



Norwegian University of Life Sciences
Faculty of Veterinary Medicine
Department of Food Safety and Infection Biology

Philosophiae Doctor (PhD)
Thesis 2019:79

Molecular characterization of *Piscine orthoreovirus* (PRV) and its pathogenesis in salmonids

Dhamotharan Kannimuthu

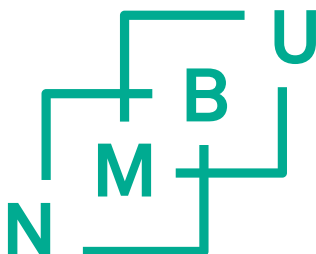
Molecular characterization of *Piscine orthoreovirus* (PRV) and its pathogenesis in salmonids

Philosophiae Doctor (PhD) Thesis

Dhamotharan Kannimuthu

Faculty of Veterinary Medicine
Department of Food Safety and Infection Biology
Norwegian University of Life Sciences

Adamstuen, 2019



Thesis number 2019:79

ISSN 1894-6402

ISBN 978-82-575-1639-0

©Dhamotharan Kannimuthu, 2019

Series of dissertations at the

Norwegian University of Life Sciences

Thesis Number 2019:79

ISSN 1894-6402

ISBN 978-82-575-1639-0

All rights reserved. No part of this publication may be reproduced or transmitted, in any form or by any means, without permission.

“Part of this research funded under grant agreement No. 652831 (AQUAEXCEL2020). This output reflects only the author’s view and the European Union cannot be held responsible for any use that may be made of the information contained therein”.

Printed in: Andvord Grafisk As

Table of contents

Acknowledgements	i
Abbreviations.....	iii
List of papers.....	v
Summary	vii
Sammendrag (Summary in Norwegian).....	ix
1. Introduction	1
1.1. Overview of Salmonids.....	1
1.2. Piscine orthoreovirus (PRV).....	4
1.2.1 Evolution and Taxonomy.....	4
1.2.2. Ultrastructure.....	5
1.2.3. Gene segments and proteins.....	7
1.2.4. Replication and transmission.....	8
1.2.5. Distribution and host range.....	9
1.3 PRV Target cells.....	10
1.3.1 Erythrocytes.....	10
1.3.2 Cardiomyocytes.....	11
1.3.3 Skeletal Muscle.....	11
1.3.4 Macrophages.....	12
1.3.5 Hepatocytes.....	12
1.4 PRV associated diseases.....	13
1.4.1 Heart and skeletal muscle inflammation (HSMI).....	13
1.4.2 HSMI-like disease in Rainbow trout.....	17
1.4.3 Erythrocytic inclusion body syndrome (EIBS).....	18
1.4.4 Jaundice syndrome.....	18
1.4.5 Black spots in Atlantic salmon.....	18
1.4.6 Proliferative darkening syndrome (PDS).....	18
1.5. Evolution of viral virulence.....	19
1.5.1. Viral virulence in farmed fish.....	19
1.5.2. Virulence mechanisms.....	21
1.5.3 Co-evolution of viral proteins.....	23
2. Aims of study.....	25
3. Summary of papers.....	27
4. Results and general discussion.....	29
4.1 Phylogenetic analysis of PRV suggests that virulence differences are related to differences in viral RNA sequences.....	29
4.2. PRV-1 is cleared from the heart but persist in blood cells.....	34
4.3. Molecular and antigenic characterization of PRV-3.....	37
4.4. Challenge experiment with purified PRV-3 confirm the causation in rainbow trout.....	42

5. Methodological considerations.....	45
5.1 <i>PRV detection methods</i>	45
5.2 <i>Polyclonal antibody production</i>	45
5.3 <i>Western blot</i>	46
5.4 <i>Realtime PCR</i>	47
5.5 <i>Immunohistochemistry and in situ hybridization</i>	48
5.6 <i>Electron microscopy</i>	49
5.7 <i>Next-generation sequencing</i>	49
6. Main conclusions.....	51
7. Future perspectives.....	53
8. References.....	57
9. Scientific Papers I-IV.....	71

Acknowledgements

I gratefully acknowledge the financial support received from Indian council of agricultural research (ICAR) through NS-International fellowship program, the research council of Norway (NFR) and European unions' Horizon 2020 research and innovation program under grant agreement No. 652831 (AQUAEXCEL²⁰²⁰). Thanks to the Dean and Head of the Department, Faculty of Veterinary Medicine (VET), NMBU, Adamstuen for their support. I would like to thank the Director, DARE, ICAR-CIFE and HOD, AEHMD for granting study leave to pursue my PhD in this prestigious institute.

I express my sincere gratitude to my main supervisor Prof. Espen Rimstad for giving me this opportunity. Words are not enough to thank you for mentoring, caring, inspiring, and supporting from the beginning. Thanks to my co-supervisor Øystein Wessel for the constant support. Your strategic and organized approach in handling any research problem is contagious. Thanks to my co-supervisor Erling Olaf Koppang for the good humor, support and guidance.

I am indebted to the virology group lab engineers, Stine, Elisabeth, Ingvild, Mamata and Ingrid for welcoming me into the research group, listening to all the problems, teaching all the methods, and encouraging me throughout the study. Thanks to my fellow PhD students, Niccolò Vendramin and Håvard Bjørgen for laying the path and making it as a successful research collaboration. Their enthusiasm and interest have fueled my motivation during the study. Special thanks to my co-authors, Turhan, Maria, Torstein, Niels, Anne, Argelia, Tine for their contribution, constant support, critical inputs and brainstorming discussions.

I felt that the PhD in Atlantic salmon is incomplete without visiting a net pen and hatchery. Thanks to Prof. Henning Sørum and Øystein Klakegg for fulfilling that wish. I would like to thank my staffs and colleagues at Lindern, Mette, Preben, Ane, Grethe, Kari, Hege, Özgün, Cristopher, John, Erik, Ida, Karla, Salman, Stannis, Anne, and Ruchika. Thanks to my colleagues at CIFE, Rajendran, Gayatri, Pani Prasad, Mekha, Jeena, Husne, Aklakur, Rathi, Mujahid, Arun, for their support.

I sincerely thank my parents, sister and brother for their love and support. Heartfelt thanks to my wife Preethi whose motivation encouraged me take up the PhD This would not have been possible without her support and sacrifice. We welcome our big miracle, daughter Niralya, to our life. Thanks to my friends in Norway Prabhu, Ramalakshmi, Nila, Muthuraja, Sloba, Agni, Chandru, Amritha, Saurabh, Victor, Kumar and Binoy for their support and making me feel at home.

Abbreviations

ARV	Avian orthoreovirus
CD8	Cluster of differentiation 8
CMS	Cardiomyopathy syndrome
Ct	Cycle threshold
EIBS	Erythrocytic inclusion body syndrome
FAST-protein	Fusion associated small transmembrane protein
GCRV	Grass carp reovirus
Hct	Hematocrit
HSMI	Heart and skeletal muscle inflammation
ICTV	International Committee on Taxonomy of Viruses
IFN	Interferon
IHC	Immunohistochemistry
IHNV	Infectious hematopoietic necrosis virus
iNOS	Inducible nitric oxide synthase
i.p.	Intraperitoneal
IPNV	Infectious pancreatic necrosis virus
ISAV	Infectious salmon anaemia virus
ISVP	Infectious subviral particle
ISG	Interferon-stimulated genes
ISH	In situ hybridization
MMC	Melanomacrophage center
MRV	Mammalian orthoreovirus
Mya	million years ago
NAPC	North American pacific coast
NGS	Next generation sequencing
NO	Nitric oxide
OIE	Office International des Epizooties
ORF	Open reading frame

PAMPs	Pathogen associated molecular patterns
PCV	Packed cell volume
PD	Pancreas Disease
PDS	Proliferative darkening syndrome
PKR	Protein kinase R
PRV	Piscine orthoreovirus
PRR	Pattern recognition receptor
RBC	Red blood cells
RdRp	RNA-dependent-RNA-polymerase
RIG-I	Retinoic acid-inducible gene-I
ROS	Reactive oxygen species
RT-qPCR	Real-time quantitative polymerase chain reaction
SAV	Salmonid alphavirus
SD	Sleeping Disease
SEM	Scanning electron microscopy
TEM	Transmission electron microscopy
TLR	Toll-like receptor
UTR	Untranslated regions
VEN	Viral erythrocytic necrosis
VHSV	Viral haemorrhagic septicaemia virus
VLP	Virus-like particle

List of papers

Paper I

Evolution of the *Piscine orthoreovirus* Genome Linked to Emergence of Heart and Skeletal Muscle Inflammation in Farmed Atlantic Salmon (*Salmo salar*)

Authors: Dhamotharan K, Tengs T, Wessel Ø, Braeen S, Nyman IB, Hansen EF, Christiansen DH, Dahle MK, Rimstad E and Markussen T

Published: Viruses, 11(5), 465, DOI: 10.3390/v11050465

Paper II

Temporal changes and localization of *Piscine orthoreovirus* (PRV) in Atlantic Salmon (*Salmo salar*) during the development of heart and skeletal muscle inflammation

Authors: Dhamotharan K, Øystein Wessel, Håvard Bjørgen, Muhammad Salman Malik, Ingvild B. Nyman, Turhan Markussen, Maria K. Dahle, Erling Olaf Koppang, Espen Rimstad

Submitted: To Veterinary Research

Paper III

Molecular and Antigenic Characterization of *Piscine orthoreovirus* (PRV) from Rainbow Trout (*Oncorhynchus mykiss*)

Authors: Dhamotharan K, Vendramin N, Markussen T, Wessel Ø, Cuenca A, Nyman IB, Olsen AB, Tengs T, Dahle MK and Rimstad E

Published: Viruses, 10(4), 170, DOI: 10.3390/v10040170

Paper IV

***Piscine orthoreovirus* subtype 3 (PRV-3) causes heart inflammation in rainbow trout (*Oncorhynchus mykiss*)**

Authors: Vendramin N*, Dhamotharan K*, Olsen AB, Cuenca A, Teige LH, Wessel Ø, Iburg TM, Dahle MK, Espen Rimstad, Niels Jørgen Olesen

* Shared authorship,

Published: Veterinary Research, 50 (1), 14, DOI: 10.1186/s13567-019-0632-4

Summary

Piscine orthoreovirus (PRV) is a virus of salmonid fish. PRV has been associated with different diseases in various salmonid fish species, including heart and skeletal muscle inflammation (HSMI) in Atlantic salmon and more recently a disease resembling HSMI in rainbow trout. In general, PRV appears to be widely distributed, with detection in diseased as well as non-diseased fish. For some of the diseases, a causative relationship has been established, confirming PRV as the etiological agent of the disease, whereas for others the disease association is questioned. The combination of multiple salmonid species and discovery of multiple PRV variants, compose a complex landscape to study disease association. This calls for basic studies revealing the characteristics of the virus, combined with targeted and controlled experiments to settle disease association. The present thesis focuses on PRV-1 infection of Atlantic salmon and PRV-3 in Rainbow trout. The work encompasses the basic characterization of PRV and provides important information on the pathogenesis and disease association.

The first study addressed potential virulence differences between PRV-1 strains infecting Atlantic salmon. A full genome sequence analysis of different PRV-1 strains was conducted. The analysis of HSMI-associated PRV-1 strains and low virulent North American pacific coast (NAPC) isolates revealed connection foremost with genomic segments S1 and M2 and the HSMI trait. Reassortment of these two genomic segments and/or possibly the accumulation of mutations have contributed to the evolution of the virulent strains. Some of the PRV-1 isolates showed segment reassortments, indicating that this mechanism contributes to PRV evolution. PRV strains from archived samples, revived by *in vivo* propagation and full-genome sequenced, confirmed the presence of different variants of PRV during the pre-HSMI period in Norway. The HSMI associated genotypes are adapted to farmed Atlantic salmon, as indicated by the sequences of S1 and M2 segments being stable for the last 20 years.

The second study looked into viral kinetics, the differential peak of PRV RNA and protein during HSMI development. Following experimental infections, irrespective of the challenge method, PRV-1 infection of erythrocytes has a clear peak. The virus particles release from erythrocytes into plasma in large numbers in the peak period and spread to other organs. Cardiomyocytes are particularly permissive for infection with PRV-1, and the resulting immune response to the infected cells causes the typical HSMI histopathological changes, i.e. epicarditis, myocarditis in spongy and compact cardiomyocytes. The immune response clears

the virus from the cardiomyocytes. However, the virus persists in erythrocytes as observed by detection of PRV RNA by RT-qPCR and *in situ* staining.

The third study focused on a new PRV variant infecting rainbow trout, which had been associated with an HSMI-like disease. Genetic and antigenic characterization of the virus were conducted to study the relation to PRV-1. Based on full genome sequence analysis, the virus was assessed as a new PRV variant and named PRV-3. The overall nucleotide identity to PRV-1 was 80%. Western blot analysis showed cross-reaction with antibodies raised against PRV-1 proteins for all homolog PRV-3 proteins tested. The antigenic analysis did not indicate that PRV-3 was a new serotype. The protein structure and functions are conserved between PRV-1 and PRV-3. The screening for PRV-3 by RT-qPCR revealed the presence of this virus in Denmark, Italy, Germany, and Scotland.

The fourth study continued to focus on PRV-3 and aimed to look at the relationship between PRV-3 and the HSMI-like disease in rainbow trout. A ten-week long cohabitation challenge experiment was conducted to prove a causal relationship with the disease. The virus was purified and shown to be morphologically indistinguishable from PRV-1 in transmission electron microscopy (TEM). The study showed that PRV-3 infection causes inflammation and pathological changes in the heart of both shedders and cohabitants. The viral infection induced innate antiviral immune responses, as measured by gene expression analysis. The PRV-3 infection in rainbow trout showed differential viral kinetics compared to PRV-1 in Atlantic salmon. PRV-3 is cleared in rainbow trout, whereas PRV-1 persists in erythrocytes of Atlantic salmon.

To summarize, 1) We have shown that PRV-1 was present in Norway before the report of HSMI appeared. The M2/S1 segment pair links to the evolution of virulence in PRV-1 in Atlantic salmon. 2) The PRV peak in erythrocytes coincides in time with infection of heart and liver. PRV-1 is cleared from cardiomyocytes, but persist in erythrocytes. 3) The genetic and antigenic characterization of PRV from rainbow trout showed close relation to PRV-1. The new virus is a distinct PRV subtype, named as PRV-3. 4) PRV-3 is present in rainbow trout and brown trout in other European countries. 5) Finally, we proved that PRV-3 causes heart pathology in rainbow trout using purified PRV-3 in a challenge study.

Sammendrag (Summary in Norwegian)

Piscine orthoreovirus (PRV) infiserer salmonide fiskearter, laksefisk. Viruset er assosiert med ulike sykdommer hos salmonider, inkludert hjerte- og skjellettmuskel betennelse (HSMB) i Atlantisk laks (*Salmo salar*), og nylig også en sykdom i regnbueørret (*Oncorhynchus mykiss*) med likhetstrekk til HSMB. PRV er vidt utbredt og finnes hos HSMB-syk og frisk fisk.

For noen sykdommer, slik som HSMB er PRV bekreftet årsak, mens for andre sykdommer er eventuell assosiasjon til PRV blitt stilt spørsmålsteget ved. Kombinasjonen av mange ulike varianter av PRV og mange arter salmonider gjør det komplisert å studere assosiasjon til sykdom. Dette krever detaljert karakterisering av virus og målrettede og kontrollerte forsøk for å studere assosiasjon mellom sykdoms og virus nærmere.

Denne avhandlingen fokuserer på PRV-1 infeksjon i Atlantisk laks og PRV-3 infeksjon i regnbueørret. Arbeidet omfatter grunnleggende karakterisering av PRV og gir viktig informasjon om patogenese og assosiasjon til sykdom.

Den første studien tok for seg mulige virulensforskjeller mellom ulike PRV-1 stammer fra atlantisk laks. En analyse av fullgenom sekvenser av forskjellige PRV-1-stammer ble utført. Analyse av HSMB-assosierte PRV-1-stammer og av lavvirulente stammer fra den nordamerikanske stillehavskysten (NAPC) viste en sammenheng mellom evnen til å inducere HSMB og sekvenser i virusets gensegmenter S1 og M2. Reassortering av disse to gen segmentene eller muligens akkumulering av mutasjoner har bidratt til utviklingen av virulente stammer. Noen PRV-1 stammer er et resultat av reassortering av gensegmenter, noe som indikerer at dette er en viktig mekanisme for evolusjon av virus. PRV-stammer fra arkiverte frosne prøver ble gjenopplivet ved injeksjon i laks og fullgenomsekvensert. Dette viste at PRV var til stede i Norge før HSMB ble beskrevet første gang. HSMB-assosierte genotyper er tilpasset atlantisk laks i oppdrett, noe som blant annet er indikert ved at sekvensene til S1 og M2-segmentene har vært tilnærmet stabile de siste 20 årene.

Den andre studien så på virus kinetikk, og PRV RNA- og protein-mengder i atlantisk laks ved utvikling av HSMB. Ved eksperimentelle infeksjoner, uavhengig av metoden som brukes, gir PRV-1-infeksjon i erytrocytter en klar topp relativt tidlig i infeksjonsforløpet. Viruspartiklene frigjøres fra erytrocytter til plasma i stort antall i topp-perioden og spres til ulike organer. Kardiomyocytter er spesielt mottagelige for infeksjon med PRV-1. Dette gir en immunrespons mot infiserte kardiomyocytter, som histopatologiske er karakterisert som epikarditt og myokarditt i spongiose og kompakte deler av hjertet. Dette kalles typiske

HSMB-histopatologiske forandringer. Immunresponsen mot infisert hjertevev fjerner virusinfiserte kardiomyocytter, men PRV-1 persisterer i erytrocytter, noe som kan observeres ved påvisning av PRV RNA ved RT-qPCR og in situ hybridisering.

Den tredje studien fokuserte på en PRV-variant som infiserer regnbueørret, og var assosiert med en HSMB-lignende sykdom i denne arten. Genetisk og antigen karakterisering av dette viruset ble utført med henblikk på relasjon til PRV-1. Basert på sekvensanalyse av fullgenom ble viruset vurdert som en ny PRV variant og kalt PRV-3. Identiteten med PRV-1 på nukleotidsekvensnivå var ca 80%. Western blot-analyser viste at antistoffer laget mot forskjellige PRV-1-proteiner kryssreagerte og gjenkjente homologe PRV-3-proteiner. Antigenanalyse indikerte derfor ikke at PRV-3 var en ny serotype. Proteinstrukturen og -funksjoner er bevart mellom PRV-1 og PRV-3. Undersøkelse for PRV-3 ved hjelp av RT-qPCR viste at dette viruset også er tilstede i Danmark, Italia, Tyskland og Skottland.

Den fjerde studien fokuserte også på PRV-3 og hadde som mål å se på forholdet mellom PRV-3 og HSMB-lignende sykdom hos regnbueørret. Et ti uker lang eksperimentell smittestudie med kohabitant smittemodell ble utført for å kartlegge potensiell årsakssammenheng med sykdom. Viruset ble først rensset og vist å være morfologisk lik PRV-1 i transmisjonselektronmikroskopi. Studien viste at PRV-3-infeksjon forårsaker HSMB-lignende patologiske forandringer i hjertet til både utskillere og kohabitant fisk, men ikke i så sterk grad som PRV-1 gjør i atlantisk laks. Virusinfeksjonen induserer en rekke medfødte antivirale immunresponser, noe som ble målt ved genekspressjonsanalyse. PRV-3-infeksjonen i regnbueørret viste forskjellig viruskinetikk sammenlignet med PRV-1 hos atlantisk laks. PRV-3 infeksjon er begrenset og fjernes fra regnbueørret, mens PRV-1 infeksjon persisterer i atlantisk laks.

Oppsummert: 1) Vi har vist at PRV-1 var til stede i Norge før HSMB dukket opp. M2 / S1-segmentene er knyttet til evnen å gi HSMB, det vil til virulens hos PRV-1 i atlantisk laks. 2) PRV-toppen i infeksjon av erytrocytter sammenfaller i tid med at infeksjonen etableres i hjerte og lever. Immunresponsen bidrar til at PRV-1 forsvinner fra kardiomyocytter, men infeksjonen vedvarer i erytrocytter. 3) Den genetiske og antigen karakteriseringen av PRV fra regnbueørret viste nær relasjon til PRV-1. Det nye viruset er en distinkt PRV-undertype som ble kalt PRV-3. 4) PRV-3 finnes i både regnbueørret og brunørret i flere europeiske land. 5) Til slutt viste vi at rensset PRV-3 forårsaker hjertepatologi hos regnbueørret.

1. Introduction

1.1. Overview of Salmonids

Salmonids are globally important fish species in aquaculture, capture fisheries and recreational fishing. The family Salmonidae encompasses 3 subfamilies and 11 genera. The subfamily Salmoninae consists of the genera *Salmo*, *Oncorhynchus*, *Salvelinus* and *Hucho* (1). Salmonids are cold-water fishes, native to temperate waters of subarctic regions (2). The top two important species in salmonid aquaculture are Atlantic salmon (*Salmo salar*) and rainbow trout (*Oncorhynchus mykiss*). Atlantic salmon is native to the North Atlantic basin and rainbow trout is native to North Pacific regions (Fig. 1). The speciation of *Oncorhynchus* is estimated to have happened before 28.2 Mya (± 1.6 Mya) (3). Despite the Atlantic and Pacific salmon native stocks regions, salmonids have been introduced to non-native regions for aquaculture and recreational fishing (2, 4) (Fig. 1). Rainbow trout is the most successfully adapted salmonid species; introduced to many countries for farming and sports fishing (5, 6).

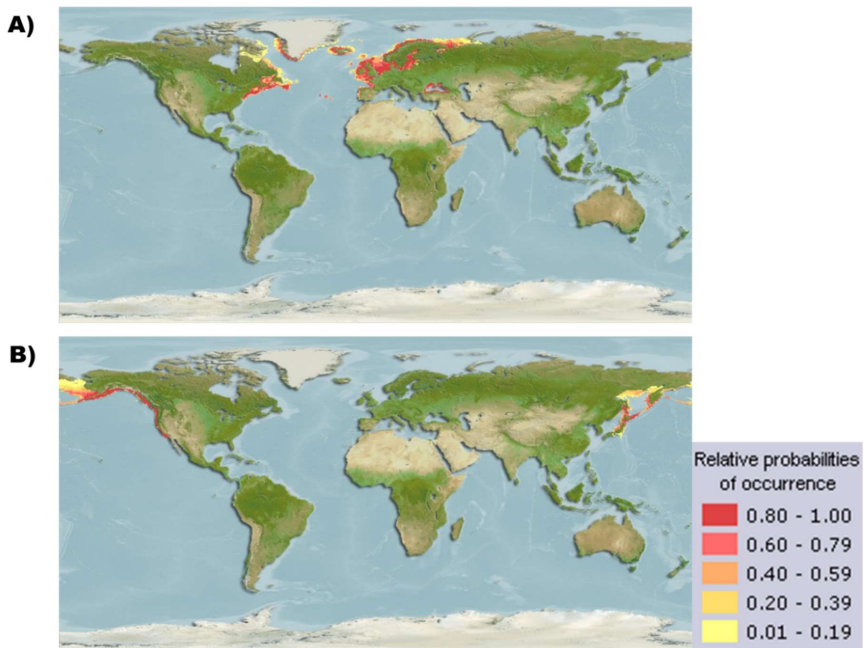


Figure. 1. Natural Distribution of A) Atlantic salmon (*Salmo salar*) and B) Rainbow trout (*Oncorhynchus mykiss*) (adapted from Fishbase). (7, 8). The relative probabilities of occurrence is given in yellow to red color code.

Atlantic salmon is an anadromous species, but also have land-locked, freshwater resident stocks (2). The anadromous Atlantic salmon return after feeding and maturation in seawater, to freshwater for spawning in streams or rivers. Rainbow trout have both anadromous migratory form (known as steelhead trout) and freshwater resident forms (9). Pacific salmon, i.e. the *Oncorhynchus* spp., shows mass migration to spawning rivers, which contrast that of Atlantic salmon (10).

Worldwide, Atlantic salmon and rainbow trout together is the most traded fish commodity by value (18% of total trade value) (11). Of the total global aquaculture production of salmonids 3.32 mmt (million metric tons), Atlantic salmon contributes 68% (2.25 mmt) and Rainbow trout 24% (0.81 mmt) (Fig. 2), the remaining 8% contributed by coho salmon and other salmonid species. The important farmed Atlantic salmon producing countries are Norway, Chile, UK and Canada, but it is also farmed in USA, Ireland, Denmark, the Faroe Islands and Australia. Rainbow trout is farmed in more than 80 countries where Iran, Turkey, Norway, Chile and Peru contribute significantly to the production (11). Salmon farming is highly industrialized in Norway. Of the total farmed fish production of 1.33 mmt (2016), Atlantic salmon contributed 93% and rainbow trout 6.6% (11).

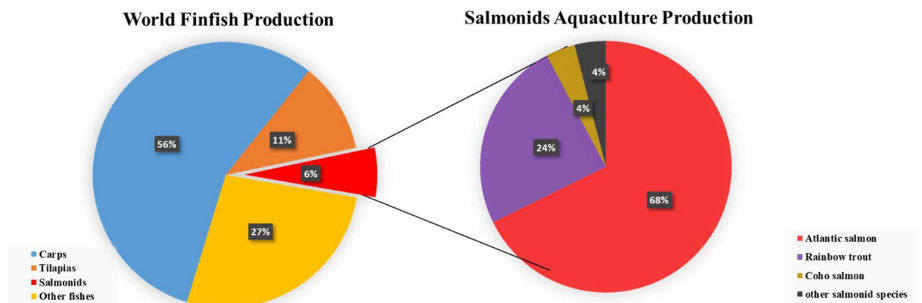


Figure. 2. Global aquaculture production of finfish. Salmonids contributes with 6% to the total finfish culture production by quantity (tons). Atlantic salmon and rainbow trout contribute 92% to the total salmonids production (FAO, 2018) (12).

In Norway, Atlantic salmon and rainbow trout farming follow similar culture practice. The smolts are produced predominantly in onshore land-based, freshwater flow through or partial recirculating systems. (13). The grow-out production of Atlantic salmon and rainbow trout is dominated by net pens in seawater. Freshwater facilities are used for broodfish.

In a land-based smolt facility, strict biosecurity measures such as the selection of water source, water filtration, ozonation, and UV radiation are applied to prevent pathogen entry through the water. It is not possible to implement such strict biosecurity measures for sea site net-pens where there are continuous exchange and interaction with the surrounding environment (6).

The transfer process from freshwater to seawater facility, stocking in a new environment and the smoltification processes itself make the smolts susceptible to infection. Hence, many viral diseases strike in the period just after seawater transfer (14). The farmed fish is more or less continuously exposed to some form of physical, chemical or biological stress during the grow-out stage, particularly due to the campaign to keep salmon louse numbers low. Hence, the loss after seawater transfer during grow-out stage is estimated to staggering 53 million smolts for Atlantic salmon and 3.2 million Rainbow trout (15). Environmental and host factors are managed to keep the impact of stress on fish health and immunity at a low level (16, 17). The newer and advanced net-pen systems such as offshore cages, closed or semi-closed system are developed to reduce infection and sea lice infestation during the grow-out stage (Figure 3).



Figure 3. Atlantic salmon net-pen in a farm site in Trøndelag, Norway. An experimental closed cage system for reducing sea lice infection (Photo: Dhamo)

One of the main challenges in salmonid farming is outbreaks of viral diseases. Such disease outbreaks may have a devastating impact on the affected farm but also at a regional or national level. Therefore, monitoring, prevention and control of fish diseases are important for the ecosystem, sustainable farming and international trade. In order to combat a viral pathogen, basic characterization of its genomic, protein, phylogeny and virulence features are necessary. This aids in the development of proper diagnostic, control measures and prophylaxis. The present thesis focuses on *Piscine orthoreovirus* (PRV) infection in Atlantic salmon and rainbow trout which is an emerging viral pathogen in farmed salmonids. Specific focus is given on the genetic and pathological characterization of PRV in Atlantic salmon and rainbow trout.

1.2. Piscine orthoreovirus (PRV)

1.2.1 Evolution and Taxonomy

PRV belongs to the family *Reoviridae*. Reovirus is derived from the acronym **R**espiratory **E**nteric **O**rphan virus, as the virus can be isolated from respiratory and enteric organs, originally described as “orphan” - virus as they lacked clear association to a clinical disease (18). The dsRNA viral genome was first described in 1963 and reovirus was one of the virus groups to be described to have dsRNA genome (19, 20). Reoviruses are non-enveloped, icosahedral symmetric viruses, which infect a wide range of species, mammals, reptiles, birds, insects, plants and fungi. *Reoviridae* is divided into subfamilies *Spinoreovirinae* and *Sedoreovirinae*. *Spinoreovirinae* has large spikes and turrets, contains nine genera including *Orthoreovirus*, *Aquareovirus*. *Sedoreovirinae* has a spherical or smooth surface, contains six genera comprising *Rotavirus* and *Orbivirus* (21).

Orthoreoviruses have been shown to infect mammals, reptiles and birds whereas the *Aquareoviruses* have been reported from many freshwater and seawater fish, crustaceans and molluscs (21). *Orthoreovirus* and *Aquareovirus* are closely related and are hypothesized to have derived from a common ancestor 49-520 million years ago (22). Co-speciation of orthoreoviruses with the host has been proposed based on the mutation rate and sequence identity among orthoreoviruses. Phylogenetically *Orthoreovirus* evolution reflects the host evolution and co-divergence (23). This can be observed in conserved enzymatic surfaces of core proteins $\lambda 1$, $\lambda 2$, $\lambda 3$, and $\sigma 2$ in both virus groups (24). Some diverged species of *Aquareovirus* and *Orthoreovirus* share outer fiber protein and lack fusion-associated small transmembrane (NS-FAST) proteins, which further confirm common origin (25).

PRV was first identified in HSMI diseased fish by next-generation sequencing (NGS) in 2010 (26). Sequence analysis revealed PRV to be the first *Orthoreovirus* infecting fish (26). The *Orthoreovirus* genus splits into fusogenic and non-fusogenic viruses. PRV is like its mammalian counterpart mammalian orthoreovirus (MRV), a non-fusogenic virus, which lack FAST proteins. The differentiating features of the PRV group have a distinct cytotoxic non-fusogenic, integral membrane protein, p13, and an outer fiber protein σ 1, different from other orthoreoviruses (27). The presence of internal reading frames and the encoded protein differ from MRV. The nucleotide and amino acid percentage identity also meet the criteria for classifying an orthoreovirus species by ICTV (21). Based on these properties and genome sequences, PRV is recognized as a new species in the genus *Orthoreovirus* (25).

The PRV group includes another divergent virus named largemouth bass reovirus (LMBRV). This virus was associated with mass mortality in wild largemouth bass (*Micropterus salmoides*) in a freshwater lake, USA (28).

1.2.2. Ultrastructure

PRV proteins are structurally and functionally conserved, compared to MRV (29). The virions are spherical shaped 70 nm in diameter with two capsid layers, the inner electron-dense core is around 38 nm and virion density is 1.34 (+/-0.01) g/mL in CsCl (Fig. 4) (30). The viral genome of 10 linear dsRNA segments is covered by an inner capsid. The viral proteins necessary for replication and mRNA synthesis, λ 3 (RNA dependent RNA polymerase), and λ 1 (Helicase, NTPase, RNA triphosphatase) are placed in the inner core (Fig. 5). In MRV, the outer capsid proteins σ 3 and μ 1 contribute >60% and RNA to 14-22% of virion mass (31, 32).

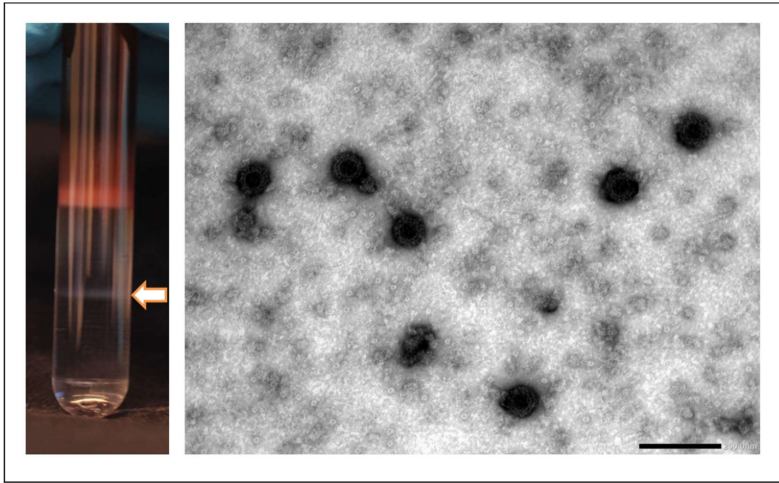


Figure 4. Purification of PRV in CsCl gradient ultracentrifugation and TEM image showing viral particles in plasma of HSMI diseased fish (Photo: Øystein Wessel)

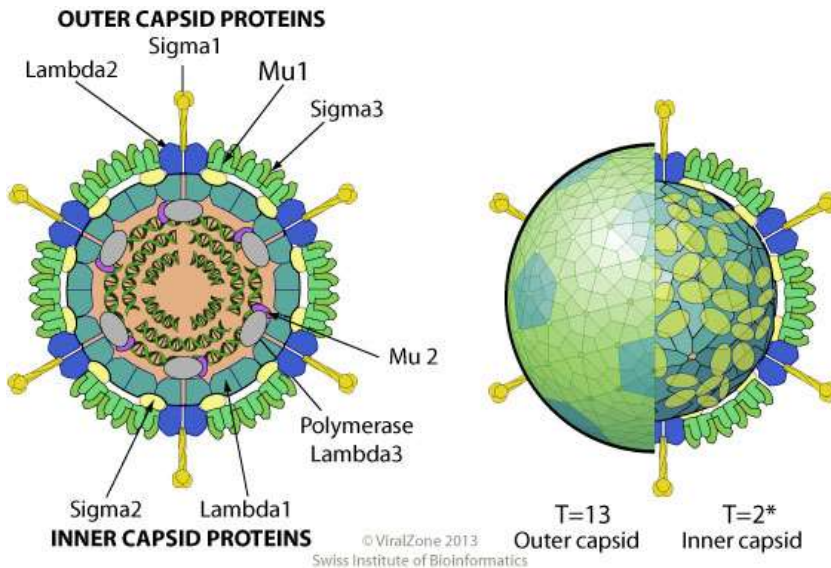


Figure 5. Orthoreovirus structure showing the overview of different viral proteins and symmetry. (Source: ViralZone:www.expasy.org/viralzone, SIB Swiss Institute of Bioinformatics).

1.2.3. Gene segments and proteins

Based on the size, the genome segments of PRV are grouped into three classes Large (L1-L3), Medium (M1-M3) and Small (S1-S4) and code for λ , μ and σ class of proteins. Every segment codes for minimum one protein (29). Each genome segment has a unique 4- or 5- bp terminal sequence specific for the species, in MRV 5'-GCUA, UCAUC-3' and in PRV it is 5'-GAUAAA and UCAUC-3' (26). The genome and coding arrangement of PRV is different from other orthoreoviruses. The S2 and L2 segments are predicted to be potential polycistronic segments, but this has to be confirmed. In PRV S1 segment is bicistronic, encodes the σ_3 , which is an outer capsid protein and the p13 proteins. In other orthoreovirus, S4 segment is bicistronic and encodes outer fiber protein and FAST protein or another protein (σ_1 s in MRV) of unclear function. In PRV, the S4 segment is not a polycistronic protein and codes for outer fiber protein and does not code of any other protein (27).

PRV segment L1 codes for λ_3 - RNA dependent RNA polymerase, which is most conserved among orthoreovirus. In the dsRNA virus, this enzyme takes part in viral genome replication and mRNA synthesis. The inner core has λ_1 , λ_3 , σ_2 and μ_2 proteins (31). The outer capsid consists of σ_3 and μ_1 proteins organized as $(\sigma_3)_3(\mu_1)_3$ heterohexamers in T=13 symmetry (33). L2 segment codes for λ_2 capping enzyme with guanylyltransferase and methyltransferase activity necessary for 5'-capping of mRNA. The λ_2 protein, arranged in pentamers of twelve copies, project the core particle and the capped mRNA exits through this protein (34). The L3 segment encodes λ_1 protein, which forms the inner capsid shell. The inner capsid (approx. 60 nm diameter) is made of 120 copies of λ_1 in T=1 symmetry (35). The protein has helicase, NTPase and RNA triphosphatase activities and binds to dsRNA and zinc (36).

The segments M1, M2 and M3 codes for μ_2 , μ_1 and μ_{NS} protein repetitively. The μ_{NS} proteins interact with cell cytoskeleton and other viral proteins. The scaffolding protein μ_{NS} is responsible for organizing the viral factories. PRV μ_{NS} protein alone can form dense, globular inclusion like structure in the cytoplasm (37). The inclusion can be either filamentous or globular for orthoreoviruses. The PRV inclusions are globular structures similar to MRV T3D type (37, 38). The S1 segment is bicistronic segment and codes for the major outer capsid protein (σ_3) and cytotoxic integral membrane protein p13, σ_3 is a dsRNA binding protein and has a zinc finger motif, conserved among orthoreoviruses (39). Among the S class proteins, the segment S2 codes for structurally conserved inner capsid structural protein - σ_2 . The non-structural σ_{NS} protein is coded from the segment S3. The protein σ_{NS} takes part in viral factory formation with μ_{NS} (40). Finally, S4 segment codes for the outer fiber protein σ_1 .

The three defined serotypes of MRV type 1 Lang (T1L), type 2 langdon (T2L) and type 3 Dearing (T3D) are classified based on the neutralization test targeting type specific $\sigma 1$ proteins (41). However, such serotype classification of PRV subtypes is hindered by the unavailability of permissive cell lines.

1.2.4. Replication and transmission

The PRV viral replication mechanisms are comparable to MRV for which the pathways are well characterized (Fig.6). The cell attachment protein, $\sigma 1$ of MRV binds to sialic acids or JAM-A receptors (42, 43) and internalized by clathrin-coated endosome (44, 45). In reoviruses, the viral morphogenesis occurs in inclusion bodies in the cytoplasm (32). The entry and disassembly are mediated by the cleavage of outer capsid protein $\sigma 3$ and $\mu 1$ which generates infectious subviral particles (ISVP), followed by transcriptionally active core viral particles (46).

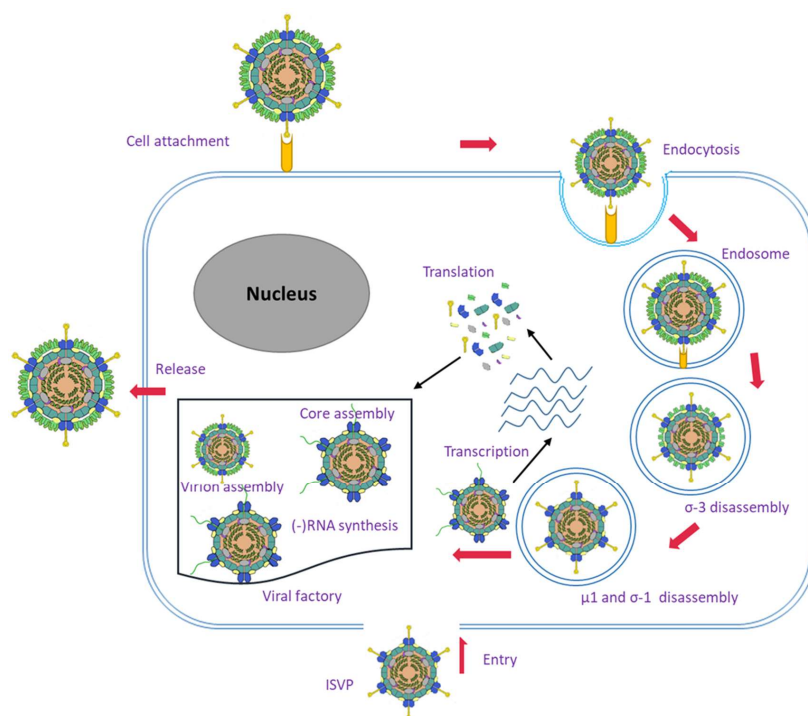


Figure. 6. Schematic diagram of MRV replication pathway. Picture modified from Sahin et al., 2013 (47) and ViralZone:www.expasy.org/viralzone, SIB Swiss Institute of Bioinformatics.

The viral genome is not exposed to the cytoplasm of the host cell to avoid host immune response. The mRNA is synthesized in subviral particles. The mRNA is capped with 5' methylation (48) and is not polyadenylated in the 3-end (49). The transcribed mRNA is translated utilizing host translational machinery. The core viral particles are assembled in viral factories packed with –ssRNA and the complementary +RNA is synthesized inside the particle to form dsRNA genome (50). Matured PRV virions are released from the cell with or without lysis. PRV enters and transmitted through the fecal-oral route and horizontal transmission is the major route for spread, vertical transmission from mother to offspring has not been shown (51).

1.2.5. Distribution and host range

PRV screening studies have reported the prevalence of PRV in several farmed and wild species with or without clinical disease. The phylogenetic analysis of PRV sequences from wild and escaped farmed Atlantic salmon showed no geographical isolation confirming the wide dispersal and exchange of PRV strains in Norway (52). PRV is detected in returning Atlantic salmon in Norwegian rivers. The PRV prevalence was in wild caught broodfish - 13.6%, hatchery-reared sea-ranched wild-caught brooders – 24.4%, and escaped farmed salmon -51.9%. The statistical analysis showed that the chances of PRV detection in returning salmon increased when the fish spends a long time at sea (53). In another study, the PRV prevalence during 2007-2009 was 13.4% in wild Atlantic salmon, 24.0% in salmon released for stock enhancement purposes, 55.2% in escaped farmed salmon and 3% of anadromous sea trout (*Salmo trutta*) without HSMI (54). PRV is detected in Atlantic cod stomach content which was feeding on straying infected Atlantic salmon (55). PRV is a virus of salmonid fish, nevertheless, it is detected in some other marine species but the Ct value was very high (56). However, the PRV infection and productive replication in other fish species require further research.

PRV is commonly detected in wild coho and Chinook salmon in the US. The prevalence was reported to be 3.4%, (77 of 2,252 fish tested positive) (57). PRV is detected in wild cutthroat trout (*Oncorhynchus clarkii*), chum salmon (*Oncorhynchus keta*), farmed steelhead trout (*Oncorhynchus mykiss*) in Canada (58). Analysis of archived paraffin blocks of different pacific salmonids from 1974 to 2013 in British Columbia detected the presence of PRV

without typical HSMI in Chinook salmon, sockeye salmon, coho salmon and steelhead trout (59).

1.3 PRV Target cells

Orthoreovirus infect and replicate in a wide range of cells in tissues. The symptoms and clinical diseases vary depending on the target cells. MRV type 1 and 3 infect CNS and cause encephalitis in newborn mice (60). MRV type 1 Lang (T1L) induce myocarditis whereas T3D does not induce myocarditis (61, 62). Another orthoreovirus, Avian reovirus causes viral arthritis/tenosynovitis and are associated with myocarditis and hepatitis in chicken (63). Similarly, PRV infects different organs and cells of fish.

1.3.1 Erythrocytes

Fish erythrocytes like those of other lower vertebrates, birds, reptiles and amphibians are nucleated cells of oval to elliptical shaped. The nucleus is centrally located with pale eosinophilic cytoplasm and basophilic nuclei. Immature erythrocytes appear as rounded than oval and have a high nucleus to cytoplasm ratio (64). Erythrocytes are generated from hematopoietic stem cells, Megakaryocyte/erythroid progenitors by erythropoiesis (65). Erythrocytes have hemoglobin and the main function is gas exchange. The life span of erythrocytes in fish varies from 13 to 500 days, compared to 120 days in humans (66). Normal erythrocyte number of Atlantic salmon varies between $0.85\text{--}1.10 \times 10^{12} \text{ l}^{-1}$ and the hematocrit (Hct) values are 44–49% (67). Normal packed cell volume (PCV) is 20-45% and value less than 20% considered anemic. The erythrocyte number and packed cells volume is influenced by age, sex, nutritional, reproductive status and other environmental factors (68). In fish, anemia could be caused by toxic chemicals, nutritional deficiency, viral, bacterial or parasitic infections.

Among erythrocytic viral infection, viral erythrocytic necrosis (VEN) and EIBS are important in salmonids. VEN is widespread and reported from chum salmon and pink salmon (69) and EIBS reported from coho and Chinook salmon. Both EIBS and VEN are infections of erythrocytes and forms viral inclusions in the cytoplasm. In TEM, VEN virus (VENV) appears as hexagonal shaped Iridovirus-like particles of average 190 nm in size (69) and EIBS viruses are spherical particles of average 75 nm diameter. Both VEN and EIBS infection cause hemolytic anemia, lowers erythrocyte count, hematocrit and hemoglobin levels (70). Recent sequencing study has confirmed that VENV is a putative new genus in the family *Iridoviridae* (71) and EIBS is caused by an orthoreovirus, PRV-2 (72). PRV-1 infection in Atlantic salmon

targets erythrocytes and causes viremia (73). PRV-1 cytoplasmic inclusions are similar to EIBS. VENV and PRV are not cultivable in cell lines. PRV can be cultivated ex-vivo in Atlantic salmon erythrocytes (74).

1.3.2 Cardiomyocytes

The fish heart has three chambers, atrium, ventricle and bulbous arteriosus. The ventricle of the fish heart has a thicker wall than the atrium. The blood from the ventricle pass to bulbous arteriosus. The ventricle has a discrete outer compact muscle layer (*stratum compactum*) and inner spongy layer (*stratum spongiosum*). The thickness of the outer compact layer varies depending on the species. There are numerous trabeculae in the spongy layer. The coronary vessel covers the outer ventricle and supplies oxygenated blood to the compact layer (75). Unlike mammalian heart, cardiomyocytes in fish can regenerate in adults (76).

Both farmed Atlantic salmon and rainbow trout are affected by many heart diseases and disorders such as idiopathic heart pathology (77), myocardial necrosis (78) coronary arteriosclerosis (79) and abnormal shaped heart (80). Viral diseases like cardiomyopathy syndrome (CMS), pancreas disease (PD), sleeping disease, heart and skeletal muscle inflammation (HSMI) also cause heart lesions. Coinfection of PRV with PMCV in heart tissues has been observed during freshwater and seawater stage (81, 82). Hypoxic tolerance and cardiac performance are significantly reduced in HSMI diseased Atlantic salmon (83). In such cardiac conditions stressors like handling, transportation and other environmental factors invigorates and increases the mortality rate of affected fish. When the cardiac function is impaired by a viral infection or other injuries, the performance is compensated by adaptive responses like hypertrophy and hyperplasia (84, 85).

1.3.3 Skeletal Muscle

The muscle tissues of fish are organized as myomeres. Further, based on the fiber types they are divided into red muscle fibers (*muscularis lateralis superficialis*) and white fibers (*muscularis lateralis profundus*). Functionally these fibers are either aerobic or anaerobic, slow or fast contracting. In addition, the salmonids have pink fibers in between white and red muscles. The red muscles are well vascularized compared to white. Both muscle tissues are affected by various parasitic, bacterial and viral diseases. Depending on the extent of damage, muscle tissue can regenerate or be replaced with fibrous scar (75). Sleeping disease by salmonid alphavirus causes necrosis and atrophy of skeletal muscle in rainbow trout (86) and inflammation and degeneration of red and white skeletal muscles in Atlantic salmon (87).

PRV infects skeletal muscle and causes inflammation and necrosis resulting in loss of striation, eosinophilia and vacuolation of myocytes (88).

1.3.4 Macrophages

Macrophages develop from circulating partially differentiated monocytes (75). They remove metabolic waste, dead or infected cells, foreign materials and infectious agents by phagocytosis. They utilize different mechanisms like the generation of reactive oxygen species to inactivate the pathogens (89). Macrophages are polarized by different inflammatory cytokines and are themselves a source of cytokines and chemokines that modulate inflammatory processes (90). They form a link between innate and adaptive immunity, also present antigen to CD8⁺ cells by MHC I molecule (91). Melanomacrophages (MMC) (named due to melanin, hemosiderin and lipofuscin pigments) are organized as aggregates known as melanomacrophage centers (MMC) in fish liver, spleen and head kidney (92). The number and distribution of MMCs are affected by various environmental factors, stress and infection (93).

In mammals and other higher vertebrates, viral infection of macrophages has been observed in many diseases (94). Some of the fish viruses target macrophages or macrophage-like cells for replication, spread or persistence. In fish, *in vitro* and *in vivo* infection of turbot aquareovirus in macrophages have been demonstrated (95). PRV-infected macrophage/macrophage-like cells and melanomacrophages have been observed and persistence of PRV in these cells is suggested (96). Other viruses, like infectious salmon anaemia virus (ISAV) (97) and IPNV also infect macrophages (98).

1.3.5 Hepatocytes

Hepatocytes are the functional unit of the liver, arranged as polygonal cells and interspersed with sinusoids. In addition to the primary role in digestion and metabolism, the liver also has hemopoietic and melanomacrophage centers in fish (75). Increase in innate and adaptive immune genes are reported following virus infection in the liver (99). The liver is targeted as a primary infection site or infected due secondary to viremia. Hepatocytes are infected by IPNV (100), VHSV (101), ISAV (102) and Aquareovirus (103). PRV associated jaundice/anaemia has been reported in Chinook salmon (104).

1.4 PRV associated diseases

1.4.1 Heart and skeletal muscle inflammation (HSMI)

Heart and skeletal muscle inflammation was first reported in 1999 in Hitra/Frøya area of Trøndelag county in Norway as a disease of unknown etiology. The name HSMI was given due to typical lesions observed in heart and skeletal muscle of diseased fish. From 1999, studies were started to find the causative agent of the disease. A TEM study of HSMI diseased fish found five different viral particles of varying shape and size. One of the viruses was 80-100 nm sized found in erythrocytes and head kidney cells similar to viral particles observed in EIBS infected fish (105). In another trial, a cohabitation challenge experiment with infectious material from diseased fish caused characteristic lesions in heart and skeletal muscle. Based on the results HSMI was described as an infectious disease and viral etiology was suggested (106). In an early challenge experiment inoculum treated with chloroform also induced heart inflammation confirming the agent as a non-enveloped virus (107). The histopathological lesions were observed from 4 weeks in the injected groups and after 8 weeks in the cohabitant fish (106). Soon the disease was listed as a notifiable disease at the national level. Recently, the cause of HSMI is proved as *Piscine orthoreovirus* (30). Since then the number of HSMI outbreak has increased, peaked in 2014 with 181 cases. The number has reduced to 93 in 2017 but the real number may be higher than the original report as the disease is removed from the notifiable list from 2014 (Fig. 7). The disease is most frequently observed in seawater farms.

PRV is often present in pre-smolts during the freshwater stage and the HSMI outbreaks occur classically after seawater transfer during spring or early summer. The viral load decreases at the end of the grow-out period close to slaughter (18 months) (108). In a longitudinal farm study, HSMI outbreaks were recorded five months after seawater transfer but the disease was continued to present even after a year. The mortality is influenced by the occurrence of other diseases like IPN, CMS, parvicapsulosis, proliferative gill inflammation, etc., (109). HSMI-like disease with severe heart pathology and regeneration has been diagnosed in farmed Atlantic salmon in Scotland (110). HSMI was diagnosed in a longitudinal farm study in Canada in 2013 (111). However, in a laboratory challenge trial, PRV failed to cause HSMI in Canada (112). A recent study showed that PRV-1 from Pacific Canada is a low virulent and causes moderate heart inflammation in Mowi-McConnell strain of Atlantic salmon (113). HSMI and HSMI-like diseased have been reported from farmed Atlantic and coho salmon in Chile (114).

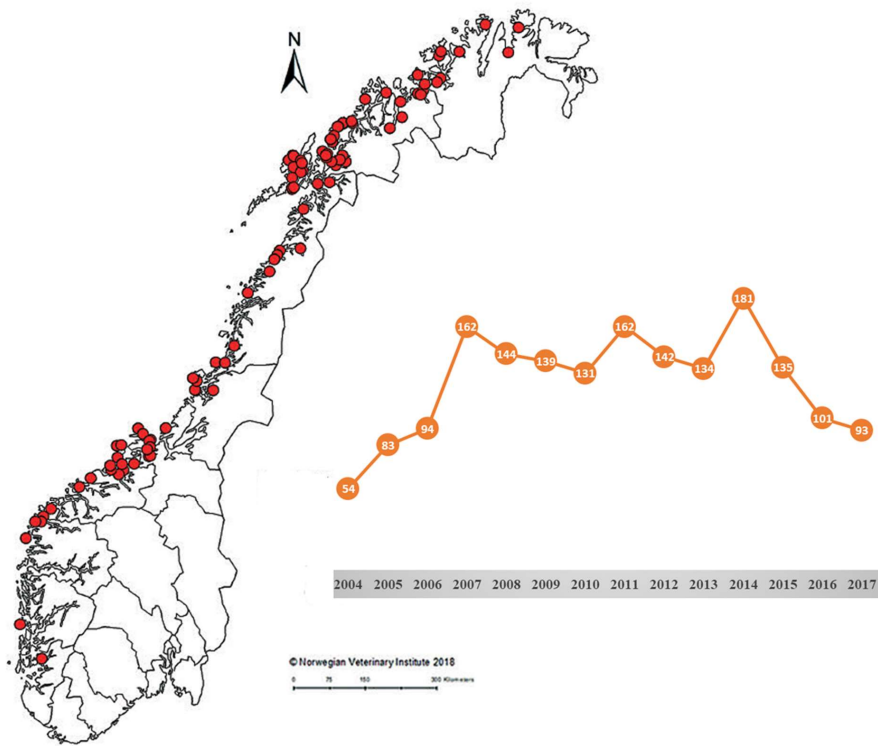


Figure. 7. Number and distribution of HSMI outbreaks in Norway in 2017 (Fish Health report 2018, Norwegian veterinary institute).

1.4.1.1 Clinical signs and histopathology

Clinically diseased fish are anorexic and show abnormal swimming. Macroscopical observations are pale heart, pericardial hemorrhage, ascites and a pale or stained liver (106), petechiae in perivisceral fat, swollen spleen (88) (Fig. 8). During the disease outbreak, asymptotic, clinically diseased, morbid or dead fish can be observed (88). High morbidity and mortality from 0 to 20 %, influenced by other stressors, are observed during the outbreak (106). Histologically, PRV infected fish show severe myocarditis in spongy and compact myocardium, and epicarditis, mild to moderate focal inflammation in skeletal muscles, infiltration of mononuclear cells and degeneration and vacuolization of skeletal muscle fibers (106). In liver, multifocal necrotic foci of varying size and shape are observed, the lesions in the liver are commonly observed in severely diseased fish with circulatory disturbances (109).

Other findings are the accumulation of erythrocytes in kidney, spleen and gills and moderate to severe peritonitis (88). Hemorrhages in all the organs, haemosiderosis with erythrophagocytosis, mononuclear infiltration in spleen and kidney are observed. HSMI-like diseased coho salmon had nephritis, spontaneous spinal fracture and kidney rupture (114). Heart, plasma, kidney/spleen and liver tissues of diseased fish are all infective (107). Macroscopic pathological changes have similarities to other viral diseases like PD and CMS, but they are distinguishable by histopathology (106).

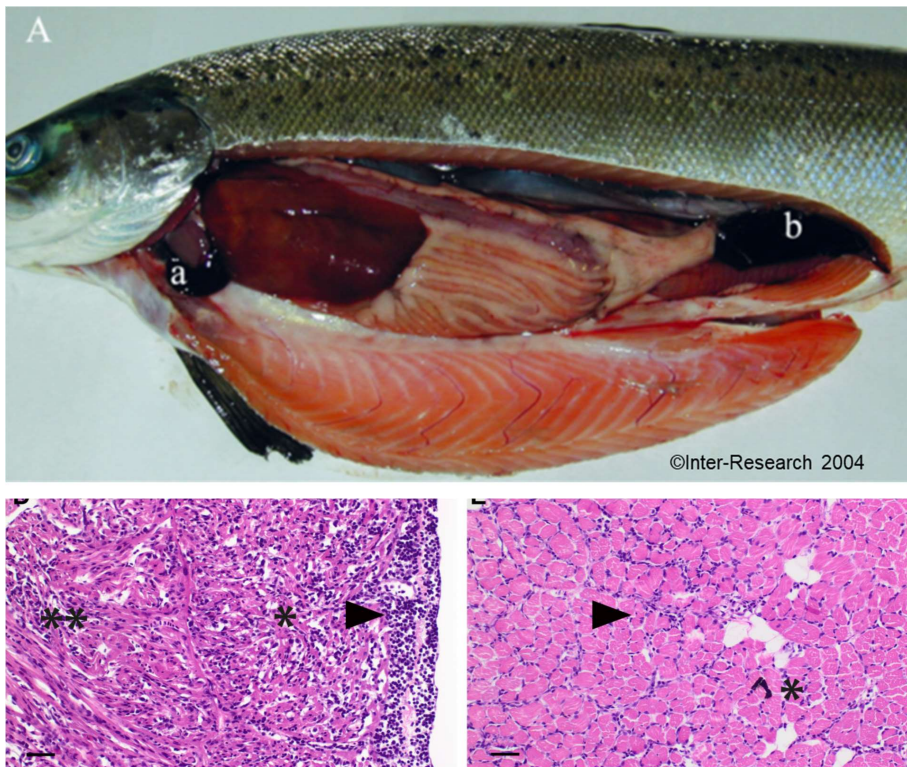


Figure 8. HSMI diseased fish peritoneal cavity with pale heart (a) and swollen liver (b) (88) (with permission from DAO, Inter-Research). Histological sections of heart and skeletal muscles showing typical lesions, epicarditis (▶) and myocarditis (*, **) in heart and myositis (▶) and melanin (*) in the muscle (30).

1.4.1.2 Innate and adaptive immune responses

As nucleated cells, fish erythrocytes have the transcription and translational systems for protein expression. Fish erythrocytes express proteins necessary for cell maintenance, metabolism, cell-to-cell interaction and immune genes. Innate and adaptive immune markers are characterized in fish erythrocytes. Immune genes like pattern recognition receptor (PRR) for the recognition of pathogen-associated molecular patterns (PAMP), innate antiviral proteins and antigen presenting molecules are expressed. This identifies erythrocytes as the first line of defense against infectious agents (115). The antiviral response halts or aborts VHSV and IPNV infection in erythrocytes ((116) 13, 26)).

The viral dsRNA will be recognized by endosomal TLR3 and induce PRR signaling pathways (116). The interferon induction further stimulates the production of Interferon stimulated genes (ISG) such as Mx, viperin, PKR, ISG and establishes antiviral state (117). In MRV infection, the interferon activates the protein kinase (PKR) which phosphorylates Serine51 of eIF2-a protein that further halts translation initiation (118). In MRV, the cellular translation inhibition is strain dependent. MRV T3D has minimal translational inhibition (119).

Interferon induced innate antiviral genes like IFN alpha, Mx, IRF-1, RIG-1, PKR, viperin, and ISG15 proteins are upregulated in PRV infected erythrocytes (115, 120). PRV infection also downregulates and suppresses the expression of erythrocyte cellular proteins (115). The ex vivo infected erythrocytes have also shown similar upregulation of IFN- α , Mx, RIG-I, and PKR immune genes (74).

In HSMI diseased fish heart, the innate antiviral immune genes, IFN γ , MX, IL-10, IL-12 and granzyme increased significantly. The innate immune response correlates with viral load, and both peak at the same time (121), suggesting an arms race between pathogen and host immune response. The release of cytokines and chemokines during the viral infection attracts inflammatory cells to the site of infection (122). Both CD4 and CD8 gene expression increased significantly correlating with the heart inflammatory score. The infiltrating inflammatory cells in compact and spongy myocardium are characterized as CD3+ and CD8+ T cells (121, 123).

T cells have T cell receptor and CD3 molecules to interact with the MHC molecules. The MHC I present peptides to CD8+ cytotoxic T cells (CTL) and MHC II to CD4+ helper T cells. CTLs are part of cell-mediated cytotoxicity and confer protection against acute viral infection. CTL secrete granzymes and perforins and kill the target cell by inducing apoptosis (124, 125).

Increase in MHC I, rTNF⁺ and MHC II staining was observed in heart tissue of HSMI diseased fish indicating an increase in antigen presentation, pro-inflammatory cytokines and infiltration of leucocyte lineage cells (dendritic cells, macrophages, B cells and T cells). PCNA, a marker of cell proliferation increased in the HSMI heart tissues (123).

1.4.1.3 Management

Farms with previous outbreaks or HSMI outbreak in nearby farms have increased chances of getting the disease (126). The multivariable modelling has also predicted infection pressure from a nearby farm, geographical location, stocking season and weight of the fish at stocking as an important risk factor for the development of HSMI (127). Hence, managing these factors would reduce infection pressure and risk factor associated with HSMI. High morbidity caused during HSMI outbreak could be improved by minimizing the stressors during seawater transfer. The use of feeds with reduced fat content and increased EPA level is shown to reduce heart inflammation caused by PRV in Atlantic salmon (128). Vertical transmission of PRV has not been confirmed. Proper disinfection of eggs would reduce the transmission of PRV from eggs to offspring. Experimental inactivated PRV and DNA vaccine have significantly reduced the occurrence of heart pathology in vaccinated fish (129, 130). Hence, the use of vaccine is promising for PRV infection; however, the unavailability of cell culture method is a bottleneck for developing vaccine on a commercial scale. Selective breeding for disease resistance has been successfully used in Atlantic salmon for IPN and development of HSMI resistant fish lines is another alternative (131, 132).

1.4.2 HSMI-like disease in Rainbow trout

In 2013, rainbow trout farms reported a disease outbreak in Norway. Infected fish showed circulatory failure, ascites, anemia and HSMI like lesions in the heart. The disease outbreak continued from hatcheries to net pens in seawater. A systematic analysis for the etiological agent revealed the presence of a new variant of PRV in the diseased fish (133). The blood homogenate samples from the disease outbreak were used in challenge trial to confirm the cause of disease as a new variant of PRV. Virus-infected blood homogenates injected shedders and cohabitants developed mild to moderate heart lesions and one fish had lesions in red skeletal muscles (134). Partial S1 segment sequence was available at that time. Hence, full genome characterization was done in paper III of this thesis.

1.4.3 Erythrocytic inclusion body syndrome (EIBS)

Erythrocytic inclusion body syndrome (EIBS) classically causes severe anemia and mass mortality in coho salmon farms in Japan, resulting in significant economic losses. EIBS was reported from salmonids coho and Chinook salmon (135, 136). EIBS cause less severe disease in rainbow trout and cutthroat trout indicating these are not particularly susceptible hosts. In Norway, viral inclusions similar to those seen in EIBS were described in hatchery-reared and wild Atlantic salmon in 1989. The viral particles were about 75-100 nm size (137). EIBS associated with high mortality was recorded in farmed Atlantic salmon in Ireland (138). EIBS infected fish recover from anemia and the hematocrit levels become normal after 30 days (136). PRV-2 is the causative agent of EIBS in Japanese coho salmon and Chinook salmon.

1.4.4 Jaundice syndrome

Jaundice syndrome is reported in farmed Chinook salmon in BC, Canada. The diseased fish show yellow discoloration of the abdomen and periorbital region. It is an acute or peracute syndrome associated with mortality. Histologically, affected fish have renal tubular epithelial necrosis. Diseased fish are infected with PRV-1; however, causal relation is not confirmed for this disease (139).

1.4.5 Black spots in Atlantic salmon

Black spots in the fillet of Atlantic salmon cause significant economic losses to the industry due to their appearance and inferior quality. Histologically, melanized spots are characterized by regeneration, fibrosis, chronic inflammation with well-organized granulomas and infiltration with melanomacrophages. PRV has been detected in melanized focal (black spot) changes in white skeletal muscle of Atlantic salmon. PRV positive macrophage-like cells, macrophages and melanomacrophages are observed in granulomas (96). The causative relation of blackspot and PRV has not been confirmed.

1.4.6 Proliferative darkening syndrome (PDS)

Proliferative darkening syndrome (PDS) is a severe disease in central Europe in brown trout (*Salmo trutta fario*) and can cause mortality up to 100%. The diseased fish are emaciated and have exophthalmia, black sub-cutaneous spots. Histopathological changes include inflammation in liver, hemorrhages in liver, spleen and kidney, necrosis in liver, spleen and nephrosis of kidney (140). The causative agent of this disease has not been clearly defined yet. A recent study has demonstrated the presence of PRV-3 in diseased fish as a possible

etiological agent. However, this was refuted by another study by showing an absence of PRV-3 in severely diseased fish (141).

1.5. Evolution of viral virulence

1.5.1. Viral virulence in farmed fish

The aquatic environment is a reservoir for viruses that coevolve with the fish. Recent viral metagenomics studies have confirmed the presence of many ancestral virus genomes of higher vertebrate viruses in fish and the aquatic environment (142, 143). The viral agents in aquaculture originate from the wild and they undergo selection and adaptation in a farm environment and may spread back to wild fish as more virulent pathogens (16, 144-146). Direct transmission of highly virulent VHSV from wild to farmed fish has also been observed (146). Many fish viruses like infectious salmon anaemia virus (ISAV), salmonid alphavirus (SAV) and PRV are present in wild fish, but clinical diseases due to these agents, which is frequent in aquaculture, are seldom observed in wild fish. Farmed fish is exposed to various physical, chemical, mechanical and biological stress. The immune system functions may be impaired by these stress factors.

The outcome of an infection depends on the host, virus and environment factors:

- Host – species, age, strain, immune status, stress level etc.
- Virus – virulence differences, transmission rate etc.
- Environment – handling, transportation, physical injury, sea lice treatment, temperature and other water quality parameters, feed, crowding during feeding, etc.

In the wild, the host availability is limited and diseased fish often succumb to death or are eaten, making bottlenecks for the survival and spread of highly virulent pathogens (147). These bottlenecks of transmission affect the evolution of viruses (148). Hence, the viral fitness in wild fish is harmonized with the ability to live along with the host. Whereas in the farmed environment the number of hosts is (almost) unlimited and less diverse. This and other factors (summarized in Table 1) offer a niche for selection for higher virulence, transmission and replication rates for the pathogen (149). The horizontal transmission pathways select for higher virulence due to high interhost competition among the virus strains (148), hence usually the high virulent strains prevail in aquaculture.

SI. No	Farmed environment	Wild
1	Almost unlimited host availability	Limited stock availability
2	Formulated Feed	Natural feed
3	Limited genetic diversity and selective bred stocks	heterogeneous, natural selection
4	Confined environment	Open
5	High density and crowding during feeding	May be crowded in a feeding ground or at breeding
6	Infectious agent circulates within the system due to various transmission factors	Infectious agents associated with mortality is eliminated with the dead fish
7	Vertical transmission is most often prevented and horizontal transmission dominates	Both can occur
8	Vaccination and antibiotic or chemical treatment make selective pressures on pathogen	No vaccination or treatment
9	Direct life cycle of pathogen	Complex life cycle of parasites are possible
10	Short culture period	Normal life span
11	Opportunistic pathogens may flourish in a farmed environment.	Less occurrence of opportunistic agents than in farming.

Table. 1. Factors and practices in farmed and wild fish environment linked to evolution of pathogen virulence (149-151).

1.5.2. Virulence mechanisms

Mutations, reassortment and recombination mechanisms contribute to the evolution of virulence in segmented RNA viruses. Horizontal gene transfer events due to interaction with other viruses and hosts are also reported for the evolution of reovirus (152). These mechanisms shape the viral evolution, disease emergence, evasion of host immune response and help in cross-species transmission (153, 154). During replication, viruses produce mutants which help to improve viral fitness and adapt to the new environment. The spontaneous mutations contribute to viral diversity (155). The population mutation frequency is affected by selection pressure, recombination and other mechanisms and is different from mutation rate (156). The mutation rate is determined by the error rate, genome size, and replication mode and strand sense of RNA virus. In general, the dsRNA virus has a lower rate of mutation due to their stamping mode of replication. Other ecological factors also affect the mutation rate (157). The mutation rate of dsRNA viruses is similar to dsDNA viruses, the molecular evolutionary rate of dsRNA viruses estimated to be 10^{-8} to 10^{-9} mutations/nucleotide/year (158). The single-stranded RNA viruses show a higher mutation rate and cross-species infection compared to DNA viruses. There are many important ssRNA viruses in aquaculture (159). When the virus is well adapted to the host or ecosystem, more mutation is not beneficial and the deleterious mutations are removed by purifying selection. In contrast, when the virus is introduced in a new environment it is not well adapted, and mutations may be beneficial (160).

Reassortment is a recombinant mechanism common in segmented RNA viruses such as *Arenaviridae*, *Birnaviridae*, *Bunyavirales*, *Orthomyxoviridae*, *Picobirnaviridae*, and *Reoviridae* (161). Co-infection with multisegmented virus can result in recombination/reassortment (Fig. 9). During co-infection and viral replication, packaging of new progeny with compatible segments from different infecting viruses may generate reassortants. In recombination, the recombinant/chimeric gene is generated by template switching among the related sequence from another virus or host gene (162). These mechanisms are important for the repair/revoke of defective RNA or deleterious mutation in the virus genome (163). It can also attenuate/reduce the fitness advantage if the resultant progeny has suboptimal RNA-RNA, RNA-protein or protein-protein interaction (164). Co-infection and co-transmission is a pre-requisite for the replication of multipartite viruses but not for segmented viruses. Co-infection is promoted by aggregation of viral particles, intestinal bacterial flora or by membrane vesicles (163). The successful reassortant generation

is dependent on co-infection, ability to overcome host interference of superinfection, interaction and compatible packaging signals (161). The protein-protein interaction is another driving factor for reassortment of segments. Reassortments are common among orthoreoviruses, rotavirus, and orbivirus. Reassortants of mammalian orthoreovirus strains have been isolated from humans (165), bats (166, 167), common vole (168), Florida white-tailed deer (169), least horseshoe bat (170) and many other species. Reassortment can affect the virus protein function and interaction (171, 172), increase or decrease the virulence. Increase in virulence is well known from influenza viruses. The reassortment can affect the interaction of the generated protein. If incompatible proteins are generated, it can affect the viral phenotypes.

Reassortment is possible only in segmented RNA viruses whereas recombination can occur in any RNA virus. It generates virus diversity and can repair the genome (173). In *orthoreovirus* homologous recombination events have been reported from Rotavirus (174) and bluetongue viruses (175). In the phylogenetic analyses, phylogenetic incongruences could be used to identify these events. Nevertheless, specific bioinformatics tools are developed for the identification of reassortment or recombination events (176-178). In the metagenomics based shotgun sequencing, identification of reassortment/recombination is still challenging in the segmented viral genome when assigning the progeny segments to the parental strain (162).

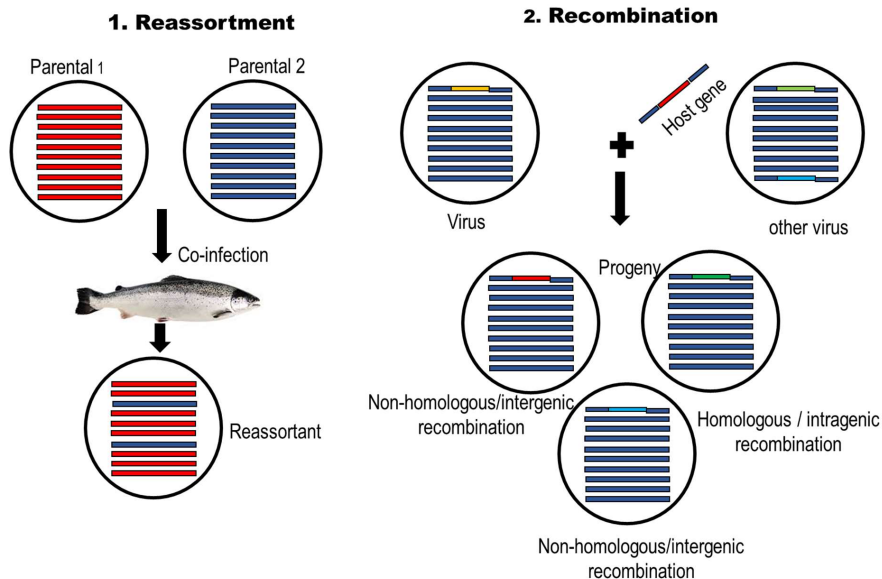


Figure. 9. Schematic diagram showing reassortment and recombination mechanisms in segmented viruses.

1.5.3 Co-evolution of viral proteins

Viral proteins interact with each other and with host proteins, structurally and functionally throughout the viral life cycle. Viral proteins also have RNA and zinc finger motifs for interaction. At the genome level, RNA-RNA interaction occurs for packaging in the segmented genome (179). The compatibility and interaction can influence the efficiency of viral replication, transmission and virulence. Co-evolution and correlated mutation of interacting proteins occur in order to maintain the interaction. In such cases, a mutation in one of the protein can cause compensatory mutation in other protein (180, 181). The mutation/reassortment restricted to one of the proteins can affect protein interaction. In MRV, recombination of $\sigma 1$ protein from another parent strain affected the $\sigma 1 - \lambda 2$ interaction in the progeny. The mismatch affected the infection efficiency (171).

2. Aims of study

Main objective

The aim of the present study was molecular, antigenic and pathogenesis characterization of *Piscine orthoreovirus* (PRV)

Sub-goals

1. Characterization of *Piscine orthoreovirus-1* genome evolutionary mechanisms in Atlantic salmon
2. Determination of dispersal and kinetics of *Piscine orthoreovirus-1* infection in Atlantic salmon
3. Molecular and antigenic characterization of *Piscine orthoreovirus-3* from rainbow trout
4. Study the causative relation of *Piscine orthoreovirus-3* infection and heart pathology in rainbow trout

3. Summary of papers

Paper I

Evolution of the *Piscine orthoreovirus* Genome Linked to Emergence of Heart and Skeletal Muscle Inflammation in Farmed Atlantic Salmon (*Salmo salar*)

PRV is ubiquitous and prevalent in farmed in wild Atlantic salmon and is not always associated with the disease. To study the PRV genomic diversity and evolution of virulence, we sequenced near-complete genome of seven new PRV-1 variants. Phylogenetic analyses grouped the viral sequences into two main monophyletic clusters, HSMI PRV strains present in farmed Atlantic salmon in Norway and Chile was in one group whereas the other one included low-virulent and non- HSMI PRV. This was particularly evident for segments S1 and M2. Only a limited number of amino acids were unique to the association with HSMI, and they all located to S1 and M2 encoded proteins. The observed evolution of the S1-M2 pair coincided in time with the emergence of HSMI, and may have evolved through accumulation of mutations and/or reassortment. Sequences of the S1-M2 suggest clonal expansion of the HSMI associated pair in salmon industry and have remained almost unchanged since 1997.

Paper II

Temporal changes and localization of *Piscine orthoreovirus* (PRV) in Atlantic Salmon (*Salmo salar*) during the development of heart and skeletal muscle inflammation

PRV-1 causes Heart and Skeletal Muscle Inflammation (HSMI) in Atlantic salmon. Here, the dispersal and temporal changes in PRV RNA and proteins were analyzed in low dose purified PRV infected Atlantic salmon. PRV primarily infects erythrocytes, replicates in cytoplasmic viral factories and subsequently spread to other organs and infects cardiomyocytes and hepatocytes. The viral RNA levels were stably detected at higher level in erythrocytes contrast to acute peak in protein level. The viral RNA and protein were cleared from fish cardiomyocytes but persist in erythrocytes. Histopathological evaluation demonstrated that PRV infection causes lesions typical of HSMI, like epicarditis and myocarditis. ISH staining of Arginase 2 showed increase in expression in infiltrating leukocyte like cells in cardiomyocytes suggesting tissue regeneration.

Paper III

Molecular and Antigenic Characterization of *Piscine orthoreovirus* (PRV) from Rainbow Trout (*Oncorhynchus mykiss*)

A new variant of PRV associated with HSMI like heart pathology in rainbow trout was reported in Norway. To find out the genetic and antigenic relatedness of this PRV, we used infected blood originated from the field to rise the viral inoculum and purified viral particles. The genome sequencing has revealed that this is indeed a different variant of PRV, which we named as PRV-3. The percentage of identities varied from 76.5–87.9% and 79.1–96.7% for the nucleotide and the amino acid sequences, respectively. Phylogenetic analysis showed that PRV-3 belongs to a separate cluster, suggesting co-evolution of PRV-3 with the host. Screening of PRV S1 segments revealed that PRV-3 strains were also found in rainbow trout in other European countries. These sequences clustered together, but were distant from PRV-3 rainbow trout in Norway. Rabbit antisera raised against purified virus or various recombinant virus proteins from PRV-1 all cross-reacted with PRV-3.

Paper IV

Piscine orthoreovirus subtype 3 (PRV-3) causes heart inflammation in rainbow trout (*Oncorhynchus mykiss*)

PRV-3 is resistant to cultivation in cell culture. We have purified the virus from the blood of infected fish and conducted cohabitation challenge experiment to prove the causation of heart pathology in rainbow trout. Both injected and cohabitant group showed increase in viral load by RT-qPCR and western blot. PRV-3 infected erythrocytes and cardiomyocytes caused inflammation and heart pathology without anaemia. The immune gene analysis confirmed that the PRV-3 infection induced innate antiviral immune genes, interferon, mx and viperin response. PRV-3 antibodies were detected in serum of infected fish. PRV-3 infection caused acute infection in erythrocytes and cleared whereas PRV-1 in Atlantic salmon persist in erythrocytes.

4. Results and general discussion

Prior to initiation of this study, we knew that PRV is ubiquitous in farmed Atlantic salmon in the marine phase, widely prevalent in wild salmonid species and not always associated with clinical disease. The presence of specific PRV subtypes in different salmonid species and their varying disease outcome i.e., PRV-1 - HSMI in Atlantic salmon, PRV-2 - EIBS in Coho salmon and PRV-3 - Heart inflammation in Rainbow trout, demand molecular characterization and species-specific pathogenesis characterization of PRV. In the first paper we set out to study PRV-1 evolution and identify evolutionary mechanisms by characterizing PRV-1 genomes from different geographic regions and time periods. This provided insights on the evolution of PRV-1 and virulence differences associated with genomic segments. In the second paper, a time course analysis of PRV-1 proteins and RNA kinetics provided a better understanding of the pathogenesis in different organs in relation to the development of HSMI. With the established method for virus purification, the pipeline for sequencing and available antibodies for PRV-1, we approached molecular and antigenic characterization of variants of PRV associated with HSMI-like disease in rainbow trout. The study determined the relationship between PRV-1 and PRV-3. At the same time, other researches have confirmed that different subtypes of PRV cause species-specific diseases. The pathogenicity, disease susceptibility and diseases outcome varied between species that encouraged us to prove causation of PRV disease in rainbow trout using purified PRV-3 virus.

4.1 Phylogenetic analysis of PRV suggests that virulence differences are related to differences in viral RNA sequences

After the first description of HSMI in Atlantic salmon in Norway in 1999 (106) and characterization of PRV in 2010 (26), many surveillance studies have reported the prevalence of PRV using RT-qPCR, and a few studies have reported S1 segment sequence (52, 54-56, 59). The results showed that PRV is widespread in farmed Atlantic salmon in freshwater and ubiquitous in seawater habitats and present in healthy hosts. In order to understand the evolutionary mechanisms and possibly identify sequences linked to virulence, we sequenced near-complete genomes of seven new PRV-1 isolates (paper I). The samples were collected from healthy fish, HSMI outbreaks and one case of a historic, unresolved suspected ISA outbreak, together representing the period 1988-2019 in Norway. Besides, two PRV-1 strains from healthy Atlantic salmon from the Faroes islands were sequenced. The sequence analysis was performed along with other available PRV sequences in GenBank.

Virulence is a complex trait dependent on host, virus and environment factors and their interaction. The outcome of the disease can vary even within the population. Virulence measures the morbidity or mortality or it can be used to assess sub-lethal changes such as weight loss, behavioral change or damage to a specific organ in a host. (182, 183). Following host jump, the virulence level is similar in closely related hosts, and the host phylogenies reflected virulence level (184). In the phylogenetic analysis, the PRV-1 sequences separated in two clusters. In one monophyletic cluster, the North American pacific coast (NAPC) (BC and USA) sequences grouped together for all segments. Most of the strains in BC cluster is not associated with the disease except one strain associated with HSMI, and another with jaundice (104), however, the causative relationship has not been established yet. The challenge studies with the BC PRV strains have reported differences in virulence and failure to cause HSMI (112, 113). There was no report of an increase in HSMI outbreak in BC region. Hence, the BC PRV cluster was named as low virulent PRV group. Another cluster groups all the Norwegian and Chilean HSMI PRV strains. This group was named as HSMI-PRV group. The NAPC low virulent group also included a PRV-1 strain from Norway sampled in 1988 and the two Faroes PRV isolates, which confirmed that NAPC-like sequences were present in Norway before 1999.

As cell culture based isolation is not available for PRV, the screening is mainly by RT-qPCR that may have been combined with histology. HSMI or HSMI-like disease have been reported from Chile (114), Canada (111) and Scotland (110).

PRV-1, or more correctly positive RT-qPCR results, has been reported from:

1. Farmed and wild Atlantic salmon, wild sea trout (*Salmo trutta*) (54, 185) and marine fish species such as great silversmelt (*Argentina silus*), capelin (*Mallotus villosus*), Atlantic horse mackerel (*Trachurus trachurus*) and Atlantic herring (*Clupea harengus*) (56) in Norway.
2. Farmed Atlantic salmon, wild coho (*Oncorhynchus kisutch*), pink (*Oncorhynchus gorbuscha*), chinook (*Oncorhynchus tshawytscha*), sockeye salmon (*Oncorhynchus nerka*) and steelhead trout (*Oncorhynchus mykiss*), in Canada (59, 186).
3. Farmed Atlantic salmon, wild coho and chinook salmon in USA (186-188).
4. Farmed Atlantic salmon, coho salmon and rainbow trout in Chile (114, 189)
5. Wild Atlantic salmon in Denmark, Sweden, Faroe Islands and Ireland (187).

PRV-3 prevalence has been reported from farmed coho salmon and rainbow trout in Chile (114, 189). The wild sea trout (*Salmo trutta*) is positive for both PRV-1 and PRV-3 in Norway

(190, 191) and coinfection of PRV-1 and PRV-3 in rainbow trout is reported from Chile (189). We have reported the presence of PRV-3 farmed rainbow trout and brown trout in other European countries (192).

The geographical and habitat isolation allows parallel independent evolution of viruses (193). Phylogenetic analysis showed that the NAPC cluster grouped monophylogenetically and there were no findings of reassortment in this cluster, however, the nucleotide sequences for all genomic segments are very homogenous and an eventual reassortment would not be easy to spot. The nucleotide changes in the group are mainly due to mutations. The PRV-1 isolate from 1988 grouped with the HSMI-PRV strains for all segments except L1, S1, and M2, where it grouped with the NAPC and Faroese isolates. Some of the HSMI PRV strains switched to NAPC group for segments L3 (KR337475) and M3 (MK675850) indicating possible reassortment events. *In vitro* and *in vivo* reassortments are reported in reoviruses and other segmented RNA viruses (194). Co-infection and superinfection of viruses are common in farmed Atlantic salmon (81, 195) which can facilitate the occurrence of reassortment or recombination mechanisms. Co-infection of PRV-1 and PRV-3 has been reported from rainbow trout in Chile (189). The compatibilities between proteins and cis-acting elements in the segments can favor the reassortment of a particular segment (175).

The phylogenetic analysis mirrored the phenotypes of PRV-1 especially for the segments M2 and S1 (Fig. 10). The segments M2/S1 might have evolved through reassortment and accumulation of mutations. Considering the genetic relatedness, except segment M2/S1, the current HSMI PRV strains might have possibly originated from strains related to the NOR-1988. The dsRNA viruses have low mutation rate in general, however, the environmental factors like farming can influence the selection pressure (196) for segments associated with virulence and pathogenesis. As there are relatively few sequences available before 1999, definitive evidence lacked to conclude on either of these mechanisms. The dominance of these segments in a distinct environment specifies the selection of these segments. The maladapted or intermediary strains might have been purged from the population.

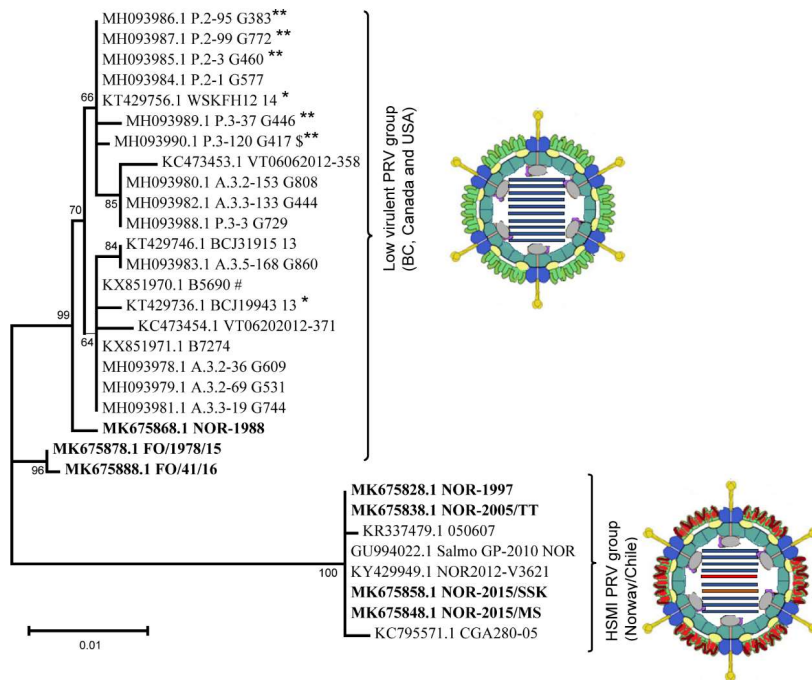


Figure 10. Phylogenetic analysis of PRV-1 S1 segment showing two different clusters. The same cluster pattern was observed for the M2 segment. The tree is unrooted and prepared with the best predicted maximum likelihood model and 1000 bootstrap replication.

For the two groups, low virulent PRV and HSMI PRV, the high number of amino acid changes and SNPs for segments M2 and S1 indicate a link for these two segments with associated virulence. The M2 segment had 60 nt SNPs and 3 aa change whereas S1 segment had 30 nt SNPs, 10 aa change in $\sigma 3$ and 7 aa in p13 indicating dN/dS ratio less than 1. (dN – synonymous mutation – which change the amino acid, dS – non-synonymous mutation which does not change the amino acid). In purifying selection or negative selection of viruses the dN/dS < 1, where the deleterious mutations are removed (183). The outer capsid consists of $\mu 1$ and $\sigma 3$ structural proteins (Fig. 11). The heterohexameric nature of $(\mu 1)_3(\sigma 3)_3$ protein in the virus particle (33) makes it likely that a gene linkage is involved for S1 and M2, indicating that only one of the proteins may be linked to the HSMI trait, while the other could be forced to co-evolve /reassort along. For segmented RNA viruses, the virulence differences often are multigenic, and two or more segments are associated with virulence (197). The $\sigma 3$ protein has

dsRNA binding domain and affect the PKR activation and downstream ISG response (198, 199). In MRV the strain specific differences in induction of myocarditis are linked to IFN- α/β responses (200). It is shown that a single amino acid difference in M2 encoded $\mu 1$ proteins is associated with the induction of IFN- β response and further myocarditis (62). This implies that the significant number of amino acid variances observed between HSMI-trait and low virulent groups could be associated with the observed virulence differences.

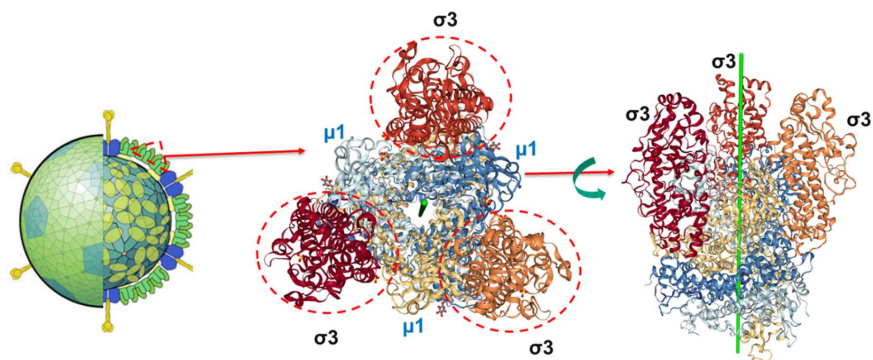


Figure. 11. MRV viral particles outer capsid proteins $\sigma 3\mu 1$ heterohexameric complex (33).

The available whole-genome PRV sequences are limited, while numerous sequences are available for the S1 segment. Therefore, we analyzed the segment S1 for eventual similar phenotypic separation in the phylogenetic analysis as observed for the whole genome analysis. The results showed that the NAPC low virulent group also included sequences of some Norwegian and Chilean PRV sequences without any known history of HSMI. This confirmed that NAPC like sequences are also present today in Norway and Chile. This group includes sequences from many salmonids, Atlantic, Chinook, coho, pink, sockeye salmon, and rainbow trout.

In the HSMI PRV group, in addition to PRV from confirmed HSMI outbreaks, PRV from escaped, hatchery-reared and wild-caught salmon were also in the same cluster, confirming wide dispersal and exchange of pathogens as found earlier (52). The pathogen exchange can occur between farmed and wild fish (191, 201). We hypothesized that the HSMI PRV is more adapted to the farming industry. The S1 sequence has been conserved within the HSMI PRV groups for more than 20 years. Similarly very low diversity $\leq 1.1\%$ was observed in low

virulence NAPC PRV group for more than 13 years. However, 3% nucleotide difference was observed between the two groups.

4.2. PRV-1 is cleared from the heart but persist in blood cells

Erythrocytes are target cells for PRV-1, PRV-2 and PRV-3. The subsequent pathological consequences vary depending upon the infected species and virus isolate. PRV-1 – heart and skeletal muscle inflammation in Atlantic salmon, jaundice/anaemia in Chinook salmon, PRV-2 – anemia and in coho and Chinook salmon (72), PRV-3 – heart pathology and anemia in rainbow trout (133). Thus the pathogenesis of a PRV infection in different hosts varies. In this study, we investigated PRV-1 viral RNA and protein kinetics in targeted organs during HSMI development in Atlantic salmon. The viral kinetics was studied in Atlantic salmon injected with purified PRV-1 of the HSMI group, but using a low viral load. The viral RNA, protein clearance and regeneration of heart tissues were observed.

In the present study, we have observed that the PRV-1 infection peak in erythrocytes at 4 wpc. Viruses use different strategies for their protein translation utilizing host machinery (202). Fish RBC are nucleated cells and support transcription and translation of the virus genome. The peak of viral RNA and proteins correlates during the early phase of infection. During the peak viremia in blood cells, the viral load also peak in plasma, confirming the erythrocytes are the source of virus in plasma. It is shown that the peak in viremia coincides with viral shedding through fecal route and infection of cohabitants. In another PRV-1 study, the shedding continued and the naïve cohabitants were infected even after 9 and 15 weeks but at a low level, suggesting a reduction in shedding of infectious viral particles (113). In PRV-2, following the peak of virus infection, the hematocrit values are reduced significantly and the RNA levels in the organs increased suggesting erythrocyte lysis (72). PRV-3 showed different viral kinetics where the viral RNA is cleared from erythrocytes in 10 weeks. In PRV-1 BC strains challenge trial, the viral RNA persisted in erythrocytes for 59 weeks post challenge in cohabitants. However, virus shedding was not observed at that time (71).

Following the acute peak, the protein levels are drastically reduced in erythrocytes but the RNA persists for a long time with no correlation of viral protein and RNA levels after the peak phase. This can be explained by various mechanisms,

1. Translational shutoff mechanisms of erythrocytes - Transcriptome analysis of PRV infected erythrocytes downregulated the host proteins like hemoglobin in infected

blood cells (115). For MRV, virus induced translational shutoff associated with PKR, Elf2-a phosphorylation and RNAase-L has been observed (203). Increase in PKR expression was observed during PRV infection which explains the possible mechanism of PKR associated translational shutoff (120).

2. The viral mRNA level reduced during PRV infection (113). In MRV infection, the stress granules formed during infection sequesters the cellular and viral mRNA (204).
3. Antiviral response reduces the active infection - PRV induced interferon and interferon regulated innate antiviral gene (ISG) response in infected blood cells (115). This may be related to point 1, as induction of PKR, which is a part of the innate response, induces Elf2-a phosphorylation.

Viral agents infecting heart tissues can inflict severe injury and induce inflammation (Fig. 12). Such cardiomyopathy condition is generally referred to as viral myocarditis (205, 206). Viral myocarditis has been reported in mammals and other animals (206, 207). PRV-1 infects cardiomyocytes and at 4 wpc, few punctate ISH staining was observed in the outer compact layer of cardiomyocytes indicating the entry and early phase of infection. At 6 and 8 wpc heavy staining of blood cells in flow cytometry, IHC and ISH staining were observed in the ventricle, spongy and compact myocardial cells indicating the peak of viral infection.

In contrast to erythrocytes, PRV RNA and protein is cleared from cardiomyocytes at 10 wpc (Fig.13) and the affected cardiomyocytes tissue regenerate. Chronic or persistent infection in the heart would result in chronic inflammation and ultimate heart failure. Teleost cardiomyocytes are capable of regeneration in adult compared to mammalian heart (208). However, the mortalities occur due to circulatory failure in severely affected fish. After viremia, the virus spread to other organs such as spleen, kidney and liver. In the present study, we have observed PRV positive hepatocytes in ISH. Multifocal necrosis without any inflammation has been observed in PRV-1 infection and in case of PRV-3 infection, no lesions were observed in liver tissues (88).

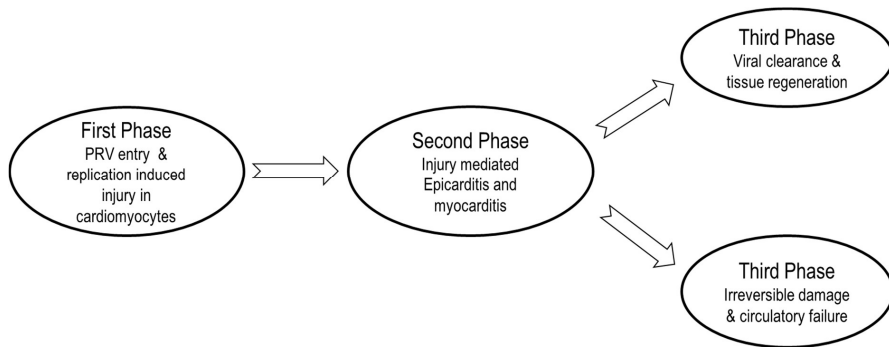


Figure. 12. Pathogenesis of PRV myocarditis (modified from Dennert et al. 2008 (209).

Macrophages are activated by either classical activation (M1) or alternate activation pathways (M2). The Th1 cytokine environment and the pro-inflammatory cytokines IFN- γ , TNF α , and GM-CSF, are part of classical activation of the macrophages. The activated macrophages produce NO and ROS with the enzyme inducible nitric oxide synthase (iNOS) from L-arginine. The Th2 cytokine environment and anti-inflammatory cytokines IL-4, IL-10, and IL-13 induce alternative activation of macrophages (M2). The arginase enzyme is a marker for M2 macrophages (90, 210, 211). The arginase converts L-arginine to L-ornithine and urea. L-ornithine is important for tissue healing and regeneration (212). In the present study, an increase in arginase was observed in the inflammatory cells. Besides the viral clearance and tissue repair, the macrophages play an important role in the adaptive immune response by presenting antigen molecules to CD⁺ T cells via MHC I molecules (91).

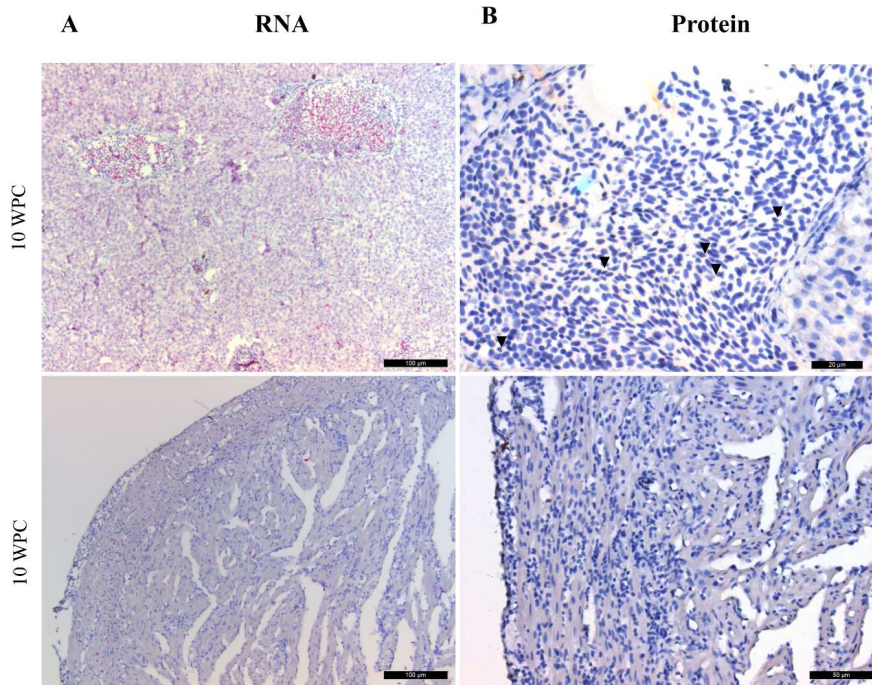


Figure. 13. PRV-1 viral RNA and protein in blood clot and heart tissues at 10 weeks post challenge (wpc).

4.3. Molecular and antigenic characterization of PRV-3

HSMI-like disease was first reported in farmed rainbow trout in Norway in 2013. A new variant of PRV was identified in diseased fish. This new PRV variant showed 85% identity to Atlantic salmon PRV in a small part of the S1 segment (133). In paper III, we have used challenge materials originated from field outbreak and passaged in healthy rainbow trout, purified virus particles and confirmed virus particles with TEM. The near-complete genome was sequenced and the viral proteins were characterized by western blot. The genome analysis confirmed that PRV in rainbow trout is related to PRV Atlantic salmon and protein structure, antigenic properties are conserved.

The virus particles were purified by CsCl gradient ultracentrifugation and were confirmed by negative staining in transmission electron microscopy. The near-complete genome sequences were generated by NGS from both plasma and purified virus samples. Both samples were proven to be the good starting material for sequencing. NGS methods are increasingly used

for novel virus discovery, genome sequencing and molecular epidemiology studies (213, 214).

Based on the molecular and antigenic analysis, PRV nomenclature was modified for consistency. The three PRVs are named as different subtypes rather than genotypes. The segmented genome makes the use of the expression genotype ambiguous i.e. it could be that the expression encompasses the whole genome or it could encompass only one or a few segments. For the influenza viruses, two segments are used in the nomenclature. All three PRVs are isolated from host with erythrocyte infections. PRV primarily infects Atlantic salmon, may cause HSMI, and is named as PRV-1. It is also associated with jaundice syndrome/anaemia in Chinook salmon (104) Another type of PRV causing erythrocytic inclusion body syndrome in coho salmon in Japan was named PRV-2 (72). Finally, PRV causes heart pathology in rainbow trout and are associated with jaundice in Chilean coho salmon (215), previously known as PRVom (134) was renamed as PRV-3. Considering the host, geographical isolation, and genome sequence, it can be hypothesized that these different PRV subtypes would have co-evolved with the host.

According to the ICTV species definition criteria for *Orthoreovirus*, the nucleotide sequence identities of homologous genome segments should be <60% equal to other orthoreoviruses, the amino acid sequence identities for more conserved proteins <65% and for more divergent outer capsid proteins <35% (21). Both PRV-1 and -3 meet these criteria. The amino acid identity was in 13-43% range compared to MRV, 14-44% to ARV and 13-38% GCRV (29). PRV is non-fusogenic and has a unique cytotoxic integral membrane protein p13 different from other orthoreovirus. Hence, PRV is classified as new species in the genus *Orthoreovirus*. Compared to each other PRV-1 vs PRV-3, the overall nucleotide identity is 80% (segment range 76.5–87.9%) and amino acid identity is 90.5% (79.1–96.7%). The L segments produce viral enzymes for transcription and replication are most conserved among reoviruses. The outer capsid protein and outer fiber protein are important for receptor binding which had 79.1% and 81.6% identity. Similarly, the non-structural factory protein, μ NS interact with host proteins have a low amino acid identity. The sequence and phylogenetic analysis confirmed that PRV-3 is more closely related to PRV-1 than to PRV-2 (Fig.14).

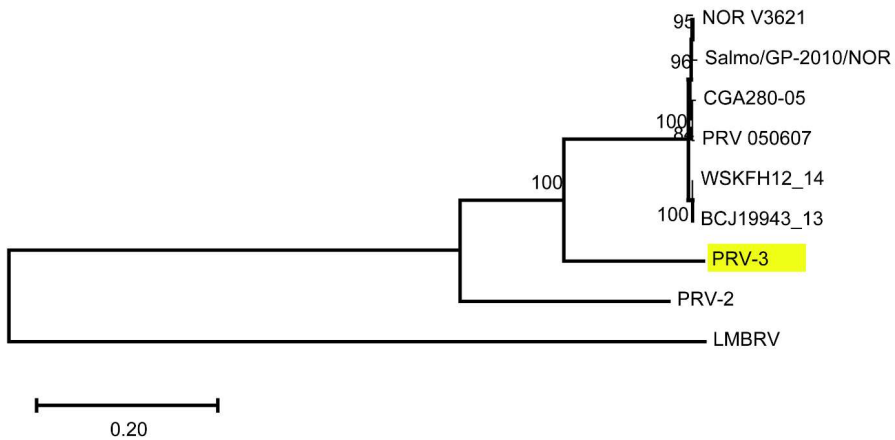


Figure. 14. Phylogenetic analysis of concatenated gene segments of selected PRV strains showing relations between different PRV subtypes.

The lowest nucleotide identity was in segment S1 between PRV1 and PRV-3 suggesting host specific selection of this segment. In the paper I, we have seen that within PRV-1 genome nucleotide and amino acid differences were very low for all the segments except M2/S1. Reassortment between different subtypes are not found in the circulating strains however, the geographical localization, common hosts and co-infection of PRV could theoretically favor reassortment of conserved and compatible segments among subtypes PRV-1 and PRV-3.

In the present study, we have reported PRV-3 in rainbow trout in Denmark, Germany, and Scotland, and brown trout in Italy. PRV-3 has been reported from rainbow trout and coho salmon in Chile. However, PRV-3 has not been reported from the North American Pacific coast where rainbow trout is an endemic native species. Hence, it raises doubt if PRV-3 has evolved with rainbow trout, or is introduced from other hosts, like brown trout or other salmonid species. The challenge studies have confirmed that Atlantic salmon is not native to PRV-3 (134). It has been shown that when a virus jumps to a new host species, the closely related species of the new host also may become susceptible to the virus (216). Following host jump, the virulence level is similar in closely related hosts and the host phylogenies reflect virulence level (184). Therefore, finding the original host for PRV-3 require further research. The S1 sequences analysis has shown that Chilean PRV is more closely related to Danish and European PRV-3 strains with 0-2 aa differences. Norwegian PRV-3 clusters separately from the other PRV-3 with 6-10 aa differences among the strains. The genetic

relatedness and few differences between them could be due to a recent introduction. Chile is the largest importer of rainbow trout eyed eggs from Denmark (217). The full genome comparison also confirmed that Danish PRV-3 is closely related to Chilean PRV-3.

The rabbit anti PRV-1 sera targeting the $\sigma 3$ (outer capsid), $\sigma 1$ (outer fiber), σNS (non-structural) and $\lambda 1$ (core shell) all cross-reacted with PRV-3 (Table 2). Differences were observed in $\mu 1$ (outer capsid protein) and μNS (non-structural factory protein) staining. Rabbit antisera raised against purified PRV-1 particles cross-reacted with PRV-3 and vice versa. The rabbit polyclonal antibodies raised against baculovirus expressed recombinant PRV-3 $\sigma 1$ (outer capsid) cross-reacted with PRV-1 in western blot, flow cytometry and immunohistochemistry (not published). The cross-reaction confirmed the antigenic relatedness of these subtypes. However, cell culture based viral neutralizing assays should be used to confirm the level cross-reactivity among the subtypes.

The $\mu 1$ protein structural analysis has shown that PRV-1 $\mu 1$ is structurally similar to the aquareovirus GCRV. The aquareovirus is another genus of reovirus that infects a wide variety of fish species. The MRV $\mu 1$ protein has a 72-96 loop where PRV-1 and GCRV have a helix. This loop stabilizes the viral capsid and influences the ISVP to ISVP* conversion. The observed differences could be due to protein adaptation to different host, environment and temperature (218). This also indicates the common origin of the genera orthoreo and aquareovirus (22).

Segments	Nucleotide Identity	Amino acid Identity	Protein in WB PRV-1	Protein in WB PRV-3
L1	80.9	95.2	-	-
L2	77.8	90.0	-	-
L3	80.3	96.7	$\lambda 1 - 141.5$	$\lambda 1 - 141.5$
M1	78.4	88.7	-	-
M2	81.2	91.5	$\mu 1$ 1 – 74.2 2 – 70.0 3 – 37.7 4 – 32.2	$\mu 1$ 1 – 70.0
M3	76.5	82.2	μNS 1 – 83.5 2 – 70.0	μNS 1 – 83.5 2 – 76.0
S1 -	80.5	79.1	$\sigma 3 - 35.6$	$\sigma 3 - 35.6$
S1-	85.6	78.2	-	-
S2	80.4	88.8	-	-
S3	87.9	94.6	$\sigma NS - 39.0$	$\sigma NS - 39.0$
S4	80.0	81.6	$\sigma 1 - 34.6$	$\sigma 1 - 34.6$

Table. 2. Nucleotide and amino acid identity between PRV-1 and 3. The band size in western blot of different proteins and its size variant observed in PRV-1 and 3.

4.4. Challenge experiment with purified PRV-3 confirm the causation in rainbow trout

We purified PRV-3 virus particles, sequenced the purified samples as well as material from the PRV-3 propagation trial in rainbow trout. Transmission electron microscopy (TEM) and sequencing confirmed the purity of the samples. Purified virus samples were used as inoculum in cohabitation challenge model as described in previous PRV studies (30). PRV-3 infected blood homogenate injected shedders and cohabitant groups were positive control groups. The viral kinetics, histopathological changes and immune responses confirmed the causative relation between PRV-3 and heart pathology in rainbow trout.

Like PRV-1, PRV-3 is not cultivable in available cell lines. Hence, purified virus particles were used in the challenge study to confirm the disease causation. The Rivers postulate for viral etiology confirmation states that the viral agent must be isolated from diseased individuals and purified viral inoculum should cause the same disease and induce specific antibodies in naïve host (219).

In TEM, PRV-3 appear as spherical viral particles of 75 nm diameter with two concentric electron-dense inner and outer core, similar to PRV-1. PRV viral proteins $\sigma 1$, $\sigma 3$ and $\mu 1$ were detected by western blot in purified virus samples. In the purified virus inoculum group, viral RNA peaked at 4 wpc in the injected group and 6 wpc in the cohabitants. The PRV viral proteins peaked at 6 wpc in both cohabitant groups. The viral RNA was cleared at 10 wpc. In PRV-1 infection in Atlantic salmon, however, the viral RNA persists in erythrocytes (Paper-II). High PRV-3 viral load was detected in infected spleen. Previous reports have reported PRV-1 positive cells in lymphoid organs, kidney, spleen suggested spread by infected erythrocytes. Highest viral load is observed in kidney and spleen in PRV-2 infection.

In the field outbreak, PRV-3 diseased fish with severe histopathological changes reported having hematocrit values of 15% or below. Histopathological observations showed lesions in red skeletal muscle, severe inflammation in heart, liver, spleen and kidney. In heart, focal to diffused inflammation, epi, endo and myocarditis, cardiomyocytes degeneration, necrosis in spongy myocardium were observed. Among the different PRV subtypes, anemia is most common in PRV-2 in EIBS whereas, PRV-1 associated anemia has been observed in Chinook salmon (104).

Despite the low viral load in the inoculum (Ct-32.67), PRV-3 induced histopathological changes in pure virus cohabitants. The changes were mild to moderate in compared to those of PRV-1. In PRV-1 severe pathological changes were observed from 6 wpc in low virus

injected groups in paper II (Fig. 15). For PRV-1 it has been shown that the viral load peak and onset of histopathology could be delayed dependent upon the viral load inoculum (30). In this study, due to low viral load in the inoculum, the histopathology appearance would have extended another two weeks, prolonging the challenge study to 12 wpc or more could have helped to identify more positive fish.

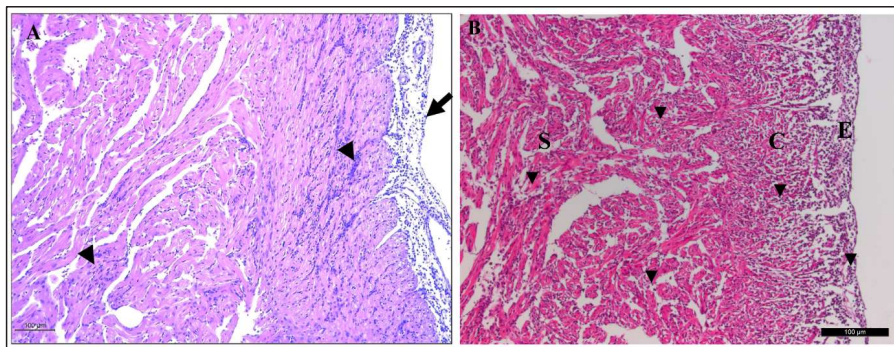


Figure. 15. Heart pathology in PRV-3 (left) (220) and PRV-1 (right) showing inflammatory changes.

PRV-3 infection induced innate antiviral response. Significant increase in interferon 1, interferon γ , mx and viperin was observed. In PRV-1, differences in eliciting immune response have been observed. PRV-1 causing HSMI in Norway induces a strong innate antiviral immune response, which coincides with viral kinetics. In contrast, low or no innate immune response observed in PRV-1 in BC, Canada. The observed differences probably link to differences in PRV-1 virus strain, however, the breed of salmon cannot be excluded. In MRV the IFN induction and myocarditis development is strain dependent (200). Similarly, in IHNV the IFN induction or inhibition is strain dependent (122). In MRV it has been shown that the IFN production is inhibited by sequestering the IRF-3 proteins into viral factory protein μ NS (221).

5. Methodological considerations

During this PhD study, I have been acquainted with many research methods, which are used routinely in a virus laboratory. This includes virus purification by ultracentrifugation, RT-qPCR, western blot, transmission electron microscopy, next-generation sequencing, basic bioinformatics tools, histology, flow cytometry, immunohistochemistry, *in situ* hybridization, cloning and recombinant protein production. Furthermore, wet lab challenge experiments have been performed in collaboration with other laboratories; NVI/NMBU wet lab, Oslo; DTU, Aqua lab, Copenhagen.

5.1 PRV detection methods

The general virus detection methods are applied for the detection of PRV. The unavailability of permissive cell lines restricts the use of cell culture-based methods for isolation, detection and serotyping of PRV. The viral nucleic acids are detected by RT-qPCR and *in situ* hybridization. The availability of PRV recombinant proteins and antibodies facilitates the use of immunohistochemistry, western blot and flow cytometry methods. The flow cytometry is an efficient tool for quantification of proteins in erythrocytes, which can be used to determine the best samples for virus purification. The RT-qPCR is the most commonly used method for screening. Blood samples are good tissue for screening and can be used for non-invasive sampling for PRV. It is important to note that viral RNA load (qPCR) and protein load do not correlate during the late stage following the peak of PRV infection. Despite high RNA load, low amounts or no protein can be detected in cardiomyocytes and erythrocytes.

5.2 Polyclonal antibody production

In the study, I have produced two polyclonal antibodies, one against whole purified PRV-3 virus and another PRV-3 $\sigma 1$ recombinant protein, produced in sf-9 cells by baculovirus. Polyclonal antibodies are quick to produce and cost effective. Polyclonal antibodies are generated by diverse B cell response against different epitopes of the protein, while monoclonal antibodies are raised against and recognize a single epitope. Polyclonal antibodies have wide application in virology. I have used the antibodies in tissue localization of virus by immunohistochemistry, to check the antigenic cross-reactivity between different virus genotypes, and quantification of the viral protein in blood by flow cytometry.

The purity of purified virus particles was checked by RT-qPCR and TEM, prior to inoculation in rabbits. Conformational epitopes are intact in purified virus particles. Despite the dialysis

of the purified virus, the samples can still contain some host proteins. This was reflected in immunohistochemical staining, where the serum raised against purified PRV-3 virus gave some background staining in non-infected blood cells, i.e. negative controls (not published) (Fig. 16). One way to overcome this obstacle is to choose affinity purification of the serum. The serum was used in western blot with proper controls to check cross-reactivity against PRV-1.

The PRV-3 $\sigma 1$ recombinant protein was produced in sf9 cells using the baculovirus system, the proteins were purified under denaturing conditions. The proteins can also be purified under native condition to better preserve epitope conformation. The antibodies showed good quality staining in immunohistochemistry, flow cytometry and western blot.

The polyclonal antiserum raised against the purified virus could recognize two or more proteins as the epitopes of the outer capsid proteins can elicit the humoral immune response. However, the antibodies against recombinant proteins are specific for a single protein but may also detect more than one protein if there is size variants of the protein.

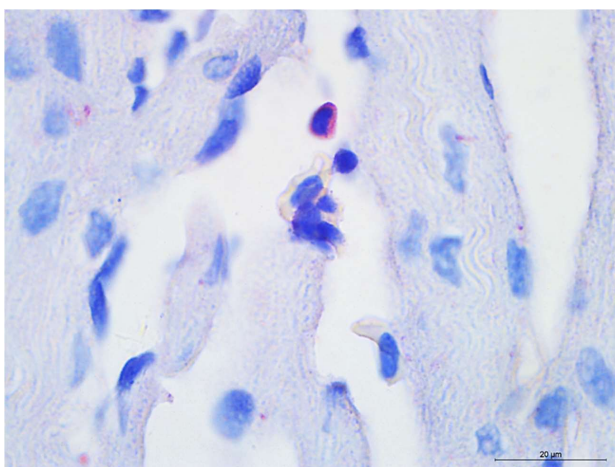


Figure. 16. Purified whole anti-PRV-3 rabbit serum stained PRV negative blood cells, proved to be not good for IHC (not published)

5.3 Western blot

Western blot method was used throughout the study to detect and quantify the viral antigens in samples. The critical steps are tissue homogenization, electrophoresis, blotting and staining. The tissue homogenization method and separation of proteins can affect the density

of bands. The NP-40 lysis buffer with complete mini protease inhibitor cocktail tablets gave good result in western blot. The protein β -actin was used as a loading control to normalize the amount of protein input. We used denaturing electrophoresis as the antibodies were made using denatured recombinant proteins for the immunization. Native gel electrophoresis could be an alternative, particularly if antibodies preferably recognize conformational epitopes. Proteins migrating on SDS-PAGE are separated mainly by molecular size.

Electrophoretic transfer to nitrocellulose or PVDF membrane can be wet, dry or semidry. I have used both the tank transfer and semidry method. The transblot turbo system is a semidry transfer system, which showed higher transfer efficiency, reproducibility and sensitivity compared to traditional transfer method. By using positive and negative controls to check the specificity of the bands and to differentiate host protein cross-reactivity (Fig. 17). Once the specificity of the antibody is checked, the samples can be diluted. In the present study, western blot method was used to check cross-reactivity of PRV-1 serum with PRV-3 proteins and to detect and quantify PRV-1/PRV-3 in blood homogenate.

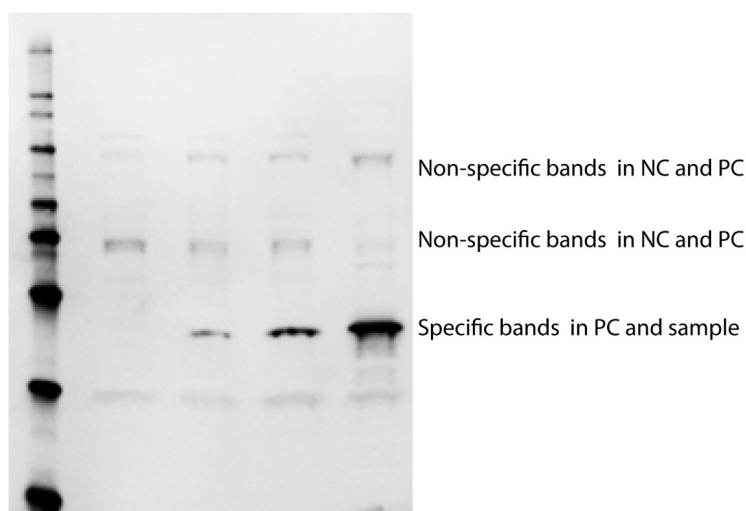


Figure. 17. Nonspecific bands are seen in negative and positive control samples.

5.4 Realtime PCR

Realtime PCR is a method to detect and quantify specific nucleic acids in a sample. In RT-qPCR, RNA is reverse transcribed to cDNA before qPCR. Realtime PCR is routinely used in

fish disease diagnostics and immune gene expression analysis. It has many advantages like high sensitivity, relatively fast, no post PCR electrophoresis, high throughput and multiplexable. The qPCR positive result does not normally differentiate between active or latent infection or if the pathogen is inactivated or viable. Other limitations are the risk of false positive/negative results and end-point variation if the number of target molecules is very low. To avoid contamination and false positive or negative results, proper controls are used during every run. In qPCR, the fluorescence level increases with the amplification cycle and depends on the initial template concentration. The Ct (cycle threshold) value is the cycle number at which the fluorescence level crosses the set threshold level (background fluorescence). Lower Ct value indicates higher template concentration in the sample. The fluorescent reported molecule in realtime PCR could be DNA binding dye (for example SYBR green) or fluorescent molecule labeled probe (for example TaqMan probe). We have used SYBR green for relative quantification of immune genes and TaqMan probe for viral quantification. In relative quantification of immune genes, the target gene expression is normalized against a stably expressed housekeeping gene and the targeted gene regulation is calculated with time-matched negative samples.

5.5 Immunohistochemistry and in situ hybridization

Histology is a valuable tool for the diagnosis of infectious disease. The cellular changes caused during virus infections are identified microscopically. However, histological changes are seldom specific. The severity of tissue damage is scored using a visual analog scale for instance from 0 to 3, based on a set of defined criteria. The slides are blinded and subjectively scored by a single person. In the formalin-fixed paraffin-embedded tissues, the architecture is well preserved, hence retrospective diagnosis is possible.

Histology combined with immunohistochemistry (IHC) or *in situ* hybridization (ISH) provides more information about viral pathogenesis. Both *in situ* and immunohistochemistry methods are useful in identifying different cells or tissues permissible for viral infection and replication. Formalin-fixed paraffin-embedded tissues were used in ISH and IHC. Proper fixation is necessary to preserve tissue morphology and RNA. Under- or over-fixation can deteriorate the tissues. We observed that over-fixed tissues drastically reduced RNA integrity and gave poor results in ISH. Incubation time with primary antibody should be standardized, overnight incubation at 4 °C gave good results in IHC. Next crucial step in IHC and ISH is endogenous peroxidase blocking and antigen retrieval. Standardization of retrieval buffer, temperature and incubation time was done to reduce the background staining. The sensitivity

and specificity of these methods have been improved a lot through recent technological advances in signal amplification methods. In immunohistochemistry, we have used the EnVision™ system for staining. The EnVision™ system uses dextran polymer technology in which many chromogenic enzymes could be attached to the polymer bone. This reduces non-specific background staining and higher sensitivity. In the RNAscope in situ hybridization method, ~20 double Z target probe pairs are designed to specifically hybridize to the target RNA sequence. The lower part of Z is complementary to target RNA and the upper Z has sequence-binding regions for preamplifiers. Preamplifiers are binding regions of amplifiers. Further, numerous fluorescence probe or chromogenic enzymes bind to the amplifiers. This enhanced the specific signals.

5.6 Electron microscopy

We chose to use TEM to check morphology and purity of purified virus samples. TEM is one of the OIE recommended presumptive diagnostic methods for many fish diseases. In TEM, the transmitted electrons pass through the samples located in EM grid. TEM has higher magnification and resolution capacity compared to SEM. Negative staining with droplet method was used to stain the virus particle. The samples were absorbed to carbon-coated copper grids and stained with uranyl acetate. Interpretation and identification of virus particles require knowledge about virus morphology. The structure of orthoreovirus and PRV-1 has been described earlier by TEM. Co-infection and presence of other virus particles could have been identified in TEM.

5.7 Next-generation sequencing

We have used NGS method for sequencing PRV dsRNA viral genome from various samples. NGS is a high-throughput, low-cost technique and it is a quick way to sequence the genome compared to other conventional methods. The primer based sequencing target the known virus sequences whereas the metagenomics sequencing allows identification of novel reassortant or recombinant or divergent virus sequences. The viral genomes can be sequenced from culture-enriched samples or directly from a clinical disease outbreak by shotgun metagenomics sequencing of random libraries (222).

Total RNA from blood pellet, plasma, heart and head kidney was used for sequencing in different NGS platforms. Another advantage in NGS is that the different samples can be multiplexed and run parallel in one lane of a sequencing flow cell. The newer and advanced NGS platforms have long read length, low run time and high output data. Total RNA of 0.1

to 4 µg is used for library preparation and the quality of RNA is very important for successful sequencing. DNA contamination can be controlled by DNAase treatment. We could not determine the RNA quality and concentration of plasma and gradient purified virus samples, due to the low total amount of RNA in such samples, nevertheless we proceeded with the samples, and the NGS sequencing yielded good coverage.

The best samples had more than 300 000 sequence reads (each 100bp length) for some segments in paired-end sequencing (2x100 PE). In such cases, the size and continuity of contigs were very high and were able to de novo map the genome without any reference genome. Some samples had poor sequence reads and coverage due to samples with low viral load. Sanger sequencing was used to close any gaps in such sequences. The size of the PRV genome is 23320 bp, however, the host RNA of the tissue sample is very high which can reduce the sensitivity. Due to the segmented PRV genome, it may be difficult to assign segments to the parental strain, if there is reassortant viruses in the sample. However, the coinfection of two related viral genotypes can be identified (223). NGS can generate chimerical sequences, point mutations, insertions and deletions (214, 224).

6. Main conclusions

Phylogenetic analysis suggests that there are virulence differences between PRV-1 strains as demonstrated by two monophyletic cluster; one associated with HSMI and one with putative low virulent isolates. This was particularly evident for M2 and S1 segments. *Piscine orthoreovirus* sequences from archived frozen samples confirmed the presence of PRV from 1988, i.e. before the first HSMI report in 1999. The phylogenetic analysis of PRV-1 strains showed indications of reassortment events. The Norwegian HSMI PRV-1 sequences formed a separate cluster distant from North American Pacific coast PRV. The nucleotide and amino acid analysis linked M2 and S1 segments with the emergence of HSMI. Reassortment or mutational accumulation events are probably linked to the evolution of these segments.

The analysis of temporal changes and localization of PRV-1 RNA and proteins revealed transient peak of viral proteins compared to viral RNA. Erythrocytes are the primary target cell for PRV. The viral load peaked in erythrocytes and plasma causing viremia, which preceded heavy infection in the heart. The hepatocytes are also infected but at a low level. High level of viral RNA and low level of PRV protein are present in persistently infected erythrocytes. PRV is cleared from cardiomyocytes, the infiltration of inflammatory cells aids in clearance and tissue regeneration.

The causative relation of PRV-3 and heart pathology in rainbow trout was confirmed by cohabitation challenge experiment with purified virus particles. The viral RNA and protein kinetics confirmed acute viral replication in blood. The PRV-3 viral RNA is cleared from erythrocytes in rainbow trout, a contrast to the persistence of PRV-1 in Atlantic salmon. PRV-3 caused epicarditis with focal to multifocal myocarditis with a significant increase in CD4 and CD8 immune genes. Increase in innate antiviral immune response was observed in infected fish. PRV-3 infection elicited antibody response was observed.

TEM examination of PRV-3 viral particles confirmed the presence of 75 nm diameter spherical viral particles with two electron-dense inner and outer capsids resembling other orthoreovirus. The near-complete genome sequencing provided insights on PRV evolution and genetic relatedness to other reoviruses. PRV-3 is more related to PRV-1 than to PRV-2. The viral protein structure and functional motifs are conserved. The antigen characterization showed similarity with PRV-1, but minor differences were observed in μ NS and μ 1C protein size variants. PRV-3 S1 sequences reported from other European countries and Chile grouped together whereas Norwegian PRV-3 formed a separate cluster.

7. Future perspectives

PRV is ubiquitously present in farmed and common in wild salmonid fish. Viruses co-evolve with their host. However, anthropogenic activities like farming pave way for the evolution of virulence. Disease development and outcome of infection depend upon virus, host, environmental factors and their interactions. Presence of various species of salmonid fish and PRV subtypes in different aquatic environment calls for systematic species-specific pathogenesis studies. A result from one particular combination of host species and PRV subtype may not fit for all species regarding virulence and pathogenesis of PRV. We can expect that farming and continuous spread of PRV will contribute to further evolution and generate new variants of PRV. However, we do not know if this will decrease or increase the virulence. Continuous monitoring, screening and good management are required.

Reassortment is common in viruses with segmented genomes and is observed in PRV. Co-infection of PRV-1 and PRV-3 in the same fish population has been reported so it is possible that reassortment can occur between subtypes if the subtype-specific packaging sequences and proteins are mutually compatible. Sequencing of PRV strains from different host species would reveal a further understanding of the PRV evolution and identify if there is reassortment between PRV-1, 2 and 3 may occur.

Based on the sequence analysis, it can be extrapolated that the HSMI PRV-1 group, as presented in the paper I, with unique M2/S1 segments would cause HSMI in wild Atlantic salmon. However, the susceptibility, pathological consequences and transmission to wild fish of PRV strains capable of inducing HSMI in farmed fish need further research. The in-depth sequence analysis signified segment S1 that encodes for $\sigma 3$ and p13, and M2 segment $\mu 1$ proteins are associated with virulence differences. The specific virulence determinants due to amino acid changes in $\sigma 3$ /p13 protein need further research. Eventually, the establishment of reverse genetics and functional studies could reveal molecular mechanisms and amino acids involved in virulence differences in PRV. With the generated PRV genome sequences, the packaging signals and potential functional internal reading frames could be identified.

There is so far no indication of virulence variants of PRV-2 or PRV-3. The volume of farming of the host of PRV-1, Atlantic salmon, is by far bigger than for the known hosts for PRV-2 and PRV-3. This indicates that there are ample possibilities for PRV-1 evolution and adaption to the farming environment, but perhaps less so for PRV-2 and PRV-3. However, if the virulence motif of PRV-1 is further deciphered, it could be guidance in PRV-2 and -3

surveillance. Rainbow trout farming is globally widespread; consequently, PRV in this species should be surveilled.

The PRV challenge experiment conducted in various host and environment has reported differing disease outcome. In future, a challenge experiment should be conducted with different PRV strains such as NOR-1998, NOR-1997, BC PRV and NOR-2012 (the latter strain was used to verify the Koch's postulate) to find out the virulence differences between virus variants in a controlled challenge model. Confirmation of virulence differences could help to develop virus-specific diagnostic methods and possibly prophylactic measures. Sequencing PRV M2/S1 segments of PRV strains prevalent in wild fish would provide more information on PRV evolution. Another potential area to focus is to understand, what is the molecular cause of the remarkable difference in the measured innate response between the HSMI inducing Norwegian strains and the low virulent BC strains? This is of pivotal importance in our understanding of the pathogenesis and outcome of the infection.

We observed a high amount of PRV viral RNA compared to proteins following an acute peak in erythrocytes. This indicates that the viral RNA is transcribed but the translation is halted. Finding out the viral proteins or molecular pathways involved in translation shutoff would be useful in developing disease preventive methods. PRV-1 is not cleared from Atlantic salmon, irrespective of the development of HSMI or not, while PRV-3 is cleared from rainbow trout and Atlantic salmon in experimental infections. What is causing PRV-1 to cause persistent infection? Can vaccination overcome persistence?

In the present study, we found a high amount of free viral particles during the peak of infection in plasma, in contrast, challenge studies performed in North-America Pacific coast did not find viruses in plasma. These differences should be studied further. The genetic and antigenic relatedness demonstrated in paper III would be useful in developing diagnostic assays, surveillance, and vaccine development. We hypothesize that PRV has co-evolved with the host, however, PRV-3 is not reported from rainbow trout in North American Pacific region where it is a native species. The absence of PRV-3 in this region highlights other salmonid species, possibly brown trout may be a natural host for PRV-3. Hence, of PRV-3 screening in other salmonid species would provide more information on host range.

Inactivated vaccines proved to be potential candidates for HSMI. However, the lack of susceptible cell lines hinders further research on PRV as well as the development of vaccines. Genome edited cell lines should be developed and checked for culturing PRV. Therefore, the cellular receptor(s) for the uptake of PRV should be mapped. Recombinant vaccine, DNA vaccine and viral-like particles (VLPs) are also promising. Complete eradication of PRV by

vaccination is probably not possible but the use of selective breeding and host resistance to heart pathology can be explored. We know that there is a virulence difference between PRV-1 variants. The possibility of using low virulence strain as a live vaccine can be tested.

8. References

1. Froese R PD. FishBase World Wide Web electronic publication. 2019 [Available from: www.fishbase.org.
2. MacCrimmon HR, Gots BL. World Distribution of Atlantic Salmon, *Salmo solar*. Journal of the Fisheries Research Board of Canada. 1979;36(4):422-57.
3. Crête-Lafrenière A, Weir LK, Bernatchez L. Framing the Salmonidae Family Phylogenetic Portrait: A More Complete Picture from Increased Taxon Sampling. PLOS ONE. 2012;7(10):e46662.
4. MacCrimmon HR. World Distribution of Rainbow Trout (*Salmo gairdneri*). Journal of the Fisheries Research Board of Canada. 1971;28(5):663-704.
5. Stanković D, Crivelli AJ, Snoj A. Rainbow Trout in Europe: Introduction, Naturalization, and Impacts. Reviews in Fisheries Science & Aquaculture. 2015;23(1):39-71.
6. Lillehaug A, Santi N, Østvik A. Practical Biosecurity in Atlantic Salmon Production. Journal of Applied Aquaculture. 2015;27(3):249-62.
7. Reyes KK. Reviewed distribution maps for *Oncorhynchus mykiss* (Rainbow trout), with modelled year 2100 native range map based on IPCC A2 emissions scenario. www.aquamaps.org, version of August 2016. 2008.
8. Ready J. Reviewed distribution maps for *Salmo salar* (Atlantic salmon), with modelled year 2100 native range map based on IPCC A2 emissions scenario. www.aquamaps.org, version of Aug. 2016. 2008.
9. Purser J. Chapter 17 Salmonids. In: Lucas JS, Southgate PC, Tucker CS, editors. Aquaculture: Farming aquatic animals and plants: Wiley-Blackwell; 2019.
10. Purser JaF, N. Salmonids. Aquaculture2013. p. 313-37.
11. FAO. FAO Yearbook. Fishery and Aquaculture Statistics 2016: Fao; 2018.
12. FAO. FAO yearbook of Fishery and Aquaculture Statistics - 2016. Rome, Italy: Food and Agriculture Organization of the United Nations; 2018. 104 p.
13. Bergheim A, Drengstig A, Ulgenes Y, Fivelstad S. Production of Atlantic salmon smolts in Europe—Current characteristics and future trends. Aquacultural Engineering. 2009;41(2):46-52.
14. Smail DA, Bain N, Bruno DW, King JA, Thompson F, Pendrey DJ, et al. Infectious pancreatic necrosis virus in Atlantic salmon, *Salmo salar* L., post-smolts in the Shetland Isles, Scotland: virus identification, histopathology, immunohistochemistry and genetic comparison with Scottish mainland isolates. J Fish Dis. 2006;29(1):31-41.
15. Hjeltmes B BJB, Haukaas A, Wlade C, S (Ed.). The Fish Health Report 2017: The Norwegian Veterinary Institute 2018; 2018.
16. Johansen LH, Jensen I, Mikkelsen H, Bjørn PA, Jansen PA, Bergh Ø. Disease interaction and pathogens exchange between wild and farmed fish populations with special reference to Norway. Aquaculture. 2011;315(3):167-86.
17. Jones SRM, Bruno DW, Madsen L, Peeler EJ. Disease management mitigates risk of pathogen transmission from maricultured salmonids. Aquaculture Environment Interactions. 2015;6(2):119-34.
18. Sabin AB. Reoviruses. A new group of respiratory and enteric viruses formerly classified as ECHO type 10 is described. 1959;130(3386):1387-9.

19. Gomatos PJ, Tamm I. ANIMAL AND PLANT VIRUSES WITH DOUBLE-HELICAL RNA. *Proceedings of the National Academy of Sciences of the United States of America*. 1963;50(5):878-85.
20. Joklik WK. *The reoviridae*: Springer Science & Business Media; 1983.
21. Attoui H, Mertens, P.P.C., Becnel, J., Belaganahalli, S., Bergoin, M., Brussaard, C.P., Chappell, J.D., Ciarlet, M., del Vas, M., Dermody, T.S., Dormitzer, P.R., Duncan, R., Fang, Q., Graham, R., Guglielmi, K.M., Harding, R.M., Hillman, B., Makkay, A., Marzachi, C., Matthijnsens, J., Milne, R.G., Mohd Jaafar, F., Mori, H., Noordeloos, A.A., Omura, T., Patton, J.T., Rao, S., Maan, M., Stoltz, D., Suzuki, N., Upadhyaya, N.M., Wei, C., Zhou, H., Family - Reoviridae. *Virus Taxonomy: Ninth Report of the International Committee on Taxonomy of Viruses*. San Diego: Elsevier; 2012. p. 541-637.
22. Attoui H, Fang Q, Jaafar FM, Cantaloube J-F, Biagini P, de Micco P, et al. Common evolutionary origin of aquarecoviruses and orthoreoviruses revealed by genome characterization of Golden shiner reovirus, Grass carp reovirus, Striped bass reovirus and golden ide reovirus (genus Aquareovirus, family Reoviridae). 2002;83(8):1941-51.
23. Geoghegan JL, Duchêne S, Holmes EC. Comparative analysis estimates the relative frequencies of co-divergence and cross-species transmission within viral families. *PLOS Pathogens*. 2017;13(2):e1006215.
24. Kim J, Tao Y, Reinisch KM, Harrison SC, Nibert ML. Orthoreovirus and Aquareovirus core proteins: conserved enzymatic surfaces, but not protein-protein interfaces. *Virus Research*. 2004;101(1):15-28.
25. Nibert ML, Duncan R. Bioinformatics of Recent Aqua- and Orthoreovirus Isolates from Fish: Evolutionary Gain or Loss of FAST and Fiber Proteins and Taxonomic Implications. *PLOS ONE*. 2013;8(7):e68607.
26. Palacios G, Lovoll M, Tengs T, Hornig M, Hutchison S, Hui J, et al. Heart and skeletal muscle inflammation of farmed salmon is associated with infection with a novel reovirus. *PLoS One*. 2010;5(7):e11487.
27. Key T, Read J, Nibert ML, Duncan R. Piscine reovirus encodes a cytotoxic, non-fusogenic, integral membrane protein and previously unrecognized virion outer-capsid proteins. *Journal of General Virology*. 2013;94(5):1039-50.
28. Sibley SD, Finley MA, Baker BB, Puzach C, Armien AG, Giehlbrock D, et al. Novel reovirus associated with epidemic mortality in wild largemouth bass (*Micropterus salmoides*). *Journal of General Virology*. 2016;97(10):2482-7.
29. Markussen T, Dahle MK, Tengs T, Lovoll M, Finstad ØW, Wiik-Nielsen CR, et al. Sequence Analysis of the Genome of Piscine Orthoreovirus (PRV) Associated with Heart and Skeletal Muscle Inflammation (HSMI) in Atlantic Salmon (*Salmo salar*). *PLOS ONE*. 2013;8(7):e70075.
30. Wessel Ø, Braaen S, Alarcon M, Haatveit H, Roos N, Markussen T, et al. Infection with purified Piscine orthoreovirus demonstrates a causal relationship with heart and skeletal muscle inflammation in Atlantic salmon. *PLOS ONE*. 2017;12(8):e0183781.
31. Joklik WK. Structure and function of the reovirus genome. *Microbiol Rev*. 1981;45(4):483-501.
32. Urbano P, Urbano FG. The Reoviridae family. *Comparative Immunology, Microbiology and Infectious Diseases*. 1994;17(3):151-61.
33. Liemann S, Chandran K, Baker TS, Nibert ML, Harrison SC. Structure of the reovirus membrane-penetration protein, Mu1, in a complex with its protector protein, Sigma3. *Cell*. 2002;108(2):283-95.
34. Reinisch KM, Nibert ML, Harrison SC. Structure of the reovirus core at 3.6 Å resolution. *Nature*. 2000;404(6781):960-7.

35. Gillies S, Bullivant S, Bellamy AR. Viral RNA polymerases: electron microscopy of reovirus reaction cores. *Science*. 1971;174(4010):694-6.
36. Dryden KA, Wang G, Yeager M, Nibert ML, Coombs KM, Furlong DB, et al. Early steps in reovirus infection are associated with dramatic changes in supramolecular structure and protein conformation: analysis of virions and subviral particles by cryoelectron microscopy and image reconstruction. *The Journal of cell biology*. 1993;122(5):1023-41.
37. Haatveit HM, Nyman IB, Markussen T, Wessel O, Dahle MK, Rimstad E. The non-structural protein muNS of piscine orthoreovirus (PRV) forms viral factory-like structures. *Vet Res*. 2016;47:5.
38. Parker JS, Broering TJ, Kim J, Higgins DE, Nibert ML. Reovirus core protein mu2 determines the filamentous morphology of viral inclusion bodies by interacting with and stabilizing microtubules. *J Virol*. 2002;76(9):4483-96.
39. Wessel O, Nyman IB, Markussen T, Dahle MK, Rimstad E. Piscine orthoreovirus (PRV) σ 3 protein binds dsRNA. *Virus Res*. 2015;198:22-9.
40. Becker MM, Peters TR, Dermody TS. Reovirus sigma NS and mu NS proteins form cytoplasmic inclusion structures in the absence of viral infection. *J Virol*. 2003;77(10):5948-63.
41. Weiner HL, Fields BN. Neutralization of reovirus: the gene responsible for the neutralization antigen. *The Journal of experimental medicine*. 1977;146(5):1305-10.
42. Barton ES, Forrest JC, Connolly JL, Chappell JD, Liu Y, Schnell FJ, et al. Junction adhesion molecule is a receptor for reovirus. *Cell*. 2001;104(3):441-51.
43. Chappell JD, Gunn VL, Wetzel JD, Baer GS, Dermody TS. Mutations in type 3 reovirus that determine binding to sialic acid are contained in the fibrous tail domain of viral attachment protein sigma1. *J Virol*. 1997;71(3):1834-41.
44. Silverstein SC, Dales S. The penetration of reovirus RNA and initiation of its genetic function in L-strain fibroblasts. *The Journal of cell biology*. 1968;36(1):197-230.
45. Maginnis MS, Mainou BA, Derdowski A, Johnson EM, Zent R, Dermody TS. NPXY motifs in the beta1 integrin cytoplasmic tail are required for functional reovirus entry. *J Virol*. 2008;82(7):3181-91.
46. Nibert ML, Furlong DB, Fields BN. Mechanisms of viral pathogenesis. Distinct forms of reoviruses and their roles during replication in cells and host. *J Clin Invest*. 1991;88(3):727-34.
47. Sahin E, Egger ME, McMasters KM, Zhou H, SJJJoCT. Development of oncolytic reovirus for cancer therapy. 2013;4(06):1100.
48. Furuichi Y, Morgan M, Muthukrishnan S, Shatkin AJ. Reovirus messenger RNA contains a methylated, blocked 5'-terminal structure: m-7G(5')ppp(5')G-MpCp. 1975;72(1):362-6.
49. Stoltzfus CM, Shatkin AJ, Banerjee AKJJoBC. Absence of polyadenylic acid from reovirus messenger ribonucleic acid. 1973;248(23):7993-8.
50. Acs G, Klett H, Schonberg M, Christman J, Levin DH, Silverstein SCJJoV. Mechanism of reovirus double-stranded ribonucleic acid synthesis in vivo and in vitro. 1971;8(5):684-9.
51. Hauge H, Dahle M, Moldal T, Thoen E, Gjevre AG, Weli S, et al. Piscine orthoreovirus can infect and shed through the intestine in experimentally challenged Atlantic salmon (*Salmo salar* L.). *Vet Res*. 2016;47(1):57.
52. Garseth ÅH, Ekrem T, Biering E. Phylogenetic evidence of long distance dispersal and transmission of piscine reovirus (PRV) between farmed and wild Atlantic salmon. *PLOS ONE*. 2013;8(12):e82202.

53. Garseth AH, Biering E, Aunsmo A. Associations between piscine reovirus infection and life history traits in wild-caught Atlantic salmon *Salmo salar* L. in Norway. *Prev Vet Med.* 2013;112(1-2):138-46.
54. Garseth AH, Fritsvold C, Opheim M, Skjerve E, Biering E. Piscine reovirus (PRV) in wild Atlantic salmon, *Salmo salar* L., and sea-trout, *Salmo trutta* L., in Norway. *J Fish Dis.* 2013;36(5):483-93.
55. Glover KA, Sorvik AG, Karlsbakk E, Zhang Z, Skaala O. Molecular genetic analysis of stomach contents reveals wild Atlantic cod feeding on piscine reovirus (PRV) infected Atlantic salmon originating from a commercial fish farm. *PLoS One.* 2013;8(4):e60924.
56. Wiik-Nielsen CR, Lovoll M, Sandlund N, Faller R, Wiik-Nielsen J, Bang Jensen B. First detection of piscine reovirus (PRV) in marine fish species. *Dis Aquat Organ.* 2012;97(3):255-8.
57. Purcell MK, Powers RL, Evered J, Kerwin J, Meyers TR, Stewart B, et al. Molecular testing of adult Pacific salmon and trout (*Oncorhynchus* spp.) for several RNA viruses demonstrates widespread distribution of piscine orthoreovirus in Alaska and Washington. *Journal of Fish Diseases.* 2018;41(2):347-55.
58. Kibenge MJ, Iwamoto T, Wang Y, Morton A, Godoy MG, Kibenge FS. Whole-genome analysis of piscine reovirus (PRV) shows PRV represents a new genus in family Reoviridae and its genome segment S1 sequences group it into two separate sub-genotypes. *Virology Journal.* 2013;10(1):230.
59. Marty GD, Morrison DB, Bidulka J, Joseph T, Siah A. Piscine reovirus in wild and farmed salmonids in British Columbia, Canada: 1974-2013. *J Fish Dis.* 2015;38(8):713-28.
60. Weiner HL, Powers ML, Fields BN. Absolute Linkage of Virulence and Central Nervous System Cell Tropism of Reoviruses to Viral Hemagglutinin. *The Journal of Infectious Diseases.* 1980;141(5):609-16.
61. Sherry B, Schoen FJ, Wenske E, Fields BN. Derivation and characterization of an efficiently myocarditic reovirus variant. *J Virol.* 1989;63(11):4840-9.
62. Irvin SC, Zurney J, Ooms LS, Chappell JD, Dermody TS, Sherry B. A Single-Amino-Acid Polymorphism in Reovirus Protein $\mu 2$ Determines Repression of Interferon Signaling and Modulates Myocarditis. *Journal of Virology.* 2012;86(4):2302-11.
63. Van Der Heide L. Viral arthritis/tenosynovitis: a review. *Avian pathology : journal of the WVPA.* 1977;6(4):271-84.
64. Clauss TM, Dove ADM, Arnold JE. Hematologic Disorders of Fish. *Veterinary Clinics of North America: Exotic Animal Practice.* 2008;11(3):445-62.
65. Kulkeaw K, Sugiyama D. Zebrafish erythropoiesis and the utility of fish as models of anemia. *Stem Cell Res Ther.* 2012;3(6):55-.
66. Arias CF, Arias CF. How do red blood cells know when to die? 2017;4(4):160850.
67. Sandnes K, Lie Ø, Waagbø R. Normal ranges of some blood chemistry parameters in adult farmed Atlantic salmon, *Salmo salar*. 1988;32(1):129-36.
68. Witeska M. Erythrocytes in teleost fishes: a review. *Zoology and Ecology.* 2013;23(4):275-81.
69. Evelyn TPT, Traxler GS. Viral Erythrocytic Necrosis: Natural Occurrence in Pacific Salmon and Experimental Transmission. *Journal of the Fisheries Research Board of Canada.* 1978;35(6):903-7.
70. Haney DC, Hursh DA, Mix MC, Winton JR. Physiological and Hematological Changes in Chum Salmon Artificially Infected with Erythrocytic Necrosis Virus. *Journal of aquatic animal health.* 1992;4(1):48-57.

71. Emmenegger EJ, Glenn JA, Winton JR, Batts WN, Gregg JL, Hershberger PK. Molecular identification of erythrocytic necrosis virus (ENV) from the blood of Pacific herring (*Clupea pallasii*). *Veterinary Microbiology*. 2014;174(1):16-26.
72. Takano T, Nawata A, Sakai T, Matsuyama T, Ito T, Kurita J, et al. Full-genome sequencing and confirmation of the causative agent of erythrocytic inclusion body syndrome in coho salmon identifies a new type of piscine orthoreovirus. *PLoS One*. 2016;11(10):e0165424.
73. Finstad OW, Dahle MK, Lindholm TH, Nyman IB, Lovoll M, Wallace C, et al. Piscine orthoreovirus (PRV) infects Atlantic salmon erythrocytes. *Vet Res*. 2014;45:35.
74. Wessel O, Olsen CM, Rimstad E, Dahle MK. Piscine orthoreovirus (PRV) replicates in Atlantic salmon (*Salmo salar* L.) erythrocytes *ex vivo*. *Vet Res*. 2015;46:26.
75. Roberts RJ. *Fish pathology*: John Wiley & Sons; 2012.
76. Matrone G, Tucker CS, Denvir MA. Cardiomyocyte proliferation in zebrafish and mammals: lessons for human disease. *Cell Mol Life Sci*. 2017;74(8):1367-78.
77. Poppe T, Børnø G, Iversen L, Myklebust E. Idiopathic cardiac pathology in seawater - farmed rainbow trout, *Oncorhynchus mykiss* (Walbaum). *Journal of fish diseases*. 2009;32(9):807-10.
78. Poppe T, Taksdal T, Bergtun P. Suspected myocardial necrosis in farmed Atlantic salmon, *Salmo salar* L.: a field case. *Journal of fish diseases*. 2007;30(10):615-20.
79. Farrell AP. Coronary arteriosclerosis in salmon: growing old or growing fast? *Comparative biochemistry and physiology Part A, Molecular & integrative physiology*. 2002;132(4):723-35.
80. Trygve TP, Renate J, Gjermund G, Brit TÅr. Heart morphology in wild and farmed Atlantic salmon *Salmo salar* and rainbow trout *Oncorhynchus mykiss*. *Diseases of Aquatic Organisms*. 2003;57(1-2):103-8.
81. Lovoll M, Wiik-Nielsen J, Grove S, Wiik-Nielsen CR, Kristoffersen AB, Faller R, et al. A novel totivirus and piscine reovirus (PRV) in Atlantic salmon (*Salmo salar*) with cardiomyopathy syndrome (CMS). *Virology*. 2010;7:309.
82. Wiik-Nielsen CR, Ski PM, Aunsmo A, Lovoll M. Prevalence of viral RNA from piscine reovirus and piscine myocarditis virus in Atlantic salmon, *Salmo salar* L., broodfish and progeny. *J Fish Dis*. 2012;35(2):169-71.
83. Lund M, Krudtaa Dahle M, Timmerhaus G, Alarcon M, Powell M, Aspehaug V, et al. Hypoxia tolerance and responses to hypoxic stress during heart and skeletal muscle inflammation in Atlantic salmon (*Salmo salar*). *PLOS ONE*. 2017;12(7):e0181109.
84. Bruno DW, Noguera PA, Poppe TT. *A colour atlas of salmonid diseases*: Springer Science & Business Media; 2013.
85. Gamperl AK, Farrell AJJEB. Cardiac plasticity in fishes: environmental influences and intraspecific differences. 2004;207(15):2539-50.
86. Biacchesi S, Jouvion G, Mérour E, Boukadiri A, Desdoutis M, Ozden S, et al. Rainbow trout (*Oncorhynchus mykiss*) muscle satellite cells are targets of salmonid alphavirus infection. *Veterinary research*. 2016;47:9-.
87. Taksdal T, Olsen AB, Bjerkås I, Hjortaa MJ, Dannevig BH, Graham DA, et al. Pancreas disease in farmed Atlantic salmon, *Salmo salar* L., and rainbow trout, *Oncorhynchus mykiss* (Walbaum), in Norway. 2007;30(9):545-58.
88. Kongtorp RT, Taksdal T, Lyngøy A. Pathology of heart and skeletal muscle inflammation (HSMI) in farmed Atlantic salmon *Salmo salar*. *Diseases of Aquatic Organisms*. 2004;59(3):217-24.

89. Hodgkinson JW, Grayfer L, Belosevic M. Biology of Bony Fish Macrophages. *Biology*. 2015;4(4):881-906.
90. Wiegertjes GF, Wentzel AS, Spaink HP, Elks PM, Fink IR. Polarization of immune responses in fish: The 'macrophages first' point of view. *Molecular Immunology*. 2016;69:146-56.
91. Grayfer L, Kerimoglu B, Yaparla A, Hodgkinson JW, Xie J, Belosevic M. Mechanisms of Fish Macrophage Antimicrobial Immunity. *Frontiers in Immunology*. 2018;9(1105).
92. Agius C, Roberts RJ. Melano-macrophage centres and their role in fish pathology. 2003;26(9):499-509.
93. Steinel NC, Bolnick DI. Melanomacrophage Centers As a Histological Indicator of Immune Function in Fish and Other Poikilotherms. *Frontiers in immunology*. 2017;8:827-.
94. Nikitina E, Larionova I, Choinzonov E, Kzhyshkowska J. Monocytes and Macrophages as Viral Targets and Reservoirs. *International journal of molecular sciences*. 2018;19(9):2821.
95. Rivas C, Bandin I, Noya M, Dopazo C, Cepeda C, Barja JJDoao. Effect of the turbot aquareovirus on fish macrophages using an in vitro model. 1996;25(3):209-16.
96. Bjorgen H, Wessel O, Fjellidal PG, Hansen T, Sveier H, Saebø HR, et al. Piscine orthoreovirus (PRV) in red and melanised foci in white muscle of Atlantic salmon (*Salmo salar*). *Vet Res*. 2015;46:89.
97. Joseph T, Kibenge MT, Kibenge FS. Antibody-mediated growth of infectious salmon anaemia virus in macrophage-like fish cell lines. *J Gen Virol*. 2003;84(Pt 7):1701-10.
98. Johansen L-H, Sommer A-I. In vitro studies of infectious pancreatic necrosis virus infections in leucocytes isolated from Atlantic salmon (*Salmo salar* L.). *Aquaculture*. 1995;132(1):91-5.
99. Castro R, Abós B, Pignatelli J, von Gersdorff Jørgensen L, González Granja A, Buchmann K, et al. Early Immune Responses in Rainbow Trout Liver upon Viral Hemorrhagic Septicemia Virus (VHSV) Infection. *PLOS ONE*. 2014;9(10):e111084.
100. Ellis AE, Cavaco A, Petric A, Lockhart K, Snow M, Collet B. Histology, immunocytochemistry and qRT-PCR analysis of Atlantic salmon, *Salmo salar* L., post-smolts following infection with infectious pancreatic necrosis virus (IPNV). 2010;33(10):803-18.
101. Brudeseth BE, Raynard RS, King JA, Evensen Ø. Sequential Pathology after Experimental Infection with Marine Viral Hemorrhagic Septicemia Virus Isolates of Low and High Virulence in Turbot (*Scophthalmus maximus* L.). 2005;42(1):9-18.
102. Simko E, Brown LL, MacKinnon AM, Byrne PJ, Ostland VE, Ferguson HW. Experimental infection of Atlantic salmon, *Salmo salar* L., with infectious salmon anaemia virus: a histopathological study. 2000;23(1):27-32.
103. Cusack RR, Groman DB, MacKinnon AM, Kibenge FS, Wadowska D, Brown N. Pathology associated with an aquareovirus in captive juvenile Atlantic halibut *Hippoglossus hippoglossus* and an experimental treatment strategy for a concurrent bacterial infection. *Dis Aquat Organ*. 2001;44(1):7-16.
104. Di Cicco E, Ferguson HW, Kaukinen KH, Schulze AD, Li S, Tabata A, et al. The same strain of Piscine orthoreovirus (PRV-1) is involved in the development of different, but related, diseases in Atlantic and Pacific Salmon in British Columbia. *FACETS*. 2018;3(1):599-641.
105. Watanabe K, Karlens M, Devold M, Isdal E, Litlabø A, Nylund A. Virus-like particles associated with heart and skeletal muscle inflammation (HSMI). *Diseases of aquatic organisms*. 2006;70(3):183-92.

106. Kongtorp RT, Kjerstad A, Taksdal T, Guttvik A, Falk K. Heart and skeletal muscle inflammation in Atlantic salmon, *Salmo salar* L: a new infectious disease. *J Fish Dis.* 2004;27(6):351-8.
107. Kongtorp R, Taksdal T. Studies with experimental transmission of heart and skeletal muscle inflammation in Atlantic salmon, *Salmo salar* L. *Journal of fish diseases.* 2009;32(3):253-62.
108. Lovoll M, Alarcon M, Bang Jensen B, Taksdal T, Kristoffersen AB, Tengs T. Quantification of piscine reovirus (PRV) at different stages of Atlantic salmon *Salmo salar* production. *Dis Aquat Organ.* 2012;99(1):7-12.
109. Kongtorp R, Halse M, Taksdal T, Falk K. Longitudinal study of a natural outbreak of heart and skeletal muscle inflammation in Atlantic salmon, *Salmo salar* L. *Journal of Fish Diseases.* 2006;29(4):233-44.
110. Ferguson H, Kongtorp R, Taksdal T, Graham D, Falk K. An outbreak of disease resembling heart and skeletal muscle inflammation (HSMI) disease diagnosed on a British Columbia salmon farm through myocardial regeneration. *Journal of fish diseases.* 2005;28(2):119-23.
111. Di Cicco E, Ferguson HW, Schulze AD, Kaukinen KH, Li S, Vanderstichel R, et al. Heart and skeletal muscle inflammation (HSMI) disease diagnosed on a British Columbia salmon farm through a longitudinal farm study. *PLOS ONE.* 2017;12(2):e0171471.
112. Garver KA, Johnson SC, Polinski MP, Bradshaw JC, Marty GD, Snyman HN, et al. Piscine orthoreovirus from western north America is transmissible to Atlantic salmon and sockeye salmon but fails to cause heart and skeletal muscle inflammation. *PLoS One.* 2016;11(1):e0146229.
113. Polinski MP, Marty GD, Snyman HN, Garver KA. Piscine orthoreovirus demonstrates high infectivity but low virulence in Atlantic salmon of Pacific Canada. *Scientific Reports.* 2019;9(1):3297.
114. Godoy MG, Kibenge MJT, Wang Y, Suarez R, Leiva C, Vallejos F, et al. First description of clinical presentation of piscine orthoreovirus (PRV) infections in salmonid aquaculture in Chile and identification of a second genotype (Genotype II) of PRV. *Virology Journal.* 2016;13(1):98.
115. Dahle MK, Wessel O, Timmerhaus G, Nyman IB, Jorgensen SM, Rimstad E, et al. Transcriptome analyses of Atlantic salmon (*Salmo salar* L.) erythrocytes infected with piscine orthoreovirus (PRV). *Fish Shellfish Immunol.* 2015;45(2):780-90.
116. Nombela I, Ortega-Villaizan MdM. Nucleated red blood cells: Immune cell mediators of the antiviral response. *PLOS Pathogens.* 2018;14(4):e1006910.
117. Robertsen B. The role of type I interferons in innate and adaptive immunity against viruses in Atlantic salmon. *Developmental & Comparative Immunology.* 2018;80:41-52.
118. Smith JA, Schmechel SC, Williams BR, Silverman RH, Schiff LA. Involvement of the interferon-regulated antiviral proteins PKR and RNase L in reovirus-induced shutoff of cellular translation. *J Virol.* 2005;79(4):2240-50.
119. Sharpe AH, Fields BN. Reovirus inhibition of cellular RNA and protein synthesis: Role of the S4 gene. *Virology.* 1982;122(2):381-91.
120. Haatveit H, Wessel Ø, Markussen T, Lund M, Thiede B, Nyman I, et al. Viral protein kinetics of piscine orthoreovirus infection in Atlantic salmon blood cells. *Viruses.* 2017;9(3):49.
121. Mikalsen AB, Haugland O, Rode M, Solbakk IT, Evensen O. Atlantic salmon reovirus infection causes a CD8 T cell myocarditis in Atlantic salmon (*Salmo salar* L.). *PLoS One.* 2012;7(6):e37269.
122. Collet B. Innate immune responses of salmonid fish to viral infections. *Developmental & Comparative Immunology.* 2014;43(2):160-73.

123. Yousaf MN, Koppang EO, Skjold K, Kollner B, Hordvik I, Zou J, et al. Cardiac pathological changes of Atlantic salmon (*Salmo salar* L.) affected with heart and skeletal muscle inflammation (HSMI). *Fish Shellfish Immunol.* 2012;33(2):305-15.
124. Nakanishi T, Shibasaki Y, Matsuura Y. T Cells in Fish. *Biology.* 2015;4(4):640.
125. Trapani JA, Smyth MJ. Functional significance of the perforin/granzyme cell death pathway. *Nature reviews Immunology.* 2002;2(10):735-47.
126. Aldrin M, Storvik B, Frigessi A, Viljugrein H, Jansen PA. A stochastic model for the assessment of the transmission pathways of heart and skeleton muscle inflammation, pancreas disease and infectious salmon anaemia in marine fish farms in Norway. *Prev Vet Med.* 2010;93(1):51-61.
127. Kristoffersen AB, Bang Jensen B, Jansen PA. Risk mapping of heart and skeletal muscle inflammation in salmon farming. *Prev Vet Med.* 2013;109(1-2):136-43.
128. Martinez-Rubio L, Morais S, Evensen Ø, Wadsworth S, Ruohonen K, Vecino JL, et al. Functional feeds reduce heart inflammation and pathology in Atlantic salmon (*Salmo salar* L.) following experimental challenge with Atlantic salmon reovirus (ASRV). *PLoS One.* 2012;7(11):e40266.
129. Wessel Ø, Haugland Ø, Rode M, Fredriksen BN, Dahle MK, Rimstad E. Inactivated Piscine orthoreovirus vaccine protects against heart and skeletal muscle inflammation in Atlantic salmon. 2018;41(9):1411-9.
130. Haatveit HM, Hodneland K, Braeen S, Hansen EF, Nyman IB, Dahle MK, et al. DNA vaccine expressing the non-structural proteins of Piscine orthoreovirus delay the kinetics of PRV infection and induces moderate protection against heart -and skeletal muscle inflammation in Atlantic salmon (*Salmo salar*). *Vaccine.* 2018;36(50):7599-608.
131. Janssen K, Chavanne H, Berentsen P, Komen H. Impact of selective breeding on European aquaculture. *Aquaculture.* 2017;472:8-16.
132. Robertsen B. Can we get the upper hand on viral diseases in aquaculture of Atlantic salmon? 2011;42(s1):125-31.
133. Olsen AB, Hjortaa M, Tengs T, Hellberg H, Johansen R. First Description of a New Disease in Rainbow Trout (*Oncorhynchus mykiss* (Walbaum)) Similar to Heart and Skeletal Muscle Inflammation (HSMI) and Detection of a Gene Sequence Related to Piscine Orthoreovirus (PRV). *PLOS ONE.* 2015;10(7):e0131638.
134. Hauge H, Vendramin N, Taksdal T, Olsen AB, Wessel Ø, Mikkelsen SS, et al. Infection experiments with novel Piscine orthoreovirus from rainbow trout (*Oncorhynchus mykiss*) in salmonids. *PLOS ONE.* 2017;12(7):e0180293.
135. Leek SL. Viral Erythrocytic Inclusion Body Syndrome (EIBS) Occurring in Juvenile Spring Chinook Salmon (*Oncorhynchus tshawytscha*) Reared in Freshwater. *Canadian Journal of Fisheries and Aquatic Sciences.* 1987;44(3):685-8.
136. Piacentini SC, Rohovec JS, Fryer JL. Epizootiology of Erythrocytic Inclusion Body Syndrome. *Journal of aquatic animal health.* 1989;1(3):173-9.
137. Rodger HD. Erythrocytic inclusion body syndrome virus in wild Atlantic salmon, *Salmo salar* L. *J Fish Dis.* 2007;30(7):411-8.
138. Graham DA, Curran W, Rowley HM, Cox DI, Cockerill D, Campbell S, et al. Observation of virus particles in the spleen, kidney, gills and erythrocytes of Atlantic salmon, *Salmo salar* L., during a disease outbreak with high mortality. 2002;25(4):227-34.
139. Garver KA, Marty GD, Cockburn SN, Richard J, Hawley LM, Muller A, et al. Piscine reovirus, but not Jaundice Syndrome, was transmissible to Chinook Salmon, *Oncorhynchus tshawytscha*

- (Walbaum), Sockeye Salmon, *Oncorhynchus nerka* (Walbaum), and Atlantic Salmon, *Salmo salar* L. *J Fish Dis.* 2016;39(2):117-28.
140. Schwaiger J FH. Pathologie und Immunstatus betroffener Bachforellenpopulationen. Schriftenreihe des Landesfischereiverbandes eV 2003 [06 Aug 2019]. Available from: <http://argefa.org/publikationen/heft-9-bachforellensterben>.
 141. Fux R, Arndt D, Langenmayer MC, Schwaiger J, Ferling H, Fischer N, et al. Piscine Orthoreovirus 3 Is Not the Causative Pathogen of Proliferative Darkening Syndrome (PDS) of Brown Trout (*Salmo trutta fario*). *Viruses.* 2019;11(2):112.
 142. Shi M, Lin X-D, Chen X, Tian J-H, Chen L-J, Li K, et al. The evolutionary history of vertebrate RNA viruses. *Nature.* 2018;556(7700):197-202.
 143. Shi M, Lin X-D, Tian J-H, Chen L-J, Chen X, Li C-X, et al. Redefining the invertebrate RNA virosphere. *Nature.* 2016;540:539.
 144. Lafferty KD, Harvell CD, Conrad JM, Friedman CS, Kent ML, Kuris AM, et al. Infectious diseases affect marine fisheries and aquaculture economics. *Annual review of marine science.* 2015;7:471-96.
 145. Ford JS, Myers RA. A Global Assessment of Salmon Aquaculture Impacts on Wild Salmonids. *PLOS Biology.* 2008;6(2):e33.
 146. Garver KA, Traxler GS, Hawley LM, Richard J, Ross JP, Lovy J. Molecular epidemiology of viral haemorrhagic septicaemia virus (VHSV) in British Columbia, Canada, reveals transmission from wild to farmed fish. *Dis Aquat Organ.* 2013;104(2):93-104.
 147. Øivind B. The dual myths of the healthy wild fish and the unhealthy farmed fish. *Diseases of Aquatic Organisms.* 2007;75(2):159-64.
 148. Bergstrom CT, McElhany P, Real LA. Transmission bottlenecks as determinants of virulence in rapidly evolving pathogens. 1999;96(9):5095-100.
 149. Kennedy DA, Kurath G, Brito IL, Purcell MK, Read AF, Winton JR, et al. Potential drivers of virulence evolution in aquaculture. *Evolutionary applications.* 2016;9(2):344-54.
 150. Menerat A, Nilsen F, Ebert D, Skorping AJEB. Intensive Farming: Evolutionary Implications for Parasites and Pathogens. 2010;37(2):59-67.
 151. Krkošek M. Population biology of infectious diseases shared by wild and farmed fish. *Canadian Journal of Fisheries and Aquatic Sciences.* 2017;74(4):620-8.
 152. Liu L, Cheng J, Fu Y, Liu H, Jiang D, Xie J. New insights into reovirus evolution: implications from a newly characterized mycoreovirus. *J Gen Virol.* 2017.
 153. Vijaykrishna D, Mukerji R, Smith GJD. RNA Virus Reassortment: An Evolutionary Mechanism for Host Jumps and Immune Evasion. *PLOS Pathogens.* 2015;11(7):e1004902.
 154. Stern A, Yeh MT, Zinger T, Smith M, Wright C, Ling G, et al. The Evolutionary Pathway to Virulence of an RNA Virus. *Cell.* 2017;169(1):35-46.e19.
 155. Hanada K, Suzuki Y, Gojobori T. A Large Variation in the Rates of Synonymous Substitution for RNA Viruses and Its Relationship to a Diversity of Viral Infection and Transmission Modes. *Molecular biology and evolution.* 2004;21(6):1074-80.
 156. Sanjuán R, Domingo-Calap P. Mechanisms of viral mutation. *Cell Mol Life Sci.* 2016;73(23):4433-48.
 157. Jenkins GM, Rambaut A, Pybus OG, Holmes ECJJoME. Rates of Molecular Evolution in RNA Viruses: A Quantitative Phylogenetic Analysis. 2002;54(2):156-65.

158. Attoui H, Mohd Jaafar F, Biagini P, Cantaloube JF, de Micco P, Murphy FA, et al. Genus Coltivirus (family Reoviridae): genomic and morphologic characterization of Old World and New World viruses. *Arch Virol.* 2002;147(3):533-61.
159. Walker PJ, Winton JR. Emerging viral diseases of fish and shrimp. *Veterinary research.* 2010;41(6):51-.
160. Duffy S. Why are RNA virus mutation rates so damn high? *PLOS Biology.* 2018;16(8):e3000003.
161. Lowen AC. It's in the mix: Reassortment of segmented viral genomes. *PLOS Pathogens.* 2018;14(9):e1007200.
162. Varsani A, Lefeuvre P, Roumagnac P, Martin D. Notes on recombination and reassortment in multipartite/segmented viruses. *Current Opinion in Virology.* 2018;33:156-66.
163. Aguilera ER, Pfeiffer JK. Strength in numbers: Mechanisms of viral co-infection. *Virus Research.* 2019;265:43-6.
164. McDonald SM, Nelson MI, Turner PE, Patton JT. Reassortment in segmented RNA viruses: mechanisms and outcomes. *Nature reviews Microbiology.* 2016;14(7):448-60.
165. Mikuletič T, Steyer A, Kotar T, Zorec TM, Poljak M. A novel reassortant mammalian orthoreovirus with a divergent S1 genome segment identified in a traveler with diarrhea. *Infection, Genetics and Evolution.* 2019;73:378-83.
166. Lelli D, Moreno A, Steyer A, Naglič T, Chiapponi C, Prosperi A, et al. Detection and Characterization of a Novel Reassortant Mammalian Orthoreovirus in Bats in Europe. *Viruses.* 2015;7(11):2908.
167. Naglič T, Rihtarič D, Hostnik P, Toplak N, Koren S, Kuhar U, et al. Identification of novel reassortant mammalian orthoreoviruses from bats in Slovenia. *BMC Veterinary Research.* 2018;14(1):264.
168. Fehér E, Kemenesi G, Oldal M, Kurucz K, Kugler R, Farkas SL, et al. Isolation and complete genome characterization of novel reassortant orthoreovirus from common vole (*Microtus arvalis*). *2017;53(2):307-11.*
169. Ahasan MS, Subramaniam K, Saylor KA, Loeb JC, Popov VL, Lednicky JA, et al. Molecular characterization of a novel reassortment Mammalian orthoreovirus type 2 isolated from a Florida white-tailed deer (*Odocoileus virginianus*) fawn. *Virus Research.* 2019:197642.
170. Wang L, Fu S, Cao L, Lei W, Cao Y, Song J, et al. Isolation and Identification of a Natural Reassortant Mammalian Orthoreovirus from Least Horseshoe Bat in China. *PLOS ONE.* 2015;10(3):e0118598.
171. Thete D, Danthi P. Protein mismatches caused by reassortment influence functions of the reovirus capsid. *bioRxiv.* 2018.
172. Thete D, Snyder AJ, Mainou BA, Danthi P. Reovirus μ 1 Protein Affects Infectivity by Altering Virus-Receptor Interactions. *Journal of virology.* 2016;90(23):10951-62.
173. Barr JN, Fearn R. How RNA viruses maintain their genome integrity. 2010;91(6):1373-87.
174. Parra GI, Bok K, Martínez M, Gomez JA. Evidence of rotavirus intragenic recombination between two sublineages of the same genotype. 2004;85(6):1713-6.
175. He C-Q, Ding N-Z, He M, Li S-N, Wang X-M, He H-B, et al. Intragenic Recombination as a Mechanism of Genetic Diversity in Bluetongue Virus. 2010;84(21):11487-95.

176. Martin DP, Murrell B, Golden M, Khoosal A, Muhire B. RDP4: Detection and analysis of recombination patterns in virus genomes. *Virus Evolution*. 2015;1(1).
177. Kosakovsky Pond SL, Posada D, Gravenor MB, Woelk CH, Frost SDW. GARD: a genetic algorithm for recombination detection. *Bioinformatics (Oxford, England)*. 2006;22(24):3096-8.
178. Nagarajan N, Kingsford C. GiRaF: robust, computational identification of influenza reassortments via graph mining. *Nucleic Acids Research*. 2010;39(6):e34-e.
179. Boyce M, McCrae MA, Boyce P, Kim JT. Inter-segment complementarity in orbiviruses: a driver for co-ordinated genome packaging in the Reoviridae? *Journal of General Virology*. 2016;97(5):1145-57.
180. Yin C, Yau SST. A coevolution analysis for identifying protein-protein interactions by Fourier transform. *PLOS ONE*. 2017;12(4):e0174862.
181. Pazos F, Helmer-Citterich M, Ausiello G, Valencia A. Correlated mutations contain information about protein-protein interaction 11 Edited by A. R. Fersht. *Journal of Molecular Biology*. 1997;271(4):511-23.
182. Bull JJ, Luring AS. Theory and empiricism in virulence evolution. *PLoS pathogens*. 2014;10(10):e1004387-e.
183. Geoghegan JL, Holmes EC. The phylogenomics of evolving virus virulence. *Nature Reviews Genetics*. 2018;19(12):756-69.
184. Longdon B, Hadfield JD, Day JP, Smith SCL, McGonigle JE, Cogni R, et al. The Causes and Consequences of Changes in Virulence following Pathogen Host Shifts. *PLOS Pathogens*. 2015;11(3):e1004728.
185. Madhun AS, Isachsen CH, Omdal LM, Bardsgjaere Einen AC, Bjorn PA, Nilsen R, et al. Occurrence of salmonid alphavirus (SAV) and piscine orthoreovirus (PRV) infections in wild sea trout *Salmo trutta* in Norway. *Dis Aquat Organ*. 2016;120(2):109-13.
186. Siah A, Morrison DB, Fringuelli E, Savage P, Richmond Z, Johns R, et al. Piscine Reovirus: Genomic and Molecular Phylogenetic Analysis from Farmed and Wild Salmonids Collected on the Canada/US Pacific Coast. *PLOS ONE*. 2015;10(11):e0141475.
187. Vendramin N, Cuenca A, Sorensen J, Alencar ALF, Christiansen DH, Jacobsen JA, et al. Presence and genetic variability of Piscine orthoreovirus genotype 1 (PRV-1) in wild salmonids in Northern Europe and North Atlantic Ocean. *J Fish Dis*. 2019.
188. Kibenge MJT, Wang Y, Gayeski N, Morton A, Beardslee K, McMillan B, et al. Piscine orthoreovirus sequences in escaped farmed Atlantic salmon in Washington and British Columbia. *Virology Journal*. 2019;16(1):41.
189. Cartagena J, Tambley C, Sandino AM, Spencer E, Tello M. Detection of piscine orthoreovirus in farmed rainbow trout from Chile. *Aquaculture*. 2018;493:79-84.
190. Åse Helen Garseth, Torfinn Moldal, Monika Hjortaas, Siri Kristine Gåsnes, Gjevne A-G. Health monitoring of wild anadromous salmonids in freshwater in Norway 2017. 2018.
191. Garseth ÅH, Moldal T, Gåsnes SK, Hjortaas MJ, Sollien VP, Gjevne A-G. Piscine orthoreovirus-3 is prevalent in wild seatrout (*Salmo trutta* L.) in Norway. 2019;42(3):391-6.
192. Adamek M, Hellmann J, Flamm A, Teitge F, Vendramin N, Fey D, et al. Detection of piscine orthoreoviruses (PRV-1 and PRV-3) in Atlantic salmon and rainbow trout farmed in Germany. *Transboundary and emerging diseases*. 2019;66(1):14-21.

193. Kurath G, Garver KA, Troyer RM, Emmenegger EJ, Einer-Jensen K, Anderson ED. Phylogeography of infectious haematopoietic necrosis virus in North America. 2003;84(4):803-14.
194. Lago M, Bandin I, Oliveira JG, Dopazo CP. In vitro reassortment between Infectious Pancreatic Necrosis Virus (IPNV) strains: The mechanisms involved and its effect on virulence. *Virology*. 2017;501:1-11.
195. Wiik-Nielsen J, Alarcon M, Jensen BB, Haugland O, Mikalsen AB. Viral co-infections in farmed Atlantic salmon, *Salmo salar* L., displaying myocarditis. *J Fish Dis*. 2016;39(12):1495-507.
196. Schrag SJ, Wiener P. Emerging infectious disease: what are the relative roles of ecology and evolution? *Trends in Ecology & Evolution*. 1995;10(8):319-24.
197. Fields BN, Byers K. The Genetic Basis of Viral Virulence. *Philos Trans R Soc Lond B Biol Sci*. 1983;303(1114):209-18.
198. Yue Z, Shatkin AJ. Double-stranded RNA-dependent protein kinase (PKR) is regulated by reovirus structural proteins. *Virology*. 1997;234(2):364-71.
199. Lanoie D, Boudreault S, Bisailon M, Lemay G. How Many Mammalian Reovirus Proteins are involved in the Control of the Interferon Response? 2019;8(2):83.
200. Sherry B, Torres J, Blum MA. Reovirus induction of and sensitivity to beta interferon in cardiac myocyte cultures correlate with induction of myocarditis and are determined by viral core proteins. *Journal of Virology*. 1998;72(2):1314-23.
201. Morton A, Routledge R, Hrushowy S, Kibenge M, Kibenge F. The effect of exposure to farmed salmon on piscine orthoreovirus infection and fitness in wild Pacific salmon in British Columbia, Canada. *PLOS ONE*. 2017;12(12):e0188793.
202. Walsh D, Mathews MB, Mohr I. Tinkering with translation: protein synthesis in virus-infected cells. *Cold Spring Harb Perspect Biol*. 2013;5(1):a012351.
203. Smith JA, Schmechel SC, Williams BRG, Silverman RH, Schiff LA. Involvement of the interferon-regulated antiviral proteins PKR and RNase L in reovirus-induced shutoff of cellular translation. 2005;79(4):2240-50.
204. Qin Q, Hastings C, Miller CL. Mammalian Orthoreovirus Particles Induce and Are Recruited into Stress Granules at Early Times Postinfection. 2009;83(21):11090-101.
205. Yajima T. Viral myocarditis: potential defense mechanisms within the cardiomyocyte against virus infection. *Future Microbiol*. 2011;6(5):551-66.
206. McManus BM, Chow LH, Wilson JE, Anderson DR, Gulizia JM, Gauntt CJ, et al. Direct myocardial injury by enterovirus: a central role in the evolution of murine myocarditis. *Clinical immunology and immunopathology*. 1993;68(2):159-69.
207. Terheggen F, Benedikz E, Frissen PH, Brinkman K. Myocarditis associated with reovirus infection. *Eur J Clin Microbiol Infect Dis*. 2003;22(3):197-8.
208. Poss KD, Wilson LG, Keating MT. Heart regeneration in zebrafish. *Science*. 2002;298(5601):2188-90.
209. Dennert R, Crijns HJ, Heymans S. Acute viral myocarditis. *Eur Heart J*. 2008;29(17):2073-82.
210. Gordon S, Martinez FO. Alternative activation of macrophages: mechanism and functions. *Immunity*. 2010;32(5):593-604.
211. Forlenza M, Fink IR, Raes G, Wiegertjes GF. Heterogeneity of macrophage activation in fish. *Developmental & Comparative Immunology*. 2011;35(12):1246-55.





212. Caldwell RB, Toque HA, Narayanan SP, Caldwell RW. Arginase: an old enzyme with new tricks. *Trends in pharmacological sciences*. 2015;36(6):395-405.
213. Tang P, Chiu C. Metagenomics for the discovery of novel human viruses. 2010;5(2):177-89.
214. Cruz-Rivera M, Forbi JC, Yamasaki LH, Vazquez-Chacon CA, Martinez-Guarneros A, Carpio-Pedroza JC, et al. Molecular epidemiology of viral diseases in the era of next generation sequencing. *Journal of clinical virology : the official publication of the Pan American Society for Clinical Virology*. 2013;57(4):378-80.
215. Bohle H, Bustos P, Leiva L, Grothusen H, Navas E, Sandoval A, et al. First complete genome sequence of piscine orthoreovirus variant 3 infecting coho salmon (*Oncorhynchus kisutch*) farmed in southern Chile. *Genome Announcements*. 2018;6(24).
216. Longdon B, Day JP, Alves JM, Smith SCL, Houslay TM, McGonigle JE, et al. Host shifts result in parallel genetic changes when viruses evolve in closely related species. *PLOS Pathogens*. 2018;14(4):e1006951.
217. Sernapesca. Estadística Importación de Ovas a julio de 2019: Servicio Nacional de Pesca y Acuicultura, Chile; 2019 [Available from: http://www.sernapesca.cl/sites/default/files/estadistica_importacion_de_ovas_a_julio_2019.pdf].
218. Sarkar P, Danthi P. The mu1 72-96 loop controls conformational transitions during reovirus cell entry. *J Virol*. 2013;87(24):13532-42.
219. Rivers TM. Viruses and Koch's Postulates. *Journal of bacteriology*. 1937;33(1):1-12.
220. Vendramin N, Kannimuthu D, Olsen AB, Cuenca A, Teige LH, Wessel Ø, et al. Piscine orthoreovirus subtype 3 (PRV-3) causes heart inflammation in rainbow trout (*Oncorhynchus mykiss*). 2019;50(1):14.
221. Stanifer ML, Kischnick C, Rippert A, Albrecht D, Boulant S. Reovirus inhibits interferon production by sequestering IRF3 into viral factories. *Scientific Reports*. 2017;7(1):10873.
222. Capobianchi MR, Giombini E, Rozera G. Next-generation sequencing technology in clinical virology. *Clinical microbiology and infection : the official publication of the European Society of Clinical Microbiology and Infectious Diseases*. 2013;19(1):15-22.
223. Tang Y, Lin L, Sebastian A, Lu H. Detection and characterization of two co-infection variant strains of avian orthoreovirus (ARV) in young layer chickens using next-generation sequencing (NGS). *Scientific Reports*. 2016;6:24519.
224. Barzon L, Lavezzo E, Militello V, Toppo S, Palu G. Applications of next-generation sequencing technologies to diagnostic virology. *International journal of molecular sciences*. 2011;12(11):7861-84.

9. Scientific Papers I-IV

I

Article

Evolution of the *Piscine orthoreovirus* Genome Linked to Emergence of Heart and Skeletal Muscle Inflammation in Farmed Atlantic Salmon (*Salmo salar*)

Kannimuthu Dhamotharan ¹, Torstein Tengs ², Øystein Wessel ¹, Stine Braaen ¹, Ingvild B. Nyman ¹, Elisabeth F. Hansen ¹, Debes H. Christiansen ³, Maria K. Dahle ⁴, Espen Rimstad ^{1,*} and Turhan Markussen ¹

- ¹ Faculty of Veterinary Medicine, Norwegian University of Life Sciences, 0454 Oslo, Norway; dhamokan@nmbu.no (K.D.); oystein.wessel@nmbu.no (Ø.W.); stine.braaen@nmbu.no (S.B.); ingvild.nyman@nmbu.no (I.B.N.); elisabeth.hansen@nmbu.no (E.F.H.); turhan.markussen@nmbu.no (T.M.)
 - ² Faculty of Chemistry, Biotechnology and Food Science, Norwegian University of Life Sciences, 1433 Ås, Norway; torstein.tengs@nmbu.no
 - ³ Faroese Food and Veterinary Authority, National Reference Laboratory for Fish Diseases, FO-110 Tórshavn, Faroe Islands; debesc@hfs.fo
 - ⁴ Department of Immunology, Norwegian Veterinary Institute, 0454 Oslo, Norway; maria.dahle@vetinst.no
- * Correspondence: espen.rimstad@nmbu.no; Tel.: +47-672-32-227

Received: 27 March 2019; Accepted: 20 May 2019; Published: 22 May 2019



Abstract: Heart and skeletal muscle inflammation (HSMI) in farmed Atlantic salmon (*Salmo salar*) was first diagnosed in Norway in 1999. The disease is caused by *Piscine orthoreovirus*-1 (PRV-1). The virus is prevalent in farmed Atlantic salmon, but not always associated with disease. Phylogeny and sequence analyses of 31 PRV-1 genomes collected over a 30-year period from fish with or without HSMI, grouped the viral sequences into two main monophylogenetic clusters, one associated with HSMI and the other with low virulent PRV-1 isolates. A PRV-1 strain from Norway sampled in 1988, a decade before the emergence of HSMI, grouped with the low virulent HSMI cluster. The two distinct monophylogenetic clusters were particularly evident for segments S1 and M2. Only a limited number of amino acids were unique to the association with HSMI, and they all located to S1 and M2 encoded proteins. The observed co-evolution of the S1-M2 pair coincided in time with the emergence of HSMI in Norway, and may have evolved through accumulation of mutations and/or segment reassortment. Sequences of S1-M2 suggest selection of the HSMI associated pair, and that this segment pair has remained almost unchanged in Norwegian salmon aquaculture since 1997. PRV-1 strains from the North American Pacific Coast and Faroe Islands have not undergone this evolution, and are more closely related to the PRV-1 precursor strains not associated with clinical HSMI.

Keywords: PRV-1; *Piscine orthoreovirus*; HSMI; virulence; reassortment; viral evolution

1. Introduction

Atlantic salmon (*Salmo salar*) aquaculture is a significant food production industry. Farmed fish are kept at high rearing densities, and outbreaks of infectious diseases strongly impact productivity and economic output [1]. Heart and skeletal muscle inflammation (HSMI) was reported for the first time in 1999, occurring during the seawater production phase in farmed Atlantic salmon in Mid-Norway [2], and rapidly emerged as an important disease. A few years later, disease outbreaks were reported from farms all along the Norwegian coast, and a maximum number of 181 outbreaks were registered in 2014,

after which HSMI was taken off the national list of notifiable fish diseases. Since then, recordings of HSMI outbreaks have not been complete. In a questionnaire to fish health professionals in 2017, HSMI was judged as the most important viral disease in salmon farms from the northern and mid regions of Norway (severity score of 4.6 out of 5) [3]. HSMI is caused by *Piscine orthoreovirus* (PRV) [4,5], a virus which uses salmonid erythrocytes as main target cells and causes subsequent infection of myocytes and inflammation of heart and red skeletal muscles [6].

PRV belongs to the genus *Orthoreovirus* in the family Reoviridae, and has a non-enveloped double protein capsid containing a 10-segmented double-stranded RNA (dsRNA) genome. The genomic segments sort into three size groups; large (L1–L3), medium (M1–M3), and small (S1–S4) [4,7]. The genome encodes at least 11 proteins. Based on similarity with the well characterized mammalian orthoreovirus (MRV) and functional studies on PRV [5,7–10], eight proteins are structural components of the virus particle (inner capsid $\lambda 1$, $\lambda 3$, $\mu 2$, $\sigma 2$, and outer capsid $\lambda 2$, $\mu 1$, $\sigma 3$, $\sigma 1$) and three are non-structural (σNS , μNS , p13). The S1 and M2-encoded proteins $\sigma 3$ and $\mu 1$ form a heterohexamer, $(\mu 1)_3(\sigma 3)_3$ in the outer capsid [11]. In the structurally coupled $\sigma 3$ and $\mu 1$ in MRV, mutations in the $\sigma 3$ protein is linked to suppressor mutations in $\mu 1$ protein [12]. Similarly, in Vero-cell adapted MRV-3, $\sigma 1$ and $\mu 1$ co-adaptation is linked to alterations in viral infection [13]. Proteolytic cleavage of $\sigma 3$ and $\mu 1$ in the endosomes after endocytic viral uptake is important for entry and infectivity of reoviruses [14]. After entering the cellular cytoplasm, $\sigma 3$ binds dsRNA, a function shown to modulate the host cell immune response [10]. The S1 segment also encodes p13, a non-fusogenic cytotoxic integral membrane protein [7,15]. In reoviruses, the replication of the dsRNA genome takes place after packaging of (+) ssRNA strands into the protein capsid. In case of an infection with two different genotypes of the reovirus in the same cell, this packaging may result in reassortants containing a mix of segments from the two viruses [16]. In addition, RNA viruses can genetically evolve through point mutations and recombination. In general, the mutation rate of RNA viruses is higher than in DNA viruses, and among RNA viruses, ssRNA viruses have a higher mutation rate than dsRNA viruses. The genome size, replication mode, and host factors influences the mutation rates in RNA viruses. The lower mutation rate of dsRNA viruses is likely due to their stamping machine mode of replication [17]. Reassortment can cause the emergence of strains with altered virulence and antigen properties, and have been linked to interspecies transmission [18].

Three subtypes of PRV, called PRV-1, -2 and -3, have been identified in salmonids. PRV-1 can cause HSMI in Atlantic salmon [5] and jaundice syndrome in Chinook salmon (*Oncorhynchus tshawytscha*) [19]. PRV-2 causes erythrocytic inclusion body syndrome (EIBS) in coho salmon (*Oncorhynchus kisutch*) [20] and PRV-3 causes pathological heart lesions in rainbow trout (*Oncorhynchus mykiss*) [21]. PRV-3 Germany was suggested as the likely causative agent of proliferative darkening syndrome (PDS) in brown trout (*Salmo trutta*) [22], but evidence lacked to conclude this [23]. The genome sequence of PRV-3 Germany is closely related to PRV-3 from coho salmon in Chile [22,24]. The species specificity is not absolute, and one genotype can infect several salmonid species. Pairwise nucleotide and amino acid sequence identities between PRV genotypes are 70%–90% [25], while within the PRV-1 genogroup, which is the most studied genogroup, the percent identity is in the upper 90's [7]. Variability in the PRV-1 sequences, with a particular focus on the S1 segment, has been reported earlier and two genotypes have been proposed [26]. Genetic homogeneity was observed in the PRV-1 S1 sequences from a vast geographic range in the North American Pacific Coast (NAPC) over a 13-year period [27]. PRV-1 is reported to be widespread in Alaska and Washington state, and detected at 3.4% prevalence level in coho and Chinook salmon [28]. A higher prevalence was reported in Chinook salmon on the west coast of Vancouver Island exposed to aquaculture [29].

PRV-1 infection is reported to be common in wild returning salmon and sea trout in Norwegian rivers [30], but uncommon in landlocked salmon and brown trout [31]. Farmed Atlantic salmon in Norway became infected with PRV-1 a few months after transfer to seawater, but the infection may not necessarily manifest clinically [32]. During an outbreak, typical pathological lesions of HSMI can be found in the cardiac and skeletal muscles of most fish in the affected sea cage. However, the mortality

is usually low, from insignificant to 20%, and influenced by many factors [2]. PRV infection is common in most countries with Atlantic salmon farming, like Chile [33], Canada [34], and Scotland [35], but some countries, like the Faroe Islands and Iceland, have not reported HSMI. PRV-1 is widespread in the NAPC region, and found in other Pacific salmon species like coho salmon, Chinook salmon, and sockeye salmon [28,36]. DiCicco et al. found HSMI histopathological lesions in farmed Atlantic salmon in British Columbia (BC), Canada, but the clinical signs were very mild with no elevated mortalities [37]. Recent findings from the same area point to mild heart inflammation [38], and failure to induce clinical HSMI in Atlantic salmon using PRV-containing material from BC, Canada [39]. This contrasts to the more severe pathological findings accompanied by increased mortalities and more than 100 annual outbreaks observed in Norway. The differences in disease manifestations could be due to differences in host, virus, environment, or a combination of these factors. In accordance with this, we have grouped BC strains as low virulent NAPC PRV group. The histopathological lesions of classical HSMI can be reproduced in experimental infections of Atlantic salmon using purified PRV particles from Norwegian isolates [5].

In this study, we obtained near-complete genome sequences of PRV-1 isolates collected over a 30-year period. Along with other available PRV-1 sequences from Atlantic salmon with or without a history of HSMI, phylogenetic and protein structure prediction analyses were used to explore the genetic diversity and evolutionary mechanisms of PRV-1 in farmed Atlantic salmon.

2. Materials and Methods

2.1. Virus Isolates

The coding regions were obtained by next generation sequencing technology from sea-reared Atlantic salmon from different sites of the Norwegian west coast sampled in 2005 (NOR-2005/TT), 2015 (NOR-2015/SSK), and 2015 (NOR-2015/MS). Two additional PRV genomes were retrieved from the Faroe Islands, FO/1978/15 from a smolt facility in 2015 and FO/41/16 from a sea site in 2016. Samples were plasma for NOR-2015/SSK and NOR-2015/MS, and heart and/or head kidney tissue in RNA later for the NOR-2005/TT and the Faroe samples. The sixth and seventh genomes were obtained from kidney samples from Atlantic salmon collected from sea sites in Norway in 1997 (NOR-1997) and 1988 (NOR-1988) stored at -80°C , preceding the first description of HSMI with two and eleven years, respectively. The stored kidney samples were screened for the eventual presence of common viruses of Atlantic salmon by qPCR (i.e., infectious pancreatic necrosis virus, salmonid alphavirus, infectious salmon anemia virus, PRV-1, piscine myocarditis virus) and were only found positive for PRV-1. The kidney samples NOR-1988 and NOR-1997, were homogenized and injected in experimental Atlantic salmon at VESO Vikan in Norway, and replication of PRV-1 was demonstrated by qPCR in collected blood. The viral genome of NOR-1988 was retrieved from a fish collected at 4 wpc (PRV-1 Ct-value of 15.4 in blood pellet) and sequenced obtained by next generation sequencing (NGS) from the plasma sample. The viral genome of NOR-1997 was retrieved from a fish collected at 3 wpc (PRV-1 Ct-value of 16.2 in blood pellet) and Sanger sequenced obtained directly from the blood pellet. The challenge trial was approved by the Norwegian Animal Research Authority and performed in accordance with the recommendations of the current animal welfare regulations: FOR-1996-01-15-23 (Norway). All samples were from individual fish except for samples NOR-2005/TT and NOR-2015/SSK.

2.2. RNA Isolation

Tissues that had been stored in RNA later were added 650 μL QIAzol Lysis Reagent (Qiagen, Hilden, Germany) and plasma samples (250 μL) 750 μL Trizol LS (Life Technologies, Carlsbad, California, USA), as recommended by the manufacturers. Steel beads (5 mm) was added to samples and homogenized for 2×5 min at 25 Hz using TissueLyser II (Qiagen). After the addition of chloroform, the samples were centrifuged and the aqueous phase transferred to RNeasy Mini spin columns (Qiagen, Hilden, Germany). The remaining RNA purification procedure followed the manufacturer's

instructions. Total RNA was eluted in 50 μ L RNase-free water, concentration determined using a NanoDrop ND-1000 spectrophotometer (ThermoFisher Scientific, Waltham, Massachusetts, USA), and subsequently stored at -80°C .

2.3. RT-qPCR and Sanger Sequencing

The RT-qPCR was performed using the Quantitect Probe OneStep RT-PCR kit from Qiagen. For head kidney samples, the amount of total RNA was standardized to 100 ng per reaction (5 μ L of 20 ng/ μ L). For plasma samples 5 μ L total RNA was used in each reaction. Prior to one-step RT-qPCR, the template dsRNA was denatured at 95°C for 5 min and cooled immediately on ice. The RT-qPCR targeted PRV gene segment S1 and was performed as previously described [40]. The coding regions of the revived sample from 1997 (NOR-1997) were amplified by PCR using primers shown in Table S1 and the PCR products were sequenced by Sanger sequencing (GATC Biotech AG, Konstanz, Germany).

2.4. NGS and Genome Assembly

The total RNA from the plasma, heart, and head kidney, stored at -80°C , was added to 0.1 \times volume of 3 M sodium acetate (pH 7.5) and 2 \times volume of 100% ethanol, and mixed gently. MacroGen (Seoul, Korea) performed library preparation and sequencing of all samples except sample NOR-2005/TT. This genome was assembled using 454 sequencing data (GS FLX Titanium platform) from a previously published study [41]. For Illumina sequencing of NOR-2015/SSK, library preparation was performed using TruSeq RNA Library Prep v2 Kit (Illumina Inc., San Diego, CA, USA) and de novo sequencing performed on a MiSeq platform (2 \times 300 PE). Libraries for samples NOR-2015/MS, NOR-1988, and the two samples from the Faroe Islands were also prepared using TruSeq RNA Library Prep v2 Kit without polyA enrichment or ribosomal depletion. DNaseI treatment was performed prior to library preparation. NOR-2015/MS and NOR-1988 were sequenced on a HiSeq2500 system (2 \times 100 PE) and the two Faroe Island samples on a HiSeq2000 system (2 \times 100 PE). Minor gaps in the sequences from the Faroe Islands and NOR/TT-2005 were closed using Sanger sequencing of RT-qPCR products (primers available upon request).

For the Illumina data, paired-end reads were assembled using a previously sequenced PRV genome as a reference [4] and the software BWA v0.6.2 [42]. Deviations from the reference sequence were scored and consensus sequences were generated using the software VarScan v2.3.9 [43]. Regions with low coverage and mutations deemed important were manually checked using the software BioEdit version 7.0.5 [44]. The 454 data were compared with the same reference PRV genome using BioEdit and assembly was performed manually. The final contigs were generated using AlignX software (Vector NTI Advance v11, ThermoFisher Scientific).

2.5. Phylogenetic Analyses

Multiple sequence alignments were performed using AlignX and MEGA X version 10.0.5 software (available from www.megasoftware.net) [45]. All phylogenetic trees were constructed using complete coding sequences from all the PRV genomes currently available in Genbank and the seven isolates sequenced in the present study. A separate phylogenetic analysis of segment S1 was performed including all available PRV-1 S1 sequences from GenBank spanning 830 nucleotides. Maximum likelihood (ML) was used together with the best-fitting nucleotide substitution model suggested by the MEGA X program [45]. Bootstrap values were calculated from 1000 replicates, and values above 70 were considered significant [46].

2.6. Protein Structure Analyses

Protein secondary structure predictions were performed using PSIPRED v3.3, available at <http://bioinf.cs.ucl.ac.uk/psipred/> [47]. A 3D-structure homology modeling of the σ 3 proteins from the HSMI-associated NOR-2012 isolate was performed in order to spatially visualize the sequence differences between the two groups. The 3D model(s) of the full-length PRV1 σ 3 protein was

constructed using the threading method provided by the iTasser server, available online at <https://zhanglab.ccmb.med.umich.edu/I-TASSER/> [48]. I-TASSER server identified MRV T3D $\sigma 3$ protein (PDB ID:1FN9) as the most appropriate template (best fitting model) for 3D-homology modeling with the highest TM score of 0.862. Template modeling score (TM-score) measures the similarity of protein structures (score range 0-1). In general scores higher than 0.5 assume roughly the same fold. In order to be able to target relevant sequence information from the PRV-1 sequence database (i.e., Genbank and from present work) potentially linked to virulence, the software program QlikSense Desktop (<https://www.qlik.com/us/products/qlik-sense>) was used together with multiple sequence alignment of protein sequences.

3. Results

3.1. Coding Sequences Obtained by Illumina and Sanger Sequencing

Here we present, in addition to previously published PRV-1 genomes from viruses originating from Norway, North American Pacific Coast (NAPC), and Chile, seven new isolates to the current PRV-1 genome sequence pool (Table 1). The 1997 (NOR-1997) and 1988 (NOR-1988) isolates were obtained from kidney samples from Atlantic salmon collected from sea sites in Norway and stored at $-80\text{ }^{\circ}\text{C}$, preceding the first description of HSMI with two and eleven years, respectively. Viral coding sequences were obtained from plasma following revival of these two isolates by injection of the stored frozen kidney homogenate in experimental fish. Illumina sequencing of NOR-2015/SSK, NOR-2015/MS, FO/1978/15, FO/41/16, and NOR-1988 provided full coverage of all coding regions (Table S2) except for FO/1978/15 and FO/41/16 from the Faroe Islands, where minor gaps were closed using traditional Sanger sequencing. Most of the NOR-2005/TT genome could be assembled from 454 sequencing, but overall coverage was poor with roughly 1000 PRV reads in total, and gaps were closed using Sanger sequencing. The coding sequences from NOR-1997 were obtained using Sanger sequencing only.

Table 1. *Piscine orthoreovirus-1* (PRV-1) isolates sequenced in the study.

PRV Isolate	Associated Disease Status	Tissue Origin of Sequence	Accession Numbers
NOR-1988	Healthy	Plasma	MK675862–MK675871
NOR-1997	Unresolved, suspicion of ISA	Plasma	MK675822–MK675831
NOR-2005/TT	CMS	Heart	MK675832–MK675841
NOR-2015/SSK	HSMI	Plasma	MK675852–MK675861
NOR-2015/MS	HSMI-suspected	Plasma	MK675842–MK675851
FO/1978/15	Healthy	Head kidney	MK675872–MK675881
FO/41/16	Healthy	Head kidney	MK675882–MK675891

3.2. Phylogenetic Analyses of Individual PRV Genomic Segments Revealed Diversity

Separate phylogenetic analyses of all ten genomic segments from the 31 available PRV-1 isolates revealed differential clustering depending on the segment for some isolates, with more consistent grouping patterns across the genome for other isolates. Using PRV-2 or PRV-3 as an outgroup did not change the grouping significantly, but collapsed the tree. Hence, to visualize minor differences within PRV-1 strains, the trees are presented as mid-point rooted. More specifically, PRV-1 from the NAPC grouped together in all ten gene segments with high bootstrap support, displaying lower intra-segment sequence diversity compared to the other PRV-1 isolates (Figures 1 and 2). Hence, no segment reassortment could be observed within the isolates from NAPC.

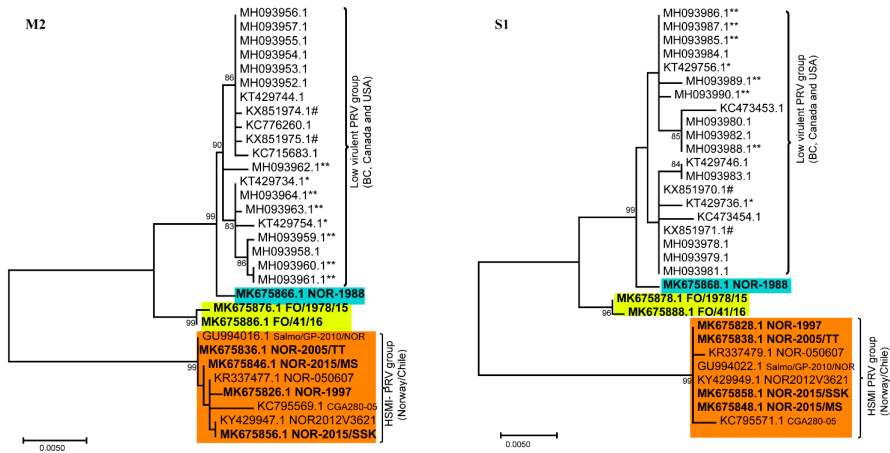


Figure 1. Phylogenetic trees constructed using M2 and S1 coding sequences from 31 PRV-1 isolates. For both gene segments, the Norwegian heart and skeletal muscle inflammation (HSMI) associated isolates, Chilean isolate, and Norwegian isolate from 1997, all group together forming a monophyletic cluster (orange background color). In contrast, the Norwegian isolate from 1988 (blue background color) and two Faroese isolates (yellow background color) group with the North American Pacific Coast isolates. Sequences obtained in the present study are shown in bold. * denotes isolates from coho and ** from Chinook salmon. # indicates PRV from BC HSMI longitudinal farm study

In the phylogenetic tree made from concatenated full genome amino acid sequences (Figure S1), Norwegian HSMI-associated isolates group separately from the monophyletic cluster generated by the NAPC and Faroe Islands.

The phylogenetic analyses showed that many HSMI isolates (orange color) changed group affiliation for the different genomic segments (Figures 1 and 2), indicating possible reassortment events. The PRV-1 isolate from 1988 (highlighted in blue color) grouped with the HSMI-associated strains (orange color) for all segments except L1, S1, and M2, where it grouped with the NAPC and Faroese isolates (yellow color). The Faroese isolates also grouped with the NAPC PRV isolates for segments L3, M2, M3, and S1. The Norwegian 050607 isolate, collected from an HSMI outbreak in 2007, grouped together with other HSMI isolates except for L3 (orange box highlighted in red outline) where it grouped with the isolates from NAPC and Faroe Islands, with high bootstrap support (Figure 2). For segment M3, the Norwegian 050607 and the Chilean CGA280-05 isolates grouped with NOR-1988. Similarly, the HSMI associated NOR-2015/MS, NOR-1997, and Chilean CGA280-05 isolates changed group affiliation for segment S3 (orange box highlighted in red outline) (Figure 2).

The bootstrap support for the two main phylogenetic clusters generated for gene segments S1 and M2 were particularly high (Figure 1) and the two groups adhered completely to HSMI association or low-virulent HSMI association, the latter group constituted by the NAPC, Faroese, and NOR-1988 isolates. The number of nucleotide differences were high for segments S1 (30 nt) and M2 (60 nt) between the HSMI and other low virulent PRVs (NOR-1988, Faroes, NAPC isolates) (Table S4). In S1, this resulted in ten amino acid changes in $\sigma 3$ and seven in p13. There were only three amino acid changes in the M2 encoded $\mu 1$. Most single nucleotide polymorphisms (SNPs) in the HSMI group were shared by all isolates within the group (i.e., 27/30 nt for S1, 51/60 nt for M2). The Faroese isolates, grouping slightly outside of the main NAPC cluster in S1 and M2, shared five and ten nucleotides, respectively, with the HSMI associated isolates. These shared nucleotides were not present in any of the NAPC isolates. Apart from this, sequence variation within the two main phylogenetic groups was very low for both segments. The high conservation of the S1 and M2 in the HSMI associated group was not found in the other segments.

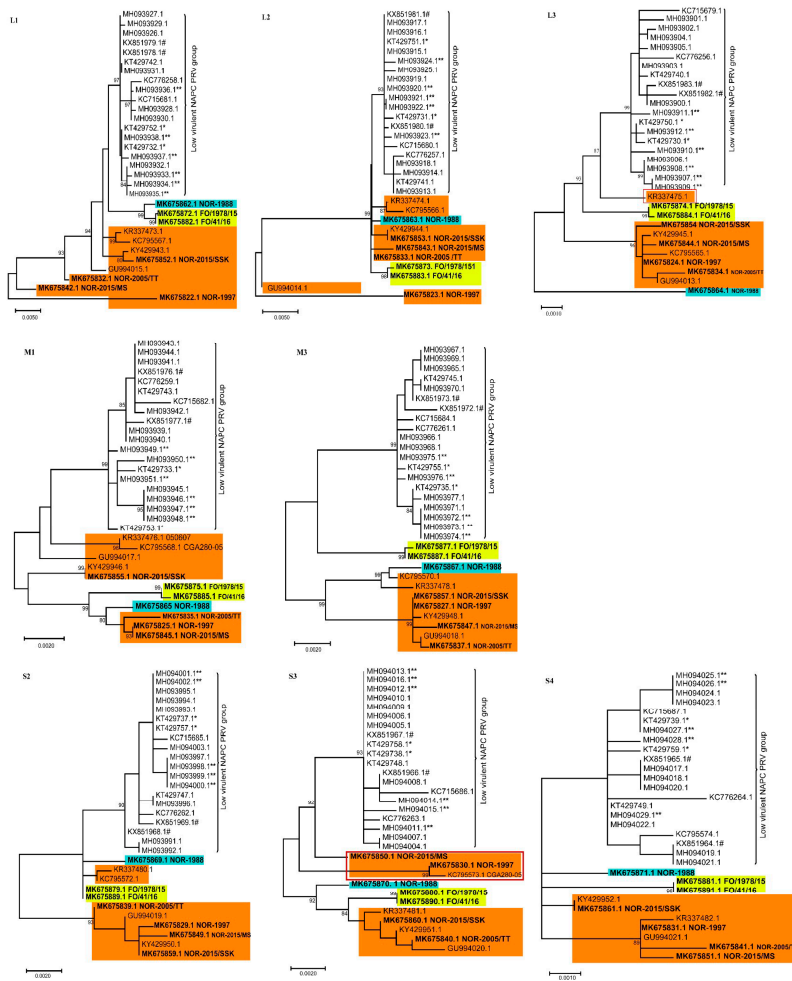


Figure 2. Phylogenetic trees constructed using coding sequences from segments L1, L2, L3, M1, M3, S2, S3, and S4 from 31 PRV-1 isolates. The North American Pacific Coast (NAPC) sequences consistently group together for all gene segments forming a monophyletic cluster. In contrast, the grouping of the Norwegian, Chilean, and Faroe Island isolates may vary from segment to segment. Color coding as in Figure 1 legend. Sequences obtained in the present study shown in bold. * denotes isolates from coho and ** from Chinook salmon. # indicates PRV from BC HSMI longitudinal farm study

3.3. None of the NAPC PRV-1 Isolates Group within the HSMI Clade

When including all available partial coding sequences of minimum 830 nt in the phylogenetic analyses of segment S1 (240 sequences in all), they separated into two distinct monophyletic clusters (Figure 3). As for the tree generated with full-length S1 coding sequences from the 31 isolates (Figure 1), the HSMI associated and low virulent HSMI associated isolates grouped separately. All isolates in the HSMI associated group originated from Norway or Chile. Similarly, the S1 sequences from the non-HSMI associated NOR-1988 grouped with the NAPC and Faroe Island isolates. There were several S1 sequences originating from Norway that group together with the NAPC isolates (Figure 3). Interestingly, most of these NAPC-like sequences from Norway originated from samples collected

from Atlantic salmon returning to rivers (wild or escaped) or from farmed salmon where no clinical information was available. Both phylogenetic analyses using complete (Figure 1) and partial (Figure 3) S1 coding sequences place the NAPC isolates within the low virulent group.

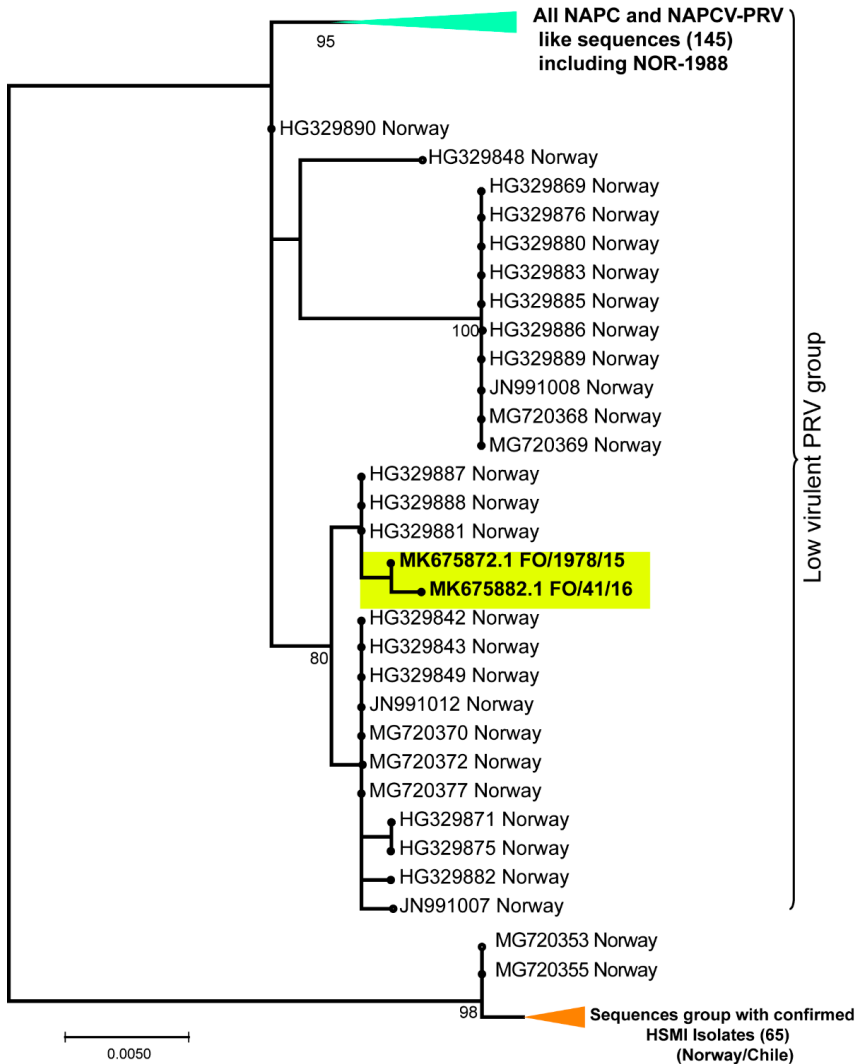


Figure 3. Phylogenetic trees constructed using partial S1 coding sequences (830 nt) of all available PRV-1 isolates in GenBank. The Faroese isolates are in the yellow box. HSMI associated isolates group separately from the NAPC sequences. Green triangle: All sequences from NAPC, and NAPC-like sequences, including NOR-1988. Orange triangle: All sequences from confirmed HSMI isolates.

3.4. Amino Acid Residues Unique to HSMI Association are Located to Proteins Encoded by S1 and M2

Comparison of amino acid sequences of proteins encoded by the two main groups of PRV-1 isolates showed remarkable conservation except for $\sigma 3$ and p13 (both encoded by S1) and $\mu 1$ (encoded by M2). No amino acid sites unique to the HSMI associated isolates were found for the other eight PRV-1 proteins ($\lambda 1$, $\lambda 2$, $\lambda 3$, $\mu 2$, μNS , $\sigma 1$, $\sigma 2$, and σNS). In segment S1, the number of amino acid sites

unique to HSMI association were ten for $\sigma 3$ and seven for p13, most differences being amino acids with similar physicochemical properties (Table S3). Only two sites in the two overlapping reading frames encoding $\sigma 3$ and p13 changed the amino acids in both proteins. The only other protein with amino acid sites unique to the HSMI associated isolates was the M2 encoded $\mu 1$ protein (three sites) (Table S3).

Finally, blast searches of all available complete and partial $\sigma 3$ and $\mu 1$ sequences revealed that none of the unique amino acid sites in the HSMI associated group were present in available sequences from NAPC isolates. The NOR-1988 isolate, sampled from an apparently healthy fish eleven years prior to the first diagnosis of HSMI, is more similar to the NAPC and Faroese isolates for segments S1 and M2. In contrast, segments S1 and M2 from the NOR-1997 isolate sampled from a fish with unresolved disease two years before the first confirmed diagnosis of HSMI, were identical to the current Norwegian HSMI associated sequences. Within PRV isolates with HSMI association, the three proteins $\mu 1$, $\sigma 3$, and p13 have identical amino acid sequences (Figure 4). The phylogenetic analysis of amino acid sequences encoded by the concatenated full PRV-1 genomes showed grouping of NAPC isolates together with NOR-1988 and Faroese isolates suggesting that these share a more recent common ancestor compared to HSMI isolates (Figure S1).

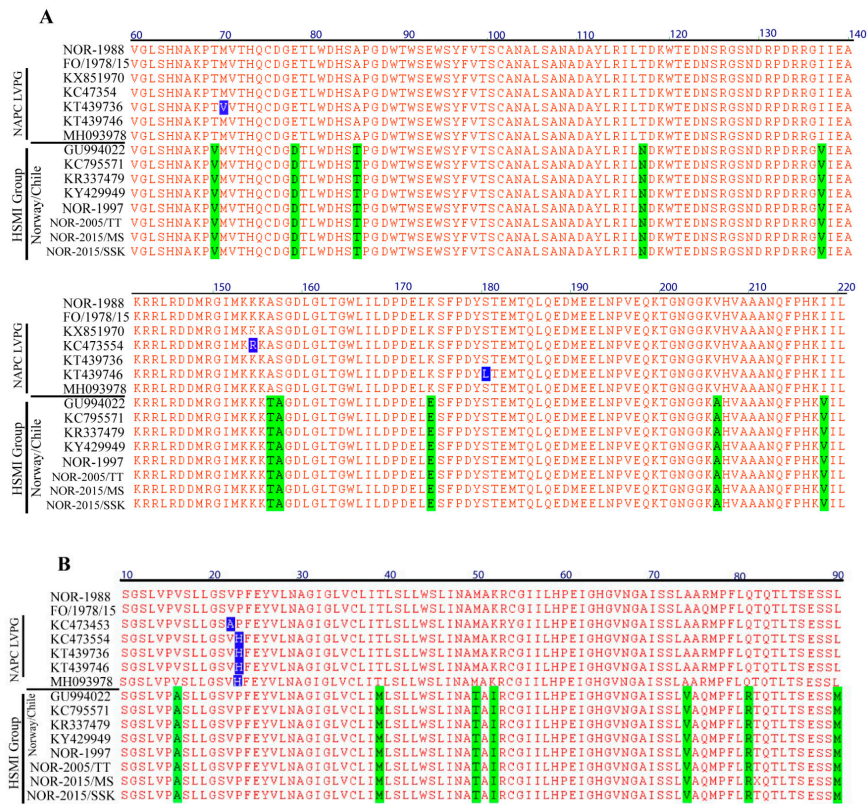


Figure 4. Sequence alignment of partial PRV-1 S1 encoded $\sigma 3$ and p13 proteins (B). For clarity, identical sequences in the low virulent group are not included in the alignment. Only sequence regions that contain variation among the isolates are presented. Amino acids unique to the HSMI associated group are shown with green background color and the amino acid differences in the low virulent group are shown with blue background color.

3.5. Predicted Differences between the HSMI Associated and Non-Associated Isolates Locate Mainly to Surface-Exposed Amino Acids in σ_3

Three-dimensional structure homology modeling of the σ_3 proteins from the HSMI-associated NOR-2012 isolate was performed in order to spatially visualize the sequence differences between the two groups. I-TASSER server identified MRV T3D σ_3 protein (PDB ID:1FN9) as the most appropriate template (best fitting model) for 3D-homology modeling with the highest TM score of 0.862. The modeled PRV-1 σ_3 structure is similar to MRV σ_3 with small and large lobes and a Zinc finger motif. Among the top five models predicted by I-TASSER, the model with the highest C score was used to visualize the protein. The amino acid sites differing between the HSMI associated and non-associated isolates seem to locate to surface exposed and more flexible coil regions (Figure 5). Only two of the ten sites locate to a predicted helical region.

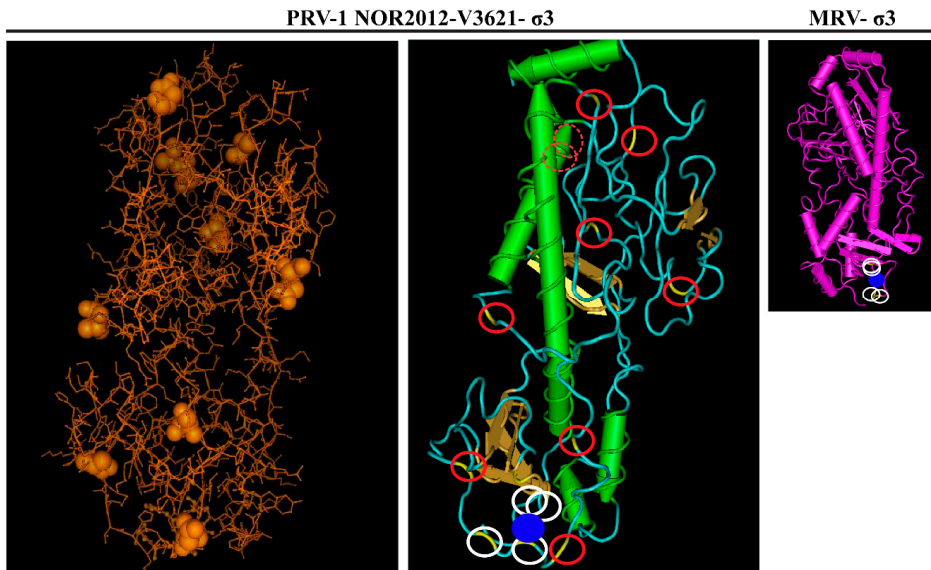


Figure 5. Visualization of the predicted 3D-structure of the NOR-2012 σ_3 protein with Vector NTI 3D molecule viewer Cn3D v4.3 following structure homology modeling using the MRV σ_3 protein (PDB ID:1FN9) as template, the most appropriate structure model to use as predicted by i-TASSER. The ten amino acid sites differing between the HSMI associated (here represented by NOR-2012) and low virulent HSMI isolates are indicated by or as yellow/brown balls (left picture) or as a yellow color enclosed by a red circle (middle picture). Amino acid side chains predicted to coordinate the Zn-ion, represented by a blue ball, are indicated by white circles. MRV- σ_3 added for comparison.

Secondary structure predictions using PSI-blast based secondary structure prediction (PSIPRED) for the σ_3 protein from HSMI and low virulent isolates showed very similar structures (Figure S2). Two of the ten amino acids that differed between the HSMI associated and non-associated groups located to a predicted sheet region and two other sites to a region containing a predicted helical structure.

4. Discussion

The analysis of 31 PRV-1 genomes collected from Atlantic salmon from Norway, the Faroes, NAPC, and Chile over a 30-year period included revived Norwegian isolates from samples collected in 1988 and 1997, pre-dating HSMI. The phylogenetic analyses revealed the presence of two distinct groups of PRV-1 sequences, which were either associated with highly virulent or low virulent strains. This

grouping was particularly evident for genomic segments S1 and M2. For these two segments, nucleotide and amino acid sequences within the HSMI associated group showed remarkable conservation over the 20 years since the emergence of HSMI.

The first recorded HSMI outbreak was recorded in 1999 in Trøndelag, Mid-Norway [49], however, the S1 and M2 sequence identity of NOR-1997 isolate to the current HSMI outbreak viruses in Norway points to a possible presence of this disease before 1999. The NOR-1997 isolate was sampled from a disease outbreak with unresolved etiology. In contrast, sequence analysis of another pre-HSMI isolate, NOR-1988, showed high similarity to the low virulent HSMI group in segments L1, S1, and M2, but to the HSMI group for the other segments. Hence, PRV-1 was present in farmed Atlantic salmon well before the reported emergence of HSMI in Norway. Approximately 100 cases of HSMI outbreaks are recorded annually in farmed Atlantic salmon in Norway, but it is not a reportable disease, so the actual number of cases is likely much higher.

A recent study of Atlantic salmon experimentally challenged with a PRV-1 isolate from BC, found only minor signs of heart inflammation, which supported the phenotypic difference between NAPC and current Norwegian PRV-1 [38]. However, an experimental challenge study using different PRV strains could minimize the effect of host or environmental related factors in disease manifestation and identify putative virulence factors linked to HSMI. The presence of unique amino acid sites in HSMI associated PRV-1 isolates in the $\sigma 3$, p13, and $\mu 1$ proteins suggest association of these proteins to the ability to induce HSMI, but the specific virulence determinants among $\sigma 3$, p13, or $\mu 1$ proteins linked to HSMI need to be explored. The heterohexameric nature of $(\mu 1)_3(\sigma 3)_3$ protein in the virus particle makes it likely that a gene linkage is involved for S1 and M2, indicating that only one of the proteins may be linked to HSMI, while the other could be forced to co-evolve. The high number of unique sites (i.e., ten for $\sigma 3$ and seven for p13), in the two S1-encoded proteins suggest that these two proteins are central for the HSMI trait. Only two of the nucleotide differences change the amino acid sequence in both proteins ($\sigma 3$, p13) on the bicistronic S1-segment, which suggest independent selection pressures.

The sequences of the S1 and M2 segments from Norwegian HSMI associated isolates differed significantly from the pre-HSMI isolate NOR-1988. One hypothesis for the emergence of HSMI in Norwegian Atlantic salmon farming is that the disease results from a reassortment event in PRV-1 introducing new S1 and M2 segments, followed by selection and spread of this S1/M2 pair. However, no donor strain of HSMI-associated S1/M2 pairs has been identified so far, and the number of available PRV sequences originating from before the emergence of HSMI is too limited to conclude about the molecular mechanisms involved in the evolution of S1 and M2. Mutational accumulation over time is an alternative hypothesis. There are few intermediate forms between the S1/M2 from HSMI associated and low virulent groups in the available selection of sequences. However, the Faroese isolates group slightly outside of the NAPC cluster in segments S1 and M2 sharing a number of nucleotides with the HSMI associated isolates that were not present in the NAPC isolates, suggesting that they might represent intermediate forms. Furthermore, the low mutation frequency, as indicated by completely conserved sequences of S1/ M2 from isolates associated with HSMI over the 20 years since the emergence of HSMI, also indicate that mutational accumulation should occur over a very long time.

Reassortment events are common for mammalian *orthoreovirus* [50], and are indicated when genetic segments from the same isolate occupy different positions on phylogenetic trees of different segments [51], like we observed here. Some of the HSMI associated isolates grouped with the NOR-1988 for segments M3 and S3, indicating reassortment for these segments as well. Successful reassortment may result in progeny viruses more suited for selective constraints compared to parental viruses (i.e., increased viral fitness). We observed that segments S1 and M2 are genetically linked, which indicate that the structure and interaction of their encoded proteins are vital for virus fitness. For MRV, an in vitro forced reassortment event has been reported to alter virus infectivity and replication efficiency due to $\lambda 2$ and $\sigma 1$ protein mismatch [52].

The secondary and 3D structure predictions did not predict significant changes between the HSMI and low virulent associated strains' $\sigma 3$ proteins. The mostly synonymous substitutions were predicted to be surface exposed and located to apparently more disorganized regions of the protein. The minor changes in amino acid sequence in $\mu 1$ may represent an adaptation to the changes occurring in $\sigma 3$ in order to maintain structural integrity of the $(\mu 1)_3(\sigma 3)_3$ heterohexameric complex. It has been shown for MRV that a single amino acid change is sufficient to affect the interaction between $\mu 1$ and $\sigma 3$ monomers and also the dsRNA binding ability of $\sigma 3$ [53,54]. The dsRNA binding activity of MRV $\sigma 3$ is an important inhibitor of the innate antiviral response, it inhibits both induction of type I interferon and activation of PKR [55]. Similarly, PRV $\sigma 3$ also binds dsRNA, although no specific domain responsible for this binding has been determined [10]. The innate immune response is important for the onset of humoral and cellular acquired immunity. Cellular immunity is central in the pathogenesis of HSMI, which is characterized by the influx of CD8 lymphocytes in heart tissue [56]. An upregulation of genes related to innate antiviral response has been demonstrated repeatedly for experimental PRV-1 infections using PRV-1 isolates able to induce HSMI [5,6,57]. However, this was not found following experimental infection using a PRV-1 NAPC isolate that did not induce HSMI, and where the innate response, measured as an expression analysis of Mx, showed only modest upregulation [39]. This could indicate that an important difference between the HSMI-inducing and non-inducing groups of PRV-1 is the ability to induce innate antiviral response. The $\sigma 3$ dsRNA binding affinity and thus its amino acid sequence could play a crucial role.

The S1 encoded p13 has a more undefined function. p13 has been defined as an integral membrane protein located to intracellular membranes [15], further characterized as Golgi-like structures [7]. PRV p13 was also reported to be cytotoxic when overexpressed in non-salmonid cells [15], but the cytotoxic function has not been determined in vivo. Potentially, p13 could play a role in viral factory formation, viral particle release or modulation of antiviral responses. Regardless of its function, p13 is likely to be involved in molecular interaction with the host, which could be affected by changes in the amino acid sequence. A previous comparison between p13 sequences [27] did not reveal an association with HSMI. However, at that time, fewer PRV sequences were available.

This study suggests that the PRV-1 genotype causing HSMI in farmed Atlantic salmon has a recent common ancestor, and evolved prior to the rapid expansion of HSMI disease outbreaks in Norwegian Atlantic salmon farming which spread from a focal zone of outbreaks to all aquaculture areas within a few years after 1999 [2]. The HSMI-associated genotype contains unique S1 and M2 sequences, and the high conservation of the S1 and M2 sequences among the Norwegian HSMI outbreak isolates over the past 20 years strongly suggests an aquaculture-specific fitness improvement and higher virulence of PRV-1. The rapid selection and spread of this segment pair implies a relatively large evolutionary advantage for viruses harboring these versions of S1/M2 in the environment of industrialized, large-scale, farming of Atlantic salmon.

A low sequence diversity was observed among low virulent-associated NAPC S1 sequences over a period of 13 years indicating that these viruses are also well adapted to their host environment. Currently, the HSMI-associated PRV-1 variants have not been found in the NAPC region [27]. The phylogenetic analysis including the coding sequences from all segments from the 31 isolates, as well as the analysis of all available partial S1 sequences showed a distinct monophyletic clade for all sequences originating from the west coast of North America. The NAPC associated PRV-1 sequences are prevalent from other salmonid species including Chinook, coho, pink salmon, and rainbow trout. This low virulent PRV-1 group also encompassed some Chilean and Norwegian isolates like the pre-HSMI NOR-1988 isolate and viral sequences retrieved from wild fish in Norway [58]. Based on the S1 segment, the NAPC like sequences are still present in Norway and sequences are similar to either NOR-1988 or Faroese isolates. This indicates that both groups of sequences are present in Norway and Chile and are each evolutionarily stable.

5. Conclusions

The unique HSMI associated PRV-1 genotype is dominant in the current Norwegian and Chilean Atlantic salmon farming industry, while a low virulent PRV-1 group is reported from broad geographic regions and other salmonid species. Further full genome sequencing of PRV-1, including PRV-1 from wild Atlantic salmon, will provide more insights into the differential virulence evolution of PRV-1 in salmon.

Supplementary Materials: The following are available online at <http://www.mdpi.com/1999-4915/11/5/465/s1>, Figure S1: Phylogenetic analysis of concatenated full genome amino acid sequences (including p13); Figure S2: Secondary structure predictions of the o3 and p13 proteins. Table S1: Primers used for Sanger sequencing of the NOR-1997 strain; Table S2: Number of reads of PRV-1 segments from the Illumina runs; Table S3: Amino acid differences between HSMI- and non-HSMI associated isolates compared to NOR-1988. Table S4. SNPs in M2 and S1 segment coding sequence of Norwegian HSMI strains

Author Contributions: K.D., T.T., T.M. and E.R. launched the project idea and participated in the overall design and coordination of the study and interpretation of data. K.D., T.M. and E.R. drafted the manuscript. T.T. and T.M. interpreted the data from the next generation sequencing. I.B.N., S.B. and E.F.H. performed sample preparations for Sanger sequencing, phylogenetic analysis, and revised the manuscript. K.D., T.T. and T.M. performed phylogenetic analyses. K.D. and T.M. performed the protein structure prediction and 3D modeling work. M.K.D. and Ø.W. participated in the coordination of the study, interpretation of data, and revised the manuscript. D.H.C. gathered the Faroese isolates and revised the manuscript. All authors approved the final manuscript.

Funding: This research was funded by The Research Council of Norway with grant #237315/E40 and #244423/E40. K.D. acknowledges the financial assistance provided by the Indian Council of Agricultural Research (ICAR) through the ICAR International Fellowship for PhD.

Acknowledgments: Thanks to Magnus Røsæg for providing access to the NOR-2015/SSK positive samples, and Håvard Bjørgen/Erling Olaf Koppang for the NOR-2015/MS sample.

Conflicts of Interest: The authors declare no conflict of interest.

References

- Ebert, D.; Bull, J.J. Challenging the trade-off model for the evolution of virulence: Is virulence management feasible? *Trends Microbiol.* **2003**, *11*, 15–20. [[CrossRef](#)]
- Kongtorp, R.T.; Kjerstad, A.; Taksdal, T.; Guttvik, A.; Falk, K. Heart and skeletal muscle inflammation in atlantic salmon, *salmo salar* L: A new infectious disease. *J. Fish Dis.* **2004**, *27*, 351–358. [[CrossRef](#)] [[PubMed](#)]
- Hjeltnes, B.W.C.; Bang Jensen, B.; Haukaas, A. *The Fish Health Report 2017*; The Norwegian Veterinary Institute: Oslo, Norway, 2018.
- Palacios, G.; Lovoll, M.; Tengs, T.; Hornig, M.; Hutchison, S.; Hui, J.; Kongtorp, R.T.; Savji, N.; Bussetti, A.V.; Solovyov, A.; et al. Heart and skeletal muscle inflammation of farmed salmon is associated with infection with a novel reovirus. *PLoS ONE* **2010**, *5*, e11487. [[CrossRef](#)]
- Wessel, O.; Braaen, S.; Alarcon, M.; Haatveit, H.; Roos, N.; Markussen, T.; Tengs, T.; Dahle, M.K.; Rimstad, E. Infection with purified piscine orthoreovirus demonstrates a causal relationship with heart and skeletal muscle inflammation in atlantic salmon. *PLoS ONE* **2017**, *12*, e0183781. [[CrossRef](#)] [[PubMed](#)]
- Wessel, O.; Olsen, C.M.; Rimstad, E.; Dahle, M.K. Piscine orthoreovirus (prv) replicates in atlantic salmon (*salmo salar* L.) erythrocytes ex vivo. *Vet. Res.* **2015**, *46*, 26. [[CrossRef](#)] [[PubMed](#)]
- Markussen, T.; Dahle, M.K.; Tengs, T.; Lovoll, M.; Finstad, O.W.; Wiik-Nielsen, C.R.; Grove, S.; Lauksund, S.; Robertsen, B.; Rimstad, E. Sequence analysis of the genome of piscine orthoreovirus (prv) associated with heart and skeletal muscle inflammation (hsmi) in atlantic salmon (*salmo salar*). *PLoS ONE* **2013**, *8*, e70075. [[CrossRef](#)]
- Haatveit, H.M.; Nyman, I.B.; Markussen, T.; Wessel, O.; Dahle, M.K.; Rimstad, E. The non-structural protein muns of piscine orthoreovirus (prv) forms viral factory-like structures. *Vet. Res.* **2016**, *47*, 5. [[CrossRef](#)]
- Haatveit, H.M.; Wessel, O.; Markussen, T.; Lund, M.; Thiede, B.; Nyman, I.B.; Braaen, S.; Dahle, M.K.; Rimstad, E. Viral protein kinetics of piscine orthoreovirus infection in atlantic salmon blood cells. *Viruses* **2017**, *9*, 49. [[CrossRef](#)] [[PubMed](#)]
- Wessel, O.; Nyman, I.B.; Markussen, T.; Dahle, M.K.; Rimstad, E. Piscine orthoreovirus (prv) o3 protein binds dsrna. *Virus Res.* **2015**, *198*, 22–29. [[CrossRef](#)]

11. Dryden, K.A.; Wang, G.; Yeager, M.; Nibert, M.L.; Coombs, K.M.; Furlong, D.B.; Fields, B.N.; Baker, T.S. Early steps in reovirus infection are associated with dramatic changes in supramolecular structure and protein conformation: Analysis of virions and subviral particles by cryoelectron microscopy and image reconstruction. *J. Cell Biol.* **1993**, *122*, 1023–1041. [[CrossRef](#)]
12. McPhillips, T.H.; Ramig, R.F. Extragenic suppression of temperature-sensitive phenotype in reovirus: Mapping suppressor mutations. *Virology* **1984**, *135*, 428–439. [[CrossRef](#)]
13. Sandekian, V.; Lemay, G. Amino acids substitutions in sigma1 and mu1 outer capsid proteins of a vero cell-adapted mammalian orthoreovirus are required for optimal virus binding and disassembly. *Virus Res.* **2015**, *196*, 20–29. [[CrossRef](#)] [[PubMed](#)]
14. Nibert, M.L.; Fields, B.N. A carboxy-terminal fragment of protein mu 1/mu 1c is present in infectious subviral particles of mammalian reoviruses and is proposed to have a role in penetration. *J. Virol.* **1992**, *66*, 6408–6418. [[PubMed](#)]
15. Key, T.; Read, J.; Nibert, M.L.; Duncan, R. Piscine reovirus encodes a cytotoxic, non-fusogenic, integral membrane protein and previously unrecognized virion outer-capsid proteins. *J. Gen. Virol.* **2013**, *94*, 1039–1050. [[CrossRef](#)] [[PubMed](#)]
16. McDonald, S.M.; Nelson, M.I.; Turner, P.E.; Patton, J.T. Reassortment in segmented rna viruses: Mechanisms and outcomes. *Nat. Rev. Microbiol.* **2016**, *14*, 448–460. [[CrossRef](#)]
17. Peyambari, M.; Warner, S.; Stoler, N.; Rainer, D.; Roossinck, M.J. A 1000 year-old rna virus. *J. Virol.* **2018**, *93*. [[CrossRef](#)]
18. Vijaykrishna, D.; Mukerji, R.; Smith, G.J.D. Rna virus reassortment: An evolutionary mechanism for host jumps and immune evasion. *PLoS Pathog.* **2015**, *11*, e1004902. [[CrossRef](#)]
19. Di Cicco, E.; Ferguson, H.W.; Kaukinen, K.H.; Schulze, A.D.; Li, S.; Tabata, A.; Guenther, O.P.; Mordecai, G.; Suttle, C.A.; Miller, K.M. The same strain of piscine orthoreovirus (prv-1) is involved in the development of different, but related, diseases in atlantic and pacific salmon in british columbia. *Facets* **2018**, *3*, 599–641. [[CrossRef](#)]
20. Takano, T.; Nawata, A.; Sakai, T.; Matsuyama, T.; Ito, T.; Kurita, J.; Terashima, S.; Yasuike, M.; Nakamura, Y.; Fujiwara, A.; et al. Full-genome sequencing and confirmation of the causative agent of erythrocytic inclusion body syndrome in coho salmon identifies a new type of piscine orthoreovirus. *PLoS ONE* **2016**, *11*, e0165424. [[CrossRef](#)]
21. Hauge, H.; Vendramin, N.; Taksdal, T.; Olsen, A.B.; Wessel, O.; Mikkelsen, S.S.; Alencar, A.L.F.; Olesen, N.J.; Dahle, M.K. Infection experiments with novel piscine orthoreovirus from rainbow trout (*oncorhynchus mykiss*) in salmonids. *PLoS ONE* **2017**, *12*, e0180293. [[CrossRef](#)]
22. Kuehn, R.; Stoeckle, B.C.; Young, M.; Popp, L.; Taeubert, J.E.; Pfaffl, M.W.; Geist, J. Identification of a piscine reovirus-related pathogen in proliferative darkening syndrome (pds) infected brown trout (*salmo trutta fario*) using a next-generation technology detection pipeline. *PLoS ONE* **2018**, *13*, e0206164. [[CrossRef](#)]
23. Fux, R.; Arndt, D.; Langenmayer, M.C.; Schwaiger, J.; Ferling, H.; Fischer, N.; Indenbirken, D.; Grundhoff, A.; Dolken, L.; Adamek, M.; et al. Piscine orthoreovirus 3 is not the causative pathogen of proliferative darkening syndrome (pds) of brown trout (*salmo trutta fario*). *Viruses* **2019**, *11*, 112. [[CrossRef](#)] [[PubMed](#)]
24. Bohle, H.; Bustos, P.; Leiva, L.; Grothusen, H.; Navas, E.; Sandoval, A.; Bustamante, F.; Montecinos, K.; Gaete, A.; Mancilla, M. First complete genome sequence of piscine orthoreovirus variant 3 infecting coho salmon (*oncorhynchus kisutch*) farmed in southern chile. *Genome Announc.* **2018**, *6*. [[CrossRef](#)]
25. Dharmotharan, K.; Vendramin, N.; Markussen, T.; Wessel, O.; Cuenca, A.; Nyman, I.B.; Olsen, A.B.; Tengs, T.; Krudtaa Dahle, M.; Rimstad, E. Molecular and antigenic characterization of piscine orthoreovirus (prv) from rainbow trout (*oncorhynchus mykiss*). *Viruses* **2018**, *10*, 170. [[CrossRef](#)]
26. Kibenge, M.J.; Iwamoto, T.; Wang, Y.; Morton, A.; Godoy, M.G.; Kibenge, F.S. Whole-genome analysis of piscine reovirus (prv) shows prv represents a new genus in family reoviridae and its genome segment s1 sequences group it into two separate sub-genotypes. *Virol. J.* **2013**, *10*, 230. [[CrossRef](#)]
27. Siah, A.; Morrison, D.B.; Fringuelli, E.; Savage, P.; Richmond, Z.; Johns, R.; Purcell, M.K.; Johnson, S.C.; Saksida, S.M. Piscine reovirus: Genomic and molecular phylogenetic analysis from farmed and wild salmonids collected on the canada/us pacific coast. *PLoS ONE* **2015**, *10*, e0141475. [[CrossRef](#)]

28. Purcell, M.K.; Powers, R.L.; Evered, J.; Kerwin, J.; Meyers, T.R.; Stewart, B.; Winton, J.R. Molecular testing of adult pacific salmon and trout (*oncorhynchus* spp.) for several rna viruses demonstrates widespread distribution of piscine orthoreovirus in alaska and washington. *J. Fish Dis.* **2018**, *41*, 347–355. [[CrossRef](#)] [[PubMed](#)]
29. Tucker, S.; Li, S.R.; Kaukinen, K.H.; Patterson, D.A.; Miller, K.M. Distinct seasonal infectious agent profiles in life-history variants of juvenile fraser river chinook salmon: An application of high-throughput genomic screening. *PLoS ONE* **2018**, *13*, e0195472. [[CrossRef](#)]
30. Garseth, A.H.; Fritsvold, C.; Opheim, M.; Skjerve, E.; Biering, E. Piscine reovirus (prv) in wild atlantic salmon, *salmo salar* L., and sea-trout, *salmo trutta* L., in norway. *J. Fish Dis.* **2013**, *36*, 483–493. [[CrossRef](#)] [[PubMed](#)]
31. Garseth, A.H.; Biering, E. Little evidence to suggest salmonid freshwater reservoirs of piscine orthoreovirus (prv). *J. Fish Dis.* **2018**, *41*, 1313–1315. [[CrossRef](#)] [[PubMed](#)]
32. Lovoll, M.; Alarcon, M.; Bang Jensen, B.; Taksdal, T.; Kristoffersen, A.B.; Tengs, T. Quantification of piscine reovirus (prv) at different stages of atlantic salmon *salmo salar* production. *Dis. Aquat. Org.* **2012**, *99*, 7–12. [[CrossRef](#)]
33. Godoy, M.G.; Kibenge, M.J.T.; Wang, Y.; Suarez, R.; Leiva, C.; Vallejos, F.; Kibenge, F.S.B. First description of clinical presentation of piscine orthoreovirus (prv) infections in salmonid aquaculture in chile and identification of a second genotype (genotype ii) of prv. *Virol. J.* **2016**, *13*, 98. [[CrossRef](#)] [[PubMed](#)]
34. Marty, G.D.; Morrison, D.B.; Bidulka, J.; Joseph, T.; Siah, A. Piscine reovirus in wild and farmed salmonids in british columbia, canada: 1974–2013. *J. Fish Dis.* **2015**, *38*, 713–728. [[CrossRef](#)]
35. Ferguson, H.; Kongtorp, R.; Taksdal, T.; Graham, D.; Falk, K. An outbreak of disease resembling heart and skeletal muscle inflammation in scottish farmed salmon, *salmo salar* L., with observations on myocardial regeneration. *J. Fish Dis.* **2005**, *28*, 119–123. [[CrossRef](#)] [[PubMed](#)]
36. Garver, K.A.; Marty, G.D.; Cockburn, S.N.; Richard, J.; Hawley, L.M.; Muller, A.; Thompson, R.L.; Purcell, M.K.; Saksida, S. Piscine reovirus, but not jaundice syndrome, was transmissible to chinook salmon, *oncorhynchus tshawytscha* (walbaum), sockeye salmon, *oncorhynchus nerka* (walbaum), and atlantic salmon, *salmo salar* L. *J. Fish Dis.* **2016**, *39*, 117–128. [[CrossRef](#)]
37. Di Cicco, E.; Ferguson, H.W.; Schulze, A.D.; Kaukinen, K.H.; Li, S.; Vanderstichel, R.; Wessel, O.; Rimstad, E.; Gardner, I.A.; Hammell, K.L.; et al. Heart and skeletal muscle inflammation (hsmi) disease diagnosed on a british columbia salmon farm through a longitudinal farm study. *PLoS ONE* **2017**, *12*, e0171471. [[CrossRef](#)]
38. Polinski, M.P.; Marty, G.D.; Snyman, H.N.; Garver, K.A. Piscine orthoreovirus demonstrates high infectivity but low virulence in atlantic salmon of pacific canada. *Sci. Rep.* **2019**, *9*, 3297. [[CrossRef](#)] [[PubMed](#)]
39. Garver, K.A.; Johnson, S.C.; Polinski, M.P.; Bradshaw, J.C.; Marty, G.D.; Snyman, H.N.; Morrison, D.B.; Richard, J. Piscine orthoreovirus from western north america is transmissible to atlantic salmon and sockeye salmon but fails to cause heart and skeletal muscle inflammation. *PLoS ONE* **2016**, *11*, e0146229. [[CrossRef](#)]
40. Finstad, O.W.; Dahle, M.K.; Lindholm, T.H.; Nyman, I.B.; Lovoll, M.; Wallace, C.; Olsen, C.M.; Storset, A.K.; Rimstad, E. Piscine orthoreovirus (prv) infects atlantic salmon erythrocytes. *Vet. Res.* **2014**, *45*, 35. [[CrossRef](#)] [[PubMed](#)]
41. Lovoll, M.; Wiik-Nielsen, J.; Grove, S.; Wiik-Nielsen, C.R.; Kristoffersen, A.B.; Faller, R.; Poppe, T.; Jung, J.; Pedomallu, C.S.; Nederbragt, A.J.; et al. A novel totivirus and piscine reovirus (prv) in atlantic salmon (*salmo salar*) with cardiomyopathy syndrome (cms). *Virol. J.* **2010**, *7*, 309. [[CrossRef](#)]
42. Li, H.; Durbin, R. Fast and accurate short read alignment with burrows-wheeler transform. *Bioinformatics* **2009**, *25*, 1754–1760. [[CrossRef](#)]
43. Koboldt, D.C.; Zhang, Q.; Larson, D.E.; Shen, D.; McLellan, M.D.; Lin, L.; Miller, C.A.; Mardis, E.R.; Ding, L.; Wilson, R.K. VarScan 2: Somatic mutation and copy number alteration discovery in cancer by exome sequencing. *Genome Res.* **2012**, *22*, 568–576. [[CrossRef](#)] [[PubMed](#)]
44. Hall, T.A. Bioedit: A User-Friendly Biological Sequence Alignment Editor and Analysis Program for Windows 95/98/nt. In *Nucleic Acids Symposium Series*; Information Retrieval Ltd.: London, UK, 1999; pp. 95–98.
45. Kumar, S.; Stecher, G.; Li, M.; Knyaz, C.; Tamura, K. Mega x: Molecular evolutionary genetics analysis across computing platforms. *Mol. Biol. Evol.* **2018**, *35*, 1547–1549. [[CrossRef](#)]
46. Hillis, D.M.; Bull, J.J. An empirical test of bootstrapping as a method for assessing confidence in phylogenetic analysis. *Syst. Biol.* **1993**, *42*, 182–192. [[CrossRef](#)]
47. Jones, D.T. Protein secondary structure prediction based on position-specific scoring matrices. *J. Mol. Biol.* **1999**, *292*, 195–202. [[CrossRef](#)]

48. Roy, A.; Kucukural, A.; Zhang, Y. I-tasser: A unified platform for automated protein structure and function prediction. *Nat. Protoc.* **2010**, *5*, 725–738. [[CrossRef](#)]
49. Kongtorp, R.T.; Taksdal, T.; Lyngøy, A. Pathology of heart and skeletal muscle inflammation (hsmi) in farmed atlantic salmon *salmo salar*. *Dis. Aquat. Org.* **2004**, *59*, 217–224. [[CrossRef](#)]
50. Wenske, E.A.; Chanock, S.J.; Krata, L.; Fields, B.N. Genetic reassortment of mammalian reoviruses in mice. *J. Virol.* **1985**, *56*, 613–616. [[PubMed](#)]
51. Svinti, V.; Cotton, J.A.; McInerney, J.O. New approaches for unravelling reassortment pathways. *BMC Evol. Biol.* **2013**, *13*, 1. [[CrossRef](#)]
52. Thete, D.; Danthi, P. Protein mismatches caused by reassortment influence functions of the reovirus capsid. *J. Virol.* **2018**, *92*. [[CrossRef](#)]
53. Mabrouk, T.; Lemay, G. The sequence similarity of reovirus sigma-3 protein to picornaviral proteases is unrelated to its role in mu-1 viral protein cleavage. *Virology* **1994**, *202*, 615–620. [[CrossRef](#)]
54. Bergeron, J.; Mabrouk, T.; Garzon, S.; Lemay, G. Characterization of the thermosensitive ts453 reovirus mutant: Increased dsrna binding of sigma 3 protein correlates with interferon resistance. *Virology* **1998**, *246*, 199–210. [[CrossRef](#)]
55. Imani, F.; Jacobs, B.L. Inhibitory activity for the interferon-induced protein kinase is associated with the reovirus serotype 1 sigma 3 protein. *Proc. Natl. Acad. Sci. USA* **1988**, *85*, 7887–7891. [[CrossRef](#)]
56. Mikalsen, A.B.; Haugland, O.; Rode, M.; Solbakk, I.T.; Evensen, O. Atlantic salmon reovirus infection causes a cd8 t cell myocarditis in atlantic salmon (*salmo salar* l.). *PLoS ONE* **2012**, *7*, e37269. [[CrossRef](#)]
57. Dahle, M.K.; Wessel, O.; Timmerhaus, G.; Nyman, I.B.; Jorgensen, S.M.; Rimstad, E.; Krasnov, A. Transcriptome analyses of atlantic salmon (*salmo salar* l.) erythrocytes infected with piscine orthoreovirus (prv). *Fish Shellfish Immunol.* **2015**, *45*, 780–790. [[CrossRef](#)]
58. Madhun, A.S.; Isachsen, C.H.; Omdal, L.M.; Einen, A.C.B.; Maehle, S.; Wennevik, V.; Niemela, E.; Svasand, T.; Karlsbakk, E. Prevalence of piscine orthoreovirus and salmonid alphavirus in sea-caught returning adult atlantic salmon (*salmo salar* l.) in northern norway. *J. Fish Dis.* **2018**, *41*, 797–803. [[CrossRef](#)]



© 2019 by the authors. Licensee MDPI, Basel, Switzerland. This article is an open access article distributed under the terms and conditions of the Creative Commons Attribution (CC BY) license (<http://creativecommons.org/licenses/by/4.0/>).

Supplementary Tables

Table S1 Primers used for Sanger sequencing of the NOR-1997 strain.

Primer name	*Nucleotide sequence (5'-3')
Lambda1 UTR_Fw	GCCGCTCGAGTCTAGAGATAATGTTT GTTTTGCCAT
Lambda1 UTR_Rw	AAACGGGGCCCTCTAGAGATGAAGTTGTCATGTTT GT
Lambda2 UTR_Fw	GCCGCTCGAGTCTAGAGATAATTGTAACGACGAAAT
Lambda2 UTR_Rw	AAACGGGGCCCTCTAGAGATGAAGAAGGAACGGCCTA
Lambda3 UTR_Fw	GCCGCTCGAGTCTAGAGATAATAATGGAGAAACCTA
Lambda3 UTR_Rw	AAACGGGGCCCTCTAGAGATGAAGAAGGATCGGCCCA
Mu2 UTR_Fw	GCCGCTCGAGTCTAGAGATAATAACTCCTTT GCCAC
Mu2 UTR_Rw	AAACGGGGCCCTCTAGAGATGAAAATCTCTTAAGCCC
Mu1 UTR_Fw	GCCGCTCGAGTCTAGAGATAAATTTGTTTAAACAGGC
Mu1 UTR_Rw	AAACGGGGCCCTCTAGAGATGAAGATTTGTCGTT CGG
MuNS UTR_Fw	GCCGCTCGAGTCTAGAGATAAAGCTTACGACACGTG
MuNS UTR_Rw	AAACGGGGCCCTCTAGAGATGAGGAGGGGAGCTCACA
Sigma1 UTR_Fw	GCCGCTCGAGTCTAGAGATAAAGATCTTAACCGCAG
Sigma1 UTR_Rw	AAACGGGGCCCTCTAGAGATGAAAAACAGGCTT ACCG
Sigma2 UTR_Fw	GCCGCTCGAGTCTAGAGATAAATTTGTTGGTGACGA
Sigma2 UTR_Rw	AAACGGGGCCCTCTAGAGATGAAGAGGGCGTGCT GACT
SigmaNS UTR_Fw	GCCGCTCGAGTCTAGAGATAATTTTGATTGCATACA
SigmaNS UTR_Rw	AAACGGGGCCCTCTAGAGATGAAGAGATGTT CGATTG
Sigma3 UTR_Fw	GCCGCTCGAGTCTAGAGATAAAGACTTCTGTACGTG
Sigma3 UTR_Rw	AAACGGGGCCCTCTAGAGATGAATAAGACCTCCT TCC

*PRV-1 sequence specific regions are shown in bold.

Table S2. Number of reads of PRV-1 segments from the Illumina HiSeq4000 run.

Segment	L1	L2	L3	M1	M2	M3	S1	S2	S3	S4
NOR-2015/SSK	3634	4460	2938	912	1016	1142	214	277	149	188
NOR-2015/MS	1047	5106	793	474	1106	505	837	690	924	933
FO/1978/15	207	270	163	120	87	98	128	52	76	40
FO/41/16	261	220	225	111	76	113	90	102	100	82
NOR-1988	211562	311365	203953	84962	72206	88916	55023	63314	72555	65535

Table S3. Amino acid differences between HSMI- and non-HSMI associated isolates compared to NOR-1988.

Seg.	*Non-HSMI isolates			HSMI Isolates							
	NOR-1988	FO/1978/15	All NAPC isolates	NOR-1997	NOR-2005/T	NOR-050607	NOR-2015/SSK	NOR-2015/MS	NOR-V3621	GP-2010	CGA-28005
L1	K ₁₆									E ₁₆	
	A ₃₀							T ₃₀			
	S ₆₀										P ₆₀
	A ₆₃	V ₆₃	V ₆₃	V ₆₃	V ₆₃	V ₆₃	V ₆₃	V ₆₃	V ₆₃	V ₆₃	V ₆₃
	I ₁₇₉			V ₁₇₉	V ₁₇₉			V ₁₇₉			
	V ₁₈₄			A ₁₈₄	A ₁₈₄			A ₁₈₄			
	T ₂₀₀							S ₂₀₀			
	D ₂₄₃										G ₂₄₃
	E ₃₄₃			G ₃₄₃							
	D ₃₄₇			E ₃₄₇							
	N ₃₇₂			D ₃₇₂				D ₃₇₂			
	V ₄₉₀			I ₄₉₀							
	I ₆₀₁										T ₆₀₁
	N ₇₅₈			S ₇₅₈	S ₇₅₈						
	D ₉₃₇			A ₉₃₇				A ₉₃₇			
	V ₉₆₂			I ₉₆₂				I ₉₆₂			
	N ₉₉₆			S ₉₉₆							
	R ₁₀₆₅										W ₁₀₆₅

	S ₃₉	P ₃₉	P ₃₉	P ₃₉	P ₃₉	P ₃₉	P ₃₉	P ₃₉	P ₃₉	P ₃₉	P ₃₉
	T ₆₉			V ₆₉	V ₆₉	V ₆₉	V ₆₉	V ₆₉	V ₆₉	V ₆₉	V ₆₉
	E ₇₈			D ₇₈	D ₇₈	D ₇₈	D ₇₈	D ₇₈	D ₇₈	D ₇₈	D ₇₈
	A ₈₅			T ₈₅	T ₈₅	T ₈₅	T ₈₅	T ₈₅	T ₈₅	T ₈₅	T ₈₅
	T ₁₁₇			N ₁₁₇	N ₁₁₇	N ₁₁₇	N ₁₁₇	N ₁₁₇	N ₁₁₇	N ₁₁₇	N ₁₁₇
	I ₁₃₇			V ₁₃₇	V ₁₃₇	V ₁₃₇	V ₁₃₇	V ₁₃₇	V ₁₃₇	V ₁₃₇	V ₁₃₇
	A ₁₅₆			T ₁₅₆	T ₁₅₆	T ₁₅₆	T ₁₅₆	T ₁₅₆	T ₁₅₆	T ₁₅₆	T ₁₅₆
	S ₁₅₇			A ₁₅₇	A ₁₅₇	A ₁₅₇	A ₁₅₇	A ₁₅₇	A ₁₅₇	A ₁₅₇	A ₁₅₇
	G ₁₆₄								G ₁₆₄		
	K ₁₇₄			E ₁₇₄	E ₁₇₄	E ₁₇₄	E ₁₇₄	E ₁₇₄	E ₁₇₄	E ₁₇₄	E ₁₇₄
	V ₂₀₆			A ₂₀₆	A ₂₀₆	A ₂₀₆	A ₂₀₆	A ₂₀₆	A ₂₀₆	A ₂₀₆	A ₂₀₆
	I ₂₁₈			V ₂₁₈	V ₂₁₈	V ₂₁₈	V ₂₁₈	V ₂₁₈	V ₂₁₈	V ₂₁₈	V ₂₁₈
S1 (p13))	V ₁₆			A ₁₆	A ₁₆	A ₁₆	A ₁₆	A ₁₆	A ₁₆	A ₁₆	A ₁₆
	T ₃₉			M ₃₉	M ₃₉	M ₃₉	M ₃₉	M ₃₉	M ₃₉	M ₃₉	M ₃₉
	M ₅₀			T ₅₀	T ₅₀	T ₅₀	T ₅₀	T ₅₀	T ₅₀	T ₅₀	T ₅₀
	K ₅₂			I ₅₂	I ₅₂	I ₅₂	I ₅₂	I ₅₂	I ₅₂	I ₅₂	I ₅₂
	A ₇₄			V ₇₄	V ₇₄	V ₇₄	V ₇₄	V ₇₄	V ₇₄	V ₇₄	V ₇₄
	R ₇₆	Q ₇₆		Q ₇₆	Q ₇₆	Q ₇₆	Q ₇₆	Q ₇₆	Q ₇₆	Q ₇₆	Q ₇₆
	Q ₈₁			R ₈₁	R ₈₁	R ₈₁	R ₈₁	R ₈₁	R ₈₁	R ₈₁	R ₈₁
	L ₉₁			M ₉₁	M ₉₁	M ₉₁	M ₉₁	M ₉₁	M ₉₁	M ₉₁	M ₉₁
S2			**								
S3	I ₃₃₆		**								V ₃₃₆
S4	A ₇₅										V ₇₅
	V ₁₀₇							A ₁₀₇			
	D ₂₅₂					N ₂₅₂	N ₂₅₂		N ₂₅₂		N ₂₅₂

*Amino acid sites consistently found in HSMI-associated isolates not present in NAPC, Faroe Island isolates and NOR-1988 are considered unique.

**The overall majority of NAPC sequences were identical to the NOR-1988 strain, but a few displayed minor differences.

Table S4. SNPs in M2 and S1 segment coding sequence of Norwegian HSMI strains compared to other NAPC and non-HSMI (NOR-1988, Faroes isolates).

S4. A

1. T80- C80	2. C189- T189	3. T203- C203 (only in CGA280-05)	4. C212- T212	5. A239- G239	6. G275- A275	7. A281- G281
8. C299- T299	9. G302- A302	10. A336- G336 (only in CGA280-05)	11. T362- C362	12. C404- G404	13. A410- G410	14. G419- A419
15. T464- C464	16. G550-C550	17. T581- C581 (In Salmo/GP-2010/NOR, NOR-2015/MS, CGA280-05)	18. C782- T782	19. G783- T783	20. T806- C806	21. T869- C869
22. C896- T896	23. C902- T902	24. C905- T905	25. G917- A917	26. T942- C942 (NOR-2015/MS, NOR-2015/SSK)	27. A944- G944	28. G950- A950
29. A960- C960	30. C983- T983	31. T1004- A1004	32. C1046- T1046	33. T1049- C1049	34. G1070- A1070	35. C1098- T1098
36. C1100- A1100	37. A1107- G1107	38. A1118- G1118 (only in NOR-2015/MS)	39. T1142- C1142	40. G1199- A1199	41. A1214- G1214	42. A1217- G1217
43. G1230- A1230 (only in NOR-2015/MS)	44. G1247- A1247	45. A1268- T1268	46. A1402- G1402 (only in NOR-2015/MS)	47. A1458- G1458 (only in NOR-2015/MS)	48. C1550- T1550	49. G1583- A1583
50. C1640- T1640	51. A1694- G1694	52. C1751- T1751	53. A1763- G1763	54. A1775- G1775	55. G1847- A1847	56. A1880- G1880
57. A1901- G1901	58. A1940- G1940	59. G1994- A1994	60. T2000- C2000 ((In NOR-1997, NOR-050607, NOR2012-V3621, NOR-2015/MS, NOR-			

			2015/SSK, CGA280-05)			
--	--	--	-------------------------	--	--	--

S4. B S1 segment

1. A68- G68 (only in CGA280-05)	2. C75- T75 (only in CGA280- 05)	3. T126- C126	4. C195- T195	5. A205- G205	6. C206- T206	7. C228- T228
8. A234- T234	9. G253- A253	10. C300- T300	11. A321- G321	12. C350- A350	13. A409- G409	14. G466- A466
15. T469- G469	16. G491- A491 (NOR- 050607)	17. T492- C492	18. G504- T504	19. C507- T507	20. A520- G520	21. G564- A564
22. T617- C617	23. A652- G652	24. A705- G705	25. T735- C735	26. A747- G747	27. A789- G789	28. C879- T879
29. C900- T900	30. T957- C957					

The non-HSMI (Faroes and NOR-1988) and other NAPC isolates nucleotides are indicated in black color with the position of nt starting from coding sequence

MH093978.1, MH093979.1, MH093980.1, MH093981.1, MH093982.1, MH093983.1, MH093984.1, MH093985.1, MH093986.1, MH093987.1, MH093988.1, MH093989.1, MH093990.1, MK675888.1 FO/41/16 MK675878.1 FO/1978/15, MK675868.1 NOR-1988, KX851971.1# KC473454.1, KT429736.1* , KX851970.1# KT429746.1, KC473453.1, KT429756.1*

The corresponding SNP in Norwegian HSMI isolates are highlighted in red color

KC795571.1 CGA280-05, MK675848.1 NOR-2015/MS, MK675858.1 NOR-2015/SSK, KY429949.1 NOR2012V3621, GU994022.1 Salmo/GP-2010/NOR, KR337479.1 NOR-050607, MK675838.1 NOR-2005/TT, MK675828.1 NOR-1997

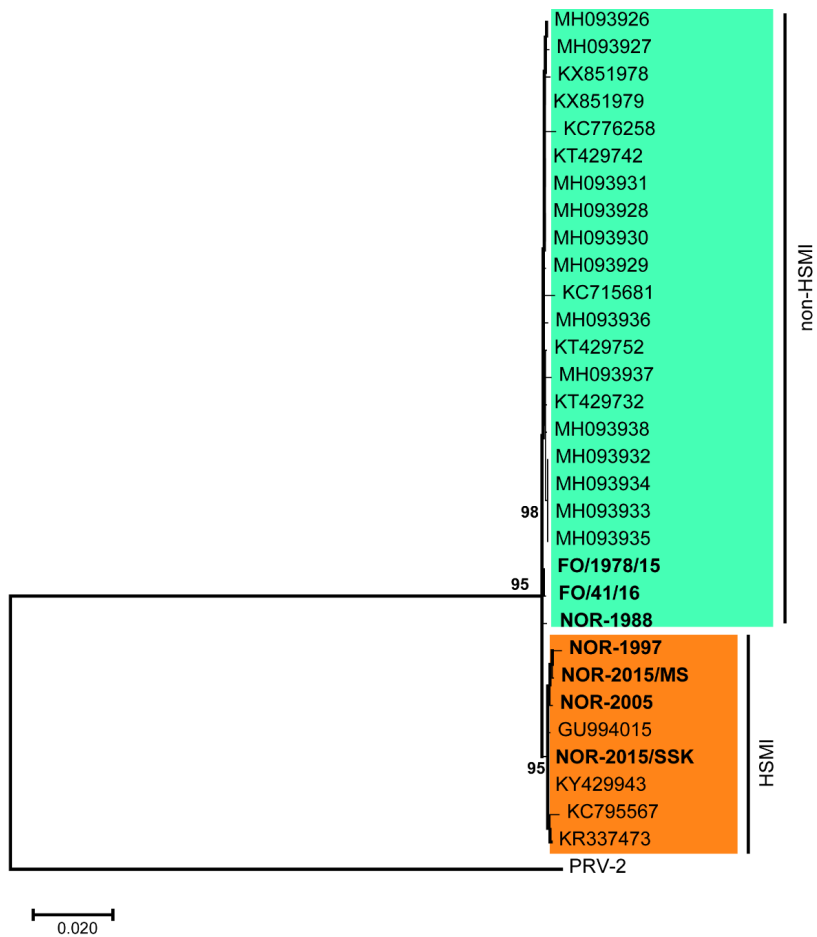
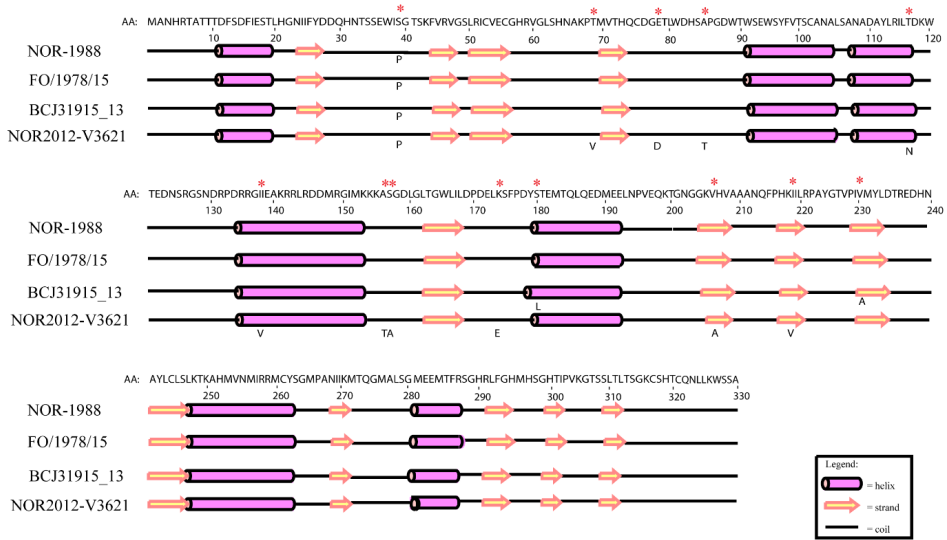


Fig. S1. Phylogenetic analysis of concatenated full genome amino acid sequences. PRV-2 is included as outgroup.

A. $\sigma 3$ protein



B. p13 protein

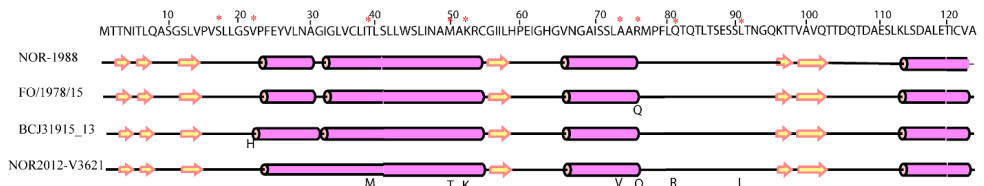


Fig. S2. Secondary structure predictions of $\sigma 3$ and p13 proteins showing similar structure between NOR2012 and selected non-HSMI-associated strains for both proteins, respectively. Amino acid differences are indicated by red asterisks. The amino acid difference is indicated below the alignment.

III

1 Temporal changes and localization of *Piscine orthoreovirus* (PRV) in
2 Atlantic Salmon (*Salmo salar*) during the development of heart and
3 skeletal muscle inflammation

4 Kannimuthu Dhamotharan¹, Håvard Bjørgen¹, Muhammad Salman Malik¹, Ingvild B. Nyman¹,
5 Turhan Markussen¹, Maria K. Dahle², Erling Olaf Koppang¹, Øystein Wessel¹, Espen Rimstad^{1*}

6 ¹Faculty of Veterinary Medicine, Norwegian University of Life Sciences, Oslo, Norway.

7 ²Department of Fish Health, Norwegian Veterinary Institute, Oslo, Norway.

8

9 *Corresponding author

10 E-mail: espen.rimstad@nmbu.no

11 **ABSTRACT**

12 *Piscine orthoreovirus* (PRV) associates with various diseases in salmonid fish such as heart and
13 skeletal muscle inflammation (HSMI) in Atlantic salmon. Here, the cellular distribution and
14 temporal changes in PRV-1 RNA and protein levels were analyzed in experimentally PRV infected
15 Atlantic salmon. Immunohistochemistry, flow cytometry and western blot were used for
16 assessment of viral proteins, and RT-qPCR and *in situ* hybridization were used for assessment of
17 viral RNA. Histopathologic evaluation demonstrated that PRV infection caused lesions typical of
18 HSMI like severe epicarditis and myocarditis with degeneration of cardiomyocytes, necrosis and
19 diffused cellular infiltration six weeks into the infectious course. Virus infection of erythrocytes
20 as well as levels of virus in plasma peaked at 4 weeks post challenge. The PRV RNA remained
21 high in erythrocytes but the protein level was abruptly reduced after 6 weeks post challenge. The
22 disproportionate RNA and protein level observed after the initial peak suggest possible

23 translational shutoff in infected erythrocytes. The peak of plasma viremia preceded PRV infection
24 in cardiomyocytes and hepatocytes. ISH demonstrated PRV positive staining of hepatocytes with
25 some multifocal intensely stained hepatocytes. The virus was cleared from regenerating heart
26 tissue and from hepatocytes, but persisted in erythrocytes. Arginase positive inflammatory cells
27 observed in the heart indicated possible polarization of M2 macrophages and early onset of
28 regenerative processes, most likely contributed to the fast onset of recovery after HSMI in this
29 trial.

30

31 INTRODUCTION

32 Heart and skeletal muscle inflammation (HSMI) is an emerging viral disease in farmed
33 Atlantic salmon (*Salmo salar*), which was first reported in Norway in 1999, and has since been
34 reported from Norway (1), Chile (2), Scotland (3) and Canada (4). HSMI is seen mainly in the
35 marine phase, but incidences have also been reported from broodstock farms and hatcheries (5).
36 Classical HSMI is caused by virulent variants of *Piscine orthoreovirus* (PRV) (6). The virus,
37 recognized as a species in the genus *Orthoreovirus*, family *Reoviridae*, packs its 10-segmented
38 dsRNA genome in a two layered, spherical shaped 80 nm diameter icosahedral particle (7). PRV
39 is a non-fusogenic orthoreovirus, and has an outer fiber protein which differ from other
40 orthoreoviruses (8). PRV is ubiquitous in the marine phase of farmed Atlantic salmon, but also
41 prevalent in wild Atlantic salmon (9) and among farmed and wild Pacific salmonids such as coho
42 and Chinook salmon (9-12). There are three known subtypes of PRV, where PRV-1 cause disease
43 in Atlantic salmon, PRV-2 in coho salmon and PRV-3 in rainbow trout.

44 Clinically, fish suffering from HSMI are anorexic and show aberrant swimming pattern,
45 and the accumulated mortality in disease outbreaks range from 0-20%. However, morbidity of

46 histopathological changes may be up to 100 % (1). In cohabitation challenge studies infected fish
47 develop histopathological changes in the heart, but no mortality (7). Histological investigations
48 show focal or diffused lesions with infiltration of inflammatory cells in the epicardium and
49 myocardium and vacuolation, loss of striation, necrosis and infiltration of mononuclear cells in red
50 skeletal muscle. In white skeletal muscle, the virus is associated with the occurrence of focal
51 melanised changes. Multifocal necrosis in liver, focal hemorrhage and accumulation of
52 erythrocytes in spleen and kidney are commonly observed in severely infected fish (13-15) .

53 Erythrocytes are the main target cells for PRV, nevertheless, PRV-1 in Atlantic salmon is
54 not reported to cause clinical anaemia (16). PRV replication occurs in the cytoplasm of infected
55 erythrocytes in inclusions called viral factories (17), and circulating infected erythrocytes are
56 found in any organ (18). In experimental infections there is a transient peak in the amount of PRV
57 proteins in erythrocytes 3-5 weeks post infection followed by a sharp drop (19), while the viral
58 RNA level stays relatively high (19).

59 PRV-1 is associated with jaundice syndrome and anaemia in Chinook salmon, but causation
60 studies are required for further confirmation. Affected fish develop degenerative necrosis in liver
61 and kidney, and necrotic hepatocytes contain high levels of hemoglobin (20). Erythrocytic
62 inclusion body syndrome (EIBS) in coho salmon in Japan is caused by PRV-2 (21). The infected
63 fish have viral inclusions in 80-100% of erythrocytes and the hematocrit value is reduced
64 significantly causing anaemia-associated mortalities (22). PRV-3 infects erythrocytes, is shown to
65 cause heart pathology in Rainbow trout (23) and is associated with jaundice in coho salmon (24).
66 Anemia is not consistently observed in PRV-3 infected Rainbow trout (25).

67 The various diseases and histopathological changes caused or associated with the subtypes
68 of PRV are mainly connected to clinical signs arising from effects on erythrocytes (anemia, EIBS),

69 heart (HSMI) and liver (jaundice). Variation in the outcome of infection could be related to virus
70 subtype and host species, but also to farming and production systems. Hence, characterization of
71 infected cells, amount of virus and mechanisms of infection throughout an experimental trial could
72 give more information on viral localization and temporal changes through the pathogenesis of
73 infection. In this study, we tracked and visualized PRV RNA and proteins in the erythrocytes, heart
74 and liver, in order to improve the understanding of the pathogenesis of PRV-1 infection in Atlantic
75 salmon. Immunohistochemistry, flow cytometry and western blot were used for PRV protein
76 assessment and RT-qPCR and ISH for evaluation of presence of viral RNA. This was combined
77 with histopathologic evaluation of morphological changes.

78 **MATERIALS AND METHODS**

79 **Challenge Experiment**

80 A challenge experiment was conducted at VESO Vikan aquatic research facility (Vikan,
81 Norway). The experiment had been approved by the Norwegian Food Safety Authority (NFDA)
82 according to the European Union Directive 2010/63/EU for animal experiments (permit number
83 11251). The experimental fish included 104 seawater-adapted Atlantic salmon (strain) with an
84 initial average weight of 100 grams. The fish were acclimatized for one week prior to challenge,
85 fed according to standard procedures and kept under 24 h light regime. The fish were confirmed
86 free of known salmon pathogens before initiation of the study. They were kept in tanks supplied
87 with particle filtered and UV treated seawater (34 ‰ salinity, 12 °C), observed minimum once a
88 day, anesthetized by bath immersion in benzocaine chloride (2-5 min, 0.5 g / 10 L water) prior to
89 handling and euthanized using concentrated benzocaine chloride (1 g / 5 L water).

90 The fish were divided into two groups. Half of the group (48 fish) was challenged by 0.1
91 uL/fish intramuscular injection with 60 000 copies of PRV-1 NOR 2012 strain, originating from

92 an HSMI outbreak in Norway (26). The virus had been purified according to previously published
93 procedures (26). The other half (48 fish) were challenged with 0.1 mL of DPBS (Thermo Fisher
94 Scientific). Eight fish were sampled prior to challenge, then eight fish from each group was
95 sampled every two weeks post challenge. Heparinized blood was collected from the caudal vein
96 for PRV analysis by RT-qPCR and flow cytometry. In addition, parallel tissue samples from heart
97 and liver were sampled in RNAlater (Life Technologies, Carlsbad, CA, USA) and 10% phosphate
98 buffered formalin, for RT-qPCR analysis, and histological analysis, immunohistochemical and in
99 situ staining, respectively.

100

101 **RNA isolation and RT-qPCR**

102 Heart tissues (25mg) and blood pellet (20 μ l) (n=6) were added 650 μ L QIAzol lysis reagent
103 (Qiagen). Samples were subsequently added 5 mm steel beads and homogenized using
104 TissueLyser II (Qiagen) for 2 \times 5 min at 25 Hz. After addition of chloroform, the samples were
105 centrifuged at 12 000 g for 15 mins and the aqueous phase was transferred to QIAcube (Qiagen)
106 for RNA extraction. The RNA purification procedure followed the manufacturer's instructions.
107 Total RNA was eluted in 50 μ L RNase-free water, concentration determined using NanoDrop ND-
108 1000 spectrophotometer (ThermoFisher Scientific). For plasma samples 10 μ l was diluted to 130
109 μ l in PBS and RNA was isolated using QIAmp viral RNA mini kit (Qiagen) following
110 manufacturer's instructions. RNA was eluted in 50 μ L elution buffer and stored at -80°C. Qiagen
111 OneStep RT-PCR kit (Qiagen) was used to perform RT-qPCR with 100 ng total RNA from tissues
112 or 5 μ l total RNA from plasma. The RNA was denatured at 95 °C for 5 mins. The reverse
113 transcription (RT) step was conducted at 50 °C for 30 min, followed by 95 °C for 15 min and 40

114 cycles of 94 °C/30 s, 55 °C/30 s, and 72 °C/30 s. The primers and probes used in the PRV-1
115 specific assay have previously been described (16).

116 **Western blot**

117 Plasma samples (n=3) from the challenge study were used in western blot analyses, and 14
118 µl plasma mixed with XT buffer and XT reducing agent (Bio-rad) were heated for 5 min at 95°C
119 and then loaded onto a 4–12% criterion XT bis-tris gel. Separated proteins were transferred onto
120 a PVDF membrane with Transblot Turbo (Bio-rad) at 15 V for 10 mins. The membranes were
121 blocked with 3% BSA in PBS and incubated overnight at 4 °C with antiserum against PRV-1 σ1
122 (1:1000) [32]. Horseradish peroxidase (HRP)-conjugated anti-rabbit IgG (Amersham, GE
123 Healthcare, Buckinghamshire, UK) (1:20,000) was used as secondary antibody. The Clarity
124 Western ECL Substrate kit was used for immunodetection (Bio-rad) and MagicMark as molecular
125 weight ladder (XP Western Protein Standard, Invitrogen). Images were acquired using ChemiDoc
126 XRS+ system and Image one software (Bio-rad).

127 **Flow cytometry**

128 Blood cells from the heparinized blood samples (n=6) were analyzed for PRV proteins σ1 flow
129 cytometry as previously described (7). In brief, 50 µL of heparinized blood was diluted 1:20 in
130 staining buffer, added into 96-well plates. The cells were fixed in IC fixation buffer (eBioscience,
131 San Diego, CA, USA) and washed in permeabilization buffer. The cells were stained with rabbit
132 polyclonal PRV-1 σ1 antibody (1:5000) for 30 mins. Followed by washing and staining with
133 secondary anti-rabbit IgG Alexa Fluor 488 (Molecular Probes, Eugene, Oregon, USA) (2 mg/mL
134 diluted 1:800) for 30 mins. The cells were counted in Gallios Flow Cytometer (Beckman Coulter,
135 Miami, FL, USA) and the data were analyzed using the Kaluza software (Becton Dickinson).

136 **Histology and Immunohistochemistry.**

137 Formalin fixed paraffin embedded (FFPE) heart tissues (n=6) were stained with hematoxylin
138 and eosin. The blocks were blinded and the histopathological changes in heart sections were scored
139 by a visual analog scale as described earlier (18). For immunohistochemistry, 4 μ m sections were
140 mounted on positively charged microscopic glass slides (Superfrost Plus, Thermo Fisher
141 Scientific, Waltham, MA) and deparaffinized for 60 mins at 60 °C followed by 2 changes in xylene
142 and absolute ethanol for 5 mins each. The sections were incubated with hydrogen peroxide for 10
143 mins to inactivate endogenous peroxidase, and then washed in distilled water and performed
144 antigen retrieval at 95-99°C for 15 mins in RNAscope target retrieval reagent. Slides were dried
145 at room temperature and a hydrophobic barrier was created around the sections with ImmEdge™
146 Hydrophobic Barrier Pen. Sections were blocked with normal goat serum diluted in 5% BSA in
147 PBS. Positive and negative control samples from previous challenge studies and 0 wpc non
148 infected samples, respectively were included. Slides were incubated overnight with anti PRV-1 σ 1
149 sera diluted (1:3000) (18) in 1% BSA in PBS, then washed with PBS and incubated with goat anti-
150 rabbit (Dako EnVision kit) HRP labelled secondary antibody. Finally, incubated with DAB
151 substrate chromogen for 5 mins to evoke color (brown) and counterstained with hematoxylin.

152 **In situ Hybridization**

153 RNAscope *in situ* hybridization or ISH, for PRV-1 L3 segment targeting nucleotides 415-
154 1379 (accession no. KY429945.1) (catalogue number 537451) and *Salmo salar* arginase targeting
155 nucleotides 1332-2053 of (XM_014190234.1) was performed using RNAscope 2.5 HD detection
156 red kit (Advanced Cell Diagnostics, Newark, CA, USA) according to manufacturer's instructions
157 and as described earlier (20). A 20 ZZ pair targeting *Salmo salar* peptidylprolyl isomerase B (ppib)
158 (PPIB) mRNA (Cat. No. 310043) was used as housekeeping control to check RNA quality, and a

159 probe against *Bacillus subtilis* strain SMY methylglyoxal synthase (mgsA) gene (cat. No. 310043)
160 was used as negative control.

161 In brief, FFPE sections were deparaffinized at 60 °C for 90 mins, transferred to xylene
162 followed by absolute ethanol 2 changes of each for 5 mins. The endogenous peroxidase blocking
163 was done with hydrogen peroxide for 10 mins at room temperature. The sections were boiled for
164 15 mins in RNAscope™ target retrieval buffer. Slides were incubated at 40°C for 15 mins with
165 RNAscope protease reagent prior to hybridization with PRV-1 RNAscope probe for 2 hrs at 40°C.
166 Slides were incubated with amplifiers, amp 1 to amp 6 for specified duration according to
167 manufacturer's recommendation and the signals were detected with fast RED. Counterstained the
168 slides with 50% Gill's Hematoxylin I for 10 mins and mounted in EcoMount. For dual staining of
169 IHC and ISH, after the antigen retrieval, slides were incubated with protease for 10 mins and
170 stained for *in situ* followed by blocking and then staining for IHC.

171 RESULTS

172

173 PRV in blood cells

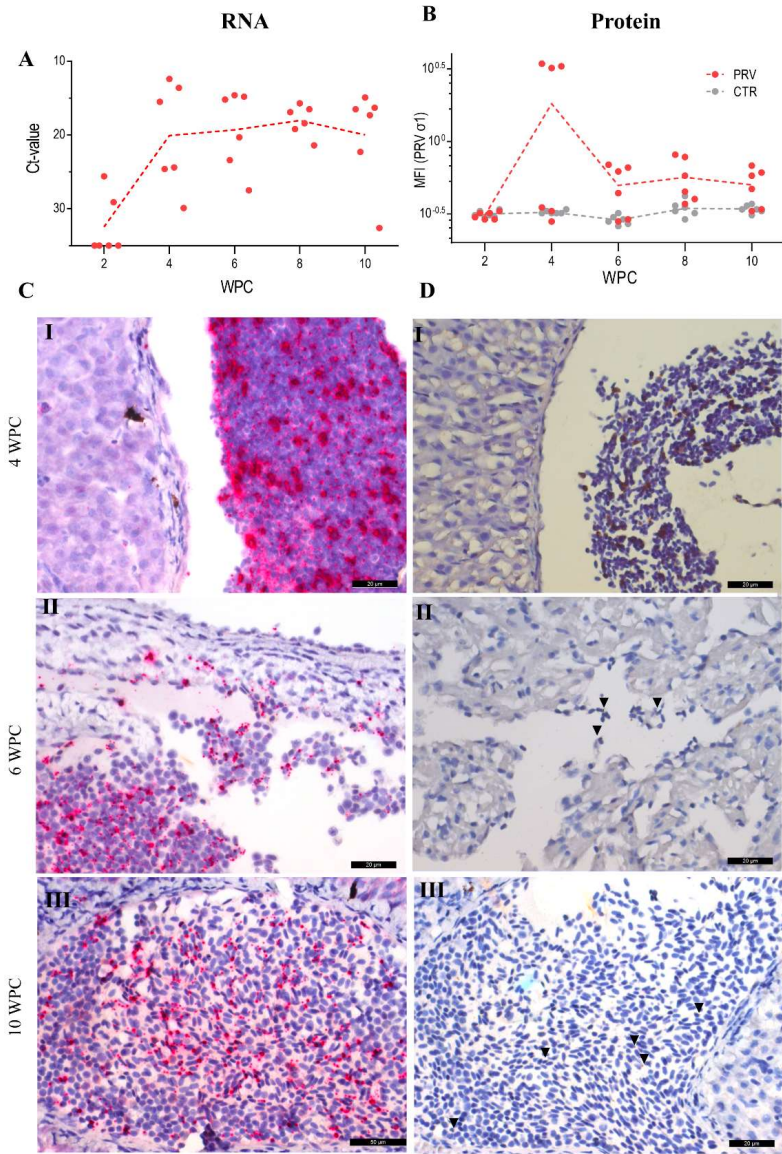
174 In blood cells, PRV RNA was first detected at 2 wpc by qPCR in two out of six fish, at
175 relatively low levels (Ct-value 25.6 and 29.1) (Fig 1A). At 4 wpc, the viral RNA load had increased
176 to a mean Ct-value of 20.0 ± 7.1 in the six fish, of which three fish presented with high loads of
177 PRV RNA (Ct-value 12.4-15.5). Thereafter, the load of viral RNA remained relatively high until
178 the end of the study at 10 wpc (Ct-value 19.9 ± 6.6).

179 PRV RNA in blood cells was also detected by *in situ* staining of tissue sections (Fig 2C). In
180 general, the PRV ISH staining in blood cells was in line with the kinetics observed by qPCR. At 4
181 wpc, many peripheral blood cells in heart and liver, assessed as mainly erythrocytes due to their

182 morphology, were heavily stained for PRV RNA (Fig 1C-I). The positive blood cells were
183 observed as peripheral cells within the cardiac chamber . At 6 wpc, both peripheral and infiltrating
184 blood cells in heart myocardium were PRV positive (Fig 1C-II). Blood cells continued to stain
185 heavily for PRV by ISH at 8 and 10 wpc (Fig 1C-III), correlating with low blood Ct-values detected
186 by qPCR.

187 Similar to PRV RNA, high loads of PRV σ 1-protein were observed by flow cytometry in
188 three out of six fish at 4 wpc (Fig 2B). This correlated with detection of PRV by
189 immunohistochemistry, where positive blood cells were found in blood clots in the heart and liver
190 (Fig 2D-I). However, post 4wpc the PRV protein level dropped substantially as observed by flow
191 cytometry (Fig 2B). Furthermore, only a limited number of faintly positive blood cells were
192 observed by immunostaining from 6-10 wpc (Fig 2 D-II and III). This is in contrast to the persistent
193 high levels of PRV RNA.

194



195

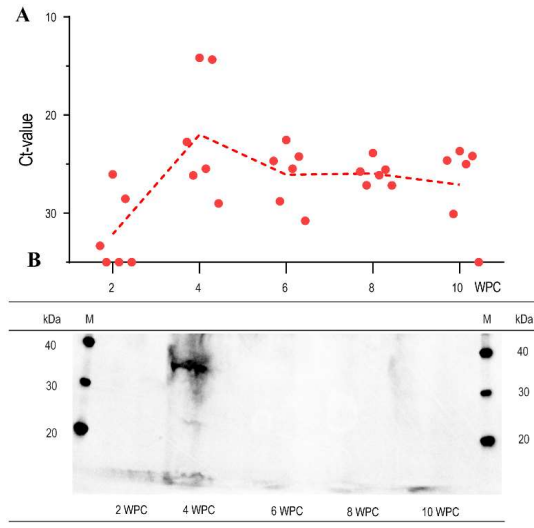
196 **Figure 1. PRV RNA and protein in blood cells**

197 A) PRV RNA detected by RT-qPCR, shown as Ct-values of individual fish (dots) and mean
 198 (dashed line) at each time point. B) PRV σ 1-protein detected by flow cytometry, shown as mean
 199 fluorescence intensity (MFI) for individual fish (dots) and mean (dashed line) at each time point.

200 Red: PRV infected group. Grey: Control group. C) PRV RNA detected in blood cells by *In situ*
201 hybridization (red color) and D) PRV σ 1-protein detected by immunohistochemistry (brown
202 staining) at 4 wpc (I), 6 wpc (II) and 10 wpc (III). Pictures show peripheral blood aggregates
203 observed in liver (I & III) and heart (II) sections. Scale bar 20 μ m. Arrowheads indicate positive
204 cells.
205

206 PRV load in plasma

207 The viral RNA load in plasma peaked at 4 wpc with mean Ct-value of 21.9 ± 6.3 , coinciding
208 with the peak of viral protein in blood cells. There was substantial individual variation, two fish
209 had especially low Ct-values 14.3 and 14.1, and with correspondingly low Ct-values of blood cells
210 (Fig. 2A). The viral RNA load in plasma decreased after 4 wpc, but was not cleared by 10 wpc
211 (mean Ct-value of 27.0 ± 4.5), i.e. at the end of the experiment. Similarly, PRV σ 1 protein were
212 detected by western blotting in plasma only at 4 wpc (Fig. 2B).



213
214

215 Figure 2. PRV-1 in plasma

216 A) Viral RNA load in plasma measured by RT-qPCR at 2, 4, 6, 8 and 10 weeks post infection
217 (wpc). Presented as individual Ct-values at each time point (n=6), including dashed line connecting
218 mean Ct-values. B) Viral protein load in plasma by western blotting using antibody targeting PRV-

219 1 σ 1 protein. The three samples with the lowest Ct-values from each sampling point were run in
220 the western blot. PRV σ 1-protein was only detected at 4 wpc (band at 35 kDa).

221
222
223

224 **PRV load in heart**

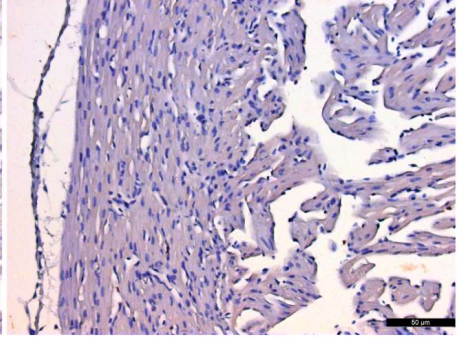
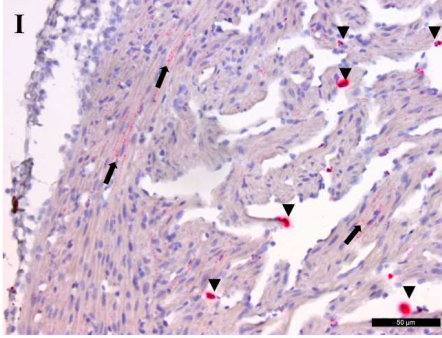
225 In the heart, PRV RNA was first detected by qPCR at 4 wpc (mean Ct-value 22.8 ± 5.2) (Fig.
226 3). Similarly, PRV RNA was detected by ISH in the heart at 4 wpc, demonstrated by less intense
227 and punctate staining of myocardial cells in stratum compactum and spongiosum (Fig. 4A-I). In
228 addition, a number of PRV positive blood cells were observed apparently attached to the
229 endothelial lining of the endocardium. At 6-8 wpc, peak ISH staining was observed in
230 cardiomyocytes, including the ventricle epicardium and in myocardial cells in the compactum and
231 spongiosum (Fig. 4A-II, III). The viral RNA load decreased thereafter with a mean Ct-value of
232 23.24 ± 2.4 at 10 wpc (Fig. 3), when only a few cardiomyocytes were positively stained by ISH.
233 However, PRV positive erythrocytes were observed intravasally and in infiltrating leukocyte-like
234 cells at 10 wpc.

235 In contrast, PRV σ 1-protein as demonstrated by IHC was present for a much shorter window
236 of time. No viral proteins could be detected in the cardiac tissue at 2-4 wpc (Fig. 4B-I). At 6 wpc,
237 PRV protein was detected in cardiomyocytes in the ventricle, where both compact and spongy
238 compartments of the myocardium were strongly stained by IHC (Fig. 4B-II). At 8 wpc, the staining
239 was reduced both by the number of positive cells and in intensity (Fig. 4B-III), and by 10 wpc no
240 positive cardiomyocytes could be detected (Fig. 4B-IV). Bulbous arteriosus was negative for
241 staining at all sampling points.

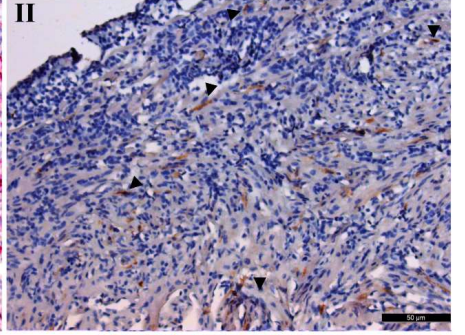
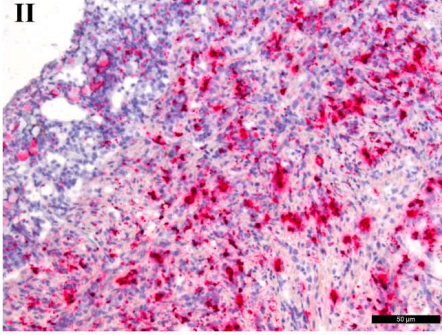
A. RNA

B. Protein

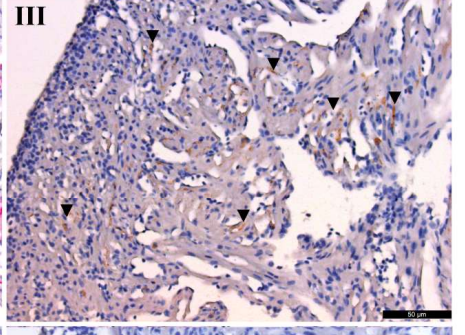
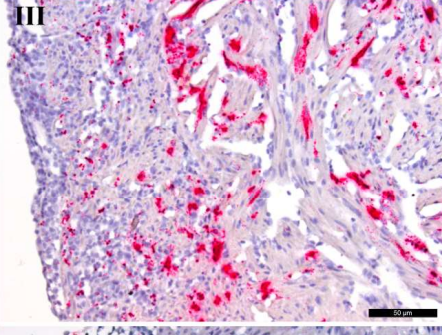
4 WPC



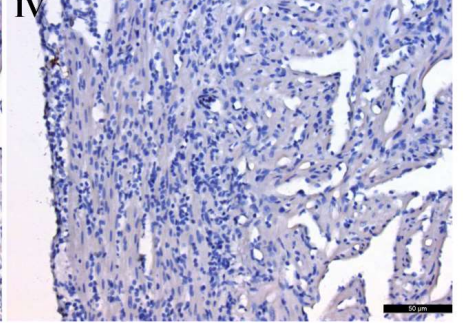
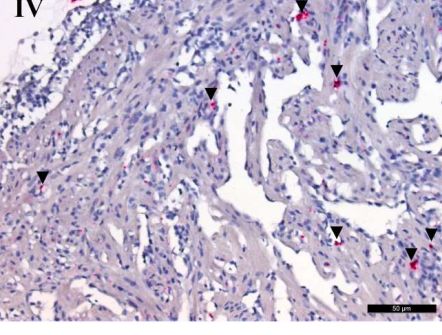
6 WPC



8 WPC



10 WPC



248 **Figure 4. PRV-1 RNA and protein in heart.**

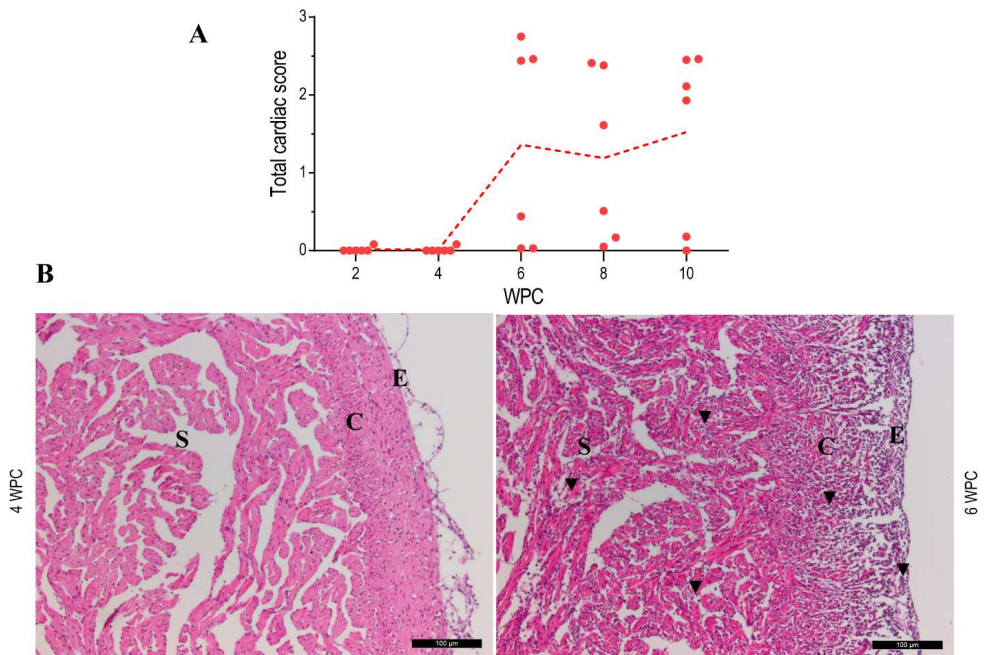
249 A) RNAScope *in situ* staining of PRV-1 L3 segment. I) Peripheral blood cells in heart tissue are
250 positive (arrow heads). Compact myocardial cell staining (arrow) appeared as few cytoplasmic
251 dots II-III) Heavy infection and staining in ventricle epicardium, endocardial cells with severe
252 epicarditis and myocarditis. IV) Cardiomyocytes are mostly negative at 10 wpc in a regenerating
253 heart tissue with positive infiltrated inflammatory cells (arrowheads) in spongy myocardium. B)
254 Immunohistochemical staining of PRV-1 $\sigma 1$ protein. II) Epicardium, compact and spongy
255 myocardium stained at 6 wpc III) Immunostained cells in spongy myocardium at 8 wpc. Scale bar
256 is given in lower right panel.

257

258 **Histological findings**

259 No histopathological changes were observed in heart or liver at 2 and 4 wpc (Fig. 5A). At
260 6wpc, severe epicarditis and myocarditis was observed (Fig. 5A). This included degeneration of
261 cardiomyocytes, loss of tissue architecture, necrosis and diffused cellular infiltration in epicardium
262 and myocardium (Fig. 5B). At 6 wpc, three out of six fish had cardiac pathology score higher than
263 2 (scale 0-3), corresponding in time to low Ct-values in heart. Most of the liver sections had normal
264 histoarchitecture, however, some of the hepatocytes showed slight degenerative changes in late
265 stage of infection, i.e. after 6 wpc.

266



267

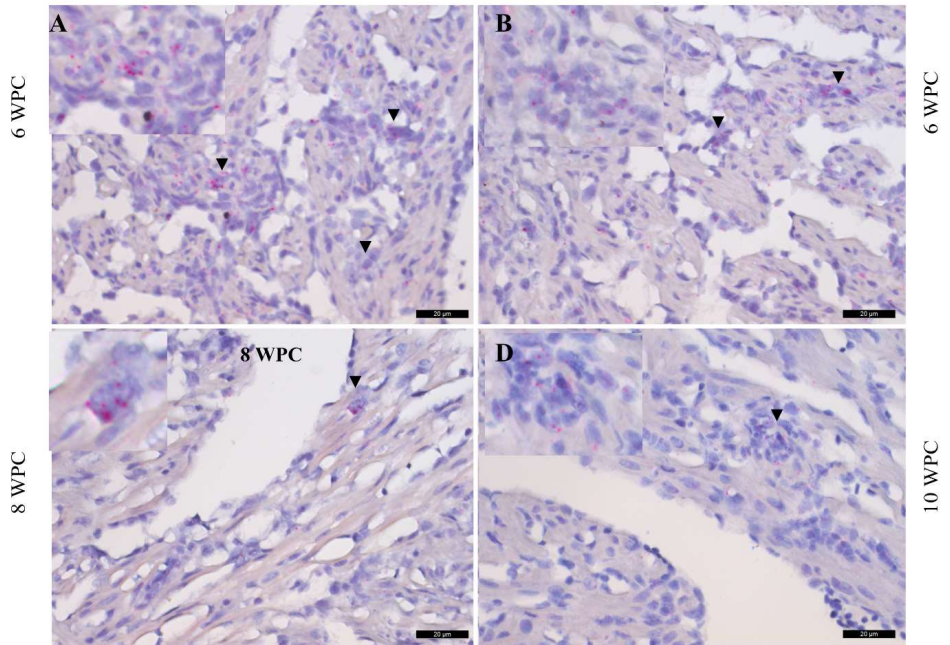
268 **Figure 5. Heart histopathology**

269 A) Histopathological score of HSMI fish (n=6) at 2, 4, 6, 8 and 10 wpc. B) Heart tissue from
 270 Atlantic salmon infected with purified PRV-1. Typical HSMI histopathological changes like
 271 severe degeneration, infiltration of inflammatory cells (highlighted in arrowheads), vacuolization,
 272 necrosis in epicardium (E), compact (C) and spongy (S) myocardium and loss of tissue architecture
 273 are visible in H & E stained tissues.

274

275 ***In situ* staining for Arginase-2 in Heart**

276 At 2 and 4 wpc, no ISH staining for arginase-2 in heart tissue was observed. Positively
 277 stained infiltrating macrophage- or leukocyte like cells were observed from 6 wpc. Highest number
 278 of positive cells were observed at 6 wpc (Fig 6).



279

280

281

282

283

284

285

PRV in liver

286

287

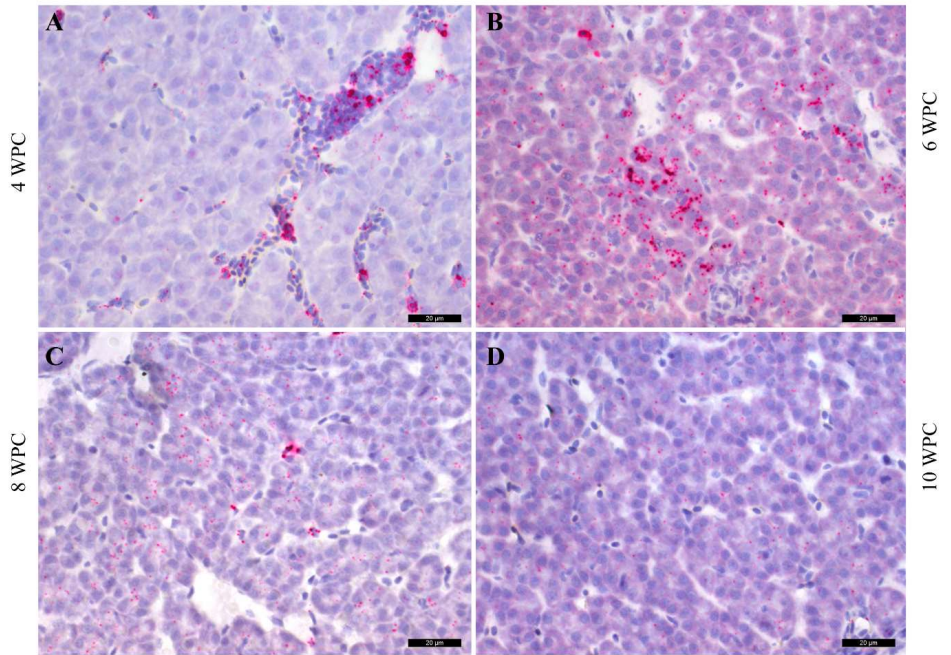
288

289

290

Figure 6. RNAscope *in situ* staining of Atlantic salmon Arginase-2 in heart tissues. Some of the infiltrating cells are immunostained (arrowheads). The magnified image is shown in subset in the top left

PRV ISH staining was negative at 2 wpc while a few hepatocytes were positive at 4 wpc (Fig. 7A). Focal intense staining of polygonal hepatocytes were observed at 6 wpc (Fig. 7B). Positive staining was observed from 8 to 10 wpc at low intensity (Fig. 7C-D). In liver sections, hepatocytes were negative by IHC staining throughout.



291

292 Figure 7. *In situ* staining of PRV-1 L3 segment. Peripheral blood erythrocytes and

293 neighboring hepatocytes stain positive from 4 to 10 wpc.

294

295 **DISCUSSION**

296 The aim of the present study was to closely monitor PRV infection and development of
297 HSMI in Atlantic salmon. Blood, heart and liver tissues were analyzed due to the central role for
298 PRV-1 pathogenesis in salmonids. All applied methods uniformly confirmed that erythrocytes are
299 the main initial target cells for PRV-1. The viral replication in erythrocytes and peak plasmic
300 viremia preceded cardiomyocytic and hepatocytic infection. The hepatocytes are permissive for
301 PRV-1, but not to the same degree as cardiomyocytes. PRV-1 was cleared from the
302 cardiomyocytes and hepatocytes while virus persisted in erythrocytes. The regeneration of the
303 heart was associated with arginase-positive macrophage-like cells. The erythrocytes were the first
304 cells observed to be infected by PRV-1, and 2 out of 6 fish were positive at 2 wpc with no other cell
305 types found virus positive at this stage. The PRV-1 load in erythrocytes peaked at 4 wpc as
306 observed by flow cytometry, immunohistochemical and *in situ* hybridization staining. At 4 wpc,
307 viral RNA and protein also peaked in plasma, which indicates that the erythrocytes are the source
308 of virus in plasma. In heart and liver, the ISH demonstrated positive staining of cells at 4 wpc, but
309 the staining was mainly on the luminal side of vessels, indicating invasion of virus to the tissue
310 from the luminal side

311 The i.p. injection of purified virus used in the present experiments assured even infection
312 load in the fish, and a similar infection course time- and dose-wise. However, this route of
313 infection does not reflect the natural port of entry. Previous experiments have demonstrated that
314 the virus dose in the inoculum influences the timing of the peak of infection, similar viral RNA
315 and protein kinetics have been observed in high and low virus dose challenge groups (7). Both
316 injection and mucosal route of infection induce HSMI, indicating that the route of exposure is not
317 essential for disease development (7). In the farming environment, virus uptake most likely occurs

318 through mucosal surfaces. “Reo” is an acronym for respiratory, enteric orphan, and as the name
319 implies, the gills and enteric system are the likely ports of entry. Anal administration has
320 demonstrated intestinal uptake of PRV (27). It is noteworthy that it takes relatively long time, i.e.
321 2 weeks after intramuscular virus injection in the present study, before PRV was detected in
322 erythrocytes. This does not indicate an immediate transfer of virus to blood and erythrocytes after
323 exposure. In the marine farm situation, with net pen populations of up to 200 000 individuals and
324 several nets, there will be ongoing virus shedding and spread for a long time.

325 In cohabitation models of PRV-1 challenge, the cohabitants are infected approximately 4
326 weeks after injection of the shedders, indicating the peak of viral shedding during this period (28).
327 At the peak of infection, cytoplasmic viral factories in erythrocytes are commonly observed (17).
328 In our experimental trial, the viral protein load declined rapidly in erythrocytes after 4 wpc., while
329 viral RNA stayed high. With a two weeks delay, i.e. after 6 wpc, a similar pattern was observed
330 in heart and liver tissues. All virus detection methods that were applied i.e. flow cytometry, IHC,
331 ISH and RT-qPCR, were in accordance with this. The sharp decline in viral protein in erythrocytes
332 has also been observed in previous studies (19). After the peak of infection, the erythrocytic viral
333 RNA level does not correspond with viral protein level (17), and in this study, similar observations
334 were made for heart and liver after 6 wpc. Salmon erythrocytes have a life span that is influenced
335 by water temperature, fish activity and many other factors (29). Young erythrocytes have a more
336 active transcription machinery than old ones (30), and will therefore probably be more suited as
337 host cells for replication of the virus.. In a former study, RTqPCR could detect viral RNA in blood
338 samples even after 59 weeks (31). The infection of erythroid progenitor cells has been indicated
339 in recent studies (32). The low viral protein level combined with a relatively high level of viral
340 RNA during later stages of infection in erythrocytes indicates that a translation shutoff mechanism

341 is activated in these cells. In MRV infected cells, translational shutoff has been demonstrated
342 through PKR and phosphorylation of the eukaryotic translation initiation factor (eIF)-2 α , as part
343 of the interferon-regulated antiviral response (33, 34). Further research would provide more
344 insights into the molecular control mechanisms of PRV replication in target cells, and the
345 persistence of PRV RNA in salmon erythrocytes. The fish erythrocyte could therefore be well-
346 suited cell type for long-term viral persistence and serve as a safe haven for persistent infection.

347 In the present study, Atlantic salmon injected with purified PRV-1 developed epicardial
348 and myocardial changes typical of HSMI from 6 wpc. The intensive PRV-1 staining observed in
349 the infected cardiomyocytes accompanying histopathologic lesions, indicated that the high viral
350 replication induce the infiltration of mononuclear cells characterized as heart inflammation and
351 pathology. The cardiomyocytic changes like vacuolation and cell death could be attributed to the
352 viral replication in these cells, or as secondary effects of the antiviral immune response. Further,
353 tissue damage would release cytokines or damage-associated molecules (DAMPs) that attract
354 immune cells to the site. The peak viral load in heart coincided with the infiltration of inflammatory
355 cells and high cardiac score, previously characterized to be dominated by CD8 positive T cells
356 (35). This indicates that cytotoxic CD8 positive cells help clear the virus from heart tissue. A
357 former study indicate that the PRV-specific antibody response also correspond in time to clearance
358 of virus and heart regeneration (36). The histopathological changes in the absence of detectable
359 viral RNA in cardiomyocytes, indicate efficient clearance of virus at 10wpc. Despite the clearance
360 in cardiomyocytes, the relatively low PRV Ct values observed by RT-qPCR in heart tissue could
361 be contributed to the presence of numerous infected circulating erythrocytes in heart vessels. It is
362 important to note here that histopathological scoring of heart tissues is independent of viral
363 presence. During a field HSMI outbreak, severely affected fish with irreparable heart damage and

364 associated circulatory failure succumb to death; however, most of the fish with severe heart
365 histopathology and high viral loads will survive the infection, as indicated by the low accumulated
366 mortality commonly observed for field outbreaks of HSMI. This indicate that most fish recover
367 through viral clearance and tissue regeneration, as teleost cardiomyocytes have the ability to
368 regenerate after an injury or infection (37).

369 Arginase expression in infiltrating cells, assumed to be mainly macrophages, were observed in
370 heart already from 6 wpc. Arginase enzyme converts L-arginine into L-ornithine and urea, and
371 ornithine is the precursor for polyamines and prolines, which is assumed necessary for wound
372 healing and regeneration (38). Thus, Arginase-2 is considered a cell marker for regenerating
373 macrophages in fish (39). Cytokines released from the infected tissue can polarize and activate
374 macrophages to participate in the regenerative processes (40). The finding of abundant cells
375 expressing arginase in the heart indicates an early onset of regenerative processes, which may
376 contribute to the relatively fast onset of recovery after HSMI. This indicates that severe HSMI
377 outcomes in the field situation may be linked to an impaired ability to regulate the regeneration
378 process.

379 In a previous PRV study where a higher virus dose was used for injection, the heart changes
380 peaked already at 4 wpc, indicating that the virus exposure dose influences the timing of the
381 infection (7). In the present study, the infection was not homogenous between the individual fish,
382 as higher vial load in cardiomyocytes could be seen by ISH at both 6 and 8 wpc in some
383 individuals. This demonstrates the impact of both infectious dose of virus and host factors
384 regarding timing and severity of heart pathologic changes.

385 Multifocal necrosis in liver tissues has been observed in Atlantic salmon with HSMI, but
386 without influx of inflammatory cells (20). In the present experiment, we observed that hepatocytes

387 stained positive for PRV RNA in ISH, and similar to the finding in heart the staining was mainly
388 at the luminal side of vessels in the liver during early infection. At 6 wpc, we found that
389 hepatocytes were in general infected at a low grade, as assessed by weak but punctuate staining,
390 whereas a few hepatocytes were more heavily infected. Whether the low grade of staining in the
391 hepatocytes mirrored actual replicating virus in the hepatocytes or merely engulfment if infected
392 erythrocytes or erythrocytic debris, were not clarified. The ISH staining of liver stayed low, and
393 did not indicate heavy virus replication. It could be concluded that the Atlantic salmon hepatocytes
394 are susceptible, but not very permissive to PRV-1 infection. This is in line with the a previous
395 study, however, extensive areas of hepatic necrosis have been observed in the heart failure cases
396 of HSMI (20). The lack of a subsequent infiltration of inflammatory cells in liver, in contrast to
397 that seen in the heart, indicates the differences in permissiveness between Atlantic salmon
398 hepatocytes and cardiomyocytes for PRV-1 replication.

399

400

401 REFERENCES

- 402 1. Kongtorp RT, Kjerstad A, Taksdal T, Guttvik A, Falk K. Heart and skeletal muscle
403 inflammation in Atlantic salmon, *Salmo salar* L: a new infectious disease. *J Fish Dis.*
404 2004;27(6):351-8.
- 405 2. Godoy MG, Kibenge MJT, Wang Y, Suarez R, Leiva C, Vallejos F, et al. First description
406 of clinical presentation of piscine orthoreovirus (PRV) infections in salmonid aquaculture in Chile
407 and identification of a second genotype (Genotype II) of PRV. *Virology Journal.* 2016;13(1):98.
- 408 3. Ferguson H, Kongtorp R, Taksdal T, Graham D, Falk K. An outbreak of disease resembling
409 heart and skeletal muscle inflammation in Scottish farmed salmon, *Salmo salar* L., with
410 observations on myocardial regeneration. *Journal of fish diseases.* 2005;28(2):119-23.
- 411 4. Di Cicco E, Ferguson HW, Schulze AD, Kaukinen KH, Li S, Vanderstichel R, et al. Heart
412 and skeletal muscle inflammation (HSMI) disease diagnosed on a British Columbia salmon farm
413 through a longitudinal farm study. *PLOS ONE.* 2017;12(2):e0171471.
- 414 5. Hjeltnes B BJB, Haukaas A, Wlode C, S (Ed.). *The Fish Health Report 2017: The*
415 *Norwegian Veterinary Institute 2018; 2018.*

- 416 6. Dhamotharan K, Tengs T, Wessel Ø, Braaen S, Nyman IB, Hansen EF, et al. Evolution of
417 the piscine orthoreovirus genome linked to emergence of heart and skeletal muscle inflammation
418 in farmed Atlantic salmon (*Salmo salar*). 2019;11(5):465.
- 419 7. Wessel Ø, Braaen S, Alarcon M, Haatveit H, Roos N, Markussen T, et al. Infection with
420 purified Piscine orthoreovirus demonstrates a causal relationship with heart and skeletal muscle
421 inflammation in Atlantic salmon. PLOS ONE. 2017;12(8):e0183781.
- 422 8. Key T, Read J, Nibert ML, Duncan R. Piscine reovirus encodes a cytotoxic, non-fusogenic,
423 integral membrane protein and previously unrecognized virion outer-capsid proteins. Journal of
424 General Virology. 2013;94(5):1039-50.
- 425 9. Garseth ÅH, Ekrem T, Biering E. Phylogenetic evidence of long distance dispersal and
426 transmission of piscine reovirus (PRV) between farmed and wild Atlantic salmon. PLOS ONE.
427 2013;8(12):e82202.
- 428 10. Garseth AH, Fritsvold C, Opheim M, Skjerve E, Biering E. Piscine reovirus (PRV) in wild
429 Atlantic salmon, *Salmo salar* L., and sea-trout, *Salmo trutta* L., in Norway. J Fish Dis.
430 2013;36(5):483-93.
- 431 11. Purcell MK, Powers RL, Evered J, Kerwin J, Meyers TR, Stewart B, et al. Molecular
432 testing of adult Pacific salmon and trout (*Oncorhynchus* spp.) for several RNA viruses
433 demonstrates widespread distribution of piscine orthoreovirus in Alaska and Washington. Journal
434 of Fish Diseases. 2018;41(2):347-55.
- 435 12. Wiik-Nielsen CR, Lovoll M, Sandlund N, Faller R, Wiik-Nielsen J, Bang Jensen B. First
436 detection of piscine reovirus (PRV) in marine fish species. Dis Aquat Organ. 2012;97(3):255-8.
- 437 13. Kongtorp RT, Taksdal T, Lyngøy A. Pathology of heart and skeletal muscle inflammation
438 (HSMI) in farmed Atlantic salmon *Salmo salar*. Diseases of Aquatic Organisms. 2004;59(3):217-
439 24.
- 440 14. Bjorgen H, Wessel O, Fjellidal PG, Hansen T, Sveier H, Saebo HR, et al. Piscine
441 orthoreovirus (PRV) in red and melanised foci in white muscle of Atlantic salmon (*Salmo salar*).
442 Vet Res. 2015;46:89.
- 443 15. Bjørgen H, Haldorsen R, Oaland Ø, Kvellestad A, Kannimuthu D, Rimstad E, et al.
444 Melanized focal changes in skeletal muscle in farmed Atlantic salmon after natural infection with
445 Piscine orthoreovirus (PRV). 2019;42(6):935-45.
- 446 16. Finstad OW, Dahle MK, Lindholm TH, Nyman IB, Lovoll M, Wallace C, et al. Piscine
447 orthoreovirus (PRV) infects Atlantic salmon erythrocytes. Vet Res. 2014;45:35.
- 448 17. Haatveit HM, Nyman IB, Markussen T, Wessel O, Dahle MK, Rimstad E. The non-
449 structural protein muNS of piscine orthoreovirus (PRV) forms viral factory-like structures. Vet
450 Res. 2016;47:5.
- 451 18. Finstad OW, Falk K, Lovoll M, Evensen O, Rimstad E. Immunohistochemical detection
452 of piscine reovirus (PRV) in hearts of Atlantic salmon coincide with the course of heart and skeletal
453 muscle inflammation (HSMI). Vet Res. 2012;43:27.
- 454 19. Haatveit H, Wessel Ø, Markussen T, Lund M, Thiede B, Nyman I, et al. Viral protein
455 kinetics of piscine orthoreovirus infection in Atlantic salmon blood cells. Viruses. 2017;9(3):49.
- 456 20. Di Cicco E, Ferguson HW, Kaukinen KH, Schulze AD, Li S, Tabata A, et al. The same
457 strain of Piscine orthoreovirus (PRV-1) is involved in the development of different, but related,
458 diseases in Atlantic and Pacific Salmon in British Columbia. FACETS. 2018;3(1):599-641.
- 459 21. Takano T, Nawata A, Sakai T, Matsuyama T, Ito T, Kurita J, et al. Full-genome sequencing
460 and confirmation of the causative agent of erythrocytic inclusion body syndrome in coho salmon
461 identifies a new type of piscine orthoreovirus. PLoS One. 2016;11(10):e0165424.

- 462 22. Okamoto N, Takahashi K, Maita M, Rohovec JS, Ikeda Y. Erythrocytic inclusion body
463 syndrome : susceptibility of selected sizes of coho salmon and of several other species of salmonid
464 fish. *Fish Pathology*. 1992;27(3):153-6.
- 465 23. Vendramin N, Kannimuthu D, Olsen AB, Cuenca A, Teige LH, Wessel Ø, et al. Piscine
466 orthoreovirus subtype 3 (PRV-3) causes heart inflammation in rainbow trout (*Oncorhynchus*
467 *mykiss*). 2019;50(1):14.
- 468 24. Bohle H, Bustos P, Leiva L, Grothusen H, Navas E, Sandoval A, et al. First complete
469 genome sequence of piscine orthoreovirus variant 3 infecting coho salmon (*Oncorhynchus kisutch*)
470 farmed in southern Chile. *Genome Announcements*. 2018;6(24).
- 471 25. Vendramin N, Alencar ALF, Iburg TM, Dahle MK, Wessel O, Olsen AB, et al. Piscine
472 orthoreovirus infection in Atlantic salmon (*Salmo salar*) protects against subsequent challenge
473 with infectious hematopoietic necrosis virus (IHNV). *Vet Res*. 2018;49(1):30.
- 474 26. Hauge H, Vendramin N, Taksdal T, Olsen AB, Wessel Ø, Mikkelsen SS, et al. Infection
475 experiments with novel Piscine orthoreovirus from rainbow trout (*Oncorhynchus mykiss*) in
476 salmonids. *PLOS ONE*. 2017;12(7):e0180293.
- 477 27. Hauge H, Dahle M, Moldal T, Thoen E, Gjevre AG, Weli S, et al. Piscine orthoreovirus
478 can infect and shed through the intestine in experimentally challenged Atlantic salmon (*Salmo*
479 *salar* L.). *Vet Res*. 2016;47(1):57.
- 480 28. Kongtorp R, Taksdal T. Studies with experimental transmission of heart and skeletal
481 muscle inflammation in Atlantic salmon, *Salmo salar* L. *Journal of fish diseases*. 2009;32(3):253-
482 62.
- 483 29. Witeska M. Erythrocytes in teleost fishes: a review. *Zoology and Ecology*. 2013;23(4):275-
484 81.
- 485 30. Götting M, Nikinmaa MJ. Transcriptomic analysis of young and old erythrocytes of fish.
486 *Front Physiol*. 2017;8:1046-.
- 487 31. Garver KA, Johnson SC, Polinski MP, Bradshaw JC, Marty GD, Snyman HN, et al. Piscine
488 orthoreovirus from western north America is transmissible to Atlantic salmon and sockeye salmon
489 but fails to cause heart and skeletal muscle inflammation. *PLoS One*. 2016;11(1):e0146229.
- 490 32. Malik MS, Bjørgen H, Dhamotharan K, Wessel Ø, Koppang EO, Di Cicco E, et al.
491 Erythroid Progenitor Cells in Atlantic Salmon (*Salmo salar*) May Be Persistently and Productively
492 Infected with Piscine Orthoreovirus (PRV). 2019;11(9):824.
- 493 33. Smith JA, Schmechel SC, Williams BRG, Silverman RH, Schiff LA. Involvement of the
494 interferon-regulated antiviral proteins PKR and RNase L in reovirus-induced shutoff of cellular
495 translation. 2005;79(4):2240-50.
- 496 34. Lanoie D, Boudreault S, Bisaillon M, Lemay G. How Many Mammalian Reovirus Proteins
497 are involved in the Control of the Interferon Response? *Pathogens*. 2019;8(2):83.
- 498 35. Mikalsen AB, Haugland O, Rode M, Solbakk IT, Evensen O. Atlantic salmon reovirus
499 infection causes a CD8 T cell myocarditis in Atlantic salmon (*Salmo salar* L.). *PLoS One*.
500 2012;7(6):e37269.
- 501 36. Teige LH, Lund M, Haatveit HM, Røsæg MV, Wessel Ø, Dahle MK, et al. A bead based
502 multiplex immunoassay detects Piscine orthoreovirus specific antibodies in Atlantic salmon
503 (*Salmo salar*). *Fish & Shellfish Immunology*. 2017;63:491-9.
- 504 37. Poss KD, Wilson LG, Keating MT. Heart regeneration in zebrafish. *Science*.
505 2002;298(5601):2188-90.
- 506 38. Caldwell RB, Toque HA, Narayanan SP, Caldwell RW. Arginase: an old enzyme with new
507 tricks. *Trends in pharmacological sciences*. 2015;36(6):395-405.

- 508 39. Wiegertjes GF, Wentzel AS, Spaink HP, Elks PM, Fink IR. Polarization of immune
509 responses in fish: The 'macrophages first' point of view. *Molecular Immunology*. 2016;69:146-
510 56.
- 511 40. Forlenza M, Fink IR, Raes G, Wiegertjes GF. Heterogeneity of macrophage activation in
512 fish. *Developmental & Comparative Immunology*. 2011;35(12):1246-55.
513
- 514

III

Article

Molecular and Antigenic Characterization of *Piscine orthoreovirus* (PRV) from Rainbow Trout (*Oncorhynchus mykiss*)

Kannimuthu Dhamotharan ¹, Niccolò Vendramin ², Turhan Markussen ¹, Øystein Wessel ¹ ,
Argelia Cuenca ², Ingvild B. Nyman ¹, Anne Berit Olsen ³, Torstein Tengs ¹,
Maria Krudtaa Dahle ⁴ and Espen Rimstad ^{1,*} 

¹ Department of Food Safety and Infection Biology, Faculty of Veterinary Medicine, Norwegian University of Life Sciences, 0454 Oslo, Norway; dhamokan@nmbu.no (K.D.); oystein.wessel@nmbu.no (Ø.W.); turhan.markussen@nmbu.no (T.M.); ingvild.nyman@nmbu.no (I.B.N.); torstein.tengs@nmbu.no (T.T.)

² National Institute of Aquatic Resources, Technical University of Denmark, 2800 Kgs. Lyngby, Denmark; niven@vet.dtu.dk (N.V.); arcun@vet.dtu.dk (A.C.)

³ Norwegian Veterinary Institute, 5003 Bergen, Norway; anne-berit.olsen@vetinst.no

⁴ Norwegian Veterinary Institute, 0454 Oslo, Norway; maria.dahle@vetinst.no

* Correspondence: espen.rimstad@nmbu.no; Tel.: +47-672-32-227

Received: 7 March 2018; Accepted: 28 March 2018; Published: 2 April 2018



Abstract: *Piscine orthoreovirus* (PRV-1) causes heart and skeletal muscle inflammation (HSMI) in farmed Atlantic salmon (*Salmo salar*). Recently, a novel PRV (formerly PRV-Om, here called PRV-3), was found in rainbow trout (*Oncorhynchus mykiss*) with HSMI-like disease. PRV is considered to be an emerging pathogen in farmed salmonids. In this study, molecular and antigenic characterization of PRV-3 was performed. Erythrocytes are the main target cells for PRV, and blood samples that were collected from experimentally challenged fish were used as source of virus. Virus particles were purified by gradient ultracentrifugation and the complete coding sequences of PRV-3 were obtained by Illumina sequencing. When compared to PRV-1, the nucleotide identity of the coding regions was 80.1%, and the amino acid identities of the predicted PRV-3 proteins varied from 96.7% ($\lambda 1$) to 79.1% ($\sigma 3$). Phylogenetic analysis showed that PRV-3 belongs to a separate cluster. The region encoding $\sigma 3$ were sequenced from PRV-3 isolates collected from rainbow trout in Europe. These sequences clustered together, but were distant from PRV-3 that was isolated from rainbow trout in Norway. Bioinformatic analyses of PRV-3 proteins revealed that predicted secondary structures and functional domains were conserved between PRV-3 and PRV-1. Rabbit antisera raised against purified virus or various recombinant virus proteins from PRV-1 all cross-reacted with PRV-3. Our findings indicate that despite different species preferences of the PRV subtypes, several genetic, antigenic, and structural properties are conserved between PRV-1 and-3.

Keywords: *Piscine orthoreovirus*; heart- and skeletal muscle inflammation; PRV-3; rainbow trout

1. Introduction

Rainbow trout (*Oncorhynchus mykiss*) is farmed in a variety of aquaculture systems in many countries [1]. Traditionally, rainbow trout is farmed in freshwater systems for production of portion size fish (300 g), while larger fish (3–5 kg) can be produced when fish are kept in seawater for the major grow-out period. In Norway, rainbow trout is primarily produced in seawater, and the loss of fish through the seawater stage has been estimated to 19% of the fish, mostly linked to infectious diseases [2].

In 2013, a new infectious disease was reported in rainbow trout in Norway. The disease occurred in freshwater hatcheries lasting until after sea transfer, and was characterized by lesions resembling those of heart and skeletal muscle inflammation (HSMI) in Atlantic salmon (*Salmo salar*), and by anemia [3]. HSMI in Atlantic salmon is caused by *Piscine orthoreovirus* (PRV) [4,5]. Screening for pathogens in the diseased rainbow trout revealed the presence of a PRV-like virus, and the nucleotide sequence that was obtained for a 562 nt region of the S1 genomic segment revealed 85% identity to PRV [3]. Experimental challenge studies in rainbow trout using blood as infective material, showed efficient viral replication in blood cells and in heart [6]. Recently, a PRV that was genetically similar to the rainbow trout PRV was reported in Coho salmon (*Oncorhynchus kisutch*) in Chile, suffering from an HSMI-like disease [7].

HSMI was first reported in Atlantic salmon in Norway in 2004, and occurs primarily in the marine phase. The disease leads to low to moderate mortality (0–20%), but has usually close to 100% morbidity [8]. The fish appear lethargic and anorectic and the histopathological changes include mild to severe inflammatory changes in the compact and spongy layer of the myocardium with similar, but milder changes in red skeletal muscle [9]. Disease outbreaks were initially reported to occur primarily five to nine months after seawater transfer [10], but now commonly occur earlier with an increasing number being detected already in the fresh water stage prior to sea water transfer [2].

PRV is recognized as a species of the genus *Orthoreovirus*, sub-family *Spinareovirinae*, family *Reoviridae*. It is a non-enveloped, icosahedral non-fusogenic virus with a double-stranded RNA (dsRNA) genome consisting of 10 linear segments L1-3, M1-3, S1-4 [4,11]. PRV is ubiquitous in seawater farmed Atlantic salmon, but has also frequently been detected in apparently healthy wild Atlantic salmon and in sea trout (*Salmo trutta*) [12]. The causality between a Norwegian PRV isolate and HSMI in Atlantic salmon was recently proven [5], but others report experimental PRV infection without pathology [13]. No viral genetic markers that were linked to virulence have been identified so far. In farmed Atlantic salmon, PRV is now found to be present from freshwater pre-smolts until slaughter, and the prevalence of infection increases after the sea transfer [14]. PRV infection in Atlantic salmon and cases of HSMI have also been reported from Scotland, Chile, and western North America [7,15–17].

A third variant of PRV, named PRV-2, was recently recognized as the causative agent of erythrocytic inclusion body syndrome (EIBS) in Coho salmon in Japan [18]. As the name of the disease implies, erythrocytes are the main target cells for PRV-2, which are similar to PRV in Atlantic salmon. The genomic organization of the Coho salmon PRV closely resembles that of the Atlantic salmon PRV. Comparisons at the whole genome level revealed however that the Coho salmon virus is genetically distinct, with a nucleotide identity of 73.4% in the coding regions [18]. In addition, a virus resembling PRV has been isolated from wild freshwater fish, largemouth bass (*Micropterus salmoides*), during a disease outbreak, and named large mouth bass reovirus (LMBRV) [19].

In this study, we have sequenced and analyzed the coding regions and the protein sequences of the PRV variant infecting rainbow trout, and analyzed the antigenic properties of this virus when compared to the PRV variant causing HSMI in Atlantic salmon. The phylogenetic analyses revealed that the rainbow trout PRV is genetically different from Atlantic salmon PRV. In line with the nomenclature used for the PRV infecting Coho salmon in Japan, i.e., PRV-2, we propose to name the PRV subtype infecting Atlantic salmon PRV-1, and the PRV subtype infecting rainbow trout PRV-3 (previously named PRV-Om).

2. Materials and Methods

2.1. Challenge Experiments

An *in vivo* experiment to generate PRV-3 positive material was carried out in the experimental facilities at DTU-VET in Denmark in accordance with the recommendations that are outlined in the current animal welfare regulations, under license No. 2013-15-2934-00976. The experimental protocols were approved by the Danish Animal Research Authority. The health status of the fish and

environmental conditions were monitored on a daily basis during the experiments. Rainbow trout eyed eggs were provided by a commercial Danish fish farm that is officially free of infectious pancreatic necrosis virus (IPNV), infectious hematopoietic necrosis virus (IHNV), viral hemorrhagic septicemia virus (VHSV), and bacterial kidney disease (BKD). Following disinfection with iodine, the fish eggs were hatched and grown in the wet laboratory facilities at the European Union Reference Laboratory for fish disease (EURL, Copenhagen, Denmark) in UV-disinfected, recirculated tap water. Prior to infection, the rainbow trout were moved into a high containment facility harboring flow-through fresh water system, with a temperature of $12\text{ }^{\circ}\text{C} \pm 1\text{ }^{\circ}\text{C}$. For the production of challenge material, fish ($n = 15$) with an average weight of 270 g were anesthetized in water containing benzocaine (80 mg/L, Sigma) and injected i.p. with 0.1 mL homogenized blood cell pellet from PRV-3 infected fish diluted 1:4 (*v/v*) in L-15 medium. The virus isolate (NOR/060214) originated from a rainbow trout hatchery in Norway. The PRV-3 levels were monitored weekly by non-lethal blood sampling from five fish, which were marked by clipping of the adipose fin to avoid repeated sampling of the same fish. At three weeks post challenge (wpc), all of the fish were euthanized by immersing fish in water containing high concentration of benzocaine (800 mg/L). Blood was collected in heparin tubes, tested for PRV-3 levels by RT-qPCR, and stored at $4\text{ }^{\circ}\text{C}$. Plasma samples from the blood pellet were used for Illumina sequencing.

Another challenge trial was carried out in the NMBU aquarium research facility in Oslo, Norway in accordance with the recommendations of current animal welfare regulations, and the protocols were approved by the Norwegian Animal Research Authority. Rainbow trout from AquaGen AS ($n = 22$), average weight of 580 g were used. Upon challenge, the fish were anesthetized, as described above, and i.p. injected with 0.1 mL lysate from PRV-3-infected blood cells (1:3 dilution) originating from the previous experiment (Ct 22.8). The fish were reared in 500 L tanks with flow through freshwater and hand-fed a commercial diet (Skretting, Stavanger, Norway), at a rate of 2% of calculated biomass/tank/day. The PRV-3 viral load was determined weekly by RT-qPCR of blood collected by non-lethal blood sampling from the caudal vein of three anesthetized fish, which were marked by clipping of the adipose fin to avoid repeated sampling. When the Ct level for PRV-3 in 100 ng blood cell RNA were below lower than 25, the fish were euthanized, and blood collected on heparinized tubes. PRV-3 was purified from two blood samples (Ct 17.8 and 19.7). Purified virus was used for transmission electron microscopy and western blotting.

2.2. Virus Purification

Purification of PRV particles was performed, as previously described using CsCl density gradient and optimized for PRV from heparinized salmon blood sample [5,20]. In brief, 0.5 mL heparinized blood was mixed with 4.5 mL L15 medium and homogenized by sonication at 20 kHz for 30 s. Then, 10% sodium deoxycholate (SOC) was added (1:50), the samples were vortexed and left to stand for 5 min. This was repeated once, and samples were then incubated for 30 min on ice, emulsified with solvent vertrel XF, and centrifuged at $9000\times g$ for 10 min at $4\text{ }^{\circ}\text{C}$ to remove cell debris. The supernatant (4.2 mL) was layered over a CsCl gradient composed of 4.2 mL, 1.22 g/mL, and 4.2 mL 1.45 g/mL. Ultracentrifugation was performed at $30,000\times \text{rpm}$ for 16 h, $4\text{ }^{\circ}\text{C}$ using a SW 40TI rotor (Beckman Coulter, Brea, CA, USA) in an Optima LE 80K Ultracentrifuge (Beckman). Fractions of 0.5 mL were collected using a syringe with a 23 G needle. The density of the fractions was determined by cross referencing the refractive index [21]. The viral loads of all the fractions were estimated by RT-qPCR [5]. Fractions with a density corresponding to that of PRV-1 and low Ct values were chosen for dialysis. Samples were injected into Slide-A-Lyzer Cassette (G2 3.5 kDa MWCO, Thermo Fisher Scientific) and dialyzed at $4\text{ }^{\circ}\text{C}$ with Dulbecco's PBS without Mg or Ca (Sigma-Aldrich) for 1 h, 3 h, and then finally 12 h, separated by buffer changes.

2.3. Transmission Electron Microscopy (TEM)

Ten microliters of the dialyzed samples were used for TEM imaging. Samples were placed on paraffin film, and the 100 mesh carbon coated copper grids were placed over the drop for 1 min, washed 5× with distilled water, and stained with 4% aqueous uranyl acetate acid for 3 s. Excess liquid was removed and the grids were inspected in JEM 1400 Electron Microscope (JEOL Ltd., Tokyo, Japan), equipped with a TVIPS TemCam-F216 camera (TVIPS GmbH, Gauting, Germany).

2.4. RNA Isolation and RT-qPCR

Total RNA was isolated from pelleted blood cells, purified viral particles, and plasma. A total of 10 µL purified virus and plasma were diluted to 130 µL in PBS and added 420 µL Trizol LS (Life Technologies). For blood pellet, a volume of 20 µL was added to 650 µL Qiazol (Qiagen). The samples were homogenized in QIAzol Lysis Reagent using 5 mm steel beads and TissueLyser II (Qiagen) for 2 × 5 min at 25 Hz. After the addition of chloroform, the samples were centrifuged and the aqueous phase was transferred to RNeasy Mini spin column (Qiagen, Hilden, Germany). The RNA purification followed the manufacturer's instructions. The RNA was stored at −80 °C. The RT-qPCR assays were performed using the Qiagen OneStep RT-PCR kit (Qiagen) adding 5 µL total RNA to each reaction tube, following the reaction conditions that were recommended by the manufacturer. The reverse transcription (RT) step was conducted at 50 °C for 30 min, followed by 95 °C for 15 min and 40 cycles of 94 °C/30 s, 55 °C/30 s, and 72 °C/30 s. The primers and probes used in the PRV-3 specific assay have previously been described [3].

2.5. Illumina Sequencing and Genome Assembly

Total RNA extracted from 2 mL of pooled plasma originating from two individuals (Ct 25.78 and 26), from challenge trial 1 was added 0.1 volumes of 3 M sodium acetate (pH 7.5) and 2X volumes of 100% ethanol, and mixed gently. Macrogen (Seoul, Korea) performed library preparation using the TruSeq RNA Library Prep Kit v2 (Illumina Inc., San Diego, CA, USA), followed by whole genome de novo sequencing (101 bases, paired-end reads) on an Illumina HiSeq4000 platform (1/7th lane). Sequences were de novo assembled using the genome assembler software SPAdes (version 3.10.1) [22].

2.6. Sequence and Phylogenetic Analyses

Multiple sequence alignments were performed using AlignX (Vector NTI Advance™ 11 package, InfoMax, Inc.) and phylogenetic analysis in MEGA7 software [23]. Pairwise nucleotide and amino acid sequence identities were calculated using the Sequences Identities and Similarities (SIAS) server (<http://imed.med.ucm.es/Tools/sias.html>). Protein secondary structure predictions were performed using PSIPRED v3.3, which is available at <http://bioinf.cs.ucl.ac.uk/psipred/> [24]. The mVISTA methods of alignment was used for the comparison of concatenated complete coding sequences of PRV-3 genome segments with PRV-1, -2, and LMBRV [25]. Phylogenetic trees were constructed using the RNA-dependent RNA polymerase (RdRp) sequence obtained for PRV-3 in the present study, together with those from selected PRV-1 strains, PRV-2, Largemouth bass orthoreovirus (LMBRV), and representative orthoreoviruses from mammals, fish, birds, and reptiles. Maximum likelihood (ML) was used with the general time-reversible model of nucleotide substitution (best-fit substitution model that was suggested by the program) with gamma distribution and invariable sites [26]. Bootstrap values were calculated from 1000 replicates and values above 70 were considered to be significant [27,28].

Partial S1 sequences were obtained from PRV-3 strains from Europe (Denmark (3), Scotland (1), Germany (1) and Italy (2)) in 2017-2018 (Table S1). Primers PRV-3S1-ORF_F ATGGCGAACCATAGGACGCGA and PRV-3-S1-ORF_R-TCACGCCGATGACCACTGAGCA were used in PCR. Amplification was carried out using Qiagen OneStep RT-PCR Kit (Qiagen), according to the manufacturer's instructions, with 25 pmol of each primer and 5 µL of template. RT-PCR conditions were 30 min at 50 °C, 15 min at 95 °C, 30 cycles consisting in 30 s at 94 °C, 30 s at 70 °C (−0.5 °C per

cycle), and 1 min at 72 °C, followed by additional 30 cycles of 30 s at 94 °C, 30 s at 55 °C, and 1 min at 72, and a final extension at 70 °C for 10 min. PCR products were separated by electrophoresis on a 1.2% (*w/v*) agarose gel and the DNA bands obtained extracted and purified, following the protocol of the QIAquick Gel Extraction Kit (Qiagen). Sequencing was done by Eurofins Genomics (Germany) using the same primers as above.

Phylogenetic analysis of the partial S1 segment (876 nt) included the European PRV-3 strains, the Norwegian isolate (NOR/060214), and PRV sequences from Norway, Canada, Chile, and Japan were retrieved from GenBank (Table S1). Sequences were aligned by translation using MUSCLE v.3.8.425 [29]. ML tree was estimated with the RAxML v.8.2.11 package [30], using the GTM model with 1000 fast bootstrap replicates and 50% consensus Neighbor-Joining trees was also estimated, as implemented in Geneious v.11.0.2 (Biomatters Ltd., Auckland, New Zealand)

2.7. SDS-PAGE and Western Blot

Heparinized blood from rainbow trout challenged with PRV-3 collected at 0 wpc and 5 wpc were used in western blot (WB) analyses. Blood from Atlantic salmon, naïve or infected with PRV-1 were used as negative and positive controls, respectively [31]. Pelleted blood cells of equal volume were added Nonidet-P40 lysis buffer containing complete ultra mini protease inhibitor cocktail (1:5) (Sigma). Lysis was performed on ice for 30 min and the samples were then centrifuged at 5000 × *g* for 5 min. Supernatant mixed with XT buffer and XT reducing agent (Bio-rad) were heated for 5 min at 95 °C and then loaded onto a 4–12% criterion XT bis-tris gel. Separated proteins were transferred onto a PVDF membrane and incubated overnight at 4 °C with antiserum against PRV-1 proteins; anti- σ 1 (1:1000) [32], anti- σ 3 (1:500) [13], anti- σ NS (1:500) anti- μ NS (1:1000) [33], anti- μ 1C (1:500) [32], anti- λ 1 (1:500), and anti-PRV-1 (1:25) (antiserum against purified PRV-1 particles) [5]. Horse radish peroxidase (HRP)-conjugated anti-rabbit IgG (Amersham, GE Healthcare, Buckinghamshire, UK) (1:20,000) was used as secondary antibody. The Clarity Western ECL Substrate kit was used for immunodetection (Bio-rad) and MagicMark as molecular weight ladder (XP Western Protein Standard, Invitrogen). Images were acquired using ChemiDoc XRS+ system and Image one software (Bio-rad).

3. Results

3.1. Morphology of Purified PRV-3 Viral Particles

PRV-3 infected blood pellet (Ct 17.8 and 19.7) that was harvested from rainbow trout at 5 wpc was used for purification. The CsCl gradient centrifugation did not yield a visible virus band, and fractions were therefore collected blindly. Fractions with densities between 1.35 and 1.33 g/cm³ were pooled and dialyzed. PRV-3 particles appeared in TEM as spherical, with an approximately 75 nm diameter. The icosahedral capsids had two concentric electron dense layers (Figure 1). The appearance of the viral particles are similar to from that previously observed for PRV-1 [5].

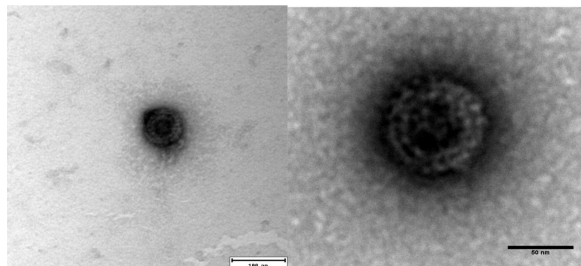


Figure 1. Transmission Electron microscope (TEM) image of negatively stained *Piscine orthoreovirus* (PRV)-3 showing approximately 75 nm diameter, spherical shaped virion.

3.2. The PRV-3 Genome

The genome sequencing and analysis confirmed that PRV-3 is closely related to PRV-1. A total of 106,257,190 Illumina reads (53,128,595 pairs) were generated, and de novo assembly produced a large number of contigs. Several contigs had a high degree of amino acid sequence similarity to PRV-1. Careful examination of high coverage contigs revealed that the PRV-3 genome consists of 10 gene segments, similar to the orthoreoviruses.

Very high coverage was obtained for all segments, with average coverage ranging 430–652 \times (Table S2), but there was poorer coverage of the segment ends. These sequences could not be determined for all of the genomic segments. The complete 3'-end sequence was determined for segment L2 only, being identical to that of ortho- and aquareoviruses, (i.e., UCAUC-3') [4,34,35]. The sequence at the 5'-ends were obtained for segments L1, L2, and S2, and was identical to that of PRV-1 (5'-GAUAAA/U), differing from other orthoreoviruses [4]. All the sequences of the coding regions of the PRV-3 genome were submitted to GenBank (MG253807-MG253816).

A detailed comparison of the PRV-3 coding sequences to PRV-1, PRV-2, and LMBRV was performed (Figure 2). The comparison showed conserved regions across L, M, and S segments among PRV, but only conservation between PRV and LMBRV was mainly seen for L1, L3, and M2. It has previously been reported that PRV-2 λ 1, μ 1, and p13 contain amino acid residue gaps when compared to PRV-1 [18]. The PRV-2 λ 1 amino acid residue gap (T₁₃) was shared by PRV-3. The remaining 10 open reading frames (ORFs) in the PRV-3 and PRV-1 genomes were of equal size.

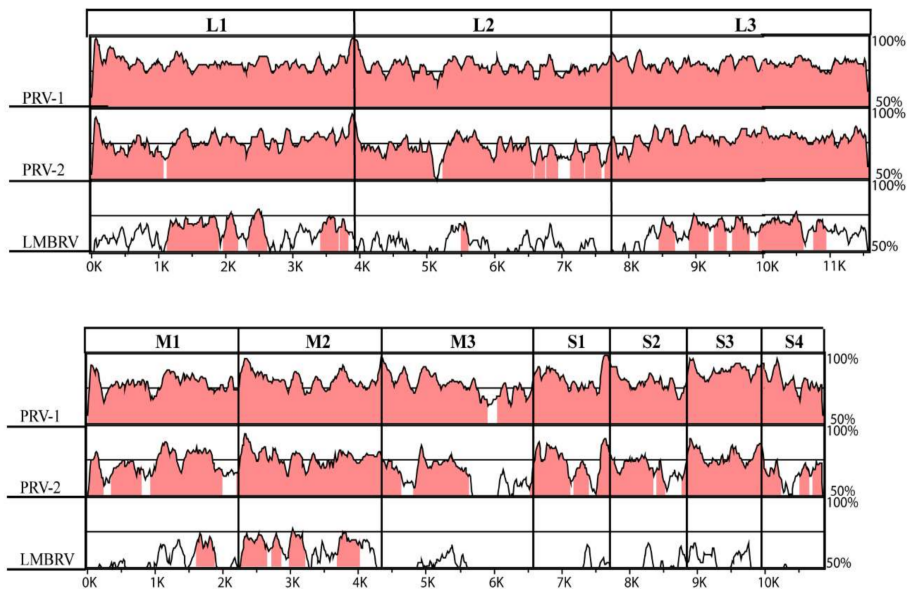


Figure 2. Stacked pair-wise conservation profile analysis. PRV-3 was used as a base sequence in an mVISTA alignment comparing whole genome segments with PRV-1, PRV-2, and LMBRV. Areas in pink colored regions illustrate >70% identities. The X-axis indicates the nucleotide sequence length in kb.

Pairwise nucleotide- and amino acid sequence identities between PRV-1 and -3 were 80.1% (segment range 76.5–87.9%) and 90.5% (79.1–96.7%) for the nucleotide and the amino acid sequences, respectively. For PRV-3 versus PRV-2, the corresponding values were 72.9% (62.6–78.3%) and 80.0% (59.7–93.0%), respectively (Table 1). The amino acid identities of PRV-1 and PRV-3 were higher than the nucleotide identities for all the proteins, except σ 3 and p13.

Table 1. Identities of nucleotide and amino acid sequences of ORFs of PRV-1, -2, and -3. ^a Protein nomenclature is based on PRV-1.

Segment	Protein Name ^a	Predicted Function	PRV-3 & PRV-1		PRV-3 & PRV-2		PRV-1 & PRV-2	
			nt	aa	nt	aa	nt	aa
L1	λ3 (Core RdRp)	RNA-dependent RNA polymerase	80.9	95.2	76.1	88.4	77.3	89.0
L2	λ2 (Core turret)	Guanylyltransferase, methyltransferase	77.8	90.0	70.9	77.1	71.1	76.9
L3	λ1 (Core shell)	Helicase, NTPase, RNA triphosphatase	80.3	96.7	78.3	93.0	77.5	92.7
M1	μ2 (Core NTPase)	NTPase, RNA triphosphatase, RNA binding	78.4	88.7	72.0	78.3	72.2	78.1
M2	μ1 (Outer shell)	Outer capsid protein, membrane penetration	81.2	91.5	76.4	84.3	76.4	85.1
M3	μNS (NS-factory)	Non-structural protein	76.5	82.2	62.6	59.7	62.3	59.3
S1	σ3 (Outer clamp)	σ3: outer capsid protein, zinc metalloprotein	80.5	79.1	71.3	69.7	71.6	69.7
	p13	p13: cytotoxic, integral membrane protein	85.6	78.2	78.1	63.7	77.3	62.9
S2	σ2 (Core clamp)	Inner capsid, RNA binding	80.4	88.8	70.1	73.8	70.2	77.1
S3	σNS (NS-RNA)	Non-structural protein	87.9	94.6	77.8	85.3	76.6	84.7
S4	σ1 (Outer fibre)	Cell attachment protein	80.0	81.6	64.5	64.4	65.5	66.7
	Concatenated coding sequences		80.1	90.5	72.9	80.0	73.4	80.3

3.3. High Conservation of Putative Functional Protein Domains between the Three PRV Subtypes

The RNA polymerase encoded by segment L1 displayed highest sequence conservation, while the μNS (M3), σ3 (S1), and σ1 (S4) proteins displayed the lowest (Table 1). Detailed analyses of all 11 known proteins that were encoded by PRV revealed that most previously predicted secondary structures and putative functional domains are conserved between PRV-3 and PRV-1 [11].

The PRV S1 segment is bicistronic, encoding the outer capsid σ3 protein and a cytotoxic integral membrane protein, p13. The p13 is encoded by an overlapping internal reading frame of the S1 segment (nt 108–482). The predicted transmembrane helical region of p13, aa 26–48 is conserved among the PRVs. The conserved TM helix of p13 is encoded by the same region as the conserved Cx₂Cx₁₆Hx₁C zinc-binding motif in the overlapping reading frame of the σ3 protein (Figure 3). Similarly, the conserved putative dsRNA binding helical region of σ3 also corresponds to a conserved part of p13. Notably, due to the restrictive nature of the overlapping reading frames, and conserved functional domains, the S1 segment nucleotide identity is higher than the amino acid identity/similarity between the PRVs.



Figure 3. Alignment of deduced amino acid sequence of S1 segment of PRV-1, PRV-2, and PRV-3. The $\sigma 3$ and $p13$ proteins are encoded in overlapping reading frames. The conserved transmembrane (TM) helix of $p13$ are encoded by the same region that encodes the conserved Zn finger motifs of $\sigma 3$ (motifs labeled with *). Amino acid residues are numbered above. Identical sequence regions in all three PRVs are indicated by yellow background, identical amino acids shared by only two PRVs are in blue, and similar amino acids are shown with green background color.

A sequence motif that differ between PRV-3 and PRV-1 was the putative cleavage site in the $\mu 1$ protein, where the $\mu 1C$ is split in as $\mu 1\delta$ and $\mu 1\phi$ (Figure 4). This site was for PRV-1 suggested to be located at the position F387 [33], which in PRV-3 is replaced by Y387. The secondary structure prediction and structural comparison of the $\mu 1$ protein showed that PRV-3 $\mu 1$ protein lacks the aa 72–96 loop and the alpha helix (aa 279–295) as compared to *Mammalian orthoreovirus* (MRV) $\mu 1$ (Figure S1). The δ/ϕ cleavage site for MRV is located in the latter domain.

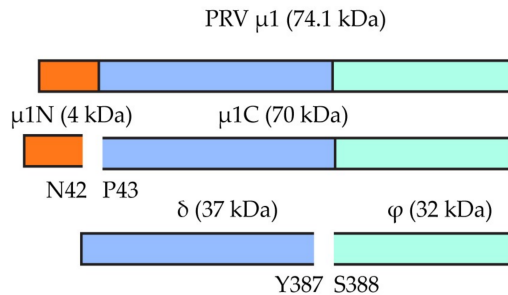


Figure 4. Putative cleavage sites of PRV $\mu 1$ protein. The top bar shows the full length $\mu 1$ protein, the middle bar shows the cleavage site of the N-myristoylated fragment $\mu 1N$ and the bottom picture represent $\mu 1C$ cleavage. The second cleavage site at position 387, which generates the δ/ϕ fragments, has a F387 for PRV-1, which in PRV-3 is replaced by Y387.

3.4. Phylogenetic Analyses

The evolutionary relationship of PRV-3 to other PRV subtypes and members of the genera *Orthoreovirus* and *Aquareovirus* was determined by phylogenetic analysis. A phylogenetic tree was constructed using complete RNA dependent RNA polymerase (RdRp) coding sequence (Figure 5). The tree shows that piscine orthoreoviruses cluster separately from mammalian and avian orthoreoviruses. Within this cluster, a single monophyletic group was generated by PRV-1 strains with high bootstrap support. Corresponding phylogenetic trees were constructed for all the coding sequences, revealed similar tree topologies, placing PRV-3 closer to the PRV-1, than to the PRV-2 subtype (Figure S2).

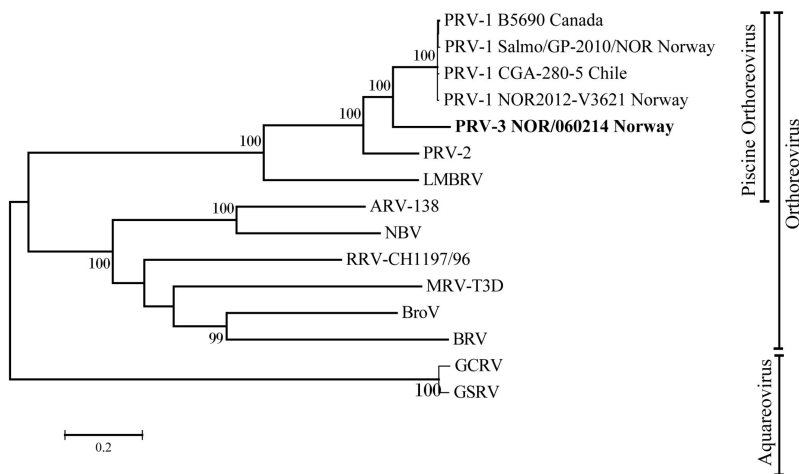


Figure 5. Phylogenetic tree based on complete coding sequences of PRV-3 RdRp (L1) of orthoreoviruses and aquareoviruses. MRV = *Mammalian orthoreovirus*, ARV = *Avian orthoreovirus*, NBV = *Nelson Bay orthoreovirus*, RRV = *Reptilian orthoreovirus*, BroV = *Broome virus*, BRV = *Baboon orthoreovirus*, GCRV = *Grass carp reovirus*, GSRV = *Golden shiner reovirus*.

The results of pairwise comparison of nucleotide and amino acid sequences of S1 (σ_3) are summarized in Table S3. The ML phylogenetic tree based on 876 nt of S1 segment showing the genetic relationship between available PRV-3 isolates is shown in Figure 6. In both ML and NJ phylogenetic analyses, PRV-3 is recovered as monophyletic group, with 100% bootstrap support. Within PRV-3, there are two well supported clades; one clade (3a) includes only the Norwegian isolate NOR/060214; whereas, the second clade (3b) includes sequences belonging to strains from different countries worldwide, including Chile, Denmark, Scotland, Germany, and Italy. Differences between PRV-3a and PRV-3b are 35 to 40 nt, or 6 to 10 aa in σ_3 ORF. Within clade 3b, European sequences form a well-supported group (BS = 92%), different from the Chilean PRV-3 sequences. Within European sequences, differences of 0 to 2 aa are observed; whereas, the aa differences range from 2 to 7 aa when comparing the Chilean sequences with the European ones (Table S3). In summary, the three variants of PRV each form a monophyletic group.

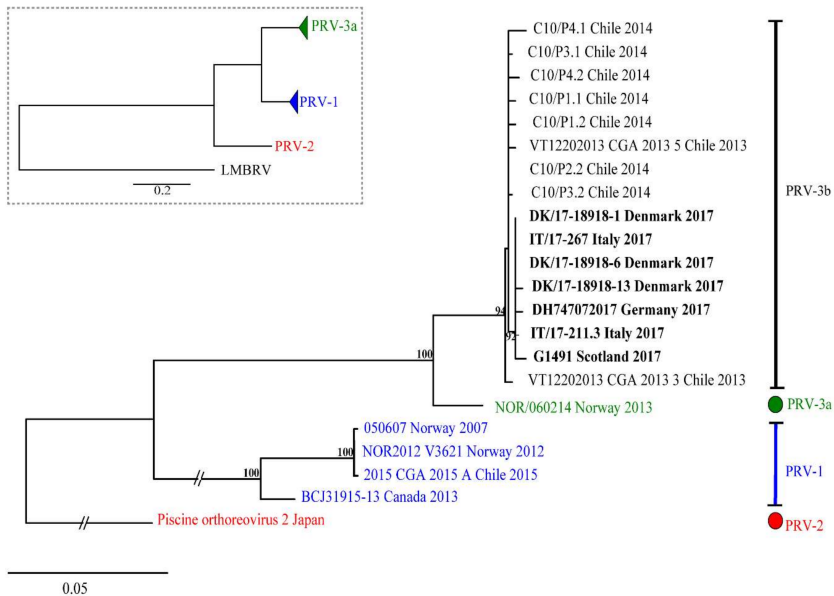


Figure 6. Phylogenetic analysis of partial nucleotide sequence of S1 segment of various PRV-3 isolates. The inner box represent the tree topography drawn in scale 0.5. Tree shows two PRV-3 clades, PRV-3a, and PRV-3b with strong support.

3.5. Serological Cross-Reaction between PRV-1 and PRV-3

The specificities of rabbit polyclonal antisera previously raised against the recombinant variants of PRV-1 $\sigma 3$, $\sigma 1$, σNS , μNS , $\mu 1C$, and $\lambda 1$ were tested towards PRV-3 on western blot (Figure 7). The sera targeting the $\sigma 3$ (outer capsid), $\sigma 1$ (outer fiber), σNS (non-structural), and $\lambda 1$ (core shell) all cross-reacted with PRV-3, producing bands that were corresponding to protein sizes of 35.6 kDa ($\sigma 3$), 34.6 kDa ($\sigma 1$), 39 kDa (σNS), and 141.5 kDa ($\lambda 1$), respectively. The pattern of staining was identical to that observed for PRV-1. The antiserum targeting μNS identified two size variants from the PRV-3 sample, one of 83.5 kDa, and one weakly present at 76 kDa. Only the 76 kDa variant was seen for PRV-1 (Figure 7, lane 4), but two size variants have been observed in a previous study [33]. The 83.5 kDa band corresponds to the full-length protein. The 76 kDa band possibly represents secondary translation initiation at M₅₇ (77.5 kDa) or M₈₅ (74.4 kDa).

The antiserum against PRV-1 $\mu 1$ produced a 70 kDa band from PRV-3 infected blood cells on WB (Figure 7). Previous study of PRV-1 infected blood cells recognized four different variants of the $\mu 1$ protein, with sizes of 74.1, 70, 37, and 32 kDa, emerging at different stages during infection [33]. According to proteomic analysis of the PRV-1 $\mu 1c$ fragments, the full-length PRV-1 $\mu 1$ protein of 74.2 kDa is most likely cleaved at N₄₂P₄₃ to form $\mu 1N$ and the 70 kDa $\mu 1C$. The smaller fragments are likely to be generated following the second proteolytic cleavage of $\mu 1C$, possibly at F₃₈₇S₃₈₈, releasing the δ (37.7 kDa) and ϕ (32.1 kDa) fragments [33].

Rabbit antisera raised against purified PRV-1 particles produced bands of 70, 35 kDa in WB of PRV-1 virus particles, and similar for PRV-3 (Figure 8). The two bands most likely represent the outer capsid proteins of PRV, i.e., the $\mu 1$ (70 kDa), $\sigma 3$ (37 kDa), and $\sigma 1$ (35 kDa). In addition, more weakly stained bands were seen for purified PRV-1 corresponding to protein sizes of around 60 (apparent dual band) and 50 kDa.

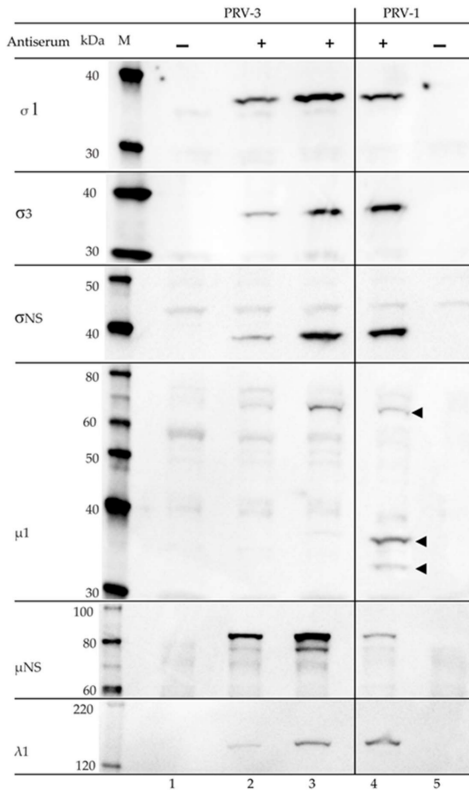


Figure 7. Western blots of PRV-3 and PRV-1 blood pellets using polyclonal antisera developed against recombinant proteins of PRV-1 $\sigma 1$, $\sigma 3$, σNS , $\mu 1$, μNS , and $\lambda 1$. Lane 1-3 Rainbow trout: L1 negative control, L2-L3 PRV-3 infected samples. Lane 4-5 Atlantic salmon: L4 PRV-1 infected, L5: negative control. Arrowheads denote differing $\mu 1$ fragments in PRV-1.

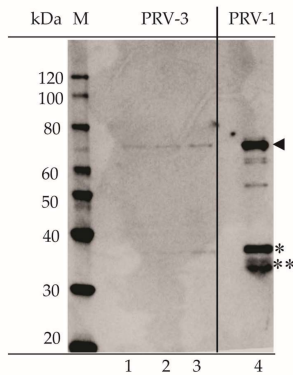


Figure 8. Purified PRV-3 (Lanes 1–3; Ct values for loaded virus particles were 22.7, 20.6 and 20.6, respectively) and PRV-1 (Lane 4; Ct value 17.1) particles analyzed by western blotting using antiserum against PRV-1. \blacktriangleleft $\mu 1$, * $\sigma 3$, ** $\sigma 1$.

4. Discussion

The aims of the present study were to perform genetic and antigenic characterization of the PRV variant recently identified in farmed rainbow trout. Complete coding nucleotide sequences of all the genomic segments were obtained from RNA isolated from plasma of infected fish. To classify as a new species within genus *Orthoreovirus*, the nucleotide sequence identities of homologous genome segments should be <60% equal to other orthoreoviruses, the amino acid sequence identities for more conserved proteins <65% and for more divergent outer capsid proteins <35% [36]. The new PRV from rainbow trout does not fulfill these criteria, thus it classifies as a *Piscine orthoreovirus*, together with PRV-1 and PRV-2. Furthermore, the 5'-terminal sequences are conserved for the particular orthoreovirus species. The 5'-terminal sequences were obtained for segments L1, L2, and S2 and were identical to those of PRV-1. We therefore propose the name PRV-3.

Previous studies have shown that important structural and functional motifs in proteins of orthoreoviruses are highly conserved [11,37]. The PRV-1, PRV-2, and PRV-3 showed the highest sequence conservation in the L class segments, which encode proteins that are involved in transcription and replication, and in the core virus structure. The single amino acid (T₁₃) gap observed in λ 1 for both PRV-3 and PRV-2 when compared to PRV-1 is preceded by a highly basic N-terminal region (M₁ERLKRKDKYKNT₁₃ ...). It is interesting that the single aa gap is shared by two subtypes that were separated by large geographical distance and possibly differing host specificities. This may indicate a functional or structural role of this gap.

During the virus entry, the μ 1 is autocleaved at N-terminal N₄₂P₄₃ and the release N-myristoylated fragment μ 1N to facilitate core delivery [38,39]. This autolytic cleavage site residue is conserved between PRV and other orthoreoviruses [11]. In MRV, the second cleavage of the C-terminal μ 1 generates the ϕ fragment, which is linked to optimal infectivity [40]. The third domain of MRV μ 1 protein consists of five α helices and contain a protease cleavage site for δ - ϕ cleavage [41]. The differences in this second cleavage site and the generation of differently sized δ and ϕ fragments observed between PRV and MRV could be linked to structural differences that were observed in this region; the loop region aa 72–96 of MRV μ 1 protein is shown to contribute to the stabilization of the capsids [42]. PRV, avian orthoreovirus (ARV), and aquareoviruses all lack this loop [43,44], which could be linked with evolutionary adaptation of the virus to different host species [42].

The lowest overall conservation for PRV-3 segments was observed for the M3 segment. The major gene product from this gene segment is the non-structural protein μ NS, which is a multifunctional protein that is interacting with and recruiting other viral proteins to viral factories [45]. Although this segment has the lowest identity to other orthoreoviruses, it still has highly conserved predicted secondary structure [11]. The multifunctionality of μ NS protein is likely a major contributing factor to the low conservation at the primary sequence level.

The phylogenetic analysis using the ORF for the RdRp showed that the fish orthoreoviruses, PRV1-3 and LMBRV form part of a larger monophyletic group that is separate from the other orthoreoviruses, with high bootstrap support. Within this larger fish orthoreovirus group, the PRVs form a monophyletic group. The phylogenetic analysis of the individual segments and of the concatenated sequences confirms that PRV-3 is genetically divergent and represents a new subtype of PRV.

The S1 sequence has high genetic homogeneity (96.1–100%) between PRV-1, but the identity between S1 of PRV-1 and PRV-3 was significantly lower (80.8%). Interestingly, the S1 segment of a PRV from Coho salmon in Chile with HSMI-like disease, together with sequences that were obtained from rainbow trout in Chile [7] cluster with the PRV-3 subtype and show high nucleotide identity to the clade of European PRV-3. Interestingly, PRV-3 has been detected in different countries in Europe both in clinical disease outbreaks in rainbow trout and in surveillance samples collected from healthy brown trout, which expands the list of susceptible species for this new PRV subtype.

A high conservation of protein structure in general between homologous PRV-1 and PRV-3 proteins were supported by secondary structure predictions. The ability of PRV-3 to infect both

rainbow trout and Atlantic salmon and to target the same cell types as PRV-1 confirms the close relationship between PRV-1 and PRV-3 [6]. The cross-reaction of the PRV-1 $\sigma 1$ antiserum with PRV-3 in western blot suggests that linear, but not necessarily conformational, epitopes of the outer fiber receptor-binding protein are conserved between PRV-1 and PRV-3. There are three serotypes in MRV and more than 11 serotypes that were described for ARV. For the serotyping of PRV, virus neutralization tests would have to be developed. This would require the ability to propagate the virus in cell cultures, which has not been successful for PRV so far.

Reoviruses are characterized by broad genetic diversity, which can be increased by their capacity of genome segment reassortment [46]. Investigation of the genetic diversity of PRV variants will aid in studies of pathogenesis of various host species and pathogen tracing. Atlantic salmon and rainbow trout are usually not stocked in the same farm, but can be present in different farms in close proximity. The occurrence of PRV-1 and PRV-3 infected fish in the dense and highly populated farming situations increase the risk of interactions between these PRV subtypes. The high level of sequence similarities, and the fact that PRV-3 can infect Atlantic salmon [6], increases the probability that new variants of PRV may evolve through the compatible reassortment of gene segments following a co-infection, as observed for ARV and MRV [47].

Reoviruses are ubiquitous in aquatic environment and are associated with fish diseases and mortality [19,48]. The finding of PRV variants in salmonid species other than Atlantic salmon have linked these PRV variants to diseases symptoms different from those of HSMI, in particular with anemia [3,18]. This indicates species-specific mechanisms of pathogenesis. Whether the species-specific disease characteristics are due to genetic differences in the PRV subtypes, salmonid host specific factors or a combination of both remains to be elucidated. The PRV-3 genome sequence that is reported in this study could be useful for studies of molecular pathogenesis and molecular epidemiology, and the observed antigenic relatedness between the PRVs could potentially be used for the development of vaccines and diagnostic methods. Future studies will aim to phenotypically characterize PRVs to better understand their tissue tropism, virulence, and possible re-assortment.

5. Conclusions

PRV-3 is a novel subtype of *Piscine orthoreovirus* reported from diseased rainbow trout. This is the first study describing the complete coding genome sequences of PRV-3 and the antigenic relationship between PRV-1 and PRV-3. The genome sequence was obtained by Illumina sequencing of plasma from infected fish. This study also reports for the first time that PRV-3 is present in several European countries.

Supplementary Materials: The following are available online at <http://www.mdpi.com/1999-4915/10/4/170/s1>: Figure S1: The secondary structure prediction and structural comparison of the $\mu 1$ protein; Figure S2: Phylogenetic trees constructed with genome segments of PRV-3; Table S1: List of sequences used for analysis and its NCBI accession numbers; Table S2: Number of reads targeting each PRV-3 segment from the Illumina HiSeq4000 run; Table S3: Nucleotide and amino acid variation between the partial S1 (nt 876) sequences of PRV isolates used in the phylogenetic analysis.

Acknowledgments: This research work was supported by grant 237315/E40 of Research Council of Norway. K.D. acknowledges the financial assistance provided by the Indian Council of Agricultural Research (ICAR) through the ICAR International Fellowship for PhD. A special thanks to Anna Toffan, IZSve, Eann Munro, Marine Scotland Science; Mikolaj Adamek, University of Hannover for providing access to PRV-3 positive samples. Thanks to Elisabeth F. Hansen and Stine Braeen for their technical assistance. All the Aquatic animal health group at DTU-AQUA is acknowledged for the support in testing European samples.

Author Contributions: For research K.D.: study design, experiments, analysis, interpretation of data, drafting, revising and approving the manuscript. N.V.: challenge experiment, S1 sequencing, revising and approving the manuscript. T.M.: sequence analysis and interpretation, writing, revising and approving the manuscript. Ø.W.: study design, virus purification, interpretation of data revising and approving the manuscript. A.C.: S1 sequence analysis, revising and approving the manuscript. I.B.N.: sigma NS expression, revising and approving the manuscript. A.B.O.: experiments, revising and approving the manuscript. M.K.D.: study design, interpretation of data drafting, revising and approving the manuscript. T.T.: NGS data curation, revising and approving the manuscript. E.R.: Study design, analysis, interpretation of data, drafting, revising and approving the manuscript.

Conflicts of Interest: The authors declare that no financial or commercial conflict of interest exists in relation to the content of this article.

References

1. FAO. *Fao Yearbook of Fishery and Aquaculture Statistics—2014*; Food and Agriculture Organization of the United Nations: Rome, Italy, 2016.
2. Hjeltnes, B.; Bornø, G.; Jansen, M.D.; Haukaas, A.; Walde, C. *The Fish Health Report 2015*; Norwegian Veterinary Institute: Oslo, Norway, 2016.
3. Olsen, A.B.; Hjortaa, M.; Tengs, T.; Hellberg, H.; Johansen, R. First description of a new disease in rainbow trout (*Oncorhynchus mykiss* (Walbaum)) similar to heart and skeletal muscle inflammation (HSMI) and detection of a gene sequence related to piscine orthoreovirus (PRV). *PLoS ONE* **2015**, *10*, e0131638. [[CrossRef](#)] [[PubMed](#)]
4. Palacios, G.; Lovoll, M.; Tengs, T.; Hornig, M.; Hutchison, S.; Hui, J.; Kongtorp, R.T.; Savji, N.; Bussetti, A.V.; Solovyov, A.; et al. Heart and skeletal muscle inflammation of farmed salmon is associated with infection with a novel reovirus. *PLoS ONE* **2010**, *5*, e11487. [[CrossRef](#)] [[PubMed](#)]
5. Wessel, O.; Braaen, S.; Alarcon, M.; Haatveit, H.; Roos, N.; Markussen, T.; Tengs, T.; Dahle, M.K.; Rimstad, E. Infection with purified piscine orthoreovirus demonstrates a causal relationship with heart and skeletal muscle inflammation in atlantic salmon. *PLoS ONE* **2017**, *12*, e0183781. [[CrossRef](#)] [[PubMed](#)]
6. Hauge, H.; Vendramin, N.; Taksdal, T.; Olsen, A.B.; Wessel, O.; Mikkelsen, S.S.; Alencar, A.L.F.; Olesen, N.J.; Dahle, M.K. Infection experiments with novel piscine orthoreovirus from rainbow trout (*Oncorhynchus mykiss*) in salmonids. *PLoS ONE* **2017**, *12*, e0180293. [[CrossRef](#)] [[PubMed](#)]
7. Godoy, M.G.; Kibenge, M.J.; Wang, Y.; Suarez, R.; Leiva, C.; Vallejos, F.; Kibenge, F.S. First description of clinical presentation of piscine orthoreovirus (PRV) infections in salmonid aquaculture in chile and identification of a second genotype (Genotype II) of PRV. *Viol. J.* **2016**, *13*, 98. [[CrossRef](#)] [[PubMed](#)]
8. Kongtorp, R.T.; Kjerstad, A.; Taksdal, T.; Guttvik, A.; Falk, K. Heart and skeletal muscle inflammation in atlantic salmon, *Salmo salar* L.: A new infectious disease. *J. Fish Dis.* **2004**, *27*, 351–358. [[CrossRef](#)] [[PubMed](#)]
9. Kongtorp, R.T.; Taksdal, T.; Lyngoy, A. Pathology of heart and skeletal muscle inflammation (HSMI) in farmed atlantic salmon *Salmo salar*. *Dis. Aquat. Organ.* **2004**, *59*, 217–224. [[CrossRef](#)] [[PubMed](#)]
10. Kongtorp, R.T.; Taksdal, T. Studies with experimental transmission of heart and skeletal muscle inflammation in atlantic salmon, *Salmo salar* L. *J. Fish Dis.* **2009**, *32*, 253–262. [[CrossRef](#)] [[PubMed](#)]
11. Markussen, T.; Dahle, M.K.; Tengs, T.; Lovoll, M.; Finstad, O.W.; Wiik-Nielsen, C.R.; Grove, S.; Lauksund, S.; Robertsen, B.; Rimstad, E. Sequence analysis of the genome of piscine orthoreovirus (PRV) associated with heart and skeletal muscle inflammation (HSMI) in atlantic salmon (*Salmo salar*). *PLoS ONE* **2013**, *8*, e70075. [[CrossRef](#)]
12. Garseth, A.H.; Fritsvold, C.; Opheim, M.; Skjerve, E.; Biering, E. Piscine reovirus (PRV) in wild atlantic salmon, *Salmo salar* L., and sea-trout, *Salmo trutta* L., in Norway. *J. Fish Dis.* **2013**, *36*, 483–493. [[CrossRef](#)] [[PubMed](#)]
13. Garver, K.A.; Johnson, S.C.; Polinski, M.P.; Bradshaw, J.C.; Marty, G.D.; Snyman, H.N.; Morrison, D.B.; Richard, J. Piscine orthoreovirus from western north america is transmissible to atlantic salmon and sockeye salmon but fails to cause heart and skeletal muscle inflammation. *PLoS ONE* **2016**, *11*, e0146229. [[CrossRef](#)] [[PubMed](#)]
14. Lovoll, M.; Alarcon, M.; Bang Jensen, B.; Taksdal, T.; Kristoffersen, A.B.; Tengs, T. Quantification of piscine reovirus (PRV) at different stages of atlantic salmon *Salmo salar* production. *Dis. Aquat. Organ.* **2012**, *99*, 7–12. [[CrossRef](#)] [[PubMed](#)]
15. Di Cicco, E.; Ferguson, H.W.; Schulze, A.D.; Kaukinen, K.H.; Li, S.; Vanderstichel, R.; Wessel, O.; Rimstad, E.; Gardner, I.A.; Hammell, K.L.; et al. Heart and skeletal muscle inflammation (HSMI) disease diagnosed on a British Columbia salmon farm through a longitudinal farm study. *PLoS ONE* **2017**, *12*, e0171471. [[CrossRef](#)] [[PubMed](#)]
16. Ferguson, H.W.; Kongtorp, R.T.; Taksdal, T.; Graham, D.; Falk, K. An outbreak of disease resembling heart and skeletal muscle inflammation in Scottish farmed salmon, *Salmo salar* L., with observations on myocardial regeneration. *J. Fish Dis.* **2005**, *28*, 119–123. [[CrossRef](#)] [[PubMed](#)]

17. Marty, G.D.; Morrison, D.B.; Bidulka, J.; Joseph, T.; Siah, A. Piscine reovirus in wild and farmed salmonids in British Columbia, Canada: 1974–2013. *J. Fish Dis.* **2015**, *38*, 713–728. [[CrossRef](#)] [[PubMed](#)]
18. Takano, T.; Nawata, A.; Sakai, T.; Matsuyama, T.; Ito, T.; Kurita, J.; Terashima, S.; Yasuike, M.; Nakamura, Y.; Fujiwara, A.; et al. Full-genome sequencing and confirmation of the causative agent of erythrocytic inclusion body syndrome in coho salmon identifies a new type of piscine orthoreovirus. *PLoS ONE* **2016**, *11*, e0165424. [[CrossRef](#)] [[PubMed](#)]
19. Sibley, S.D.; Finley, M.A.; Baker, B.B.; Puzach, C.; Armien, A.G.; Giehlbrock, D.; Goldberg, T.L. Novel reovirus associated with epidemic mortality in wild Largemouth Bass (*Micropterus salmoides*). *J. Gen. Virol.* **2016**, *97*, 2482–2487. [[CrossRef](#)] [[PubMed](#)]
20. Mendez, I.I.; Hermann, L.L.; Hazelton, P.R.; Coombs, K.M. A comparative analysis of freon substitutes in the purification of reovirus and calicivirus. *J. Virol. Methods* **2000**, *90*, 59–67. [[CrossRef](#)]
21. Bruner, R.; Vinograd, J. The evaluation of standard sedimentation coefficients of sodium RNA and sodium DNA from sedimentation velocity data in concentrated NaCl and CsCl solutions. *Biochim. Biophys. Acta* **1965**, *108*, 18–29. [[CrossRef](#)]
22. Bankevich, A.; Nurk, S.; Antipov, D.; Gurevich, A.A.; Dvorkin, M.; Kulikov, A.S.; Lesin, V.M.; Nikolenko, S.I.; Pham, S.; Pribelski, A.D.; et al. Spades: A new genome assembly algorithm and its applications to single-cell sequencing. *J. Comput. Biol.* **2012**, *19*, 455–477. [[CrossRef](#)] [[PubMed](#)]
23. Kumar, S.; Stecher, G.; Tamura, K. Mega7: Molecular evolutionary genetics analysis version 7.0 for bigger datasets. *Mol. Biol. Evol.* **2016**, *33*, 1870–1874. [[CrossRef](#)] [[PubMed](#)]
24. Jones, D.T. Protein secondary structure prediction based on position-specific scoring matrices. *J. Mol. Biol.* **1999**, *292*, 195–202. [[CrossRef](#)] [[PubMed](#)]
25. Frazer, K.A.; Pachter, L.; Poliakov, A.; Rubin, E.M.; Dubchak, I. Vista: Computational tools for comparative genomics. *Nucleic Acids Res.* **2004**, *32*, W273–W279. [[CrossRef](#)] [[PubMed](#)]
26. Tamura, K. Estimation of the number of nucleotide substitutions when there are strong transition-transversion and G+C-content biases. *Mol. Biol. Evol.* **1992**, *9*, 678–687. [[PubMed](#)]
27. Hungnes, O.; Jonassen, T.O.; Jonassen, C.M.; Grinde, B. Molecular epidemiology of viral infections—How sequence information helps us understand the evolution and dissemination of viruses. *Appl. Microbiol.* **2000**, *108*, 81–97. [[CrossRef](#)] [[PubMed](#)]
28. Tamura, K.; Stecher, G.; Peterson, D.; Filipi, A.; Kumar, S. Mega6: Molecular evolutionary genetics analysis version 6.0. *Mol. Biol. Evol.* **2013**, *30*, 2725–2729. [[CrossRef](#)] [[PubMed](#)]
29. Edgar, R.C. Muscle: A multiple sequence alignment method with reduced time and space complexity. *BMC Bioinform.* **2004**, *5*, 113. [[CrossRef](#)] [[PubMed](#)]
30. Stamatakis, A. Raxml version 8: A tool for phylogenetic analysis and post-analysis of large phylogenies. *Bioinformatics (Oxford, England)* **2014**, *30*, 1312–1313. [[CrossRef](#)] [[PubMed](#)]
31. Lund, M.; Rosaeg, M.V.; Krasnov, A.; Timmerhaus, G.; Nyman, I.B.; Aspehaug, V.; Rimstad, E.; Dahle, M.K. Experimental piscine orthoreovirus infection mediates protection against pancreas disease in atlantic salmon (*Salmo salar*). *Vet. Res.* **2016**, *47*, 107. [[CrossRef](#)] [[PubMed](#)]
32. Finstad, O.W.; Falk, K.; Lovoll, M.; Evensen, O.; Rimstad, E. Immunohistochemical detection of piscine reovirus (PRV) in hearts of atlantic salmon coincide with the course of heart and skeletal muscle inflammation (HSMI). *Vet. Res.* **2012**, *43*, 27. [[CrossRef](#)] [[PubMed](#)]
33. Haatveit, H.M.; Wessel, O.; Markussen, T.; Lund, M.; Thiede, B.; Nyman, I.B.; Braaen, S.; Dahle, M.K.; Rimstad, E. Viral protein kinetics of piscine orthoreovirus infection in atlantic salmon blood cells. *Viruses* **2017**, *9*, 49. [[CrossRef](#)] [[PubMed](#)]
34. Attoui, H.; Fang, Q.; Mohd Jaafar, F.; Cantaloube, J.F.; Biagini, P.; de Micco, P.; de Lamballerie, X. Common evolutionary origin of aquareoviruses and orthoreoviruses revealed by genome characterization of golden shiner reovirus, grass carp reovirus, striped bass reovirus and golden ide reovirus (genus *Aquareovirus*, family *Reoviridae*). *J. Gen. Virol.* **2002**, *83*, 1941–1951. [[CrossRef](#)] [[PubMed](#)]
35. Duncan, R. Extensive sequence divergence and phylogenetic relationships between the fusogenic and nonfusogenic orthoreoviruses: A species proposal. *Virology* **1999**, *260*, 316–328. [[CrossRef](#)] [[PubMed](#)]
36. Attoui, H.; Mertens, P.P.C.; Becnel, J.; Belaganahalli, S.; Bergoin, M.; Brussaard, C.P.; Chappell, J.D.; Ciarlet, M.; del Vas, M.; Dermody, T.S.; et al. Family—Reoviridae. In *Virus Taxonomy: Ninth Report of the International Committee on Taxonomy of Viruses*; Elsevier: San Diego, CA, USA, 2012; pp. 541–637.

37. Xu, W.; Coombs, K.M. Conserved structure/function of the orthoreovirus major core proteins. *Virus Res.* **2009**, *144*, 44–57. [[CrossRef](#)] [[PubMed](#)]
38. Nibert, M.L.; Fields, B.N. A carboxy-terminal fragment of protein mu 1/mu 1C is present in infectious subvirion particles of mammalian reoviruses and is proposed to have a role in penetration. *J. Virol.* **1992**, *66*, 6408–6418. [[PubMed](#)]
39. Nibert, M.L.; Odegard, A.L.; Agosto, M.A.; Chandran, K.; Schiff, L.A. Putative autocleavage of reovirus $\mu 1$ protein in concert with outer-capsid disassembly and activation for membrane permeabilization. *J. Mol. Biol.* **2005**, *345*, 461–474. [[CrossRef](#)] [[PubMed](#)]
40. Snyder, A.J.; Danthi, P. Cleavage of the c-terminal fragment of reovirus $\mu 1$ is required for optimal infectivity. *J. Virol.* **2018**, *92*. [[CrossRef](#)] [[PubMed](#)]
41. Liemann, S.; Chandran, K.; Baker, T.S.; Nibert, M.L.; Harrison, S.C. Structure of the reovirus membrane-penetration protein, $\mu 1$, in a complex with its protector protein, $\sigma 3$. *Cell* **2002**, *108*, 283–295. [[CrossRef](#)]
42. Sarkar, P.; Danthi, P. The $\mu 1$ 72–96 loop controls conformational transitions during reovirus cell entry. *J. Virol.* **2013**, *87*, 13532–13542. [[CrossRef](#)] [[PubMed](#)]
43. Zhang, X.; Jin, L.; Fang, Q.; Hui, W.H.; Zhou, Z.H. 3.3 Å Cryo-EM structure of a nonenveloped virus reveals a priming mechanism for cell entry. *Cell* **2010**, *141*, 472–482. [[CrossRef](#)] [[PubMed](#)]
44. Zhang, X.; Tang, J.; Walker, S.B.; O'Hara, D.; Nibert, M.L.; Duncan, R.; Baker, T.S. Structure of avian orthoreovirus virion by electron cryomicroscopy and image reconstruction. *Virology* **2005**, *343*, 25–35. [[CrossRef](#)] [[PubMed](#)]
45. Haatveit, H.M.; Nyman, I.B.; Markussen, T.; Wessel, O.; Dahle, M.K.; Rimstad, E. The non-structural proteins of piscine orthoreovirus (PRV) forms viral factory-like structures. *Vet. Res.* **2016**, *47*, 5. [[CrossRef](#)] [[PubMed](#)]
46. Goral, M.I.; Mochow-Grundy, M.; Dermody, T.S. Sequence diversity within the reovirus S3 gene: Reoviruses evolve independently of host species, geographic locale, and date of isolation. *Virology* **1996**, *216*, 265–271. [[CrossRef](#)] [[PubMed](#)]
47. Tang, Y.; Lin, L.; Sebastian, A.; Lu, H. Detection and characterization of two co-infection variant strains of avian orthoreovirus (ARV) in young layer chickens using next-generation sequencing (NGS). *Sci. Rep.* **2016**, *6*, 24519. [[CrossRef](#)] [[PubMed](#)]
48. Fan, Y.; Rao, S.; Zeng, L.; Ma, J.; Zhou, Y.; Xu, J.; Zhang, H. Identification and genomic characterization of a novel fish reovirus, hubei grass carp disease reovirus, isolated in 2009 in China. *J. Gen. Virol.* **2013**, *94*, 2266–2277. [[CrossRef](#)] [[PubMed](#)]



© 2018 by the authors. Licensee MDPI, Basel, Switzerland. This article is an open access article distributed under the terms and conditions of the Creative Commons Attribution (CC BY) license (<http://creativecommons.org/licenses/by/4.0/>).

Supplementary Tables

Table S1. List of sequences used for analysis and its NCBI accession numbers.

Journal number.	Year	Species	Country	Subtype	GenBank Acc. No.
NOR/060214	2013	<i>Oncorhynchus mykiss</i>	Norway	PRV-3	MG983780
DK/17-18918-1	2017	<i>Oncorhynchus mykiss</i>	Denmark	PRV-3	MG983785
DK/17-18918-6	2017	<i>Oncorhynchus mykiss</i>	Denmark	PRV-3	MG983786
DK/17-18918-13	2017	<i>Oncorhynchus mykiss</i>	Denmark	PRV-3	MG983782
G1491	2017	<i>Oncorhynchus mykiss</i>	Scotland	PRV-3	MG983781
773	2017	<i>Oncorhynchus mykiss</i>	Germany	PRV-3	MG983787
IT/17-211.3	2017	<i>Salmo trutta fario</i>	Italy	PRV-3	MG983783
IT/17-267	2017	<i>Salmo trutta fario</i>	Italy	PRV-3	MG983784
C10/P4.1	2014	<i>Oncorhynchus mykiss</i>	Chile	PRV-3	KX844951
C10/P1.2	2014	<i>Oncorhynchus mykiss</i>	Chile	PRV-3	KX844964
C10/P1.1	2014	<i>Oncorhynchus mykiss</i>	Chile	PRV-3	KX844965
C10/P4.2	2014	<i>Oncorhynchus mykiss</i>	Chile	PRV-3	KX844959
C10/P3.2	2014	<i>Oncorhynchus mykiss</i>	Chile	PRV-3	KX844960
C10/P3.1	2014	<i>Oncorhynchus mykiss</i>	Chile	PRV-3	KX844961
C10/P2.2	2014	<i>Oncorhynchus mykiss</i>	Chile	PRV-3	KX844962
VT12202013-CGA-2013-3	2013	<i>Oncorhynchus kisutch</i>	Chile	PRV-3	KU131595
VT12202013-CGA-2013-5	2013	<i>Oncorhynchus kisutch</i>	Chile	PRV-3	KU131596
BCJ31915_13	2013	<i>Salmo salar</i>	British Columbia	PRV-1	KT429746
050607	2007	<i>Salmo salar</i>	Norway	PRV-1	KR337479
2015-CGA-2015-A	2015	<i>Oncorhynchus kisutch</i>	Chile	PRV-1	KU131604
NOR2012-V3621	2012	<i>Salmo salar</i>	Norway	PRV-1	KY429949

PRV-2	2012	<i>Oncorhynchus kisutch</i>	Japan	PRV-2	LC145616
LMBRV	2015	<i>Micropterus salmoides</i>	USA	PRV	KU974955
	2008	<i>Gallus gallus</i>	Canada	ARV	EU707935
	2011	<i>Pteropus poliocephalus</i>	Australia	NBV	JF342673
T3D	2002	<i>Homo sapiens</i>	USA	MRV	HM159613
	2010	<i>Pteropus scapulatus</i>	Australia	BrOV	NC_014238
	1993	<i>Papio cynocephalus</i>	USA	BRV	NC_015878
2511	2015	<i>Eucampsipoda africana</i>	South Africa	MAHLV	NC_029912
	1979	<i>Notemigonus crysoleucas</i>	Canada	GSRV	AF403399
	2000	<i>Ctenopharyngodon idellus</i>	China	GCRV	AH009795
CH1197/96	2016	<i>Testudo graeca</i>	Switzerland	RRV	KT696549

Table S2. Number of reads targeting each PRV-3 segment from the Illumina HiSeq4000 run.

Segment	L1	L2	L3	M1	M2	M3	S1	S2	S3	S4
# of reads	24936	20588	21162	10256	10733	10461	4378	5961	5213	4034

Figure S1. The secondary structure prediction and structural comparison of the $\mu 1$ protein.

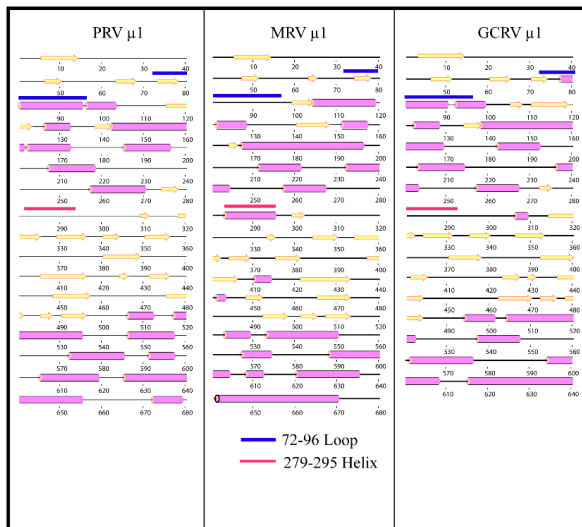


Table S3. Nucleotide and amino acid variation between the partial S1 (nt 876) sequences used in the phylogenetic analysis.

	LC 14 56 16 PR V- 2 Jap an	NO R/0 602 14 Nor wa y 201 3	KX 84 49 51 C1 DH_ 7470 7 7 2017	D K/ 17- 18 91 G1 8- 13 De n ma rk 20 17	17- 18 91 G1 1- 13 Sc otl an d 20 17	17- 192 66- 27 Ital y_ 201 7	17- 192 66- 35 Ital y_ 201 7	D K/ 17- 18 91 De n ma rk 20 17	D K/ 17- 18 91 De n ma rk 20 17	KX 844 964 C1 C1 Chi le_ 201 4	KX 844 965 C1 C1 Chi le_ 201 4	KU 131 595 VT 122 020 13 A- 201 3-3 Chi le_ 201 4	KX 844 959 C1 CG 3-3 Chi le_ 201 4	KU 131 596 VT 122 020 13 A- 201 3-5 Chi le_ 201 4	KX 844 960 C1 CG 3-5 Chi le_ 201 4	KX 844 961 C1 CG 3-5 Chi le_ 201 4	KX 844 962 C1 CG 3-5 Chi le_ 201 4	KT4 2974 6 BCJ 3191 5_13 Can ada_ 2013 ? 7	KR3 3747 9 0506 07 Nor way_ 200 7	KU 131 604 201 5- CG A- 201 5-A 21 Nor way_ 201 2	KY4 2994 9 NO R20 12- V36 21 Nor way_ 201 2		
LC145616_Piscine orthoreovirus 2_Japan		265	275	271	271	270	270	270	270	269	270	271	270	271	270	270	270	270	253	260	259	259	
NOR/060214 Norway 2013	94		40	37	37	38	36	35	35	35	37	37	36	38	37	36	36	35	166	178	176	177	
KX844951 C10/P4.1 Chile 2014	102	10		9	9	10	8	7	7	7	7	7	7	8	8	7	6	6	5	173	181	179	180
DH_747072017_Germany_2017	98	7	7		4	5	3	2	2	2	6	6	7	7	6	5	5	4	172	180	178	179	
DK/17-18918-13 Denmark 2017	97	7	7	2		5	3	2	2	2	6	6	7	7	6	5	5	4	171	178	176	177	
G1491_Scotland_2017	97	6	6	1	1		4	3	3	3	7	7	8	8	7	6	6	5	171	179	177	178	

17-19266-27 Italy_2017	97	6	6	1	1	0		1	1	1	5	5	6	6	5	4	4	3	171	179	177	178
17-19266-35 Italy_2017	97	6	6	1	1	0	0		0	0	4	4	5	5	4	3	3	2	170	178	176	177
DK/17-18918-1 Denmark 2017	97	6	6	1	1	0	0	0		0	4	4	5	5	4	3	3	2	170	178	176	177
DK/17-18918-6 Denmark 2017	97	6	6	1	1	0	0	0	0		4	4	5	5	4	3	3	2	170	178	176	177
KX844964 C10/P1.2_Chile _2014	97	8	6	5	5	4	4	4	4	4		4	5	5	4	3	3	2	170	178	176	177
KX844965 C10/P1.1_Chile _2014	98	8	6	5	5	4	4	4	4	4	4		5	5	4	3	3	2	169	177	175	176
KU131595 VT12202013- CGA-2013- 3_Chile_2013	98	7	5	4	4	3	3	3	3	3	3	3		6	5	4	4	3	167	175	173	174
KX844959 C10/P4.2_Chile _2014	99	7	5	4	4	3	3	3	3	3	3	3	2		5	4	4	3	171	179	177	178
KU131596 VT12202013- CGA-2013- 5_Chile_2013	99	7	5	4	4	3	3	3	3	3	3	3	2	2		3	3	2	169	177	175	176
KX844960 C10/P3.2_Chile _2014	99	7	5	4	4	3	3	3	3	3	3	3	2	2	2		2	1	168	176	174	175
KX844961 C10/P3.1_Chile _2014	98	6	4	3	3	2	2	2	2	2	2	2	1	1	1	1		1	167	175	175	174
KX844962 C10/P2.2_Chile _2014	98	6	4	3	3	2	2	2	2	2	2	2	1	1	1	1	0		168	176	174	175


IV

RESEARCH ARTICLE

Open Access



Piscine orthoreovirus subtype 3 (PRV-3) causes heart inflammation in rainbow trout (*Oncorhynchus mykiss*)

Niccoló Vendramin^{1*}, Dhamotharan Kannimuthu^{2†}, Anne Berit Olsen³, Argelia Cuenca¹, Lena Hammerlund Teige², Øystein Wessel², Tine Moesgaard Iburg¹, Maria Krudtaa Dahle⁴, Espen Rimstad² and Niels Jørgen Olesen¹

Abstract

Piscine orthoreovirus (PRV) mediated diseases have emerged throughout salmonid aquaculture. Three PRV subtypes are currently reported as causative agents of or in association with diseases in different salmonid species. PRV-1 causes heart and skeletal muscle inflammation (HSMI) in Atlantic salmon (*Salmo salar*) and is associated with jaundice syndrome in farmed chinook salmon (*Oncorhynchus tshawytscha*). PRV-2 causes erythrocytic inclusion body syndrome (EIBS) in coho salmon in Japan. PRV-3 has recently been associated with a disease in rainbow trout (*Oncorhynchus mykiss*) characterized by anaemia, heart and red muscle pathology; to jaundice syndrome in coho salmon (*Oncorhynchus kisutch*). In this study, we conducted a 10-week long experimental infection trial in rainbow trout with purified PRV-3 particles to assess the causal relationship between the virus and development of heart inflammation. The monitoring the PRV-3 load in heart and spleen by RT-qPCR shows a progressive increase of viral RNA to a peak, followed by clearance without a measurable change in haematocrit. The development of characteristic cardiac histopathological findings occurred in the late phase of the trial and was associated with increased expression of CD8+, indicating cytotoxic T cell proliferation. The findings indicate that, under these experimental conditions, PRV-3 infection in rainbow trout act similarly to PRV-1 infection in Atlantic salmon with regards to immunological responses and development of heart pathology, but not in the ability to establish a persistent infection.

Introduction

Piscine orthoreovirus (PRV) causes or are associated with emerging diseases in salmonid aquaculture. PRV belongs to the family *Reoviridae*, sub-family *Spinareovirinae*, genus *Orthoreovirus*. It has a double stranded RNA genome consisting of 10 segments [1]. The virion has a double protein capsid with icosahedral symmetry and no envelope [1]. PRV resists cultivation in cell culture monolayers, however, ex vivo infection of naïve red blood cells has been demonstrated [2]. Efficient propagation of

the virus relies on in vivo experimental challenge in susceptible fish.

Three subtypes of PRV have been reported and are denoted as PRV-1, PRV-2, and PRV-3. Subtypes 1 and 2 have recently been identified as aetiological agents of disease in salmonids through infection with purified virus. PRV-1 causes heart and skeletal muscle inflammation (HSMI) in Atlantic salmon (*Salmo salar*) [3]. The disease was first diagnosed in 1999 in Norway [4, 5]; HSMI has also been reported in Scotland and Canada [6]. In Norway, the causative relationship between PRV-1 and HSMI was demonstrated [3]. As the disease name implies, the major histopathological findings are in located in the heart and red skeletal muscle. Affected fish show pericarditis with epicarditis, mononuclear cell infiltrations in the atrium and spongy and compact layers of the cardiac

*Correspondence: niven@aqu.dtu.dk

[†]Niccoló Vendramin and Dhamotharan Kannimuthu contributors equally to this work

¹National Institute of Aquatic Resources, Technical University of Denmark, Kongens Lyngby, Denmark

Full list of author information is available at the end of the article



ventricle and necrotic cardiomyocytes. Severely affected fish also have red muscle inflammation [7].

PRV-2 was shown to cause erythrocytic inclusion body syndrome (EIBS) in coho salmon (*Oncorhynchus kisutch*) in 2016 [8] in Japan. The anaemic condition denoted as EIBS was first described in 1977 in rainbow trout [9] and in 1987 in chinook salmon from the Pacific Northwest of North America [10], however, as these occurrences predate the discovery of PRV-2, it remains unknown as to whether these historical EIBS cases are equivalent to the PRV-2 causing EIBS as diagnosed in Japan. To date, PRV-2 has not been reported outside of Japan.

PRV-3 was detected in 2013 following a thorough investigation of unexplained mortalities in young rainbow trout (*Oncorhynchus mykiss*) farmed in fresh water in Norway [11]. After detection of the virus, infection trials were conducted to assess its pathogenicity and the risk associated with its introduction to salmonid aquaculture in Europe. Those experimental trials showed that PRV-3 replicated in rainbow trout blood and efficiently transmitted to naïve host in a cohabitation trial, while its capacity of replicating in Atlantic salmon is limited [12]. The PRV-3 genome was sequenced and compared with PRV-1 showing that PRV-3 is more closely related to PRV-1 than PRV-2 [13].

PRV-3 antigenic properties were analyzed with antibodies raised against homologous proteins of PRV-1. Western blot analysis of PRV-3 infected blood cells have demonstrated that polyclonal rabbit antisera raised against the homologous proteins of PRV-1 cross-reacted with the PRV-3 proteins $\sigma 1$, $\sigma 3$, σNS , $\mu 1$, μNS , and $\lambda 1$ [13].

The orthoreoviruses are, in general, ubiquitous in their respective niches. The mere detection of the virus is therefore not necessarily indicative of disease causality. For example, PRV-1 is present in almost every cohort of farmed Atlantic salmon in the marine phase [3] and PRV-3 was detected in non-diseased adult rainbow trout in Norway [14]. Recently the virus was detected in several European countries, including Scotland, Germany, Italy and Denmark both from disease outbreaks and asymptomatic fish [13], the virus might also be associated with proliferative darkening syndrome (PDS) in brown trout [15]; finally PRV-3 was detected in clinically affected coho salmon in Chile [16, 17]. The main aim of our study was to demonstrate eventual causality between PRV-3 infection in rainbow trout and development of cardiac lesions as observed in field cases and previous challenge experiments. Injection with blood from infected fish was used previously in infection trials, but did not prove that PRV-3 was in fact the sole causative agent of the disease, since other pathogens/viruses could be present in the sample.

In this study, we set out to demonstrate an eventual causality between a disease recently described in rainbow trout [11], and the associated *Piscine orthoreovirus* (PRV) [13]. To achieve this goal, PRV-3 was purified from experimentally infected rainbow trout blood and used in the challenge model previously developed to compare the infection progress and disease development with a control group injected with PRV-3 infected blood.

The viral RNA kinetics in the heart and spleen and PRV protein expression in erythrocytes were assessed, along with the development of heart pathology. In addition, the immune response was monitored through gene expression analysis and detection of PRV specific antibodies.

Materials and methods

Virus purification

The challenge material, consisting of purified PRV-3 particles or PRV-3 infected blood, originated from intra peritoneal (i.p.) injected fish from a PRV-3 challenge trial described earlier [13]. PRV-3 particles (isolate NOR/060214) were purified from the PRV-3 infected blood (500 μ L, Ct 19.7) exactly as stated in [13]. Fractions of 0.5 mL were collected using a syringe with a 23 G needle. The density of the fractions was determined by cross referencing to the refractive index [18]. The quantity of PRV-3 in the fractions was determined using RT-qPCR. Fractions with a density corresponding to that of PRV were chosen for dialysis. The purity of the samples was inspected by transmission electron microscopy (TEM) and analyzed by Next Generation Sequencing (NGS) as described by Dhamotaran et al. [13].

Experimental challenge

Rainbow trout were obtained from eyed eggs provided by a Danish commercial fish farm officially registered free of IPNV, IHNV, VHSV and bacterial kidney disease (BKD). After iodophor disinfection, the eggs were hatched and fish were grown in the wet laboratory facilities of the European Union Reference Laboratory for fish disease (EURL, Copenhagen, Denmark) using recirculated tap water disinfected by UV light. Before infection, the specific pathogen free (SPF) rainbow trout were moved into the high containment infection facility with fresh water at a constant temperature of $12 \text{ }^\circ\text{C} \pm 1 \text{ }^\circ\text{C}$. Each tank was supplied with flow-through UV disinfected water (1 full water exchange per day), furthermore one recirculating unit (EHEIM Professional 4+) was added to each tank to increase water quality and reduce water usage.

A total of 500 SPF rainbow trout of 10 g in average were kept in tanks with 5 L/h flow-through fresh water renewal using the following conditions: $12 \text{ }^\circ\text{C} \pm 1 \text{ }^\circ\text{C}$, L:D 12:12, stocking density below 60 kg/m³, and feeding of 1.5% of biomass/day. The fish were divided into three

groups: Negative control; purified PRV-3 particles and positive control PRV-3 infected blood.

In order to have comparable biomass in the different groups, the negative control group of 500 Lts capacity accommodated 300 rainbow trout, the two experimental tanks accommodating fish challenged with purified PRV-3 particles and positive controls were 180 Lts accommodating 100 rainbow trout each. In all tanks the ratio between injected (shedders) and cohabitants was 50:50. To set up the cohabitation trial, shedder fish were anaesthetized by immersion in water containing benzocaine (80 mg/L water), and then i.p. injected with 0.1 ml of challenge or mock inoculum. The PRV-3 RNA load in the infected blood inoculum was Ct 26.3 per 5 μ L; whereas in the purified viral particle inoculum the PRV-3 load was assessed as Ct 32.7 per 5 μ L. Mock infection with blood from naïve fish (tested negative for PRV-3) diluted in L-15 medium was performed in the same manner on 50% of the negative control fish. Injected fish

were marked by adipose fin clipping. Sampling took place at 2, 4, 6, 8, 10 weeks post-challenge (wpc) and included six shedders and six cohabitants in the exposed tanks, whereas 2 mock injected fish and 2 negative control cohabitants were sampled. Sampling specifics are provided in Table 1.

Sampling

Upon sampling, fish were euthanized with benzocaine (800 mg/L). Blood was collected from the caudal vein in heparinized tubes (Kruuse Ltd UK). Heparinized blood was centrifuged (130 g for 10 min) and plasma and blood cells were separated. Blood was used for Western blot (WB) and plasma for assessing specific antibody. An aliquot of heparinized blood was centrifuged (12 000 g for 5 min) in glass microhematocrit tubes (Vitrex Medical A/S) with specific centrifuge (Nüve) and haematocrit (hct) assessed visually with specific scale.

Table 1 Design of the experimental trial

Group	Number of fish	Trial length (weeks)	Sampling time points (weeks post-challenge-wpc) ^a	Fish sampled per time point	Samples	Analysis
Negative control	150 mock injected	10	2, 4, 6, 8, 10	2	Blood	Antibody detection
					Heart	Virus qPCR; CD4 CD8
					Spleen	Virus qPCR; IFN
	150 cohabitants	10	2, 4, 6, 8, 10	2	Organs	Histopathology
					Blood	WB—antibody detection—Hct
					Heart	Virus qPCR; CD4 CD8
Purified PRV-3 particles	50 purified PRV-3 injected	10	2, 4, 6, 8, 10	6	Spleen	Virus qPCR; IFN
					Organs	Histopathology
					Blood	WB—antibody detection—Hct
	50 cohabitants	10	2, 4, 6, 8, 10	6	Heart	Virus qPCR; CD4 CD8
					Spleen	Virus qPCR; IFN
					Organs	Histopathology
Positive control	50 PRV-3 infected blood injected	10	2, 4, 6, 8, 10	6	Blood	Antibody detection
					Heart	Virus qPCR; CD4 CD8
					Spleen	Virus qPCR
	50 cohabitants	10	2, 4, 6, 8, 10	6	Organs	Histopathology
					Blood	WB—antibody detection—Hct
					Heart	Virus qPCR; CD4 CD8
					Spleen	Virus qPCR; IFN
					Organs	Histopathology

^a In addition 9 fish were collected prior to exposure and investigated for presence of PRV-3 and heart histopathology.

The heart was cut in two equal halves along the mid-sagittal axis; one half was stored in 10% neutral-buffered formalin for histopathological evaluation, and the other half was divided into two aliquots: one was stored in RNeasy Lysis Buffer (Qiagen) for gene expression analysis (CD4 and CD8) and one was stored in RLT buffer (Qiagen) for quantifying viral RNA. The spleen was divided into three aliquots: one was stored in 10% neutral-buffered formalin, one was stored in RNeasy Lysis Buffer (Qiagen) for gene expression analysis and one was stored in RLT buffer (Qiagen) for quantifying viral RNA. Gill, liver, pancreas and pyloric caeca, distal intestine, red and white muscle, mid kidney were also collected and stored in 10% neutral-buffered formalin for histopathological evaluation.

Quantification of PRV-3 in the heart and spleen

RT-qPCR was performed on RNA purified from fish tissue. After processing the sample with Tissue Lyser (Qiagen, Hilden, Germany), total RNA was isolated using QIAcube and the RNeasy Mini Kit (Qiagen) according to the manufacturer's recommendations.

RT-qPCR was performed with 5 μ L of template using the QuantiTect Probe RT-PCR Kit (Qiagen), primers and probes, and conditions as described elsewhere [11], with ROX as a reference dye.

All RT-qPCR analyses were performed using Agilent Mx3005P and Mx3000P qPCR-system (Agilent Technologies, Santa Clara, United States), and MxPro (v. 4.10) software, using the adaptive Baseline function. Cycle thresholds (Ct) were set manually to the same value in all the runs (dR=380), in order to be able to compare Ct values among runs. Fish were considered virus positive at Ct levels below 35 and suspect between Ct 35–40; Ct values above 40 were negative.

Western blotting

Purified PRV-3 virus particles or blood pellets pooled from three cohabitant fish were mixed with XT buffer and XT reducing agent (Bio-rad), heated for 5 min at 95 °C and loaded onto a 4–12% criterion XT bis-tris gel. Separated proteins were transferred onto a 0.2 μ m PVDF membrane using Trans Blot Turbo Transfer system (Bio-rad) and incubated overnight at 4 °C with antiserum against PRV-1 proteins; anti- σ 1 (1:1000) [19], anti- σ 3 (1:500) [1], anti- μ 1C (1:500) [19] and anti-actin (1:500) (Sigma). After washing 4 \times 15 min the membranes were incubated with the secondary antibody horse radish peroxidase (HRP)-conjugated anti-rabbit IgG (Amersham, GE Healthcare, Buckinghamshire, UK) (1:20 000). The membranes were washed 4 \times 15 min and stained with the Clarity Western ECL Substrate kit (Bio-rad). Magic-Mark was used as molecular weight ladder (XP Western

Protein Standard, Invitrogen). Images were acquired using ChemiDoc XRS+ system and Image one software (Bio-rad).

PRV immunoassay

The specific antibody response to PRV infection was measured as mean fluorescence intensity (MFI) in plasma samples of challenged rainbow trout using a bead based immunoassay as described earlier [20]. Briefly, plasma samples from cohabitant fish sampled from the the negative control, positive control and experimental groups were analysed for antibodies against μ 1C. Beads, conjugated with and PRV-1 μ 1C recombinant protein, were incubated with plasma harvested at 0, 4, 6, 8 and 10 wpc from cohabitants (n 6 per time point). The μ 1C protein has 91.5% homology at the aminoacid level between PRV-1 and PRV-3 [13].

Histopathology

Hearts from 60 fish exposed to purified PRV particles and 60 fish from the positive control group were sampled at regular intervals and examined by histopathology; in addition, 20 hearts from the negative control group were assessed. Prior to exposure 9 fish were sampled and analysed as well (Table 1).

Tissue samples collected in 10% neutral-buffered formalin were embedded in paraffin and processed into sections of 3–4 μ m, stained with haematoxylin and eosin (H&E) and examined by light microscopy. Pathological findings in the heart were classified as (1) mild (one to a few lesions), (2) moderate (more extended distribution of lesions) and (3) severe (most of the heart sample affected) [21].

Immune gene expression

In brief, tissues were homogenized in 650 μ L QIAzol lysis reagent with 5 mm steel beads in a Tissue Lyser II for 5 min. Following chloroform extraction, 350 μ L of aqueous phase was loaded into an automated QIAcube (Qiagen) for RNA purification. Total RNA concentration was measured using a NanoDrop ND-1000 spectrophotometer (Thermo Fisher Scientific). For gene expression analysis, cDNA was synthesized using 500 ng of total RNA using the QuantiTect Reverse Transcription kit (Qiagen) which includes a gDNA wipeout step. The qPCR was performed in duplicates with 10 ng of cDNA input in total volume of 10 μ L per reaction using Maxima SYBR Green/ROX qPCR Master Mix (Fisher Scientific) and 500 nM forward and reverse primers (Table 2). The assay included 95 °C for 10 min, 40 cycles of 94 °C for 15 s and 60 °C for 30 s. The melting curve analysis confirmed the specificity of each SYBR qPCR assay, and elongation factor (EF1 α) mRNA was used for normalization by

Table 2 Primers used for immune gene analysis

Gene	Primer sequences	Amplicon length	Reference	Gene Bank No.
Elongation Factor (EF1a)	GATCCAGAAGGAGGTACCA TTACGTTTCGACCTTCCATCC	150	[43]	AF498320.1
Mx	AGCTCAAACGCCTGATGAAG ACCCCACTGAAACACACCTG	142	[43]	NM_001171901
Viperin	ACGACCTCCAGTCCCAAGT GTCCAGGTGGCTTCTCTGC	173	[43]	AF076620.1
Interferon type 1	AAAACGTGGTGGGAATGAAA TGTTTCAGTCTCCTCTCAGTT	141	[43]	NM_001124531
Interferon gamma	CAAACGTAAAGTCCACTATAAGATCCCA GGTCCAGCCTTCCCCTCAC	188	[44]	FM864345.1
CD-4	CCTGCTCATCCACAGCCTAT CTTCTCTGGCTGTCTGACC	111	[43]	AY973030.1
CD-8 alpha	AGTCGTGCAAAGTGGGAAAG GTTTGAATGGCATACTAGT	123	[43]	NM_001124263

the $\Delta\Delta C_t$ method. In Figures 3C, D and 5 all the PRV-3 infected groups were compared to time-matched samples from negative control groups. At each time point, gene expression of fish exposed to purified PRV-3 particles and PRV-3 infected blood respectively were compared to the negative control at that specific time point. The fold changes in gene expression in the negative control group sampled at weeks 2, 4, 6, 8 and 10 were compared to the same group at week 0.

Statistical analysis

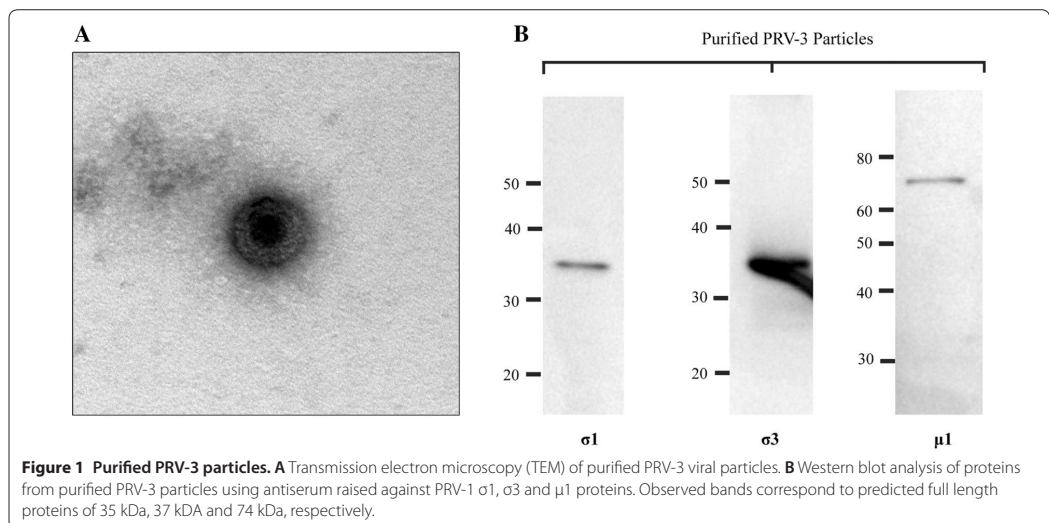
To assess the significant differences in immune gene expression between the control group and PRV-3

infected groups, the statistical analysis was performed using one way ANOVA with Dunnett's multiple comparison test [22]. The correlation between viral load and immune transcripts were done by non-parametric Spearman correlation test [23].

Results

Characterization of purified PRV-3

Purified PRV-3 particles were observed in TEM as spherical, non-enveloped virions of approximately 75 nm in diameter resembling PRV-1 particles [3] (Figure 1A). No other type of virus particles were found. In western blotting of purified virus, antibodies against PRV-1 σ_1 , σ_3



and $\mu 1$ recognized the corresponding proteins of PRV-3, observed as bands of 35, 37 and 74 kDa (Figure 1B).

PRV-3 RNA viral kinetics in heart and spleen

The PRV-3 RNA load in heart and spleen showed a similar trend for the positive control group, inoculated with PRV-3 infected blood, as for the group inoculated with purified PRV-3 particles. An acute phase characterized by a peak PRV-3 load was followed by virus clearance (Figures 2A and B).

In the positive control group (injected with PRV-3 infected blood) viral RNA peaked at 2 wpc (median Ct 26.8 in the heart and 22.5 in the spleen) while the peak occurred at 6 wpc in the cohabitants (median Ct 21 in the heart and 18.1 in the spleen). In fish challenged with purified PRV-3, viral RNA peaked at 4 wpc in the injected group (median Ct 28.9 in the heart and 24.8 in the spleen) and at 6 wpc in the cohabitants (median Ct 25 in the heart and 22.7 in the spleen).

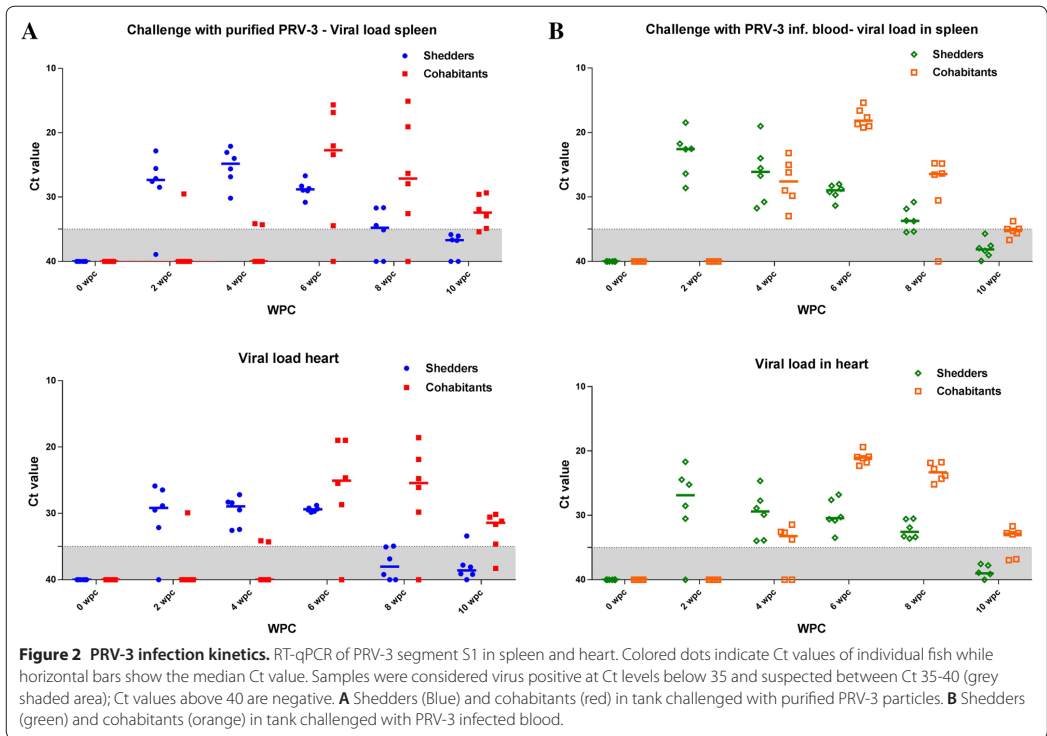
After the peak phase of infection, the number of PRV positive fish per sampling point decreased and the Ct values of the positive fish increased, indicating viral clearance. At the end of the trial (10 wpc) PRV-3 RNA could

not be detected in the spleen or heart from shedders of the positive control group and only in three spleen and four heart samples from the six cohabitants. In virus-positive samples, the Ct values were close to the set detection limit (Ct 35). A similar observation was made at 10 wpc in fish infected with purified PRV-3. No PRV-3 RNA was detected in spleen samples from shedders, whereas the five positive out of six spleen samples from the cohabitants had high Ct values (>29). Only one out of six heart samples from the shedders and five out of six from the cohabitants tested positive (Ct values >30) at 10 wpc. No PRV-3 was detected in samples from the negative control group.

No significant differences in haematocrit were observed between the groups (data not shown).

Histopathology

Histopathological findings in hearts consisting in the PRV-3 associated pathology described earlier [11, 12], were detected after peak load of PRV-3 in hearts in the respective groups. In the group challenged with purified PRV-3 particles, 2 shedders and 2 cohabitant fish had heart lesions, whereas 1 shedder and 7 cohabitants show



heart pathology in the positive control group. Prevalence and distribution of heart lesions at each time point are shown in Table 3. The lesions observed were mild to moderate in positive controls. Typical findings were epicarditis and focal to multifocal endo- and myocarditis in atrium and *stratum spongiosum* of the ventricle and perivasculitis and myocarditis in *stratum compactum* of the ventricle (Figures 3A and B). Histopathological findings consisting of epicarditis and a focal inflammatory reaction involving the interface layer between *stratum compactum* and *stratum spongiosum* were occasionally observed in all groups throughout the experiment (Additional file 1). Since they were clearly distinguishable from PRV-3 associated pathology, they were prudentially removed while assessing the development of PRV-3 pathology.

PRV-3 protein detection

Western blot analysis of blood cells from cohabitants of fish injected with PRV-3 purified particles or infected blood, detected $\sigma 1$ viral proteins at 6 wpc, correlating with the peak phase of infection. No viral proteins were detected in blood cells after 6 wpc (Figure 4A).

Development of specific antibodies against PRV

There was a significant increase in $\mu 1C$ -specific IgM in plasma from PRV-3 infected cohabitant fish compared to plasma of uninfected fish at 8 wpc, and the production continued to increase at 10 wpc. Notably, large variations between individuals were observed (Figure 4B).

At 6 wpc the group challenged with PRV-3 infected blood had higher specific antibody levels than the

purified PRV-3 particle group, but this was opposite at 10 wpc.

Immune gene expression

The innate antiviral immune response following PRV-3 infection was targeted by measuring Mx, Viperin, interferon type 1 and interferon γ gene expression patterns in spleen. The T cell response in the heart was analyzed by targeting the T-cell markers CD4 and CD8. The Mx and Viperin gene expressions were significantly upregulated in the groups challenged with PRV-3 infected blood and purified virus particles, and correlated well with the viral load (Spearman $r=0.76$) (Figure 5). In the shedders, the antiviral gene expression increased significantly along with the viral load at 2 wpc and 4 wpc, and subsided after 4 wpc. In the cohabitants, the antiviral gene expression shows an acute peak at 6 wpc corresponding with the peak viral load. Both viral load and antiviral gene expression decreased after 6 wpc. In both cohabitant groups, CD4 and CD8 expression in heart remained equivalent to the 0 wpc control level until 8 wpc. The CD8 gene expression shows a particularly high increase (100-fold) peaking at 10 wpc (Figures 3C and D). The CD4 expression was also significantly higher at 10 wpc. The T cell marker gene expression did not correlate with the viral peak, but with the inflammation scores in the heart.

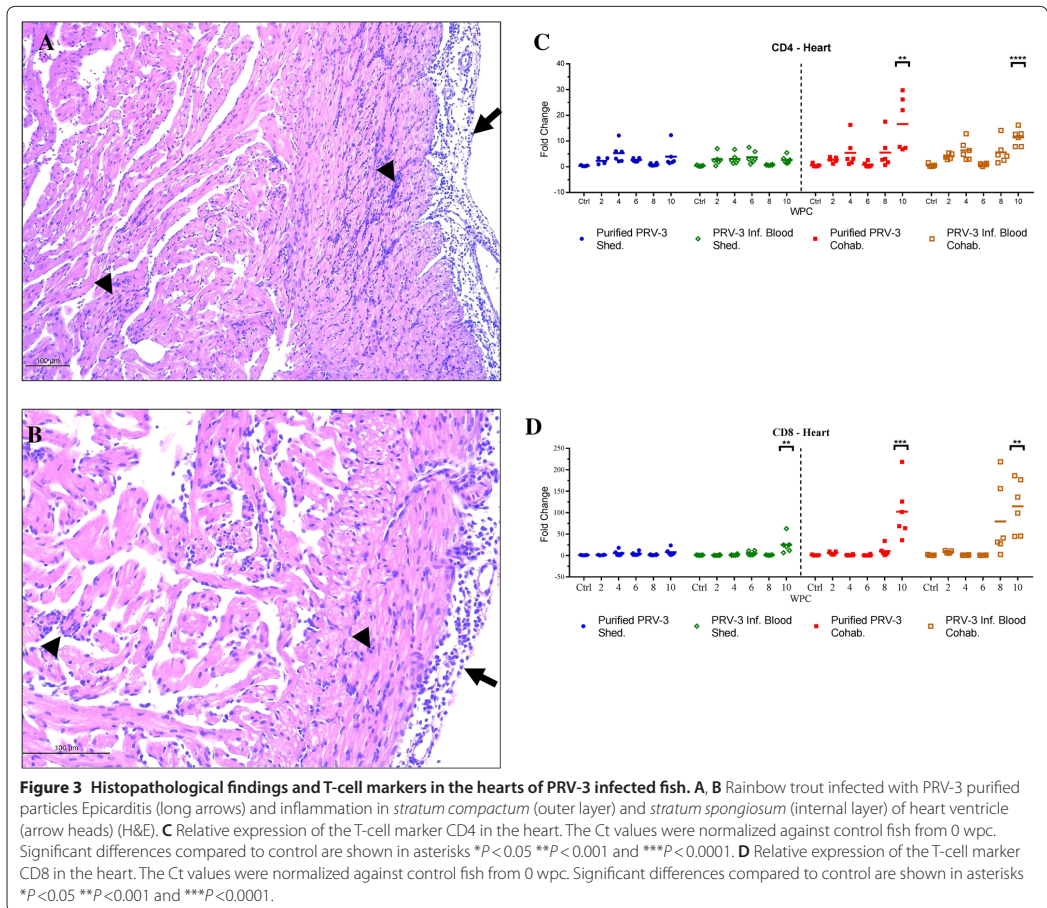
Discussion

The major aim of this study was to investigate an eventual association between PRV-3 infection in rainbow trout and the development of heart pathology consistent with cardiac lesions observed in natural disease outbreaks associated with PRV-3 infection. The detection of PRV-3 RNA in apparently healthy fish has raised

Table 3 Prevalence and scores of histopathological findings in the hearts of PRV-3 challenged fish

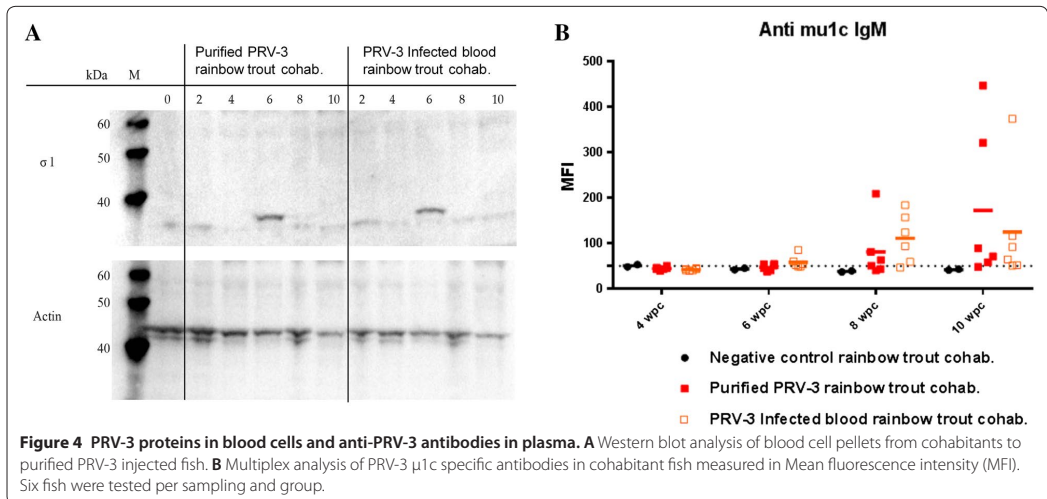
WPC	PRV-3 purified particles						PRV-3 infected blood					
	Shedder	Score	Ct	Cohab.	Score	Ct	Shedder	Score	Ct	Cohab.	Score	Ct
2	0/6			0/6			0/6			0/6		
4	0/6			0/6			0/6			0/6		
6	1/6	1	29.5	0/6			0/6			0/6		
8	0/6			0/6			0/6			2/6	1.5	21.8
											1.5	22.8
10	1/6	1	>35	2/6	1	31.2	1/6	1	>35	5/6	1	32.7
					1	30.1					1	32.7
											1	>35
											1	31.7
											1	36.8
Positive hearts	2			2			1			7		

Proportion of positive fish per time point, histopathological score and Ct values of the positive hearts are given.



questions in relation to the causative relationship between the virus and the disease. Koch's postulates have historically defined the criteria to demonstrate a causative relationship between infecting agents and disease [24]. Fulfillment of Koch's postulate relies on four main criteria, which are the presence of the disease agent in all disease cases; the possibility to isolate the agent in pure culture, the development of disease after the agent is inoculated in susceptible hosts and the re-isolation of the agent from the experimentally infected host. These criteria cannot be fulfilled for all disease-causing agents who resist culturing. According to the Rivers postulate, the viral agent should be isolated from a diseased individual and should induce the same disease when challenged with the purified viral inoculum as cell free extract and

produce antibodies in a disease free individual of the same species [25]. The development of sequence based detection methods have led to further revision [26]. In recent years Atlantic salmon farming has in particular been challenged with a number of pathogens that resist cultivation [27] such as PRV-1 [3], piscine myocarditis virus (PMCV) [28, 29], and salmon gill poxvirus (SGPV) [30, 31]. The diagnostic investigations that followed the appearance of a new disease in farmed rainbow trout in Norway in 2013 [11] led to the detection of a virus with 80% gene sequence homology to PRV-1, and further characterization of the virus concluded that it was a subtype of PRV, named PRV-3. Infectious trials were conducted to assess the risk associated with introduction of the new virus in salmonid aquaculture [12], which



indicated that the virus infects and replicates more effectively in rainbow trout than in Atlantic salmon. PRV-3 has been detected in several salmonid farming countries including Scotland, Germany, Italy, Denmark and Chile [13, 16, 17], but not always associated with clinical disease. Therefore, further investigations of the host–pathogen interaction could provide knowledge of benefit for fish health management.

The resistance of PRV to in vitro cultivation in available cell lines led to an approach where the virus was purified from experimentally infected fish as demonstrated by Wessel et al. [3] for PRV-1 and by Takano et al. [8] for PRV-2. Here, we adopted this approach by propagating PRV-3 in experimentally infected rainbow trout and purifying the virus by density CsCl gradient ultracentrifugation, as described by Wessel et al. [3]. The purity of viral particles was confirmed by analyzing the fraction by Next Generation Sequencing-NGS [13]. In EM, PRV-3 particles show similar features to the one displayed by purified PRV-1, i.e. the spherical particles with icosahedral symmetry with a diameter of approximately 75 nm, and two concentric electron dense layers representing the double capsid (Figure 1A).

Notably, fish exposed to PRV-3 by cohabitation had higher viral loads than the injected groups, suggesting that the cohabitation challenge model is suitable for investigation of PRV infection.

Fish challenged with purified PRV-3 by cohabitation were infected, as seen by the presence of σ 1 protein at 6 wpc as demonstrated by western blot of pelleted blood cells and by the increase of qPCR positive fish after

cohabitation. The timing of this is similar to PRV-1 infection in Atlantic salmon [32].

PRV-1 establishes a persistent infection in Atlantic salmon, and viral RNA can be detected for at least 57 wpc [33]. On the contrary, we observed that experimental PRV-3 infection in rainbow trout was characterized by significant clearance over time, in line with a previous study [12]. More specifically, the number of positive fish and virus levels per sampling point decreased after peak viremia. This trend of the infection kinetics was observed in both infected groups in our trial. In the positive control tank the injected fish reached peak virus levels already 2 wpc, whereas in the group injected with purified PRV-3 particles the peak was 4 wpc. Most likely, this difference can be explained by lower viral load in the initial inoculum, i.e. Ct 26.3 in PRV-3 infected blood, and Ct 32.67 in the purified PRV-3 inoculum.

The finding of PRV-specific antibody response from 8 wpc directed against the outer capsid protein PRV-1 μ 1C showed that the infection was recognized by the fish humoral response. Temporally, PRV-specific antibodies were detectable 2 weeks following the peak viral load and presumably the main shedding period which occurred at 6 wpc in cohabitants.

PRV-3 infection in rainbow trout did not cause reduced survival, neither in the positive control group nor in the group challenged with purified PRV-3 particles, consistent with what is previously observed under experimental conditions [12].

PRV-3 challenged fish developed typical heart pathology; a pancarditis, where all parts of the heart were

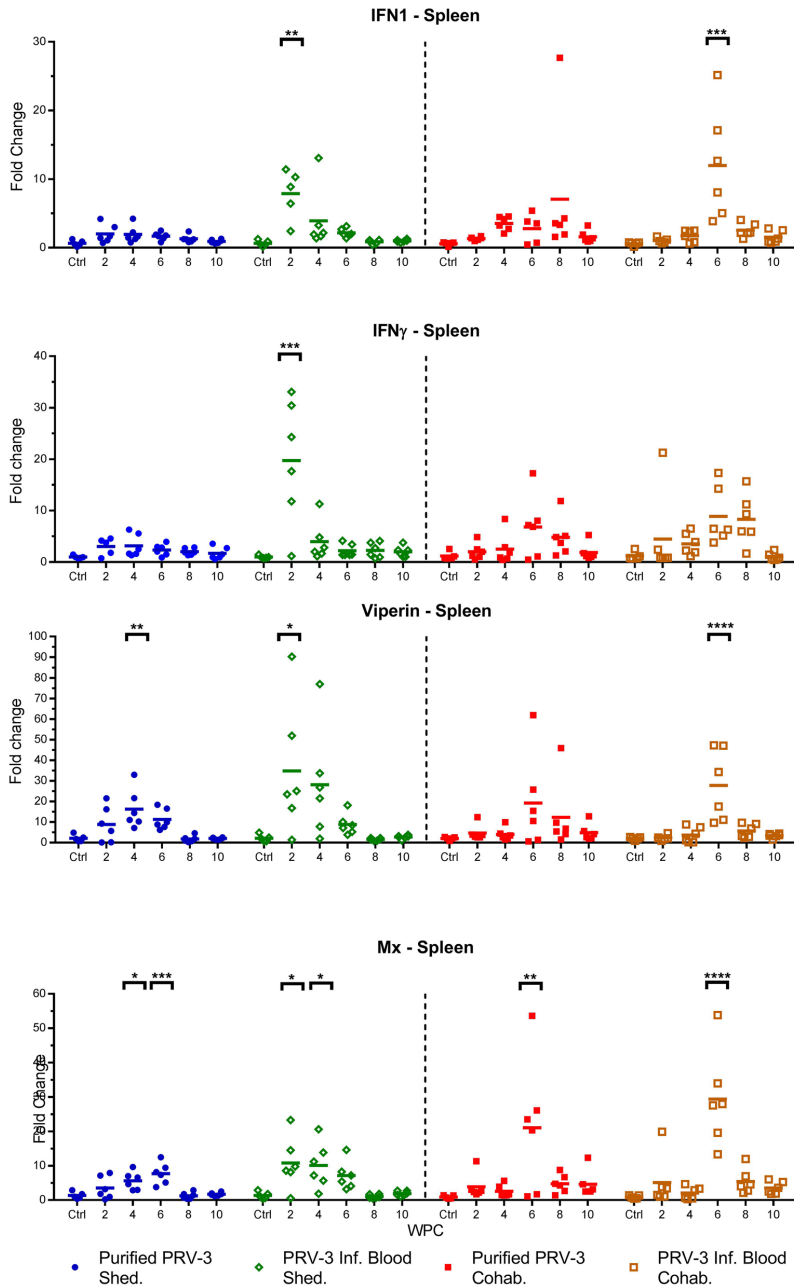


Figure 5 Innate antiviral immune gene expression in spleen of PRV-3 challenged fish. Relative expression of IFN1, IFN γ , Mx, and Viperin in controls, pure virus injected fish, blood pellet injected fish and their respective cohabitant groups (n=6). The Ct values were normalized against control fish from 0 wpc. Significant differences compared to control are shown in asterisks * $P < 0.05$, ** $P < 0.01$, *** $P < 0.001$, **** $P < 0.0001$.

affected. This was more pronounced in fish challenged with PRV-3 infected blood, nevertheless fish exposed to purified PRV-3 particles had these heart lesions. Although mild, the histopathological findings in the experimental group were consistent with a pathology described in field cases [11], from previous experiments [12] and the same as observed in the positive control group in this study.

An attempt to stain PRV antigen by immunohistochemistry in heart sections from fish with high viral loads with a polyclonal antibody against PRV-1 failed. This could be explained by low sensitivity of the antibodies in IHC, i.e. the amount of viral antigen was too low for detection. Another explanation could be conformational differences between PRV-1 and PRV-3. PRV-3 antigen can be detected in western blots under denaturing conditions, but it highlights the need for development of specific tools for identifying the localization of PRV-3 in tissue.

Our results linked the presence of the virus to the consecutive development of pathology in the heart, but furthermore also to the upregulation of CD8 and CD4 lymphocyte markers in this organ. The PRV-3 load peaked at 6 wpc in cohabitants, 4 weeks before the increased expression of CD8+ T cell population marker in the heart.

The increased level of the CD8+ T cell transcripts was associated with the observation of heart pathology, as previously observed in Atlantic salmon [32, 34]. This finding strengthens the link between CD8+ cytotoxic cells and heart inflammation, and indicates that the mechanisms of Norwegian PRV-1 induced HSMI [34] is paralleled by the pathogenesis of the PRV-3 induced heart pathology. The study highlighted some similarities between PRV-1 infection in Atlantic salmon and PRV-3 infection in rainbow trout. The two viral subtypes shares 80% homology at the genetic level [13], they target the respective host erythrocytes for replication and cause similar inflammatory lesion in the heart of infected fish. Both viral subtypes trigger similar immune responses in the respective hosts. Conversely, PRV-1 establishes a persistent infection in Atlantic salmon while our findings indicate that PRV-3 infection could be of limited duration in rainbow trout. Notably, PRV-3 affected rainbow trout in field outbreaks suffer severe anaemia [11], which is not reported for HSMI in Atlantic salmon. Furthermore typical PRV-3 outbreaks in rainbow trout occurred in fresh water, whereas HSMI is most common after sea transfer.

The innate antiviral gene regulation in the present study followed the PRV-3 kinetics, thus strengthening the association between PRV load and innate antiviral responses in infected salmonids [3, 12, 34, 35]. The innate antiviral gene upregulation in the early stage of PRV-3

infection may efficiently hamper the progression of viral infection, and lead to the decreased viral load after 6 wpc. Differences have been observed for HSMI and in innate antiviral response after PRV-1 challenge of Atlantic salmon indicating that viral and/or host genetic factors influence the outcome of a PRV-1 infection [3, 33]. For *Mammalian orthoreovirus* it has been shown that the ability to induce IFN contributes to the differences in the development of myocarditis [36, 37].

Previous studies [12] have shown how experimental infection in Atlantic salmon with PRV-3 infected blood failed to induce host innate immune response. Moreover, experimental infection in sockeye salmon (*Oncorhynchus nerka*) with PRV-1 fail to induce IFN related genes [38], whereas PRV-1 infection successfully trigger IFN related immune response modulating the susceptibility of Atlantic salmon to subsequent challenge with Infectious haematopoietic necrosis virus—IHNV or Salmonid alphavirus—SAV [35, 39, 40].

PRV infection of farmed salmonids can broadly be divided into two different clinical manifestations. (1) An acute disease, EIBS, which is a direct consequence of severe anemia at the peak of viremia, as seen in PRV-2 infection of coho salmon. It could be speculated that the jaundice syndrome described in Chinook salmon (related to PRV-1) [41] and jaundice syndrome reported in coho salmon (related to PRV-3) [16, 17] are downstream consequences of the clearance process of infected erythrocytes. Yet the role of PRV-1 and PRV-3 in the development of anaemia remains unknown. PRV-1 infection under experimental conditions failed to induce anaemia in Sockeye salmon [33, 38]. In Atlantic salmon, experimental infection with PRV-1 has only occasionally led to reduction of haematocrit and haemoglobin levels [35]. Notably, in this study, high loads of PRV-3 were generated in rainbow trout without causing a reduction of haematocrit, albeit it is described in disease outbreaks associated with PRV-3 in the field [11]. These findings might suggest that other factors, possibly related to farming conditions, are involved in the development of anaemia in clinical outbreaks. (2) HSMI, which appears a few weeks after the viraemia peak as demonstrated for PRV-1 in Atlantic salmon, is characterized by inflammation seen as influx of CD8 lymphocytes in heart tissue [34, 42]. In field outbreaks associated with PRV-3 reported by Olsen et al. [11], 113 fish were examined for histopathology. Amongst these, 80 fish showed evident clinical signs and 33 apparently looked healthy. A heart pathology resembling HSMI was described in 103 of the 113 fish examined [11]. In the current study, no clinical signs were observed, and an HSMI-like pathology was observed in a limited number of fish. Yet, in line with the timing of observation of heart pathology after PRV-1 infection in

Atlantic salmon [19], the HSMI related histopathological findings in the heart in the present experiment were observed in the later stage of the trial, i.e. at 6 wpc in the injected group and 10 wpc in the cohabitant group.

In conclusion, the findings of this study support the hypothesis that establishes the causative relationship between PRV-3 infection in rainbow trout and the development of pancarditis as described for HSMI in Atlantic salmon. Furthermore, the identification of the aetiological agent, makes a basis for the development of specific preventive tools and control strategies. The recent emergence of PRV-3 variants in rainbow trout farms associated with severe disease outbreaks [13], warrants further investigation in search of factors that modulate the severity of the disease.

Additional file

Additional file 1. Proportion of fish showing histopathological findings not consistent with PRV-induced inflammation. The findings consisted of epicarditis and a focal inflammatory reaction involving the interface layer between *stratum compactum* and *stratum spongiosum* of the ventricle. These were randomly distributed throughout the experiment and observed in all groups.

Competing interests

The authors declare that they have no competing interests.

Authors' contributions

NJO, NV and ER launched the project idea. NJO, KD, NV and ER participated in the overall design and coordination of the study, interpretation of data and drafting the manuscript. KD and NV conducted the trial, performed sampling and tested samples for viral kinetics. KD and MKD performed gene expression analysis. ABO and TMI performed histopathological examination of samples collected. LHT and MKD performed immunoassay for PRV antibody detection. ØW, TMI, MKD, AC and ABO participated in the coordination of the study, revised the manuscript and provided significant contribution to figures and text. All authors read and approved the final manuscript.

Acknowledgements

This study was co-funded by the European Reference Laboratory for Fish diseases at DTU AQUA National Institute of Aquatic Resources and H2020 INFRAIA-1-2014/2015 Aquaexcel grant agreement No 652831. Immune gene analysis and immunoassays were financed by the Norwegian Research Council (NRC) (Bioforsk Grant # 237315/E40) (ViVaFish). K.D. acknowledges the financial assistance provided by the Indian Council of Agricultural Research (ICAR) through the [National Bureau of Agriculturally Important Microorganisms (ICAR International Fellowship)] for his PhD. Histopathology was financed by the Norwegian Veterinary Institute (NVI). A special thanks to the Unit for fish and shellfish diseases at DTU-AQUA and the teams at NVI in Oslo and Bergen for technical support during the study.

Author details

¹ National Institute of Aquatic Resources, Technical University of Denmark, Kongens Lyngby, Denmark. ² Department of Food Safety and Infection Biology, Norwegian University of Life Sciences, Oslo, Norway. ³ Norwegian Veterinary Institute, Bergen, Norway. ⁴ Norwegian Veterinary Institute, Oslo, Norway.

Ethics approval and consent to participate

The experiments were carried out in the facilities at DTU-VET (Frederiksberg, Denmark) in accordance with the recommendations in the current animal

welfare regulations under the license 2013-15-2934-00976. The protocols were approved by the Danish Animal Research Authority.

Publisher's Note

Springer Nature remains neutral with regard to jurisdictional claims in published maps and institutional affiliations.

Received: 31 August 2018 Accepted: 3 January 2019

Published online: 18 February 2019

References

- Markussen T, Dahle MK, Tengs T, Lovøll M, Finstad ØW, Wiik-Nielsen CR, Grove S, Lauksund S, Robertsen B, Rimstad E (2013) Sequence analysis of the genome of piscine orthoreovirus (PRV) associated with heart and skeletal muscle inflammation (HSMI) in Atlantic salmon (*Salmo salar*). *PLoS One* 8:e70075
- Wessel Ø, Olsen CM, Rimstad E, Dahle MK (2015) Piscine orthoreovirus (PRV) replicates in Atlantic salmon (*Salmo salar* L.) erythrocytes ex vivo. *Vet Res* 46:26
- Wessel Ø, Braaen S, Alarcon M, Haatveit H, Roos N, Markussen T, Tengs T, Dahle MK, Rimstad E (2017) Infection with purified Piscine orthoreovirus demonstrates a causal relationship with heart and skeletal muscle inflammation in Atlantic salmon. *PLoS One* 12:e0183781
- Palacios G, Lovøll M, Tengs T, Hornig M, Hutchison S, Hui J, Kongtorp RT, Savji N, Bussetti AV, Solovyov A, Kristoffersen AB, Celone C, Street C, Trifonov V, Hirschberg DL, Rabadan R, Egholm M, Rimstad E, Lipkin WI (2010) Heart and skeletal muscle inflammation of farmed salmon is associated with infection with a novel reovirus. *PLoS One* 5:e11487
- Kongtorp RT, Kjerstad A, Taksdal T, Guttvik A, Falk K (2004) Heart and skeletal muscle inflammation in Atlantic salmon, *Salmo salar* L.: a new infectious disease. *J Fish Dis* 27:351–358
- Di Cicco E, Ferguson HW, Schulze AD, Kaukinen KH, Li S, Vanderstichel R, Wessel Ø, Rimstad E, Gardner IA, Hammell KL, Miller KM (2017) Heart and skeletal muscle inflammation (HSMI) disease diagnosed on a British Columbia salmon farm through a longitudinal farm study. *PLoS One* 12:e0171471
- Kongtorp RT, Taksdal T, Lyngoy A (2004) Pathology of heart and skeletal muscle inflammation (HSMI) in farmed Atlantic salmon *Salmo salar*. *Dis Aquat Organ* 59:217–224
- Takano T, Nawata A, Sakai T, Matsuyama T, Ito T, Kurita J, Terashima S, Yasuike M, Nakamura Y, Fujiwara A, Kumagai A, Nakayasu C (2016) Full-genome sequencing and confirmation of the causative agent of erythrocytic inclusion body syndrome in coho salmon identifies a new type of piscine orthoreovirus. *PLoS One* 11:e0165424
- Landolt ML, MacMillan JR, Patterson M (1977) Detection of an intra-erythrocytic virus in rainbow trout (*Salmo gairdneri*). *Fish Health News* 6:4–6
- Leek SL (1987) Viral erythrocytic inclusion body syndrome (EIBS) occurring in juvenile spring chinook salmon (*Oncorhynchus tshawytscha*) reared in freshwater. *Can J Fish Aquat Sci* 44:685–688
- Olsen AB, Hjortaa M, Tengs T, Hellberg H, Johansen R (2015) First description of a new disease in rainbow trout (*Oncorhynchus mykiss* Walbaum) similar to heart and skeletal muscle inflammation (HSMI) and detection of a gene sequence related to piscine orthoreovirus (PRV). *PLoS One* 10:e0131638
- Hauge H, Vendramin N, Taksdal T, Olsen ABAB, Wessel Ø, Mikkelsen SS, Alencar ALF, Olesen NJ, Dahle MK (2017) Infection experiments with novel Piscine orthoreovirus from rainbow trout (*Oncorhynchus mykiss*) in salmonids. *PLoS One* 12:e0180293
- Dhamotharan K, Vendramin N, Markussen T, Wessel Ø, Cuenca A, Nyman IBIB, Olsen ABAB, Tengs T, Dahle MK, Rimstad E (2018) Molecular and antigenic characterization of piscine orthoreovirus (PRV) from rainbow trout (*Oncorhynchus mykiss*). *Viruses* 10:E170
- Gjevne AG, Modahl I, Spilberg B, Lyngstad TM (2016) The surveillance programme for virus associated with disease in rainbow trout (PRVom) in 2016. The Norwegian Veterinary Institute 2016. https://www.vetinst.no/overvaking/Piscine-orthoreovirus-Oncorhynchus-mykiss-PRVom-fisk/_/attachment/download/d6ff8741-307e-4c30-8456-50b85002b678:1c508

- 8843c6f2c7dd4bc6e80c1d8fdcaad7c921/2017_OK_PRVom_2016.pdf. Accessed June 2018
15. Kuehn R, Bc Stoeckle, Young M, Popp L, Tæubert E, Pfaffl MW, Geist J (2018) Identification of a piscine reovirus-related pathogen in proliferative darkening syndrome (PDS) infected brown trout (*Salmo trutta fario*) using a next-generation technology detection pipeline. *PLoS One* 13:e0206164
 16. Bohle H, Bustos P, Leiva L, Grothusen H, Navas E, Sandoval A, Bustamante F, Montecinos K, Alvaro Gaete MM (2018) First complete genome sequence of piscine orthoreovirus variant 3 infecting coho salmon (*Oncorhynchus kisutch*) farmed in southern Chile. *Genome Announc* 6:e00484-18
 17. Godoy MG, Kibenge MJT, Wang Y, Suarez R, Leiva C, Vallejos F, Kibenge FSB (2016) First description of clinical presentation of piscine orthoreovirus (PRV) infections in salmonid aquaculture in Chile and identification of a second genotype (Genotype II) of PRV. *Virology* 13:98
 18. Bruner R, Vinograd J (1965) The evaluation of standard sedimentation coefficients of sodium RNA and sodium DNA from sedimentation velocity data in concentrated NaCl and CsCl solutions. *Biochim Biophys Acta* 108:18–29
 19. Finstad ØW, Falk K, Løvoll M, Evensen Ø, Rimstad E (2012) Immunohistochemical detection of piscine reovirus (PRV) in hearts of Atlantic salmon coincide with the course of heart and skeletal muscle inflammation (HSMI). *Vet Res* 43:27
 20. Teige LH, Lund M, Haatveit HM, Røsæg MV, Wessel Ø, Dahle MK, Storset AK (2017) A bead based multiplex immunoassay detects Piscine orthoreovirus specific antibodies in Atlantic salmon (*Salmo salar*). *Fish Shellfish Immunol* 63:491–499
 21. Kongtorp RT, Halse M, Taksdal T, Falk K (2006) Longitudinal study of a natural outbreak of heart and skeletal muscle inflammation in Atlantic salmon, *Salmo salar* L. *J Fish Dis* 29:233–244
 22. Dunnett CW (1955) A multiple comparison procedure for comparing several treatments with a control. *J Am Stat Assoc* 50:1096–1121
 23. Spearman C (1904) The proof and measurement of association between two things. *Am J Psychol* 15:72–101
 24. Cohen J (1890) The evolution of Koch's postulates. In: Cohen J, William PG, Steven OD (eds) *Infectious Diseases*, 4th edn. Elsevier
 25. Rivers TM (1937) Viruses and Koch's postulates. *J Bacteriol* 33:1–12
 26. Fredricks DN, Relman DA (1996) Sequence-based identification of microbial pathogens: a reconsideration of Koch's. *Clin Microbiol Rev* 9:18–33
 27. Tengs T, Rimstad E (2017) Emerging pathogens in the fish farming industry and sequencing-based pathogen discovery. *Dev Comp Immunol* 75:109–119
 28. Haugland O, Mikalsen AB, Nilsen P, Lindmo K, Thu BJ, Eliassen TM, Roos N, Rode M, Evensen O (2011) Cardiomyopathy syndrome of Atlantic salmon (*Salmo salar* L.) is caused by a double-stranded RNA virus of the *Totiviridae* family. *J Virol* 85:5275–5286
 29. Garseth H, Fritsvold C, Svendsen JC, Bang Jensen B, Mikalsen AB (2018) Cardiomyopathy syndrome in Atlantic salmon *Salmo salar* L.: a review of the current state of knowledge. *J Fish Dis* 41:1–26
 30. Gjessing MC, Yutin N, Tengs T, Senkevich T, Koonin E, Rønning HP, Alarcon M, Ylving S, Lie K-I, Saure B, Tran L, Moss B, Dale OB (2015) Salmon gill poxvirus, the deepest representative of the *Chordopoxvirinae*. *J Virol* 89:9348–9367
 31. Gjessing MC, Thoen E, Tengs T, Skotheim SA, Dale OB (2017) Salmon gill poxvirus, a recently characterized infectious agent of multifactorial gill disease in freshwater- and seawater-reared Atlantic salmon. *J Fish Dis* 40:1253–1265
 32. Haatveit HM, Wessel Ø, Markussen T, Lund M, Thiede B, Nyman IB, Braeen S, Dahle MK, Rimstad E (2017) Viral protein kinetics of piscine orthoreovirus infection in Atlantic salmon blood cells. *Viruses* 9:E49
 33. Garver KA, Johnson SC, Polinski MP, Bradshaw JC, Marty GD, Snyman HN, Morrison DB, Richard J (2016) Piscine orthoreovirus from western North America is transmissible to Atlantic salmon and sockeye salmon but fails to cause heart and skeletal muscle inflammation. *PLoS One* 11:e0146229
 34. Mikalsen AB, Haugland O, Rode M, Solbakk IT, Evensen O (2012) Atlantic salmon reovirus infection causes a CD8 T cell myocarditis in Atlantic salmon (*Salmo salar* L.). *PLoS One* 7:e37269
 35. Vendramin N, Alencar ALF, Iburg TM, Dahle MK, Wessel O, Olsen AB, Rimstad E, Olesen NJ (2018) Piscine orthoreovirus infection in Atlantic salmon (*Salmo salar*) protects against subsequent challenge with infectious hematopoietic necrosis virus (ihnv). *Vet Res* 49:30
 36. Sherry B, Torres J, Blum MA (1998) Reovirus induction of and sensitivity to beta interferon in cardiac myocyte cultures correlate with induction of myocarditis and are determined by viral core proteins. *J Virol* 72:1314–1323
 37. Irvin SC, Zurney J, Ooms LS, Chappell JD, Dermody TS, Sherry B (2012) A single-amino-acid polymorphism in reovirus protein $\mu 2$ determines repression of interferon signaling and modulates myocarditis. *J Virol* 86:2302–2311
 38. Polinski MP, Bradshaw JC, Inkpen SM, Richard J, Fritsvold C, Poppe TT, Rise ML, Garver KA, Johnson SC (2016) De novo assembly of Sockeye salmon kidney transcriptomes reveal a limited early response to piscine reovirus with or without infectious hematopoietic necrosis virus superinfection. *BMC Genomics* 17:848
 39. Røsæg MV, Lund M, Nyman IB, Markussen T, Aspehaug V, Sindre H, Dahle MK, Rimstad E (2017) Immunological interactions between Piscine orthoreovirus and Salmonid alphavirus infections in Atlantic salmon. *Fish Shellfish Immunol* 64:308–319
 40. Lund M, Røsæg MV, Krasnov A, Timmerhaus G, Nyman IB, Aspehaug V, Rimstad E, Dahle MK (2016) Experimental Piscine orthoreovirus infection mediates protection against pancreas disease in Atlantic salmon (*Salmo salar*). *Vet Res* 47:107
 41. Di Cicco E, Ferguson HW, Kaukinen KH, Schulze AD, Li S, Tabata A, Günther OP, Mordecai G, Suttle CA, Miller KM (2018) The same strain of Piscine orthoreovirus (PRV-1) is involved with the development of different, but related, diseases in Atlantic and Pacific Salmon in British Columbia. *Facets* 3:599–641
 42. Yousaf MN, Koppang EO, Skjødt K, Hordvik I, Zou J, Secombes C, Powell MD (2013) Comparative cardiac pathological changes of Atlantic salmon (*Salmo salar* L.) affected with heart and skeletal muscle inflammation (HSMI), cardiomyopathy syndrome (CMS) and pancreas disease (PD). *Vet Immunol Immunopathol* 151:49–62
 43. Ballesteros NA, Rodriguez Saint-Jean S, Perez-Prieto SI (2015) Immune responses to oral pcDNA-VP2 vaccine in relation to infectious pancreatic necrosis virus carrier state in rainbow trout *Oncorhynchus mykiss*. *Vet Immunol Immunopathol* 165:127–137
 44. Wangkahart E, Scott C, Secombes CJ, Wang T (2016) Re-examination of the rainbow trout (*Oncorhynchus mykiss*) immune response to flagellin: *Yersinia ruckeri* flagellin is a potent activator of acute phase proteins, antimicrobial peptides and pro-inflammatory cytokines in vitro. *Dev Comp Immunol* 57:75–87

WPC	Neg. control		Purified PRV-3		PRV-3 infected blood	
	Shedder	Cohab.	Shedder	Cohab.	Shedder	Cohab.
2						
4	1 / 2				2 / 6	
6		2 / 2				
8	1 / 2		2 / 6	2 / 6	1 / 6	
10			1 / 6	4 / 6	1 / 6	1 / 6

Acknowledgement

This project has received funding from the European unions's Horizon 2020 research and innovation programme under grant agreement No. 652831(AQUAEXCEL²⁰²⁰). This output reflects only the author's view and the European Union cannot be held responsible for any use that may be made of the information contained therein.'

ISBN: 978-82-575-1639-0

ISSN: 1894-6402



Norwegian University
of Life Sciences

Postboks 5003
NO-1432 Ås, Norway
+47 67 23 00 00
www.nmbu.no